NSF/CEE-81096

PB82-212945

CALIFORNIA INSTITUTE OF TECHNOLOGY

EARTHQUAKE ENGINEERING RESEARCH LABORATORY

DYNAMIC BEHAVIOR OF ROCKING STRUCTURES ALLOWED TO UPLIFT

By

Ioannis N. Psycharis

EERL 81-02

A Report on Research Conducted Under a
Grant from the National Science Foundation

Pasadena, California

August 1981

INFORMATION RESOURCES
NATIONAL SCIENCE FOUNDATION

A portion of this investigation was sponsored by Grant No. PFR77-23687 from the National Science Foundation, Division of Problem-Focused Research Applications, under the supervision of P. C. Jennings. Any opinions, findings, and conclusions or recommendations expressed in this publication are those of the author and do not necessarily reflect the views of the National Science Foundation.

DYNAMIC BEHAVIOR OF ROCKING STRUCTURES ALLOWED TO UPLIFT

Thesis by

Ioannis N. Psycharis

In Partial Fulfillment of the Requirements
for the Degree of
Doctor of Philosophy

California Institute of Technology

Pasadena, California

1982

(Submitted August 20, 1981)

ACKNOWLEDGEMENTS

I wish to express my sincere gratitude to my advisor, Professor P. C. Jennings, for his guidance, encouragement and helpful suggestions provided during the course of this investigation. The assistance of other members of the faculty of Civil Engineering, and especially of Professors G. W. Housner and R. F. Scott, is also acknowledged. Special thanks are due to Professor A. Rutenberg of the Technion-Israel Institute, Haifa, for many interesting discussions and valuable suggestions.

The financial support provided by the California Institute of Technology is gratefully appreciated. The partial support of this investigation by a grant from the National Science Foundation is also acknowledged.

I would like to thank Mr. Dirceau Bothelo for his assistance with some of the computations. Thanks are also expressed to my friends Stelios Kyriakides and Yanis Yortsos for their help in numerous ways.

Special thanks are owed to Mrs. Gloria Jackson and Mrs. Sharon Beckenbach for all they have done in preparing this manuscript.

ABSTRACT

Strong shaking of structures during large earthquakes may result in some cases in partial separation of the base of the structure from the soil. This phenomenon of uplifting, which can affect the dynamic behavior of the structure significantly, even if the amount of uplift is small, is examined in this thesis. First the case of a rocking rigid block is investigated and then more complicated, flexible superstructures are introduced. Two foundation models which permit uplift are considered: the Winkler foundation and the much simpler "two-spring" foundation. Several energy dissipating mechanisms are also introduced into these models. It is shown that an equivalence between these two models for the foundation can be established, so that one can always work with the much simpler two-spring foundation. In this way complete analytical solutions can be derived in most cases. Moreover, simple approximate methods for the calculation of the apparent fundamental period of the rocking system are developed and simplified methods of analysis are proposed.

In general, uplift leads to a softer vibrating system which behaves nonlinearly, although the response is composed of a sequence of linear responses. As a result, the apparent fundamental resonant frequency of the uplifting system is always less than the fundamental resonant frequency of both the soil-structure interacting system, in which lift-off is not allowed, and the superstructure itself. The second and higher resonant frequencies of the superstructure, however, are not affected significantly by lift-off. For damped foundations, the ratio of

critical damping associated with the apparent fundamental mode decreases, in general, with the amount of lift-off. These effects of uplift on the dynamic properties of the rocking system can alter the response of the structure significantly during an earthquake. Nevertheless, it cannot be said a priori whether they are favorable to the behavior or not; this depends on the parameters of the system and the time history of the excitation.

TABLE OF CONTENTS

LIST OF SYMBOLS

I. LATIN

Symbol	Meaning
a	width of the superstructure
a_0	amplitude of harmonic ground acceleration
A	amplitude of harmonic oscillations of Y
A_r	$= \sum_{i=1}^{n} m_i h_i \eta_i^{(r)}$
b	height of the superstructure
B	maximum value of the parabolic terms in equation (2.3.69)
B_r	$= \sum_{i=1}^{n} m_i \eta_i^{(r)}$
c	damping coefficient for the two-spring foundation
c_0	damping coefficient for the Winkler foundation
c_{11}, c_{12}, c_{22}	elements of [C] matrix
c^*	damping coefficient of the dashpot of the impact mechanism
C	damping coefficient of the single-degree-of-freedom superstructure
CF	correction factor
C_i	damping coefficient of the $(i-1)^{th}$ floor of the multistory superstructure
C_ϕ	damping coefficient of rotational dashpot modeling the elastic half space

Symbol	Meaning
C_1, C_2	constants of integration
[C]	damping matrix
d	depth of the superstructure
e	base of Napierian logarithms
f_i	forcing term of the equation of motion corresponding to the i^{th} mode of the superstructure
F_W	vertical force from the Winkler foundation (total)
F_0	yield force of the two-spring foundation (elasto-plastic springs)
F_1, F_2	vertical foundation forces
F_{2s}	vertical force from the two-spring foundation (total)
$\underset{\sim}{F}$	forcing term in the equations of motion
g	acceleration of gravity (= 9.81 m/sec^2, or, 32.2 ft/sec^2)
G_1, G_2, G_3	functions defined by equations (I.19), (I.20) and (I.25)
$G_1(s^2)$, $G_2(s^2)$, $G_3(s^2)$, $G_4(s^2)$	functions of the Laplace variable, s, defined by equations (4.3.23), (4.3.24), (4.3.26) and (4.3.27)
h, h_c	height of the center of mass measured from the base
h_i	height of the i^{th} floor measured from the base
$\underset{\sim}{h}$	= $\{h_i\}$
H_i	height of the i^{th} floor measured from the $(i-1)^{th}$ floor
$\underset{\sim}{H}_{CM}$	total angular momentum with respect to the center of mass

Symbol	Meaning
$\underset{\sim}{H}'_{CM}$	angular momentum with respect to the center of mass associated with $\underset{\sim}{\omega}_0$
$\underset{\sim}{H}''_{CM}$	angular momentum with respect to the center of mass associated with $\underset{\sim}{\Omega}_i$'s
$\underset{\sim}{H}_i$	angular momentum of mass m_i with respect to its center of mass
$\underset{\sim}{H}'_i$	angular momentum of mass m_i with respect to its center of mass, associated with $\underset{\sim}{\omega}_0$
$\underset{\sim}{H}''_i$	angular momentum of mass m_i with respect to its center of mass, associated with $\underset{\sim}{\Omega}_i$
i	$= \sqrt{-1}$
I	vertical impulse during impact
I_A	horizontal impulse during impact
I_{CM}	moment of inertia about the center of mass
I_h	horizontal impulse excitation
I_i	centroidal moment of inertia of i^{th} mass
I_M	moment of inertia about the midpoint of the base, M
I_P	moment of inertia about the pole of rotation, P
I_O	moment of inertia about the point O or O'
$[I]$	unit matrix
$[I_i]$	inertia matrix of mass m_i
k	stiffness of springs for the two-spring foundation
k_0	stiffness of springs for the Winkler foundation
K	stiffness of the single-degree-of-freedom superstructure

Symbol	Meaning
K_i	stiffness of the $(i-1)^{th}$ floor for the case of a multistory superstructure
K_ϕ	stiffness of rotational spring modeling the elastic half-space
[K]	stiffness matrix
ℓ	distance of the pole of rotation from the midpoint of the base, M
ℓ_1	$= \frac{a}{2} - \ell$
m	total mass of the superstructure
m_i	mass of the i^{th} floor
m_i^*	$= \sum_{\ell=i}^{n} m_\ell$
m_0	mass of the base
M_{CM}	moment of external forces about the center of mass
M_W	moment of foundation forces about the center of mass for the Winkler foundation
M_{2s}	moment of foundation forces about the center of mass for the two-spring foundation
[M]	mass matrix
n	number of floors of the multistory building (including the roof, excluding the base)
N_i	axial force between the $(i-1)^{th}$ and i^{th} floors
[N]	modal matrix
p	apparent rocking frequency for the rigid superstructure

Symbol	Meaning
p_1, p_2	characteristic foundation frequencies during full contact for the two-spring foundation (undamped)
p_1^*, p_2^*	characteristic foundation frequencies during full contact for the Winkler foundation (undamped)
p_{1d}, p_{2d}	damped characteristic foundation frequencies during full contact for the two-spring foundation
p_{1d}^*, p_{2d}^*	damped characteristic foundation frequencies during full contact for the Winkler foundation
P_1, P_2	characteristic foundation frequencies after lift-off for the two-spring foundation (undamped)
q	displacement vector in principal coordinates
Q	reduction of kinetic energy during impact
Q_i	shear force between the $(i-1)^{th}$ and i^{th} floors
r	$= \frac{1}{2}\sqrt{a^2 + b^2}$
r_e	radius of equivalent circular base
r_M	radius of gyration about the midpoint of the base, M
$\underset{\sim}{r}$	$= \begin{Bmatrix} y \\ \xi\phi \end{Bmatrix}$
R_A	horizontal force from the foundation
s	Laplace variable
S	length of contact, after lift-off, for the Winkler foundation
$\tilde{S}$	average value of S with respect to time
t	time
t_0	time at which the structure first lifts off

Symbol	Meaning
t_1	time at which the angle of rotation attains its maximum value (in the first half period), measured from the time of uplift
T	apparent rocking period for the rigid superstructure
T_1	fundamental period of the superstructure (fixed-base response)
T_c	rocking period of the system during full contact
T_{1c}	fundamental rocking period of the soil-structure interacting system during full contact
u	shear deformation of the single-degree-of-freedom superstructure
u_c	deflection of the superstructure at the level of the center of mass
u_i	deflection of the superstructure at the level of the i^{th} floor
$\underset{\sim}{u}$	$= \{u_i\}$
v	$= x + u$
$(v_i)_r$	relative velocity of center of mass of i^{th} floor with respect to the system (x_0, y_0, z_0)
x	horizontal displacement of the center of mass because of the rotation $(= h\phi)$
x_G	horizontal ground displacement
$x_{xG}(t)$, $x_{yG}(t)$	Green's functions defined by equations (2.3.40)
$X_y(s)$, $X_x(s)$, $X_p(s)$, $X_{xG}(s)$	Laplace functions defined by equations (2.3.36)

Symbol	Meaning
y	vertical displacement of the center of mass, positive upwards
y_G	vertical ground displacement, positive upwards
y_M	vertical displacement of the midpoint of the base, M, positive upwards
y_0, $y_{0'}$	vertical displacement of point 0 or 0', positive upwards
$y_{xG}(t)$, $y_{yG}(t)$	Green's functions defined by equations (2.3.40)
$\dot{y}_1$, $\dot{y}_2$	vertical velocities before and after impact
Y	vertical displacement of point 0 or 0', positive downwards
$Y_x(s)$, $Y_y(s)$, $Y_p(s)$, $Y_{xG}(s)$	Laplace functions defined by equations (2.3.36)
Y_1^e, Y_2^e	elastic deformation of springs (elastoplastic springs)
Y_1^p, Y_2^p	plastic deformation of springs (elastoplastic springs)
z	$= S\phi$
z'	$= (S-\xi)\phi$
$\tilde{Z}_i$	i^{th} apparent ratio of critical damping after lift-off for the soil-structure interacting system

II. GREEK

Symbol	Meaning
α	$= \phi_{cr}/\theta_1$
α^*	$= \phi_{cr}/\theta$
α_1, α_2	powers of the dimensionless terms used in the empirical formula of $\tilde{S}$
$\tilde{\alpha}$	$= \xi/h$

Symbol	Meaning
β	normalized impulse ($= \phi^{c}_{max}/\phi_{cr}$)
β_{2s}	value of β corresponding to the two-spring foundation
Γ	Bromwich contour
δ	static deflection
δ_{ij}	Kronecker delta
$\Delta(s)$	characteristic determinant of the Laplace system
$\Delta_i(s)$	$= s^2 + 2\zeta^{s}_{i}\omega_i + \omega_i^2$
ΔE	dissipation of energy during impact
$(\Delta E)_{max}$	maximum possible dissipation of energy during impact
Δt	operating time of impact mechanism
$\Delta\dot{y}$, $\Delta\dot{\phi}$	velocity changes during impact
ϵ	coefficient of restitution during impact
ζ	apparent ratio of critical damping in rocking for the rigid superstructure
ζ^{s}	ratio of critical damping of the single-degree-of-freedom superstructure
ζ^{s}_{i}	ratio of critical damping associated with the i^{th} mode of the multi-degree-of-freedom superstructure
$\check{\zeta}_i$	i^{th} apparent ratio of critical damping during full contact for the soil-structure interacting system
ζ_1, ζ_2	ratios of critical damping associated with the foundation during full contact, two-spring model
ζ_1^*, ζ_2^*	ratios of critical damping associated with the foundation during full contact, Winkler model
$\eta^{(i)}_{j}$	j^{th} component of i^{th} eigenvector

Symbol	Meaning
$\underset{\sim}{\eta}^{(i)}$	i^{th} eigenvector
θ	overturning angle in the case of the Winkler foundation $\left[= \tan^{-1}\left(\frac{a}{2h}\right)\right]$
θ_1	overturning angle in the case of the two-spring foundation $\left[= \tan^{-1}\left(\frac{\xi}{h}\right)\right]$
λ	$= \frac{m\xi^2}{I_M}$
μ_i $(i = 1,2)$	eigenvalues of $[M]^{-1}[K]$ matrix for the case of the rocking block on a damped two-spring foundation
$\tilde{\mu}_i$ $(i = 1,2)$	$= \mu_i/(k/m)$
ξ	position of springs of the two-spring foundation, measured from the midpoint of the base, M
ξ'	$= \frac{a}{2} - \xi$
π	$= 3.14159...$
Π_1, Π_2, Π_3	dimensionless quantities defined by equations (I.2)-(I.4)
$\underset{\sim}{\rho}_i$	distance of the center of mass of i^{th} floor from the center of mass of the system
ϕ	angle of rotation
ϕ^u	angle of rotation for the undamped foundation
$\tilde{\phi}$	angle of rotation for the equivalent linear system
ϕ_{cr}	critical angle at which lift-off first happens in the absence of vertical oscillations
$\phi_{cr}^{(2s)}$	value of ϕ_{cr} for the two-spring foundation
ϕ_{max}	maximum value of angle of rotation

Symbol	Meaning
ϕ^c_{max}	maximum angle of rotation which would happen if lift-off were not allowed (undamped foundation)
$\phi^c_{max(2s)}$	value of ϕ^c_{max} for the two-spring foundation
$\phi^c_{max(W)}$	value of ϕ^c_{max} for the Winkler foundation
ϕ^u_{max}	maximum angle of rotation for the undamped foundation
$\tilde{\phi}_{max}$	maximum angle of rotation for the equivalent linear system
ϕ_n	amplitude of rocking response following the n^{th} impact
ϕ_0, $\dot{\phi}_0$	initial conditions for the rocking response
$\dot{\phi}_1$, $\dot{\phi}_2$	rocking velocities before and after impact
ω	resonant frequency of the single-degree-of-freedom superstructure
$\tilde{\omega}$	resonant frequency of the soil-structure interacting system during full contact (single-degree-of-freedom superstructure)
ω_i	i^{th} resonant frequency of the superstructure (fixed-base response)
$\tilde{\omega}_i$	i^{th} resonant frequency of the soil-structure interacting system during full contact (multistory superstructure)
ω_0	frequency of the harmonic ground acceleration
$\underset{\sim}{\omega_0}$	angular velocity of the (x_0, y_0, z_0) system of coordinates, applied at the center of mass

Symbol	Meaning
$\tilde{\Omega}_i$	i^{th} characteristic frequency of the soil-structure interacting system after lift-off
$\underset{\sim}{\Omega}_i$	relative angular velocity of mass m_i with respect to the system (x_0, y_0, z_0)

A bar over a function denotes Laplace Transform.

CHAPTER I

INTRODUCTION

The phenomenon of partial separation (lift-off) of the base of a structure from its foundation during strong ground shaking has been observed in many earthquakes. For example, during the Arvin-Tehachapi, California earthquake of July, 1952, a number of tall, slender, petroleum-cracking towers stretched their anchor bolts and rocked back and forth on their foundations.[1] After the Alaska earthquake of March, 1964, ice was found under some oil tanks, evidence that lift-off occurred during the earthquake.[2] During the Asam, India earthquake of June, 1897, indications of rocking of some monuments and tombstones were evident;[3] in many cases, the rocking was so strong that it resulted in overturning of these small structures. In Figure 1.1, two examples of lift-off from the recent Imperial Valley, California earthquake of October 15, 1979, are shown. In Figure 1.1a the stretched grounding cable of the oil tank indicates that uplift of the tank happened during the ground shaking. From the position of this grounding cable it can be estimated that the uplift was at least 5 to 6 inches. In Figure 1.1.b lift-off of the tank is indicated by the cracked asphalt around the pipeline which was connected with the tank. The fact that partial lift-off has not yet been clearly observed for buildings does not imply that this phenomenon is impossible for such structures. It is possible that the lack of such observations is caused by the difficulty in finding evidence of the small amounts of uplift expected for buildings. Analysis of the behavior of buildings during earthquakes indicates that partial lift-off may

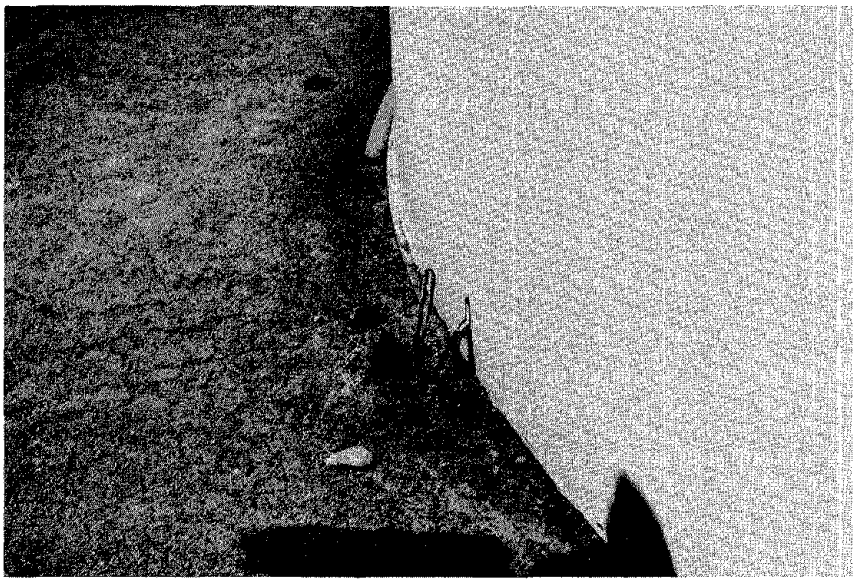

(a)

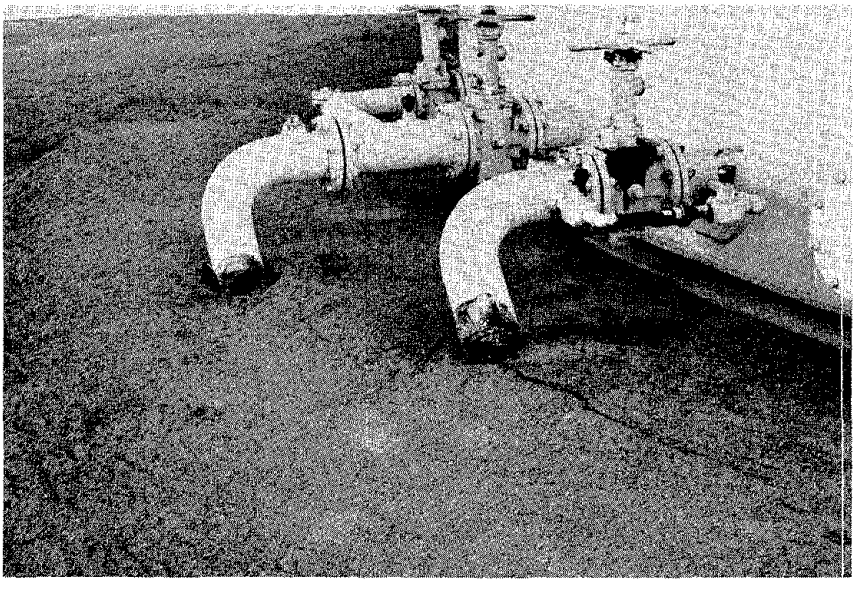

(b)

Fig. 1.1. Evidence of lift-off during the El Centro, California earthquake of October, 1979.

happen in some cases; for example, in the case of Veterans Hospital Building 41 during the San Fernando earthquake.[4]

A significant amount of work has already been done on the limiting case of tipping of bodies on a rigid foundation, especially for rigid superstructures (for example see references 1,5-13). The motive for most of this research was the prevention of overturning of objects such as tombstones, furniture or other equipment installed in buildings during earthquakes. An interesting review of the investigations done on this problem is presented by Ishiyama in reference 13. Of special interest is the work reported by Aslam, et al.,[11] who performed experiments and a computer analysis. He concluded that the rocking response of a rigid block is very sensitive to the boundary conditions, the impact coefficient of restitution, and the ground motion details. A probabilistic approach of the problem was done by Yim, et al.,[12] who also applied their results to the estimation of the intensity of ground shaking from its observed effects on tombstones, monumental columns, and other similar objects.

Housner[1] was the first to relate the problem of tipping of bodies with the good performance of some apparently unstable structures during strong ground shaking. His work was motivated by the fact that several "golf-ball-on-a-tee" types of elevated water tanks survived the ground shaking of the Chilean earthquakes of May, 1960, while other more stable appearing reinforced concrete elevated water tanks were severely damaged. In his analysis, Housner derived an expression for the amplitude dependent period of a rocking block and developed a formula to estimate the dissipation of energy which occurs during the rocking. Since the

foundation is assumed rigid, energy is lost in the impact that happens every time the pole of rotation changes from one corner of the base to the other. The beneficial effect of tipping to the earthquake response of structures was also described by Beck and Skinner[14] in their dynamic analysis of the South Rangitikei Rail Bridge pier, in New Zealand, which was designed to step. The first analytical investigation of the response of a flexible superstructure rocking on a rigid foundation was reported by Meek,[15] who examined the rocking of a single-degree-of-freedom oscillator. Meek concluded that the foundation tipping leads to a favorable reduction in the maximum transverse deformation. As it was pointed out, however, in a discussion of Meek's paper made by Sexton[16], this reduction does not necessarily happen for all excitations.

For the case of a structure supported by a sufficiently flexible foundation, the deformability of the ground affects the behavior of the superstructure and cannot be neglected. The importance of this dynamic coupling between the structure and the foundation (soil-structure interaction) to the dynamic response of the system has been realized in recent years and has attracted attention from many investigators (e.g., see references 17-24). These studies, however, do not take under consideration the possibility of partial lift-off, which is present for very strong ground motions. Efforts have been directed lately toward this subject, trying to understand the phenomenon and its effects on the seismic response of the structures (see references 26-38).

Although very little analytical work has been done on this problem, some experimental work and some studies on the computer have been

performed. First, in 1960, Muto and his associates[25], in an effort to examine the possibilities of overturning of a single mass vibrating on a rigid or flexible foundation, conducted experiments on the rocking of such a structure under earthquake excitation.

The effect of partial lift-off of a multistory building was first examined during experiments performed at the University of California, Berkeley by Huckelbridge and Clough.[26-30] They did shaking table tests on steel frame models of buildings and concluded that allowing the structure to lift-off may result in reduced requirements for the strength and ductility of the frame. The fact that uplift may markedly change the behavior of the system was also pointed out by Morris,[31] who performed experiments on the earthquake response of a rigid tower using a centrifuge. During these tests, the soil under the tower was able to deform and the tower was allowed to lift-off.

Priestley and his associates[32,33] proposed a simplified trial and error method of predicting the maximum displacement of rocking for a single-degree-of-freedom superstructure by use of displacement response spectra. An extension of Housner's analysis for the rocking block on a rigid foundation[1] was developed to establish an equivalent elastic representation of the rocking system. This method is approximate and does not take into account the elastic characteristics of the superstructure except in its initial stage. A more refined technique using time-history analysis was proposed in reference 33. Both methods were verified by experimental shaking table results for simple models.

A study of the effects of lift-off on the seismic behavior of structures using finite element techniques was done by Wolf[34,35]

and Wolf and Skrikerud[36]. Although these analyses were made for the case of a nuclear reactor, the results can be extended to other structures. They concluded that allowing the structure to lift-off leads to a reduction of the total horizontal acceleration, the overturning moment and the lateral displacement within the structure, in comparison to the results of the standard soil-structure interaction theory in which lift-off is not allowed. Because of the resulting beneficial reduction in the strength requirements of the structure, they concluded that there is no need to prevent lift-off but, on the contrary, it is desirable to permit it. Similar results were obtained by Singh[37] who used a computer model to analyze a six-story split K-braced frame with foundation conditions allowing lift-off. A technique to handle the nonlinear effect of uplift in numerical studies was also presented by Bervig and Chen[38].

In this thesis, we present an analytical investigation of the effects of lift-off on the dynamic behavior of structures, along with simplified methods of analysis which permit the designer to take these effects under consideration. First the case of a rigid superstructure is examined and then a multistory building is considered. The foundation is elastic, with damping, and two different cases are studied: the Winkler model, commonly used in soil mechanics, and the simplified two-spring foundation in which the structure is supported by only two springs (in a two-dimensional representation). It is assumed that the springs cannot take tension, therefore, lift-off happens when the upward displacement of a portion of the base is greater than the static deflection.

The coefficients of the foundation models are assumed constant, independent of amplitude or frequency. It has been proven (e.g., see reference 39) that a representation of the elastic half-space by springs and dashpots implies frequency dependent coefficients. However, it seems permissible in many cases to use representative, constant values for these coefficients. Similarly, a linear model for the soil is used for simplicity, with dissipation modeled by viscous damping. The advantage of this approximate method is that it leads to differential equations of motion with constant coefficients. It should be mentioned that the determination of the appropriate foundation parameters is by no means trivial and requires a careful investigation. Since this is one of the main problems of soil-structure interaction theory, it attracted the attention of several investigators and much research has been done on this subject (for example, see references 17, 19, 21-22, 39-47).

Posing the problem in this way, two different regimes of the response can be distinguished: (i) the case of full contact, during which the base of the structure is in full contact with the foundation. In this regime, the equations of motion are linear for small displacements and the classical theory of soil-structure interaction can be applied, (ii) the case after lift-off, during which partial separation of the base from the foundation has occurred. For this case, and for the two-spring foundation, linearized equations of motion can be derived; in constrast, the equations of motion corresponding to the Winkler foundation are highly nonlinear, because of the varying degree of contact between the body and the foundation. However, even for the two-spring foundation, the overall response of the system is nonlinear because the

system continuously changes from one linear regime to the other. As a result, the principle of superposition does not hold for the overall response.

The amount of lift-off, which depends on the excitation and the parameters of the structure and the foundation, dramatically affects the response of the system. For an impulse excitation, this quantity is measured by the so-called "normalized impulse," which is denoted by β and is equal to the ratio of the maximum angle of tilting which would occur if lift-off were not allowed, divided by the angle of rotation at which uplift occurs in the absence of vertical oscillations. Impulse excitations are used extensively in this study, first because an impulse is the simplest excitation that captures some of the dynamic features of the earthquake problem, and second because it provides information for the determination of the apparent resonant frequency of the system as a function of the amount of lift-off. The word "apparent" is used, since the uplifting system does not possess resonant frequencies in the classical sense.

For the dynamic behavior of a building supported by an elastic foundation, it was shown by Jennings and Bielak[19] that the effect of the horizontal translation of the base is usually negligible in comparison to the effect of the rocking, especially for tall buildings. In this analysis, the horizontal translation is neglected and the assumption that no slipping is permitted between the base and the foundation is employed. It should be mentioned that these assumptions may not be applicable for very short structures, for which the horizontal movement might be significant. Such structures, however, are not the main concern

in this thesis; the principal emphasis is on more slender structures.

In Chapter II, the dynamics of a rigid block supported by an elastic foundation are examined. No dissipation of energy is considered. This simple case, apart from its usefulness because some structures can be represented this way, aids the understanding of the phenomenon of lift-off for flexible structures. It is shown in this chapter that the simple two-spring foundation can be defined in such a way that it can model the rocking response of the much more complicated Winkler foundation. Although many results employ an impulse excitation, they can be extended to apply for other, more complex excitations.

In Chapter III, three different energy dissipative mechanisms are introduced into the foundation models of Chapter II and they are examined individually. The superstructure is again a rigid block. These mechanisms model the energy dissipation in the foundation, wich results from inelastic behavior of the soil and/or radiation of energy in the form of stress waves. An equivalence between the Winkler and the two-spring model is also established in this case.

The effect of lift-off on the dynamic response of a flexible superstructure is investigated in Chapter IV. The cases of a simple shear oscillator and a more general model of a multistory building are considered. In the latter case, it is assumed that the building possesses classical normal modes. Although the analysis is restricted to the two-spring foundation, the results can be extended to the Winkler model, and hence to practical problems, by use of the equivalence defined in Chapter III. It is shown that a small amount of lift-off may dramatically affect the behavior of the structure, compared to the

response without uplift. An approximate method of analysis, which allows the use of response spectra for the calculation of the maximum deformation, is also proposed in this chapter.

A summary of the results obtained in this thesis is presented in Chapter V, along with conclusions and recommendations for future study.

CHAPTER II

DYNAMICS OF A RIGID BLOCK

2.1. INTRODUCTION

The dynamics of a rigid block rocking on a rigid foundation were first studied by Housner,[1] and a review of this work is given in section 2.2. In section 2.3 an analysis is made of a block supported symmetrically by two elastic springs. The springs are not permitted to take tensile forces and thus, separation of the block from one of the springs may occur for strong excitations. This simple system illustrates many of the important features of the dynamics of elastically supported tipping structures. A more realistic model for the foundation is examined in Section 2.4, where the block is supported by an elastic foundation, modeled by continuous elastic springs (the familiar Winkler model). Lift-off of the block from the base, with the amount of separation of the base from the foundation dependent on the rotation and displacement of the block, can occur in this case, too.

The equations of motion for the "two-spring" case can be linearized and closed-form expressions for the motion of the block are presented. In contrast, the Winkler foundation leads to complicated nonlinear equations because of the varying amount of contact at the foundation. In Section 2.5, an equivalence between the two models is established so that for many engineering purposes, one can use the equivalent "two-spring" model to approximate the effects of a continuous elastic foundation.

2.2. RIGID BLOCK ON RIGID FOUNDATION

George W. Housner[1] was the first to analyze the dynamic response of a rigid block rocking on a rigid foundation. This work was motivated by the response of inverted pendulum-type structures during the Chilean earthquake of 1960. A review of Housner's analysis is presented here.

The block shown in Fig. 2.2.1 will vibrate about the poles of rotation O and O´ when it is set to rocking; it is assumed that the block cannot slip horizontally. Let a and b be the width and height of the block respectively, m its mass and I_0 the moment of inertia about the points O and O´. If ϕ is the angle of tilting of the block, measured from the vertical, the equation of free vibrations is

$$I_0\ddot{\phi} + mgr \sin(\theta-\phi) = 0 \qquad (2.2.1)$$

where $r = \frac{1}{2}\sqrt{a^2 + b^2}$, $\theta = \tan^{-1}\left(\frac{a}{b}\right)$ and g is the acceleration of gravity. For small vibrations of tall, slender blocks, having the angles θ and ϕ less than about 20°, small angle approximations permit this equation to be written as

$$I_0\ddot{\phi} - mgr\,\phi = - mgr\,\theta \qquad (2.2.2)$$

Assuming initial conditions $\phi = \phi_0 < \theta$ and $\dot{\phi} = 0$ at $t = 0$, which represent the block released from rest with initial displacement ϕ_0, equation (2.2.2) has the solution:

$$\phi(t) = \theta - (\theta - \phi_0) \cosh pt \qquad (2.2.3)$$

where $p^2 = mgr/I_0$ and $0 \leq \phi \leq \phi_0$.

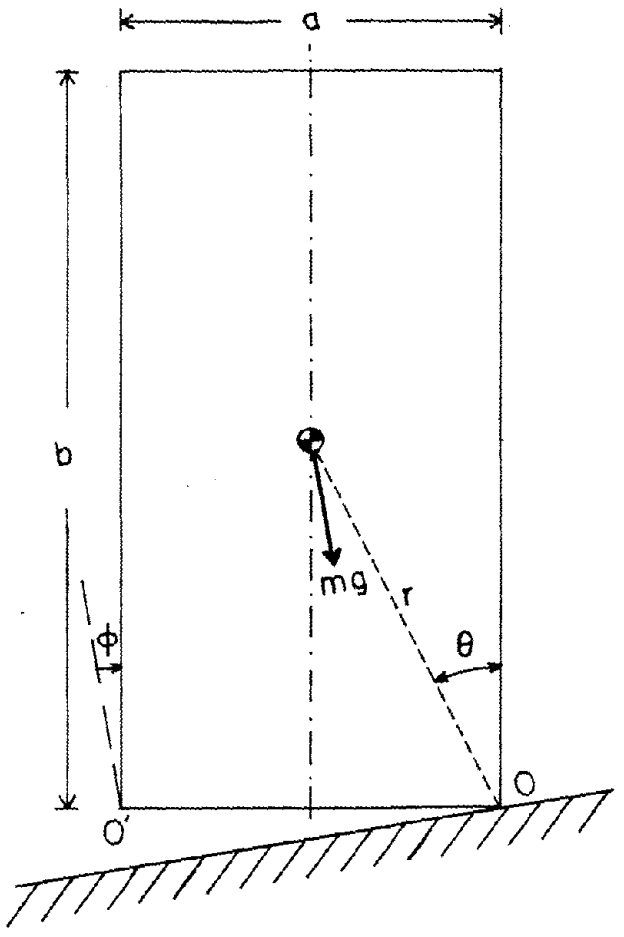

Fig. 2.2.1. Rocking block on rigid foundation.

Equation (2.2.3) describes the rotation of the block about the point O as it falls back to the vertical position. If there is negligible energy loss during impact, the block will rotate about the point O′ to an angle $\phi = -\phi_0$ and then back to the vertical position, etc. Thus, the motion is periodic and the time required for the block to fall from $\phi = \phi_0$ to $\phi = 0$ equals one quarter of the period. For $\phi = 0$ and $t = \frac{T}{4}$ equation (2.2.3) gives

$$T = 4\sqrt{\frac{I_0}{mgr}}\ \cosh^{-1}\left(\frac{1}{1 - \frac{\phi_0}{\theta}}\right) \qquad (2.2.4)$$

T being the period of the vibrations. A graph of this equation is shown in Figure 2.2.2, where it is seen that the period is strongly dependent on the amplitude. The period is long for ϕ_0 close to θ and short for ϕ_0 close to zero.

During the rocking, however, there will be dissipation of energy every time the block hits the base and changes its pole of rotation. If the impact is assumed to be inelastic, the rotation continues smoothly about the opposite pole. Let $\dot{\phi}_1$ and $\dot{\phi}_2$ be the angular velocities of the block before and after impact, respectively, and assume that the pole of rotation before impact is O. Equating the moment of momentum about O′ immediately before and after the impact, Housner found the following relation:

$$I_0\dot{\phi}_1 - mra\,\dot{\phi}_1 \sin\theta = I_0\dot{\phi}_2 \qquad (2.2.5)$$

The reduction of kinetic energy during impact is

$$Q = \left(\frac{1}{2} I_0\dot{\phi}_2^{\,2}\right) \Big/ \left(\frac{1}{2} I_0\dot{\phi}_1^{\,2}\right) = \left(\frac{\dot{\phi}_2}{\dot{\phi}_1}\right)^2$$

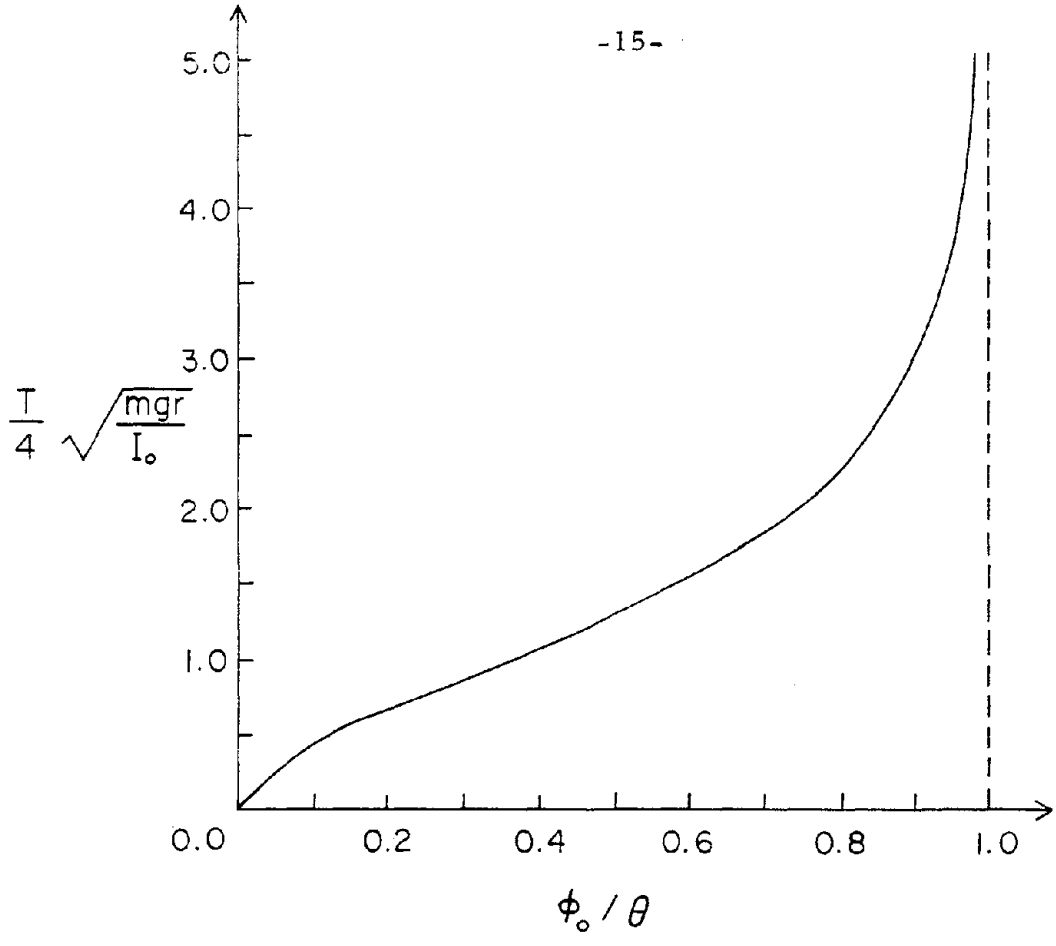

Fig. 2.2.2. Period of block rocking with amplitude ϕ_0(after Housner, 1963).

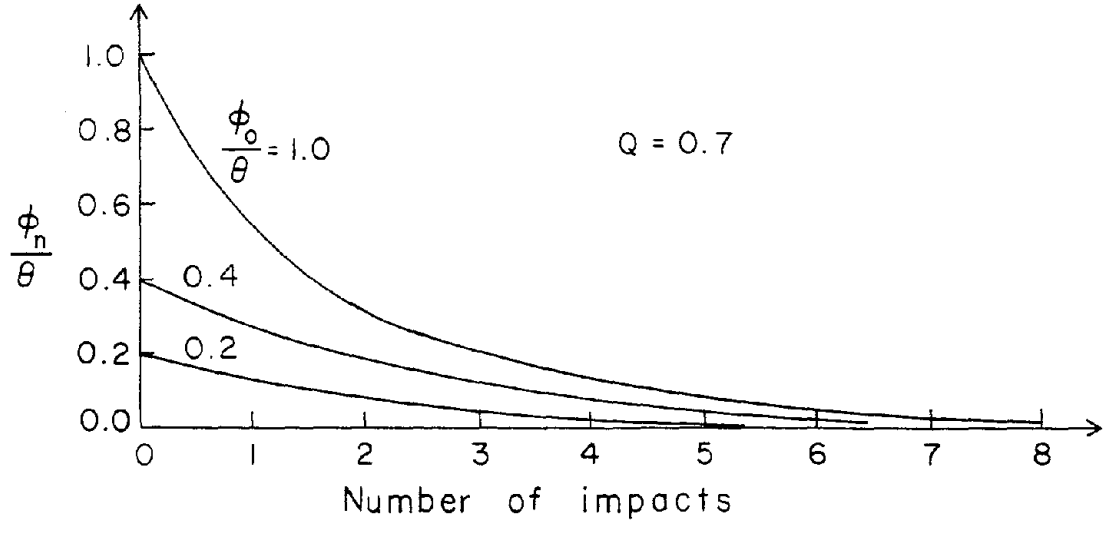

Fig. 2.2.3. Amplitude ϕ_n/θ subsequent to n^{th} impact (after Housner, 1963).

which, because of equation (2.2.5), reduces to

$$Q = \left[1 - \frac{mr^2}{I_0}\left(1 - \cos 2\theta\right)\right]^2$$

For slender blocks this relation may be written as

$$\sqrt{Q} = 1 - \frac{2mr^2\theta^2}{I_0} \qquad (2.2.6)$$

Thus, the fractional reduction of the kinetic energy depends only on the parameters of the block and not on the initial conditions.

Using the expression for the response as given by equation (2.2.3) and recalling that $\dot{\phi}_2 = \sqrt{Q}\,\dot{\phi}_1$, Housner found that the amplitude of the response, following the n^{th} impact is given by the following expression:

$$\frac{\phi_n}{\theta} = 1 - \sqrt{1 - Q^n\left[1 - \left(1 - \frac{\phi_0}{\theta}\right)^2\right]} \qquad (2.2.7)$$

A graph of this equation for Q = 0.7 is presented in Fig. 2.2.3, where the decrease in amplitude for successive n is shown for several values of the intial displacement. The successive half periods of vibration during free rocking are given by

$$\frac{T}{2} = 2\sqrt{\frac{I_0}{mgr}}\,\tanh^{-1}\sqrt{Q^n\left[1 - \left(1 - \frac{\phi_0}{\theta}\right)^2\right]} \qquad (2.2.8)$$

According to the foregoing results, the amplitude of the oscillations decreases significantly with each impact, especially for large initial displacements. As the number of the oscillations increases, however, the frequency of vibrations increases indefinitely. Since the

conditions at impact assumed in this analysis are idealized, the limiting behavior of real blocks is somewhat different. As can easily be confirmed by a simple desk-top experiment, a freely rocking block will show an increasing frequency as the amplitude decreases, but will come to rest rather quickly. The number of impacts is about six to ten for most cases, with more for slender blocks.

2.3. TWO-SPRING FOUNDATION

2.3.1. System Considered and Assumptions

As the next step in complexity, let us assume that the foundation is no longer rigid, but deformable. The simplest case, where the block is supported by two elastic springs will be examined here. Figure 2.3.1.a shows the three dimensional configuration for ground motion in the x and y-directions. The springs are placed symmetrically in the z-direction, a distance ξ from the central line MM´ of the base, and k_1 is the stiffness per unit length. The dynamic problem is reducible to the two-dimensional configuration shown in Figure 2.3.1.b. The stiffness of the springs is now $k = k_1 \cdot d$, where d is the depth of the block.

It is assumed that there is no slipping between the block and the foundation, therefore the system possesses only two degrees of freedom: vertical motion, denoted by the vertical displacement, y, of the center of mass measured from the position at rest, and rotation, measured by the angle of tilting, ϕ, from the vertical.

In order to model the inability of soil to carry tensile stresses, it is assumed that the block is just resting on the springs, without any bond between them and the block. In this way, whenever the upward

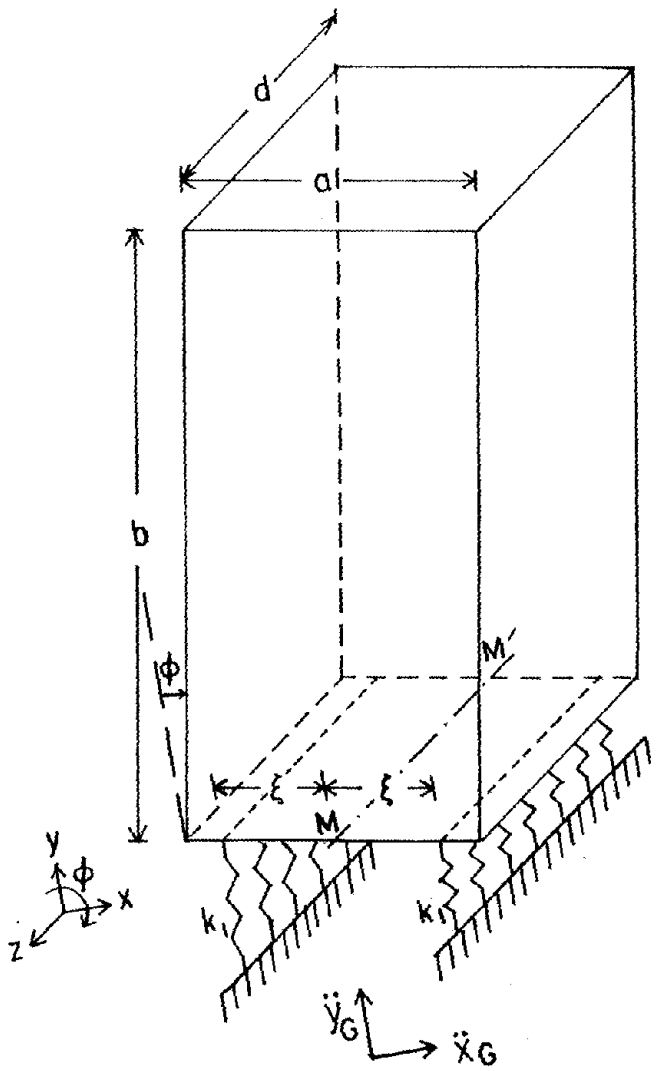

(a) Three-dimensional case

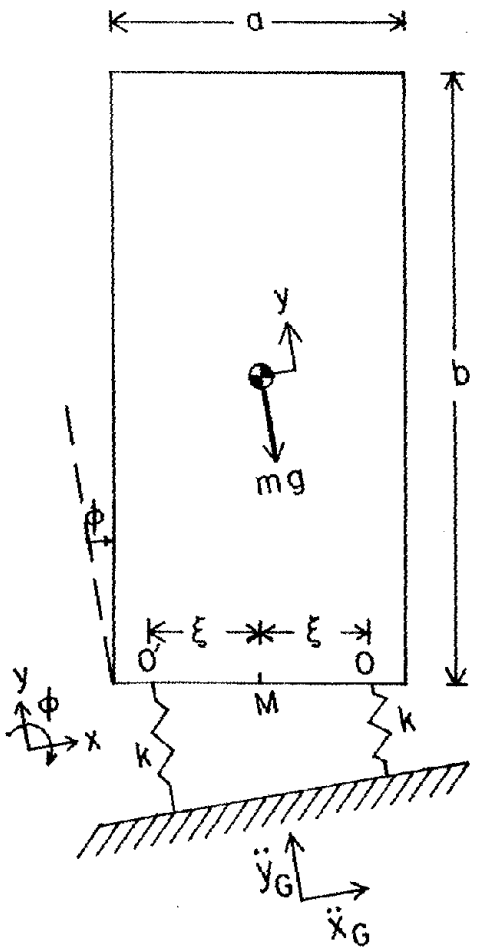

(b) Equivalent two-dimensional problem

Fig. 2.3.1. Tipping block on a "two-spring" foundation.

displacement of point O or O′ is greater than the static deflection, the block will separate from one of the springs. It should be mentioned here that complete separation of the block from both springs is possible for sufficiently strong excitations. However, this represents a special case, generally encountered for short blocks, stiff springs and extremely strong excitation, as will be shown in Section 2.3.6.

2.3.2. Equations of Motion

The equations of motion will be derived by use of Newton's second law of motion. The two cases, before and after lift-off, will be treated separately. A free body diagram for the case of full-contact is shown in Figure 2.3.2. After lift-off, the picture is similar, except that F_2, which is due to the left spring, vanishes. The ground accelerations, $\ddot{x}_G$ and $\ddot{y}_G$, are assumed to act horizontally and vertically, respectively, and, by D'Alembert's principle, can be represented by forces $-m\ddot{x}_G$ and $-m\ddot{y}_G$ applied at the center of mass of the block. Since the horizontal displacement of the block is prevented at the base, a horizontal force R_A, positive as shown, acts between the block and the foundation. We will assume that this force is acting at the right corner of the base (for positive angles of tilting). In any case, changes in the point of application of R_A along the base of the block introduce only second order changes in the equations of motion.

Let x and y be the horizontal and vertical displacements of the center of mass respectively, measured from the position of static equilibrium, and ϕ be the angle of tilting, measured from the vertical. Assuming that the corner A can move vertically, we can express x in terms of ϕ (see Fig. 2.3.3) as

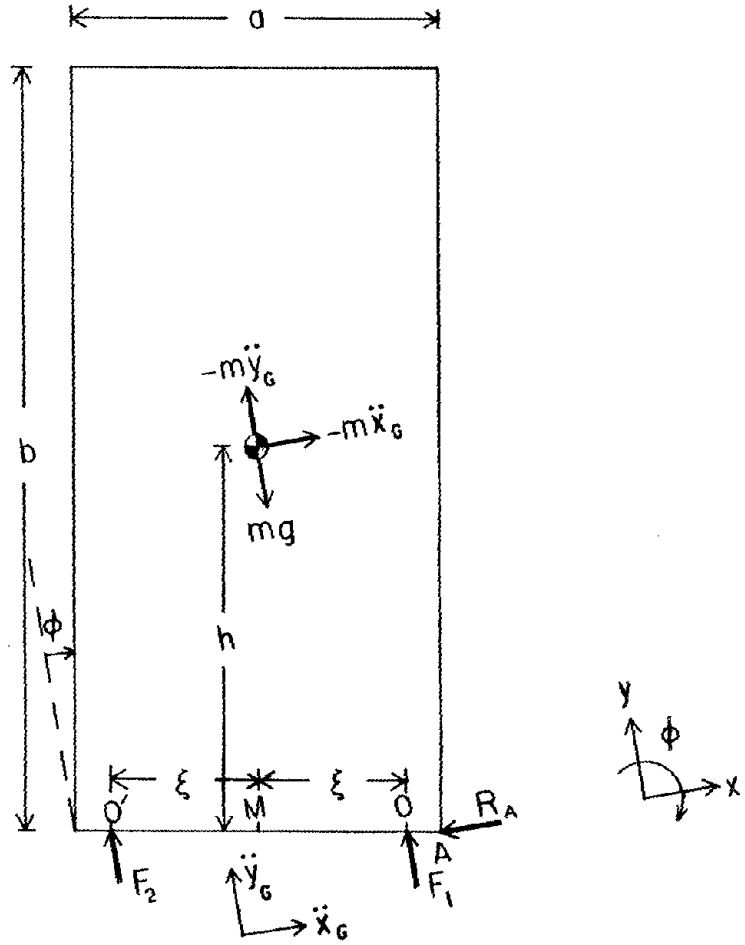

Fig. 2.3.2 Free body diagram (full contact).

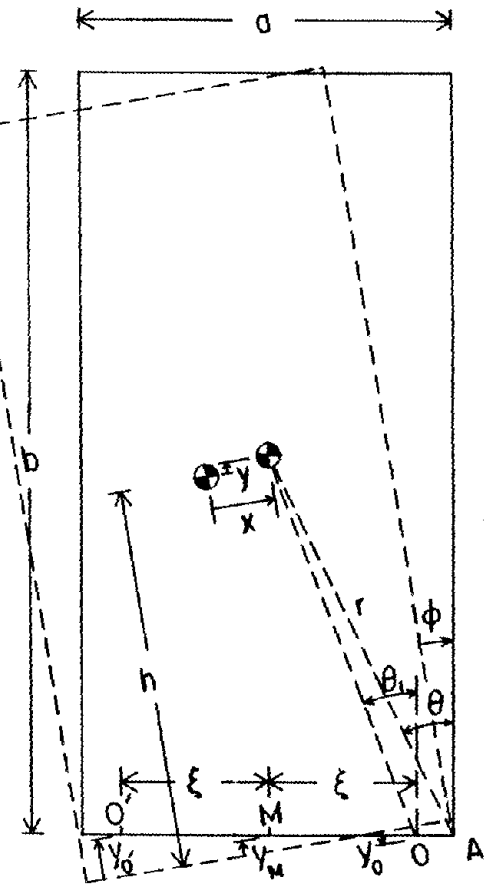

Fig. 2.3.3. Geometry of rocking block.

$$x = r \sin\theta - r \sin(\theta-\phi)$$

where $r = \sqrt{h^2 + \left(\frac{a}{2}\right)^2}$ and $\theta = \tan^{-1}\left(\frac{a}{2h}\right)$. Using the geometric relations $a = 2r \sin\theta$ and $h = r \cos\theta$, the above equation results to

$$x = \frac{a}{2} - \frac{a}{2}\cos\phi + h \sin\phi \qquad (2.3.1)$$

Let δ be the static deflection, given by

$$\delta = \frac{mg}{2k} \qquad (2.3.2)$$

and y_0 and y_0' the vertical displacements of points 0 and 0' respectively. From Fig. 2.3.3 we get

$$\left.\begin{aligned} y_0 &= y_M - \xi \sin\phi \\ y_0' &= y_M + \xi \sin\phi \end{aligned}\right\} \qquad (2.3.3)$$

where y_M is the vertical displacement of the middle point of the base, M, and can be expressed in terms of y and ϕ by the equation

$$y_M = y + h(1 - \cos\phi) \qquad (2.3.4)$$

Then, for positive angles of rotation, the spring forces, F_1 and F_2, acting on the block, are

$$F_1 = \frac{1}{2} mg - ky - kh(1 - \cos\phi) + k\xi \sin\phi \qquad (2.3.5)$$

$$F_2 = \begin{cases} \frac{1}{2} mg - ky - kh(1 - \cos\phi) - k\xi \sin\phi, & \text{before lift-off} \\ 0, & \text{after lift-off} \end{cases} \qquad (2.3.6)$$

The horizontal force, R_A, can be determined by applying Newton's second law in the x-direction, which gives

$$R_A = -m\ddot{x}_G - m\ddot{x} \tag{2.3.7}$$

in which x is given by (2.3.1).

The two equations of motion, in the rocking and vertical directions, then, are

Full contact

$$m\ddot{y} + 2ky + 2kh(1 - \cos\phi) = -m\ddot{y}_G \tag{2.3.8}$$

$$I_{CM}\ddot{\phi} - \left[\frac{1}{2}mg - ky - kh(1-\cos\phi) - k\xi\sin\phi\right]\left[r\sin(\theta+\phi) - \left(\frac{a}{2} - \xi\right)\cos\phi\right]$$
$$+ \left[\frac{1}{2}mg - ky - kh(1-\cos\phi) + k\xi\sin\phi\right]\left[r\sin(\theta-\phi) - \left(\frac{a}{2} - \xi\right)\cos\phi\right]$$
$$+ (m\ddot{x} + m\ddot{x}_G)\, r\cos(\theta-\phi) = 0 \tag{2.3.9}$$

After lift-off

$$m\ddot{y} + ky + kh(1 - \cos\phi) - k\xi\sin\phi = -\frac{1}{2}mg - m\ddot{y}_G \tag{2.3.10}$$

$$I_{CM}\ddot{\phi} + \left[\frac{1}{2}mg - ky - kh(1-\cos\phi) + k\xi\sin\phi\right]\left[r\sin(\theta-\phi) - \left(\frac{a}{2} - \xi\right)\cos\phi\right]$$
$$+ (m\ddot{x} + m\ddot{x}_G)\, r\cos(\theta-\phi) = 0 \tag{2.3.11}$$

where I_{CM} is the moment of inertia of the block about the center of mass.

These equations are valid only for positive angles of rotation. For tilting in the opposite direction, the equations of motion can be rederived, or they can be found by changing the system of coordinates. For the second approach, the y-axis remains the same, but the x-axis is

reversed and ϕ is taken positive counterclockwise. In the new system, $\ddot{x}_G$ will be negative, but otherwise, equations (2.3.10) and (2.3.11) apply as they are.

2.3.3. A Limiting Case: $k \to \infty$, $\xi \to \frac{a}{2}$

When the foundation springs are very stiff, the block is expected to behave as if it were rocking on a rigid foundation. In the limiting case, therefore, as $k \to \infty$ and $\xi \to \frac{a}{2}$, equations (2.3.10) and (2.3.11), which describe the motion after lift-off, should reduce to equation (2.2.1), which Housner derived for the rocking block on a rigid foundation. Let us assume that ϕ is positive and $\ddot{x}_G = \ddot{y}_G = 0$. Then, for $\xi = \frac{a}{2}$, equations (2.3.10) and (2.3.11) reduce to:

$$m\ddot{y} + ky + kh(1 - \cos\phi) - \frac{1}{2} ka \sin\phi = -\frac{1}{2} mg$$

and

$$I_{CM}\ddot{\phi} + \left[\frac{1}{2}mg - ky - kh(1 - \cos\phi) + \frac{1}{2}ka \sin\phi\right] r \sin(\theta-\phi) + m\ddot{x}\, r \cos(\theta-\phi) = 0$$

Substituting from the first equation into the term in brackets in the second equation yields

$$I_{CM}\ddot{\phi} + (m\ddot{y} + mg)\, r \sin(\theta-\phi) + m\ddot{x}\, r \cos(\theta-\phi) = 0 \qquad (2.3.12)$$

For $k \to \infty$, the vertical displacement of point 0 goes to zero, and thus,

$$y_M = \frac{a}{2} \sin\phi$$

Equation (2.3.4), then, gives

$$y = \frac{a}{2} \sin\phi - h(1 - \cos\phi)$$

Substituting this equation into (2.3.12) and using expression (2.3.1) finally produces

$$\left(I_{CM} + mr^2\right)\ddot{\phi} + mgr \sin(\theta-\phi) = 0 \qquad (2.3.13)$$

Since $I_{CM} + mr^2 = I_0$, the moment of inertia about point O (for $\xi = \frac{a}{2}$), equation (2.3.13) is the same as equation (2.2.1).

2.3.4. Linearized Equations of Motion

If the displacements are expected to be small, the equations of motion can be greatly simplified. First, for small angles of rotation, sin ϕ can be replaced by ϕ and cos ϕ by 1. Equations (2.3.1), (2.3.3) and (2.3.4), then, reduce to:

$$\left.\begin{aligned} x &= h\phi \\ y_0 &= y - \xi\phi \\ y_0' &= y + \xi\phi \end{aligned}\right\} \qquad (2.3.14)$$

After these simplifications and elimination of the non-linear terms, the following linearized equations of motion can be obtained from equations (2.3.8), (2.3.9), (2.3.10) and (2.3.11):

Full contact

$$m\ddot{y} + 2ky = -m\ddot{y}_G \qquad (2.3.15)$$

$$I_M\ddot{\phi} + (2k\xi^2 - mgh)\phi = -mh\ddot{x}_G \qquad (2.3.16)$$

After lift-off

$$m\ddot{y} + ky \mp k\xi\phi = -\frac{1}{2}mg - m\ddot{y}_G \qquad (2.3.17)$$

$$I_M\ddot{\phi} + \frac{1}{2}\left(2k\xi^2 - mgh\right)\phi \mp k\xi y = -mh\ddot{x}_G \mp \frac{1}{2}mg\xi \tag{2.3.18}$$

where I_M is the moment of inertia about the midpoint of the base, M, given by

$$I_M = I_{CM} + mh^2$$

Whenever a double sign appears in the above equations, the upper one corresponds to the block tilting to the right and the lower one to the left. In both cases, the positive directions of the angles and displacements are as shown in Figs. 2.3.2 and 2.3.3.

The nonlinear terms that were omitted are in the forms $\ddot{\phi}\phi$, $y\phi$ and ϕ^2. Also, the term $\frac{1}{2}ma\ddot{x}_G\phi$, which comes from the assumption that R_A acts at the corner of the base, was dropped for simplicity in the derivation of equations (2.3.16) and (2.3.18). For $|\ddot{x}_G| < g$ and $h > \frac{a}{2}$, this term is always smaller than the term $mgh\phi$ and, for values of the spring constant expected in earthquake engineering applications, is much smaller than the term $k\xi^2\phi$.

The rocking of a block on a two-spring foundation for small displacements consists, therefore, of a sequence of linear problems. Assuming that the block is initially at rest, it starts vibrating according to equations (2.3.15) and (2.3.16). If the excitation is strong enough, lift-off occurs and equations (2.3.17) and (2.3.18) are the governing equations of motion from uplift until contact is re-established. The displacements and velocities at the time of lift-off are used as initial conditions for the latter equations, etc. Continuing in this way, one can calculate the sequentially linear response, which, however, shows

nonlinear characteristics overall; for example, the period is amplitude dependent and the principle of superposition does not hold.

Equation (2.3.15) implies that for horizontal excitation, the vertical motion of the system is not excited initially. However, since equations (2.3.17) and (2.3.18) are coupled, the vertical motion is excited after lift-off happens. When the block comes back and gains contact with both springs again, it will, in general, continue to oscillate in both the rocking and the vertical modes. Typically, therefore, the only case in which the block is not moving vertically, is before the first lift-off under horizontal excitation only.

Another interesting point, which comes from equation (2.3.16), is that the value of $(2k\xi^2 - mgh)$ may be negative for very soft springs. In that case, equation (2.3.16) has a hyperbolic solution. Using equation (2.3.2), the condition for this to happen may be expressed as

$$\delta > \frac{\xi^2}{h} \tag{2.3.19}$$

But, $\frac{\xi}{h} = \tan \theta_1$ (see Fig. 2.3.3), and for slender structures, inequality (2.3.19) reduces to

$$\delta > \xi\theta_1 \tag{2.3.20}$$

By definition, lift-off occurs when the vertical displacement of point O' becomes equal to the static deflection, δ. Using equations (2.3.14), we find that the angle ϕ_{cr}, at which uplift occurs for a horizontal excitation for the first time, can be given by

$$\phi_{cr} = \frac{\delta}{\xi} \tag{2.3.21}$$

Comparing (2.3.20) and (2.3.21) we conclude that, in the case under consideration, the required angle of rotation for lift-off is bigger than θ_1, which means that overturning of the block occurs before lift-off; that is, the system is statically unstable and buckles elastically before lift-off. For this situation to occur requires extremely soft springs and is unlikely to be encountered in applications. It is therefore excluded from further consideration.

Solution of the Equations of Motion

In the case of full contact, the two equations of motion are uncoupled and their solution can be written as,

$$y(t) = y(0)\cos p_2 t + \frac{\dot{y}(0)}{p_2}\sin p_2 t - \frac{1}{p_2}\int_0^t \ddot{y}_G(\tau)\sin p_2(t-\tau)d\tau \tag{2.3.22}$$

$$h\phi(t) = h\phi(0)\cos p_1 t + \frac{h\dot{\phi}(0)}{p_1}\sin p_1 t - \frac{mh^2}{I_M p_1}\int_0^t \ddot{x}_G(\tau)\sin p_1(t-\tau)d\tau \tag{2.3.23}$$

where,

$$p_1^2 = \frac{2k\xi^2 - mgh}{I_M} \tag{2.3.24}$$

and

$$p_2^2 = \frac{2k}{m} \tag{2.3.25}$$

Recall that $h\phi$ gives the horizontal displacement of the center of mass of the block.

After lift-off, the equations of motion are coupled; however, they can be solved exactly by a number of techniques. In the following pages, a solution of these equations via the Laplace transform will be given.

For simplicity, let us consider that ϕ is positive and keep only the upper sign in equations (2.3.17) and (2.3.18). For ϕ negative, a similar analysis can be carried out. Using relations (2.3.24) and (2.3.25) the equations of motion are

$$\ddot{y} + \frac{1}{2} p_2^2 y - \frac{1}{2} p_2^2 \frac{\xi}{h} (h\phi) = -\frac{1}{2} g - \ddot{y}_G$$

$$(h\ddot{\phi}) + \frac{1}{2} p_1^2 (h\phi) - \frac{kh\xi}{I_M} y = -\frac{mh^2}{I_M} \ddot{x}_G - \frac{mgh\xi}{2I_M}$$

Making the transformation: $x = h\phi$, and taking the Laplace transform of the above equations produces,

$$s^2\bar{y} - sy(0) - \dot{y}(0) + \frac{p_2^2}{2} \bar{y} - \frac{p_2^2 \xi}{2h} \bar{x} = -\frac{g}{2s} - \bar{\ddot{y}}_G \tag{2.3.26}$$

$$s^2\bar{x} - sx(0) - \dot{x}(0) + \frac{p_1^2}{2} \bar{x} - \frac{kh\xi}{I_M} \bar{y} = -\frac{mh^2}{I_M} \bar{\ddot{x}}_G - \frac{mgh\xi}{2I_M s} \tag{2.3.27}$$

where s is the Laplace variable and a bar over a function indicates the Laplace transform. The initial conditions in the above equations are assumed to be the displacements and velocities at the time of lift-off. The solution of the system of equations (2.3.26) and (2.3.27) can be written in the form

$$\bar{y}(s) = \frac{\begin{vmatrix} -\bar{\ddot{y}}_G - \frac{g}{2s} + sy(0) + \dot{y}(0) & -\frac{p_2^2 \xi}{2h} \\ -\frac{mh^2}{I_M} \bar{\ddot{x}}_G - \frac{mgh\xi}{2I_M s} + sx(0) + x(0) & s^2 + \frac{p_1^2}{2} \end{vmatrix}}{\Delta(s)} \tag{2.3.28}$$

$$\bar{x}(s) = \frac{\begin{vmatrix} s^2 + \frac{p_2^2}{2} & -\bar{\ddot{y}}_G - \frac{g}{2s} + sy(0) + \dot{y}(0) \\ -\frac{kh\xi}{I_M} & -\frac{mh^2}{I_M}\bar{\ddot{x}}_G - \frac{mgh\xi}{2I_M s} + sx(0) + \dot{x}(0) \end{vmatrix}}{\Delta(s)} \tag{2.3.29}$$

in which,

$$\Delta(s) = \begin{vmatrix} s^2 + \frac{p_2^2}{2} & -\frac{p_2^2\xi}{2h} \\ -\frac{kh\xi}{I_M} & s^2 + \frac{p_1^2}{2} \end{vmatrix} \tag{2.3.30}$$

The zeros of the function $\Delta(s)$ are poles for the functions $\bar{y}(s)$ and $\bar{x}(s)$ ($s = 0$ is another pole) and will be used for the inversion of the Laplace transform. Using equations (2.3.24) and (2.3.25) we find that the zeros of (2.3.30) are given by the roots of the equation:

$$s^4 + \frac{1}{2}\left(p_1^2 + p_2^2\right)s^2 - \frac{kgh}{2I_M} = 0 \tag{2.3.31}$$

This is the characteristic equation for the system. A real root of this equation corresponds to a hyperbolic type of response and an imaginary root to a harmonic response. Let

$$P_1 = \frac{1}{2}\sqrt{-(p_1^2 + p_2^2) + \sqrt{(p_1^2 + p_2^2)^2 + 8\frac{kgh}{I_M}}} \tag{2.3.32}$$

$$P_2 = \frac{1}{2}\sqrt{(p_1^2 + p_2^2) + \sqrt{(p_1^2 + p_2^2)^2 + 8\frac{kgh}{I_M}}} \tag{2.3.33}$$

Then the four roots of equation (2.3.31) can be written as

$$s = \pm P_1 \quad \text{and} \quad s = \pm iP_2 \tag{2.3.34}$$

From expressions (2.3.28) and (2.3.29) we get

$$\left.\begin{aligned}
\bar{y}(s) &= \frac{Y_y(s)}{\Delta(s)} + \frac{Y_x(s)}{\Delta(s)} + \frac{Y_p(s)}{s\Delta(s)} + \frac{Y_{xG}(s)}{\Delta(s)}\,\bar{\ddot{x}}_G(s) + \frac{Y_{yG}}{\Delta(s)}\,\bar{\ddot{y}}_G(s) \\
\bar{x}(s) &= \frac{X_y(s)}{\Delta(s)} + \frac{X_x(s)}{\Delta(s)} + \frac{X_p(s)}{s\Delta(s)} + \frac{X_{xG}(s)}{\Delta(s)}\,\bar{\ddot{x}}_G(s) + \frac{X_{yG}}{\Delta(s)}\,\bar{\ddot{y}}_G(s)
\end{aligned}\right\} \tag{2.3.35}$$

wherein

$$\left.\begin{aligned}
Y_y(s) &= \left(s^2 + \frac{p_1^2}{2}\right)[sy(0) + \dot{y}(0)] \\
Y_x(s) &= \frac{p_2^2\xi}{2h}[sx(0) + \dot{x}(0)] \\
Y_p(s) &= -\frac{g}{2}\left(s^2 + \frac{p_1^2}{2} + \frac{mp_2^2\xi^2}{2I_M}\right) \\
Y_{xG}(s) &= -\frac{kh\xi}{I_M}, \quad Y_{yG}(s) = -\left(s^2 + \frac{p_1^2}{2}\right) \\
X_y(s) &= \frac{kh\xi}{I_M}[sy(0) + \dot{y}(0)] \\
X_x(s) &= \left(s^2 + \frac{p_2^2}{2}\right)[sx(0) + \dot{x}(0)] \\
X_p(s) &= -\frac{gh\xi}{2I_M}\left[m\left(s^2 + \frac{p_2^2}{2}\right) + k\right] \\
X_{xG}(s) &= -\frac{mh^2}{I_M}\left(s^2 + \frac{p_2^2}{2}\right), \quad X_{yG}(s) = -\frac{kh\xi}{I_M}
\end{aligned}\right\} \tag{2.3.36}$$

and $\Delta(s)$ can be expressed in the form

$$\Delta(s) = \left(s^2 - P_1^2\right)\left(s^2 + P_2^2\right) \tag{2.3.37}$$

The inverse Laplace transform of equations (2.3.35) is

$$\left.\begin{aligned} y(t) &= \frac{1}{2\pi i}\int_{\Gamma}\frac{1}{\Delta}\left(Y_y + Y_x + \frac{Y_p}{s}\right)e^{st}ds + \frac{1}{2\pi i}\int_{\Gamma}\left[\frac{Y_{xG}}{\Delta}\bar{\bar{x}}_G + \frac{Y_{yG}}{\Delta}\bar{\bar{y}}_G\right]e^{st}ds \\ x(t) &= \frac{1}{2\pi i}\int_{\Gamma}\frac{1}{\Delta}\left(X_y + X_x + \frac{X_p}{s}\right)e^{st}ds + \frac{1}{2\pi i}\int_{\Gamma}\left[\frac{X_{xG}}{\Delta}\bar{\bar{x}}_G + \frac{X_{yG}}{\Delta}\bar{\bar{y}}_G\right]e^{st}ds \end{aligned}\right\} \quad (2.3.38)$$

where Γ is a suitable Bromwich contour, such that all the poles are included. Using the convolution property of the Laplace transform, the last integrals in the above expressions can be written as

$$\left.\begin{aligned} \frac{1}{2\pi i}\int_{\Gamma}\frac{Y_{xG}}{\Delta}\bar{\bar{x}}_G e^{st}ds &= \int_0^t y_{xG}(t-\tau)\ddot{x}_G(\tau)d\tau \\ \frac{1}{2\pi i}\int_{\Gamma}\frac{Y_{yG}}{\Delta}\bar{\bar{y}}_G e^{st}ds &= \int_0^t y_{yG}(t-\tau)\ddot{y}_G(\tau)d\tau \\ \frac{1}{2\pi i}\int_{\Gamma}\frac{X_{xG}}{\Delta}\bar{\bar{x}}_G e^{st}ds &= \int_0^t x_{xG}(t-\tau)\ddot{x}_G(\tau)d\tau \\ \frac{1}{2\pi i}\int_{\Gamma}\frac{X_{yG}}{\Delta}\bar{\bar{y}}_G e^{st}ds &= \int_0^t x_{yG}(t-\tau)\ddot{y}_G(\tau)d\tau \end{aligned}\right\} \quad (2.3.39)$$

where y_{xG}, y_{yG}, x_{xG}, x_{yG} are the corresponding Green's functions, given by

$$\left.\begin{aligned} y_{xG}(t) &= \frac{1}{2\pi i}\int_{\Gamma} \frac{Y_{xG}}{\Delta} e^{st} ds \\ y_{yG}(t) &= \frac{1}{2\pi i}\int_{\Gamma} \frac{Y_{yG}}{\Delta} e^{st} ds \\ x_{xG}(t) &= \frac{1}{2\pi i}\int_{\Gamma} \frac{X_{xG}}{\Delta} e^{st} ds \\ x_{yG}(t) &= \frac{1}{2\pi i}\int_{\Gamma} \frac{X_{yG}}{\Delta} e^{st} ds \end{aligned}\right\} \qquad (2.3.40)$$

Substituting expressions (2.3.36) and (2.3.37) in (2.3.38) and using (2.3.39) and (2.3.40), the following expressions for the solution are obtained by application of the residue theory at the poles $s = \pm P_1$, $s = \pm iP_2$ and $s = 0$

$$y(t) = \frac{1}{(P_1^2+P_2^2)}\left\{\left[\frac{p_2^2}{2}\xi\phi(0)+\left(\frac{p_1^2}{2}+P_1^2\right)y(0)-\frac{g}{2P_1^2}\left(\frac{p_1^2}{2}+P_1^2+\frac{k\xi^2}{I_M}\right)\right]\cosh P_1 t\right.$$
$$+\left[\frac{p_2^2}{2}\xi\dot{\phi}(0)+\left(\frac{p_1^2}{2}+P_1^2\right)\dot{y}(0)\right]\frac{\sinh P_1 t}{P_1}$$
$$-\left[\frac{p_2^2}{2}\xi\phi(0)+\left(\frac{p_1^2}{2}-P_2^2\right)y(0)+\frac{g}{2P_2^2}\left(\frac{p_1^2}{2}-P_2^2+\frac{k\xi^2}{I_M}\right)\right]\cos P_2 t$$
$$\left.-\left[\frac{p_2^2}{2}\xi\dot{\phi}(0)+\left(\frac{p_1^2}{2}-P_2^2\right)\dot{y}(0)\right]\frac{\sin P_2 t}{P_2}\right\}+\frac{2\xi^2}{h}-\frac{mg}{2k}$$
$$-\frac{kh\xi}{I_M(P_1^2+P_2^2)}\int_0^t \ddot{x}_G(\tau)\left[\frac{\sinh P_1(t-\tau)}{P_1}-\frac{\sin P_2(t-\tau)}{P_2}\right]d\tau$$
$$-\frac{1}{(P_1^2+P_2^2)}\left[\left(P_1^2+\frac{p_1^2}{2}\right)\int_0^t \ddot{y}_G(\tau)\frac{\sinh P_1(t-\tau)}{P_1}d\tau\right.$$
$$\left.+\left(P_2^2-\frac{p_1^2}{2}\right)\int_0^t \ddot{y}_G(\tau)\frac{\sin P_2(t-\tau)}{P_2}d\tau\right] \qquad (2.3.41)$$

$$x(t) = h\phi(t) = \frac{1}{(P_1^2+P_2^2)}\left\{\left[\left(\frac{p_2^2}{2}+P_1^2\right)h\phi(0)+\frac{kh\xi}{I_M}y(0)-\frac{(2k+mP_1^2)gh\xi}{2I_MP_1^2}\right]\cosh P_1 t\right.$$
$$+\left[\left(\frac{p_2^2}{2}+P_1^2\right)h\dot{\phi}(0)+\frac{kh\xi}{I_M}\dot{y}(0)\right]\frac{\sinh P_1 t}{P_1}$$
$$-\left[\left(\frac{p_2^2}{2}-P_2^2\right)h\phi(0)+\frac{kh\xi}{I_M}y(0)+\frac{(2k-mP_2^2)gh\xi}{2I_MP_2^2}\right]\cos P_2 t$$
$$\left.-\left[\left(\frac{p_2^2}{2}-P_2^2\right)h\dot{\phi}(0)+\frac{kh\xi}{I_M}\dot{y}(0)\right]\frac{\sin P_2 t}{P_2}\right\}+2\xi$$
$$-\frac{mh^2}{I_M(P_1^2+P_2^2)}\left[\left(P_1^2+\frac{p_2^2}{2}\right)\int_0^t \ddot{x}_G(\tau)\frac{\sinh P_1(t-\tau)}{P_1}d\tau\right.$$
$$\left.+\left(P_2^2-\frac{p_2^2}{2}\right)\int_0^t \ddot{x}_G(\tau)\frac{\sin P_2(t-\tau)}{P_2}d\tau\right]$$
$$-\frac{kh\xi}{I_M(P_1^2+P_2^2)}\int_0^t \ddot{y}_G(\tau)\left[\frac{\sinh P_1(t-\tau)}{P_1}-\frac{\sin P_2(t-\tau)}{P_2}\right]d\tau \qquad (2.3.42)$$

For tall slender structures, equations (2.3.32) and (2.3.33) for the characteristic frequencies after lift-off can be greatly simplified. First, using expressions (2.3.24) and (2.3.25), one can write

$$\left(p_1^2 + p_2^2\right)^2 + \frac{8kgh}{I_M} = \left(\frac{2kI_0}{mI_M} - \frac{mgh}{I_M}\right)^2 + 8\,\frac{kgh}{I_M} \qquad (2.3.43)$$

where I_0 is the moment of inertia about the points O and O', given by

$$I_0 = I_M + m\xi^2$$

For slender blocks, $m\xi^2 \ll I_M$, therefore, $I_0 \cong I_M$. Then, equation (2.3.43) reduces to

$$(p_1^2 + p_2^2) + \frac{8kgh}{I_M} \cong \left(\frac{2k}{m} - \frac{mgh}{I_M}\right)^2 + 8\frac{kgh}{I_M} = \left(\frac{2k}{m} + \frac{mgh}{I_M}\right)^2$$

Using this relation and equations (2.3.24) and (2.3.25), expressions (2.3.32) and (2.3.33) give

$$p_1^2 = \frac{mgh}{2I_M} \qquad (2.3.44)$$

$$p_2^2 = \frac{p_2^2}{2} \qquad (2.3.45)$$

2.3.5. A Further Simplification for Small Rotations

The moments of the external forces about the center of mass, which affect the rocking equation of motion of the system, can be given by the following expression, for positive angles of tilting (see Fig. 2.3.2)

$$M_{CM} = F_2(\xi + h\phi) - F_1(\xi - h\phi) + R_A(h + \frac{a}{2}\phi) \qquad (2.3.46)$$

For small angles of rotation, one can neglect the term $h\phi$ in comparison with ξ and the term $\frac{a}{2}\phi$ in comparison with h, in expression (2.3.46). Note that the second simplification was implicitly used in deriving the linearized equations of motion, since the term $\frac{a}{2}\phi$ produced a nonlinear term when multiplied by R_A. After these approximations, the equations of motion become:

Full contact

$$m\ddot{y} + 2ky = -m\ddot{y}_G \tag{2.3.47}$$

$$I_M\ddot{\phi} + 2k\xi^2\phi = -mh\ddot{x}_G \tag{2.3.48}$$

After lift-off

$$m\ddot{y} + ky \mp k\xi\phi = -\frac{1}{2}mg - m\ddot{y}_G \tag{2.3.49}$$

$$I_M\ddot{\phi} \mp k\xi y + k\xi^2\phi = -mh\ddot{x}_G \mp \frac{1}{2}mg\xi \tag{2.3.50}$$

As before, in the double signs, the upper sign corresponds to positive angles of rotation and the lower one to negative angles.

Comparison of these equations with the equations of motion derived in the previous section shows that the approximations considered here produce simplified coefficients of the ϕ-terms in the rocking equations. More precisely, the term mgh has been neglected in comparison with the term $2k\xi^2$. Note that the critical angle, ϕ_{cr}, at which lift-off happens, for a horizontal excitation, is

$$\phi_{cr} = \frac{\delta}{\xi} = \frac{mg}{2k\xi}$$

and the second critical angle, θ_1, at which overturning occurs is (see Fig. 2.3.3)

$$\theta_1 = \tan^{-1}\left(\frac{\xi}{h}\right) \cong \frac{\xi}{h}$$

for tall structures. Then, writing

$$\alpha = \frac{\phi_{cr}}{\theta_1} \tag{2.3.51}$$

one observes that the ratio $\frac{mgh}{2k\xi^2}$ is equal to α. The approximation considered in this seciton, therefore, is acceptable if the critical ratio, α, is negligible in comparison to unity. This assumption is believed to be generally valid for applications, except for the case of extremely soft springs.

The notation of equations (2.3.24) and (2.3.25) reduces to

$$p_1^2 = \frac{2k\xi^2}{I_M} \tag{2.3.52}$$

$$p_2^2 = \frac{2k}{m} \tag{2.3.53}$$

and the solution during full contact is given by equations (2.3.22) and (2.3.23).

For simplicity, the solution after lift-off will be developed for positive angles of rotation only. The case of $\phi < 0$ proceeds similarly. It is convenient to introduce the transformation

$$Y = \xi\phi - y \tag{2.3.54}$$

where Y is the vertical displacement of point 0, measured from the

position at rest and being positive downwards (see Fig. 2.3.3). Substituting in equations (2.3.49) and (2.3.50) and eliminating y, finally reduces to

$$\ddot{Y} + \frac{p_2^2 I_0}{2I_M} Y = -\frac{mh\xi}{I_M}\ddot{x}_G + \ddot{y}_G + g\left(1 - \frac{I_0}{2I_M}\right) \qquad (2.3.55)$$

$$I_0\ddot{\phi} = m\xi\ddot{Y} - mh\ddot{x}_G - m\xi\ddot{y}_G - mg\xi \qquad (2.3.56)$$

The solution of equation (2.3.55) can be written as

$$Y(t) = \left[Y(0) - \delta\left(\frac{2I_M}{I_0} - 1\right)\right]\cos P_2 t + \frac{\dot{Y}(0)}{P_2}\sin P_2 t + \delta\left(\frac{2I_M}{I_0} - 1\right) - \frac{1}{P_2}\int_0^t \left(\frac{mh\xi}{I_M}\ddot{x}_G(\tau) - \ddot{y}_G(\tau)\right)\sin P_2(t-\tau)d\tau \qquad (2.3.57)$$

where

$$P_2^2 = \frac{p_2^2 I_0}{2I_M} \qquad (2.3.58)$$

and $Y(0) = \xi\phi(0) - y(0)$, $\dot{Y}(0) = \xi\dot{\phi}(0) - \dot{y}(0)$. In these equations, the origin of the time is taken at the onset of lift-off. Expression (2.3.58) can also be derived from equation (2.3.33), with p_1 given by (2.3.51) and the term $\frac{8kgh}{I_M}$ being omitted, which is consistent with the approximation considered here.

Double integration of equation (2.3.56) gives

$$h\phi(t) = \frac{m\xi h}{I_0}\left[Y(t) - \frac{h}{\xi}x_G(t) - y_G(t) - \frac{g}{2}t^2 + C_1 t + C_2\right] \qquad (2.3.59)$$

where

$$\left.\begin{aligned} C_1 &= \frac{I_0}{m\xi}\dot{\phi}(0) - \dot{Y}(0) + \frac{h}{\xi}\dot{x}_G(0) + \dot{y}_G(0) \\ C_2 &= \frac{I_0}{m\xi}\phi(0) - Y(0) + \frac{h}{\xi}x_G(0) + y_G(0) \end{aligned}\right\} \qquad (2.3.60)$$

and $x_G(t)$, $\dot{x}_G(t)$, $y_G(t)$, $\dot{y}_G(t)$ are the ground displacements and velocities in the horizontal and vertical direction, respectively.

Once $Y(t)$ and $\phi(t)$ have been found, the vertical displacement, $y(t)$, of the center of mass is found from equation (2.3.54).

The main difference of this solution from equations (2.3.41) and (2.3.42) is that the hyperbolic part of the response, which appears in equations (2.3.41) and (2.3.42), is approximated here by a parabola. The expressions for the characteristic frequencies of the system are also simplified.

As an example, let us examine the limiting case of $k \to \infty$ and $\xi \to \frac{a}{2}$ (rigid block on rigid foundation), and consider free oscillations, resulting from a horizontal impulse. Let $\dot{\phi}_0$ be the initial angular velocity. Then, $Y(t)$ vanishes and equation (2.3.59) reduces to

$$\frac{\phi(t)}{\theta} = -\frac{1}{2}(pt)^2 + \frac{\dot{\phi}_0}{p\theta}(pt) \qquad (2.3.61)$$

in which $p^2 = \frac{mgr}{I_0}$ and $\theta = \frac{a}{2r}$ (see Fig. 2.2.1). According to Housner's solution (section 2.2), the angle of rotation for this problem can be given by

$$\frac{\phi(t)}{\theta} = 1 - \cosh pt + \frac{\dot{\phi}_0}{p\theta}\sinh pt$$

Note that one of the assumptions made here is that $h\phi \ll \xi$, i.e.,

$\frac{\phi_{max}}{\theta} << 1$. Also, the above expressions for the response are valid for the first half period, only, so $0 \leq t \leq \frac{T}{2}$. Under these assumptions, and as can be verified from Fig. 2.2.2, pt is expected to be smaller than unity. Expanding cosh pt and sinh pt in Taylor series, Housner's solution reduces to

$$\frac{\phi(t)}{\theta} = -\frac{1}{2}(pt)^2 + \frac{\dot{\phi}_0}{p\theta}(pt) + O[(pt)^3]$$

Comparing this equation with (2.3.61) it is seen that the approximate solution derived in this section is good to $O[(pt)^3]$ for the limiting case of a rigid block rocking on a rigid foundation, which is acceptable for engineering purposes.

2.3.6. Some Further Observations for the Case of Free Oscillations

Let us now consider the simplified system of section 2.3.5 undergoing free oscillations in response to a horizontal impulse. Let I_h be the magnitude of the impulse, which is assumed to act at the center of mass. Applying the principle of conservation of angular momentum about the middle point of the base, M, which is the pole of rotation at time t = 0, the initial angular velocity, $\dot{\phi}_0$, can be found:

$$\dot{\phi}_0 = \frac{I_h h}{I_M} \tag{2.3.62}$$

Since all other initial conditions vanish, equations (2.3.22) and (2.3.23) reduce to:

$$\left.\begin{aligned} y(t) &= 0 \\ \phi(t) &= \phi^c_{max} \sin p_1 t \end{aligned}\right\} \tag{2.3.63}$$

where ϕ^c_{max} is the maximum angle of tilting, which would occur if lift-off was not allowed (i.e., if the springs could take tension), given by

$$\phi^c_{max} = \frac{\dot{\phi}_0}{p_1} \tag{2.3.64}$$

Equations (2.3.63) are valid only for the case of full contact. If ϕ^c_{max} is greater than the critical value

$$\phi_{cr} = \frac{\delta}{\xi} \tag{2.3.65}$$

lift-off will happen at some time, t_0, such that

$$t_0 = \frac{1}{p_1} \sin^{-1}\left(\frac{1}{\beta}\right) \tag{2.3.66}$$

where,

$$\beta = \frac{\phi^c_{max}}{\phi_{cr}} \tag{2.3.67}$$

The ratio, β, can be viewed as a measure of the excitation and the resulting amount of lift-off. For β large, $\phi^c_{max} >> \phi_{cr}$, and lift-off will happen for a relatively long time, compared to the rocking period. On the other hand, if β is close to unity, the block lifts-off only for a short time. For values of β less than one, lift-off does not occur. Since lift-off is of primary concern here, we will assume that

$$\beta > 1$$

After lift-off, the response is given by equations (2.3.57) and (2.3.59), which, for the case of free oscillations, reduce to:

$$Y(t) = \delta\left[\frac{2\lambda}{1+\lambda}\cos P_2 t + \sqrt{\frac{2\lambda}{1+\lambda}(\beta^2-1)}\sin P_2 t + \frac{1-\lambda}{1+\lambda}\right] \tag{2.3.68}$$

$$\phi(t) = \frac{\lambda}{\xi(1+\lambda)}\left[A\sin(P_2 t+\gamma) - \frac{g}{2}t^2 + \frac{\delta}{\lambda}\sqrt{\beta^2-1}\,p_1 t + \delta\left(\frac{1}{\lambda}+\frac{1-\lambda}{1+\lambda}\right)\right] \tag{2.3.69}$$

where A is the amplitude of the harmonic oscillations of Y, γ is a phase correction, t is measured from lift-off and

$$\lambda = \frac{m\xi^2}{I_M} = \left(\frac{\xi}{r_M}\right)^2 \tag{2.3.70}$$

in which r_M is the radius of gyration about point M. The following initial conditions were used for the derivation of equations (2.3.68) and (2.3.69)

$$Y(0) = \delta \quad , \quad \dot{Y}(0) = \delta p_1\sqrt{\beta^2-1}$$

$$\delta(0) = \frac{\delta}{\xi} \quad , \quad \dot{\phi}(0) = \frac{\delta}{\xi}p_1\sqrt{\beta^2-1}$$

The apparent rocking frequency of the system after lift-off is expected to be smaller than p_1, the rocking frequency during full contact, since the system becomes more flexible after uplift. On the other hand, the frequency of the vertical vibrations, which start after lift-off, is P_2. The ratio p_1/P_2 can be expressed in terms of λ only as

$$\frac{p_1}{P_2} = \sqrt{\frac{2\lambda}{1+\lambda}} \tag{2.3.71}$$

therefore, this ratio is less than one for $\lambda < 1$ and decreases as λ decreases.

For most applications in practice, λ is expected to be smaller than unity, except for the case of short, wide structures. For example, assuming that the mass of the block is uniformly distributed, the ratio λ can be expressed in terms of the dimensions of the block and the distance ξ as

$$\lambda = \frac{3\left(\frac{2\xi}{a}\right)^2}{1 + 4\left(\frac{b}{a}\right)^2} \qquad (2.3.72)$$

In Fig. 2.3.4, λ is plotted versus the aspect ratio $\frac{b}{a}$, for different values of ξ. It is seen from this plot that λ quickly approaches zero as $\frac{b}{a}$ increases. Even for the limiting case of $\xi = \frac{a}{2}$, λ is less than one for aspect ratios greater than $\frac{\sqrt{2}}{2}$.

The frequency of the rocking oscillations is, therefore, expected to be smaller than the frequency of the vertical vibrations and the rocking response of the system after lift-off consists of a harmonic function superimposed upon a parabolic one, as shown in Fig. 2.3.5. It is reasonable, then, to assume that a quarter of a period has ellapsed when the parabolic term attains its maximum value, which happens at time, t_1, after uplift, such that

$$t_1 = \frac{1}{p_1}\sqrt{\beta^2-1} \qquad (2.3.73)$$

Using equations (2.3.66) and (2.3.73), the rocking period, T, of free vibrations can be approximated by

$$T = \frac{4}{p_1}\left[\sin^{-1}\left(\frac{1}{\beta}\right) + \sqrt{\beta^2-1}\right] \qquad (2.3.74)$$

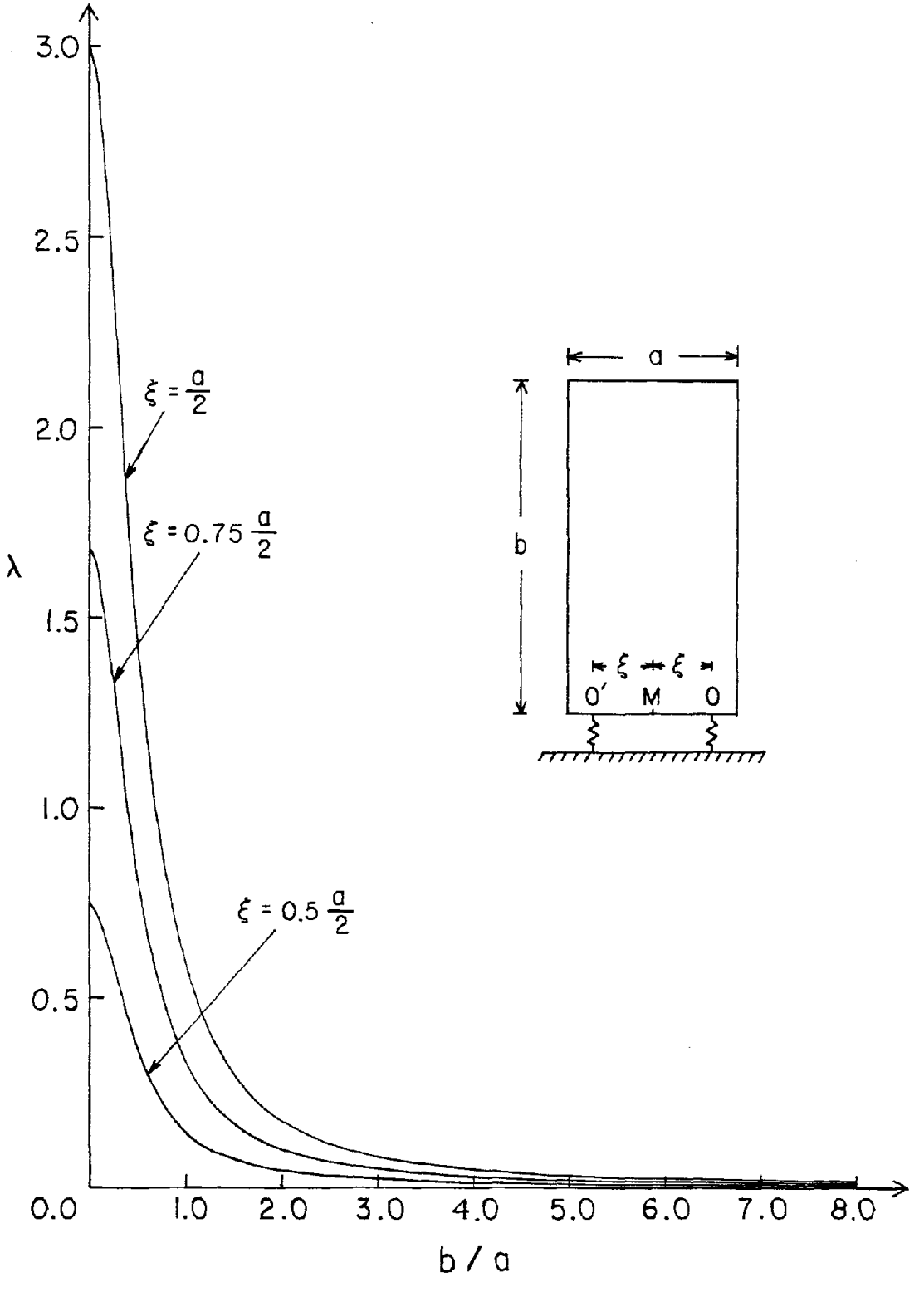

Fig. 2.3.4. Variation of λ with the aspect ration b/a.

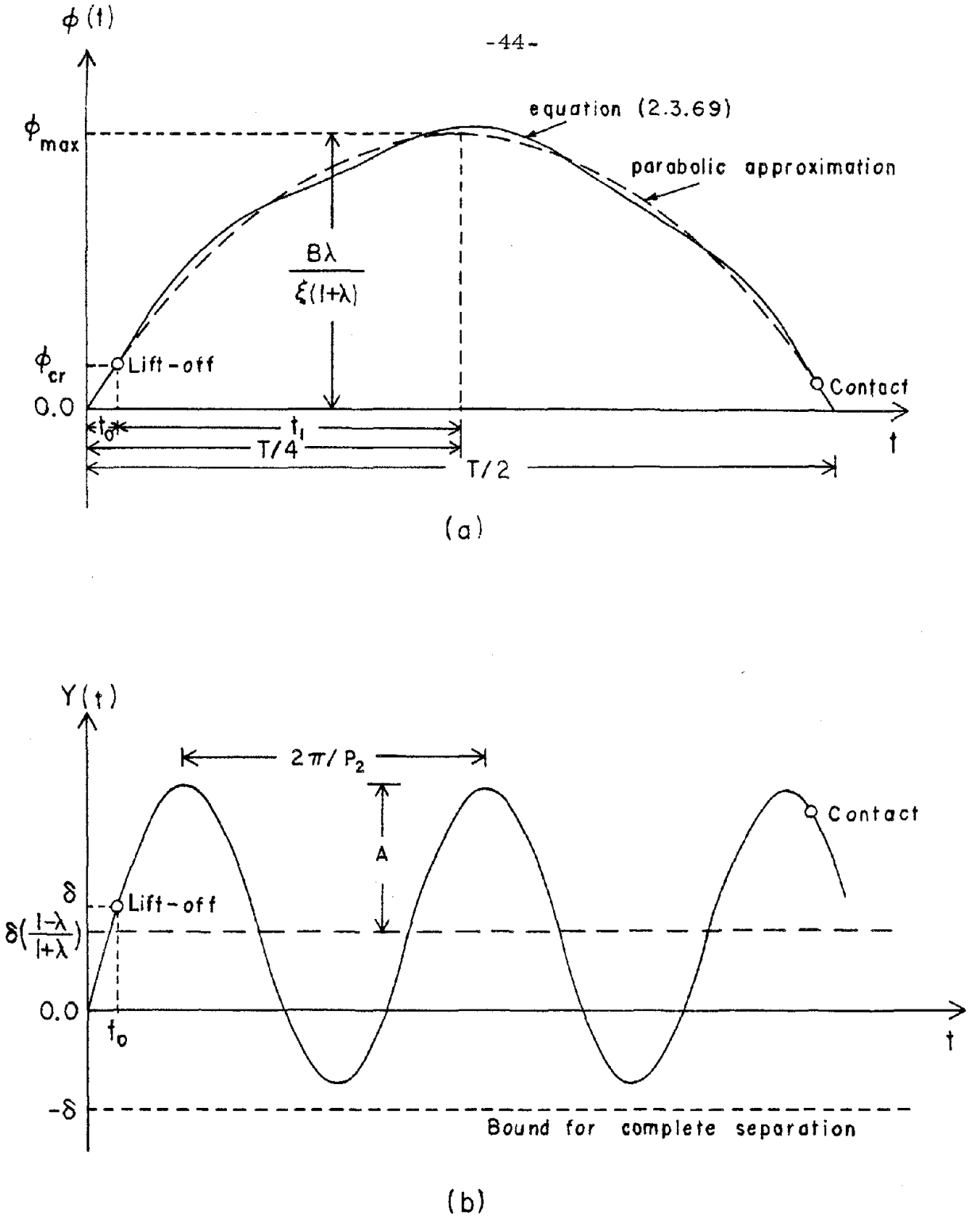

Fig. 2.3.5. Response of a freely rocking block with uplift.

If lift-off was not allowed, the rocking period, T_c, would be

$$T_c = \frac{2\pi}{p_1} \tag{2.3.75}$$

The increase in the period because of the uplift is then

$$\frac{T}{T_c} = \frac{2}{\pi}\left[\sin^{-1}\left(\frac{1}{\beta}\right) + \sqrt{\beta^2 - 1}\right] \tag{2.3.76}$$

It is seen that the elongation of the period depends only on the normalized impulse, β. In Fig. 2.3.6, a plot of equation (2.3.76) is shown; it is evident that the increase in the period is very significant for large values of β, for which $\frac{T}{T_c}$ is essentially proportional to β.

From equation (2.3.68), the amplitude, A, of the harmonic part of the vertical oscillations, Y, can be written as

$$A = \delta\sqrt{\frac{2\lambda}{1+\lambda}\left(\frac{2\lambda}{1+\lambda} + \beta^2 - 1\right)} \tag{2.3.77}$$

and the maximum value, B, of the parabolic terms (the last three) in the bracket of equation (2.3.69) as

$$B = \delta\left[\frac{1}{2\lambda}(\beta^2+1) + \frac{1-\lambda}{1+\lambda}\right] \tag{2.3.78}$$

In Fig. 2.3.7, the ratio (A/B) is plotted versus β, for different values of λ. It is seen that for small values of λ, A is much smaller than B, therefore, the harmonic part in equation (2.3.69) can be neglected. If λ is not small compared to unity, A can be neglected in comparison with B only for large values of β. In such cases, however, complete separa-

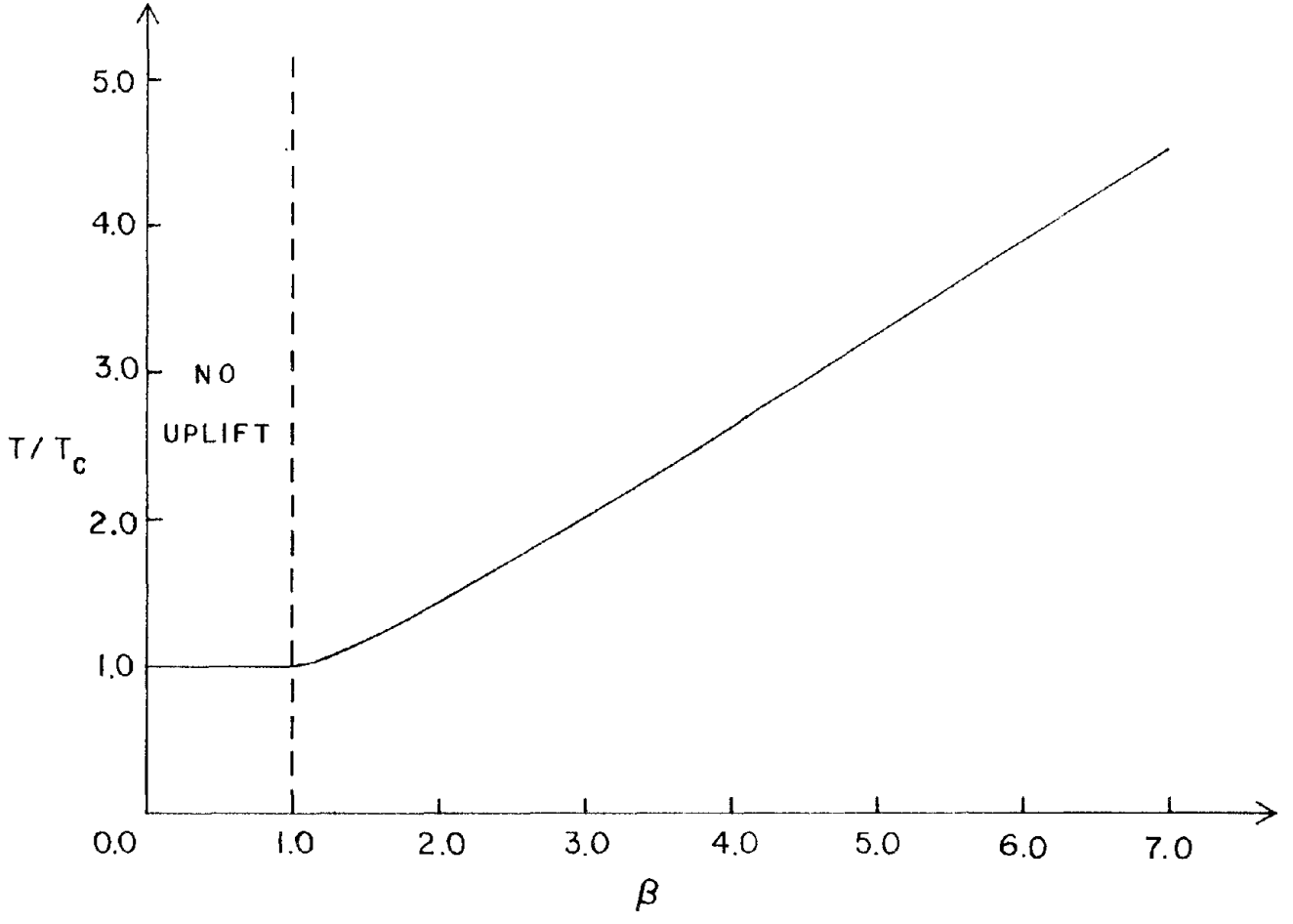

Fig. 2.3.6. Increase of the free rocking period with uplift, as a function of the normalized impulse, β.

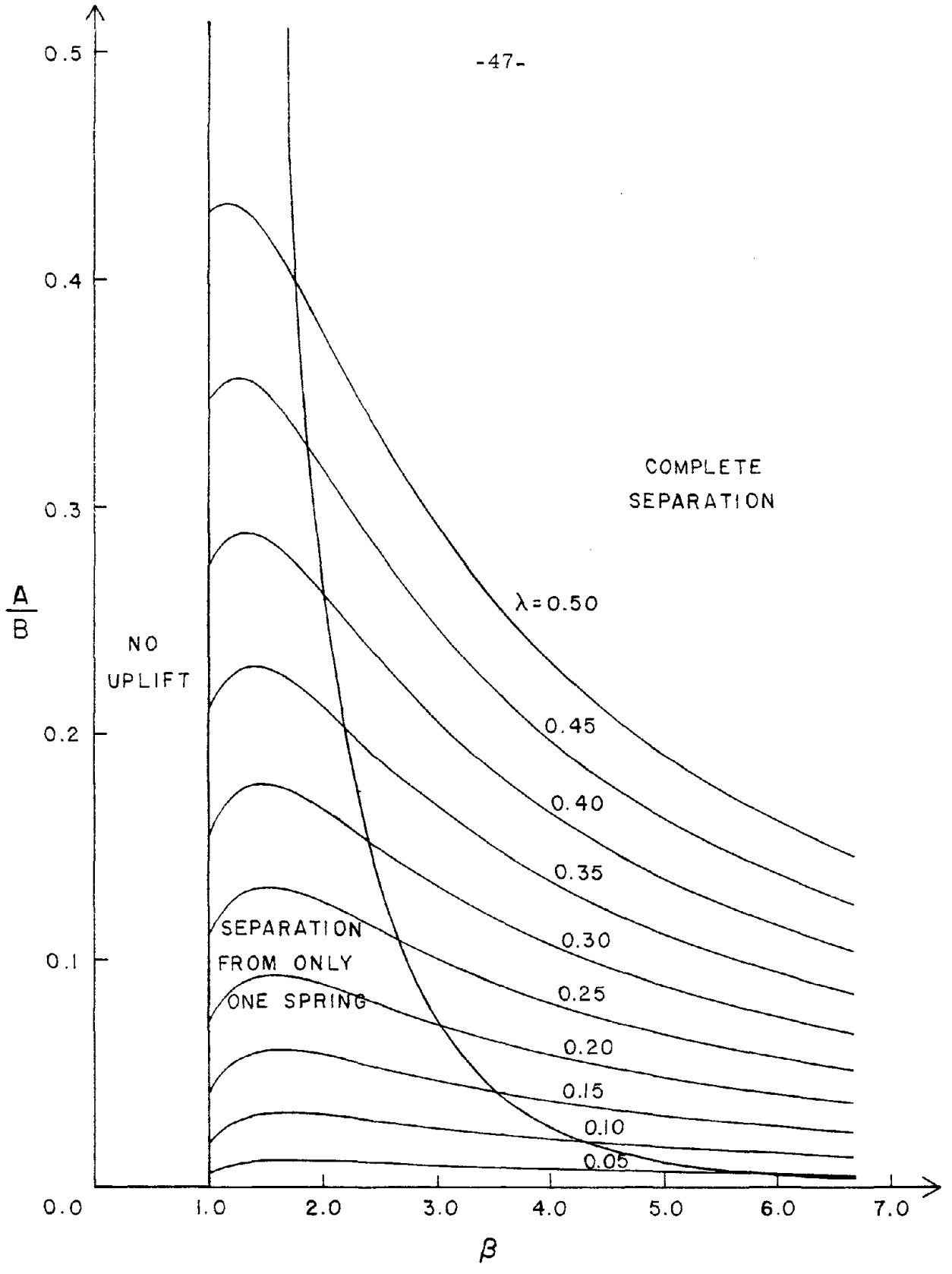

Fig. 2.3.7. Variation of the ratio A/B of the amplitudes of the harmonic and parabolic terms of the rocking response, respectively, with β and λ.

tion of the block from both springs is very likely to happen. Since Y measures the downward vertical displacement of point O, measured from the equilibrium position, complete separation will happen if $Y < -\delta$, that is

$$A - \delta\left(\frac{1-\lambda}{1+\lambda}\right) > \delta \quad . \tag{2.3.79}$$

Substituting from equation (2.3.77), this criterion can be expressed in terms of β and λ only, as

$$\beta^2 > \frac{2-\lambda}{\lambda} \tag{2.3.80}$$

In this inequality, β is a measure of the size of the impulse and the right-hand side is a geometrical factor depending on the dimensions of the block and the position of the springs.

Figure 2.3.8 shows the combinations of λ and β which cause complete separation according to inequality (2.3.80) and the condition that $\beta > 1$ for lift-off. It is interesting to note that for values of λ greater than one (e.g., a uniform block with aspect ratio less than $\frac{\sqrt{2}}{2}$), complete separation happens for all $\beta > 1$. For these values of λ, the block finally separates from both springs for all impulses strong enough to cause lift-off.

As it was discussed earlier, however, λ can be near to or greater than unity only for short, wide structures; in these cases, complete separation from the foundation is likely to happen during strong excitations, provided that the reaction force, R_A, is in fact, generated. Interestingly, the phenomenon of complete separation has occasionally been inferred from earthquake response in regions of very strong shaking

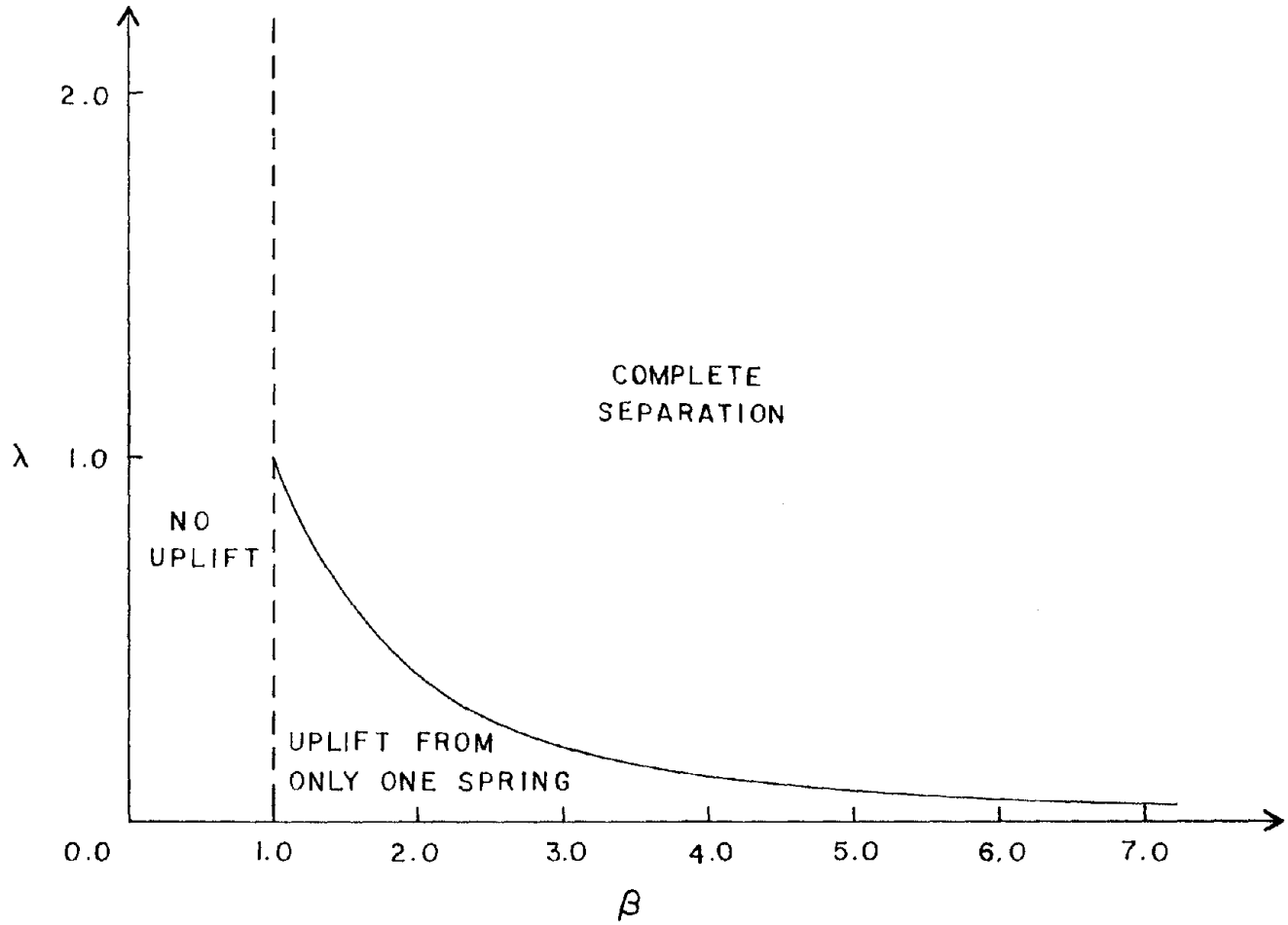

Fig. 2.3.8. Combinations of λ and β for degrees of separation in the first half period (horizontal excitation).

(e.g., see Bolt[48] and Morrill[49]). The analysis made in this thesis, however, is based on the more common condition that the value of λ is small compared to unity. The possibility of complete separation, therefore, is remote. In the following, it is assumed that the values of λ and β are such that complete separation does not happen.

When A can be neglected in comparison to B, i.e., when vertical oscillations are negligible, one can find the maximum angle of rotation by calculating the value of the parabolic term in equation (2.3.69) at time $t = t_1$. This gives

$$\phi_{max} = \phi_{cr}\left[\frac{\beta^2+1}{2(1+\lambda)} + \frac{\lambda(1-\lambda)}{(1+\lambda)^2}\right] \qquad (2.3.81)$$

In this case, then, the rocking response of the block to a horizontal impulse consists of a sequence of harmonic functions during full contact and parabolic functions during lift-off. The total response, however, resembles a sine function of period T and amplitude ϕ_{max}. It can, therefore, be approximated by the response, $\tilde{\phi}(t)$, of a similar linear system, in which the rocking period during full contact is T and lift-off is not allowed, with the amplitude modified by the following correction factor, CF

$$CF = \frac{\pi}{2\beta}\frac{\left[\frac{\beta^2+1}{2(1+\lambda)} + \frac{\lambda(1-\lambda)}{(1+\lambda)^2}\right]}{\left[\sin^{-1}\left(\frac{1}{\beta}\right) + \sqrt{\beta^2-1}\right]} \qquad (2.3.82)$$

This factor is required so that the amplitudes are matched for the same impulse.

Unfortunately, this result cannot be extended to treat the response to a horizontal ground excitation, in general, because the equivalent linear system depends on the magnitude of the impulse. Considering the continuous excitation to be a summation of pulses, a different linear system would be required for each impulse. In spite of this fact, the above results can be used for the estimation of the response to those ground motions in which a single large pulse determines the maximum response of structures over a wide range of periods. Such dominant pulses have been recorded on some earthquake records, e.g. the Pacoima Dam record from the San Fernando earthquake of 1971,[50] the Romanian earthquake of 1977,[51] and the record obtained at Cholame Shandon, station no. 2, in the Parkfield earthquake of 1966.[52] In such cases, the response can be estimated as follows:

1. Find the angle ϕ^c_{max} for the selected ground motion using equation (2.3.23). If a response spectrum is available, ϕ^c_{max} can be found by multiplying the displacement corresponding to frequency p_1 by $\frac{mh}{I_M}$.
2. Find the corresponding value of β using equation (2.3.67). If $\beta < 1$ lift-off does not happen and ϕ^c_{max} is the actual maximum amplitude of the response.
3. For $\beta > 1$, find the rocking period, T, as given by equation (2.3.74). This is the period of free oscillations excited by an impulse which will produce the same ϕ^c_{max}.
4. Consider the equivalent linear system, for which the foundation conditions are modified so that the natural rocking period during full contact is T. Find the response of this system for the excitation

under consideration, without allowing lift-off. If the maximum amplitude is desired, the response spectrum can be used to find the maximum angle of rotation, $\tilde{\phi}_{max}$, corresponding to period T, similar to the determination of ϕ^{c}_{max} in step 1.

5. Multiply this response by the correction factor, CF, to determine the response of the original problem in which uplift occurs.

Although this simple method cannot be expected to give good results if the ground motion is not dominated by a large pulse, it might still produce some useful characteristics of the response, if high accuracy is not required.

2.4. WINKLER FOUNDATION

2.4.1. System Considered and Assumptions

The two-spring foundation, which was examined in the previous section, is simple to analyze and illustrates many of the dynamic features of rocking bodies; however, the foundation is oversimplified for applications, except for the case of spring-mounted equipment. For most purposes, a continuous elastic foundation, (e.g., a Winkler model) provides a better representation of the supporting conditions. The behavior of a rocking block on a Winkler foundation is examined in this section.

In Figure 2.4.1 the two-dimensional configuration of a rocking block, supported by a continuous elastic foundation, is shown. The dimensions of the spring constant, k_0, are $[F/L^2]$. The assumptions that the block cannot slip on the foundation and that the springs cannot take tension are again employed. For ground motions acting in the

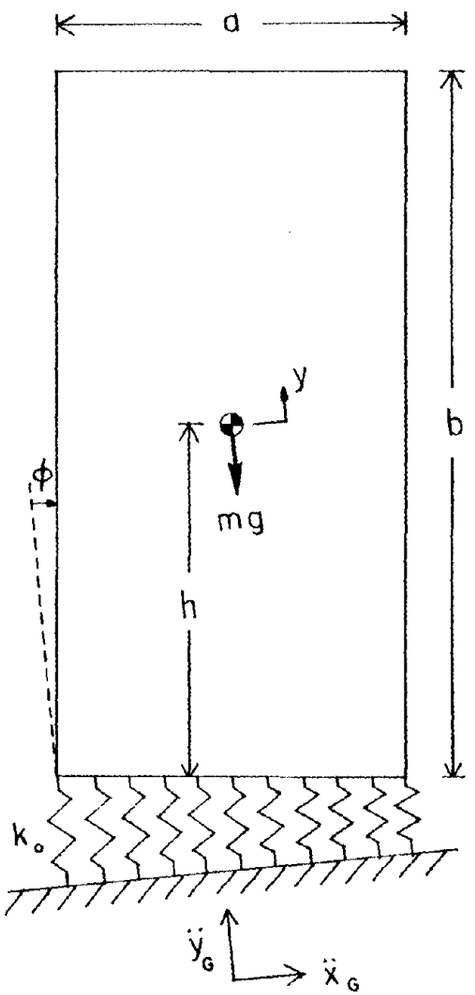

(a) Full-contact case

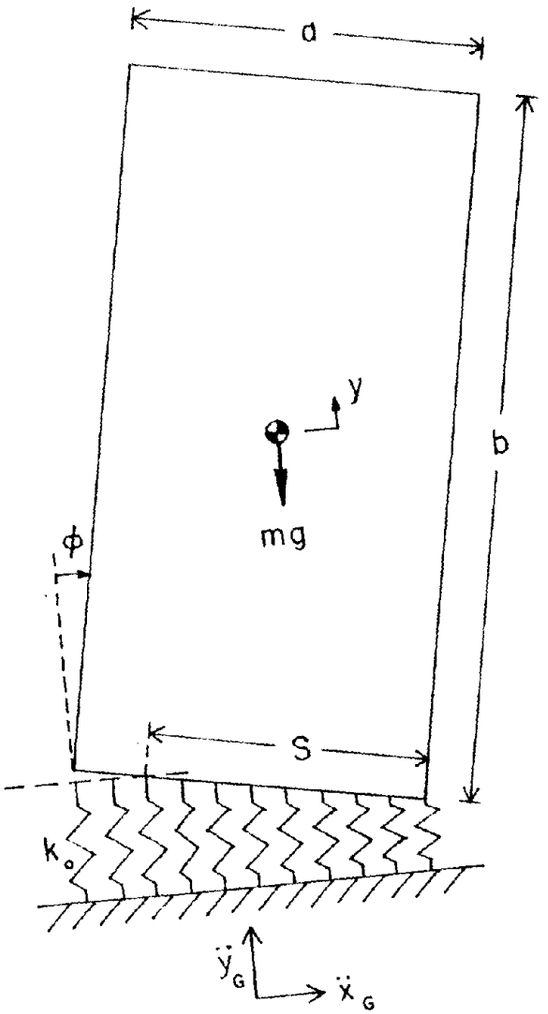

(b) After lift-off

Fig. 2.4.1. Rocking block on continuous elastic foundation (Winkler model).

x and y-directions, the system possesses only two degrees of freedom: vertical displacement, which is measured by the vertical displacement, y, of the center of mass, and rotation, measured by the angle of tilting, ϕ, from the vertical.

For sufficiently strong excitations the block will start lifting off, with the length of the base which remains in contact with the foundation dependent on the amount of uplift and being, therefore, a function of time. Complete separation of the block from the foundation may also occur for some geometries and for strong excitations, but is excluded from this analysis.

2.4.2. Equations of Motion

As in the two-spring foundation, the equations of motion can be derived using Newton's second law of motion. For small angles of rotation and tilting to the right, the resulting equations are

Full contact

$$m\ddot{y} + k_0 a y = -m\ddot{y}_G \tag{2.4.1}$$

$$I_M\ddot{\phi} + \frac{1}{2} mah\phi\ddot{\phi} + k_0 a\left(\frac{a^2}{12} - h\delta\right)\phi + \frac{1}{2} ma\ddot{x}_G\phi + k_0 ahy\phi = -mh\ddot{x}_G \tag{2.4.2}$$

After lift-off

$$m\ddot{y} - \frac{1}{2} k_0 \frac{y^2}{\phi} + k_0\delta \frac{y}{\phi} - \frac{1}{2} k_0 \frac{\delta^2}{\phi} - \frac{1}{8} k_0 a^2\phi + \frac{1}{2} k_0 ay = -\frac{1}{2} mg - m\ddot{y}_G \tag{2.4.3}$$

$$I_M\ddot{\phi} + \frac{1}{2}mah\phi\ddot{\phi} + \frac{1}{2}k_0a\left(\frac{a^2}{12} - h\delta\right)\phi + \frac{1}{2}k_0ahy\phi - k_0\left(\frac{a^2}{8} - h\delta\right)y$$
$$- \frac{1}{6}k_0\frac{\delta^3}{\phi^2} - \frac{1}{2}k_0\delta\frac{y^2}{\phi^2} + \frac{1}{2}k_0\delta^2\frac{y}{\phi^2} + \frac{1}{6}k_0\frac{y^3}{\phi^2} - \frac{1}{2}k_0hy^2 - \frac{1}{8}k_0a^2h\phi^2$$
$$+ \frac{1}{2}ma\ddot{x}_G\phi = -\frac{1}{2}k_0\delta\left(\frac{a^2}{4} - h\delta\right) - mh\ddot{x}_G \qquad (2.4.4)$$

in which δ is the static deflection given by

$$\delta = \frac{mg}{k_0a} \qquad (2.4.5)$$

For the derivation of equations of motion after lift-off, the following expression for the length of contact, S, was used

$$S = \frac{a}{2} + \frac{\delta}{\phi} - \frac{y}{\phi} \qquad (2.4.6)$$

As it can be seen from equation (2.4.1), a block, initially at rest and subjected to horizontal excitation, does not move in the vertical direction before lift-off happens. However, as in the case of two-spring foundation, vertical motion is excited after lift-off.

Since the angles and displacements were assumed to be small, the non-linear terms that appear in equation (2.4.2) can be deleted. Then, the response of the block for the full contact case can be written as

$$y(t) = y(0)\cos p_2^*t + \frac{\dot{y}(0)}{p_2^*}\sin p_2^*t - \frac{1}{p_2^*}\int_0^t \ddot{y}_G(\tau)\sin p_2^*(t-\tau)d\tau \qquad (2.4.7)$$

$$h\phi(t) = h\phi(0)\cos p_1^*t + \frac{h\dot{\phi}(0)}{p_1^*}\sin p_1^*t - \frac{mh^2}{I_Mp_1^*}\int_0^t \ddot{x}_G(\tau)\sin p_1^*(t-\tau)d\tau \qquad (2.4.8)$$

in which

$$(p_1^*)^2 = \frac{\frac{k_0 a^3}{12} - mgh}{I_M} \tag{2.4.9}$$

$$(p_2^*)^2 = \frac{k_0 a}{m} \tag{2.4.10}$$

and the following inequality was assumed to hold

$$\delta < \frac{a^2}{12h} \tag{2.4.11}$$

If the springs are very soft, so that (2.4.11) does not hold, the homogeneous equation that corresponds to (2.4.2) (after linearization) possesses a hyperbolic solution. In contrast to the two-spring foundation, where a hyperbolic solution of the homogeneous equations of motion during full contact implies static istability (overturning) before lift-off, in this case, if (2.4.11) does not hold static overturning may happen before or after lift-off depending on whether the overturning angle,

$$\theta = \tan^{-1}\left(\frac{a}{2h}\right) \cong \frac{a}{2h} \tag{2.4.12}$$

is greater or less than the critical angle,

$$\phi_{cr} = \frac{2\delta}{a} \tag{2.4.13}$$

After lift-off, the equations of motion are coupled and highly nonlinear because of the geometrical complexity. The only way they appear to be solvable is by use of numerical methods. The complexity of these equations comes from the varying length of contact, which, as can be

seen from (2.4.6), depends on both y and ϕ. Material nonlinearities in the foundation would complicate the problem even more.

2.5. EQUIVALENCE BETWEEN WINKLER AND TWO-SPRING FOUNDATION

2.5.1. General Principles

Although the Winkler foundation often provides an acceptably accurate model of the flexibility of the foundation, it leads to complicated equations of motion after lift-off, which make it difficult to apply in practice. On the other hand, the two-spring foundation is not such a realistic model, except for special cases such as spring-mounted equipment or small buildings supported by footings aligned at the corners of the base. However, the two-spring model leads to simple equations of motion, which can be easily solved analytically. From the engineering viewpoint it would be valuable to establish an equivalence between the two models. In other words, we would like to determine the parameters of the two-spring foundation in such a way that the response of a block supported by two springs nearly equals that for a given Winkler foundation. The simpler, equivalent system could then be used in solving practical problems.

The parameter which characterizes the Winkler model is the stiffness per unit length, k_0, of the springs. For the two-spring foundation there are two characteristic parameters: the stiffness, k, of the springs and their distance from the center of the base, measured by ξ. Assuming that the value of k_0 corresponding to the foundation under consideration is known, the parameters k and ξ for the two-spring model are to be found so that the two foundations lead to similar response for a given block.

Since there are two distinct regimes of response, before and after lift-off, it is logical first to determine two sets of equivalent values for k and ξ, corresponding to these two cases. Moreover, it turns out that a generally equivalent set of k and ξ can be established, which combines the two cases and which can be used to estimate the complete time history of the response.

Since the rocking block possesses two degrees of freedom, vertical displacement and rotation, its response depends only upon the vertical forces and upon the moments about the center of mass. Thus, establishing relations between the parameters of the two foundation models, such that the vertical forces and the moments about the center of mass are the same, the governing equations of motion for either type of foundation will be equivalent. During full contact, this leads to a system of two algebraic equations for the determination of the two unknown parameters, k and ξ. After lift-off, however, the procedure is not so straightforward because of the varying length of contact between the block and the foundation. Some further assumptions must be made in that case.

2.5.2. Equivalence During Full Contact

The total vertical force from the foundation, F_{2s}, and the moment about the center of mass, M_{2s}, for the two-spring foundation during full contact, are

$$F_{2s} = -2ky + mg \tag{2.5.1}$$

$$M_{2s} = -2k\xi^2\phi + mgh\phi - 2khy\phi + R_A\left(h + \frac{a}{2}\phi\right) \tag{2.5.2}$$

where R_A is the horizontal force acting at the corner of the base (see Fig. 2.3.2), given by

$$R_A = -m\ddot{x}_G - mh\ddot{\phi} \tag{2.5.3}$$

For the Winkler foundation, the corresponding forces and moments, F_W and M_W, are

$$F_W = -k_0 ay + mg \tag{2.5.4}$$

$$M_W = -\frac{1}{12} k_0 a^3 \phi + mgh\phi - k_0 ahy\phi + R_A \left(h + \frac{a}{2}\phi\right) \tag{2.5.5}$$

in which R_A is again given by (2.5.3). The principles of equivalence between the two systems, therefore, require that

$$k = \frac{k_0 a}{2} \tag{2.5.6}$$

and

$$\xi = \frac{a\sqrt{3}}{6} \tag{2.5.7}$$

The response during full contact of a block sitting on a two-spring foundation, in which the values of k and ξ are as given by equations (2.5.6) and (2.5.7), is then expected to be the same as the response of the Winkler model. The equivalence, of course, is not valid after the block lifts-off. However, if uplift happens for only a short time, relative to the period of rocking vibrations, the two responses should be similar for the whole time history. But, if uplift occurs over longer intervals of time, this equivalence is not expected to give satisfactory results.

It should be mentioned that, although equation (2.5.6) assures the same static deflection for both models, lift-off will not happen at exactly the same time. In the case of the Winkler foundation (and for a horizontal excitation) uplift occurs when the angle of rotation reaches

the value $\frac{\delta}{a/2}$, whereas the critical angle for the two-spring foundation is $\frac{\delta}{\xi}$. It is possible, therefore, that an excitation can be strong enough to cause lift-off from the Winkler foundation, but not be able to produce lift-off from the equivalent two-spring system.

2.5.3. Equivalence After Lift-Off

The resultant vertical forces from the foundation in this case are

$$F_{2s} = kz' \tag{2.5.8}$$

$$F_W = \frac{1}{2} k_0 S z \tag{2.5.9}$$

for the two-spring and the Winkler model, respectively, in which (see Fig. 2.5.1)

$$z = \delta - y + \frac{a}{2}\phi \tag{2.5.10}$$

and z' can be expressed as

$$z' = \frac{(S-\xi')}{S} z \tag{2.5.11}$$

where

$$\xi' = \frac{a}{2} - \xi \tag{2.5.12}$$

Equation (2.5.11) is based on the assumption that the angle of rotation, ϕ, and the vertical displacement, y, are the same in the two models.

Since F_W and the position of its application depend on the length of contact, S, application of the principles of equivalence would produce expressions for the parameters k and ξ, which would be functions of S. But, as it can be seen from equation (2.4.6) and Fig 2.4.1.b, S changes with time. This is shown in more detail in Fig. 2.5.2, where the dimensionless quantity $\frac{S}{a}$ is plotted versus time for the case of free

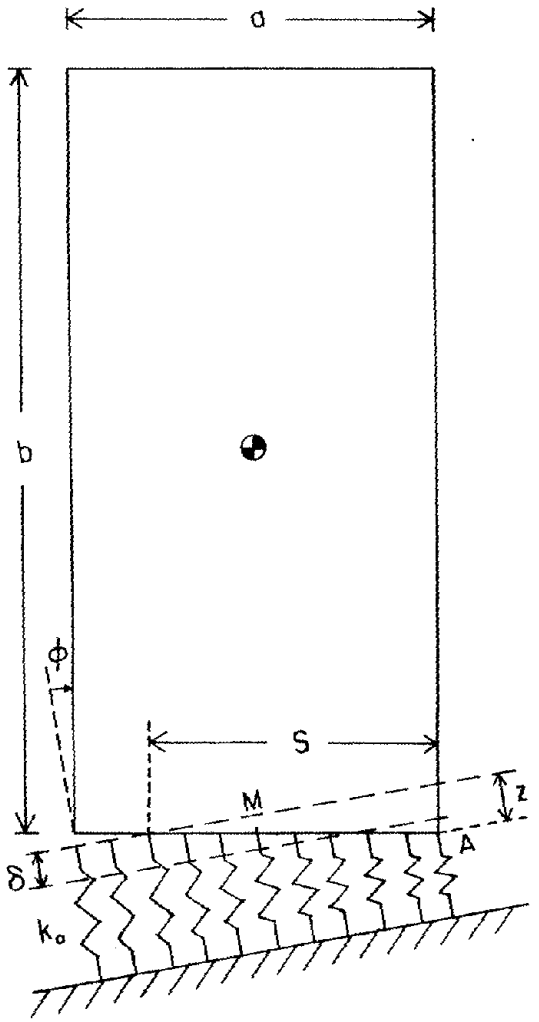

(a) Winkler foundation

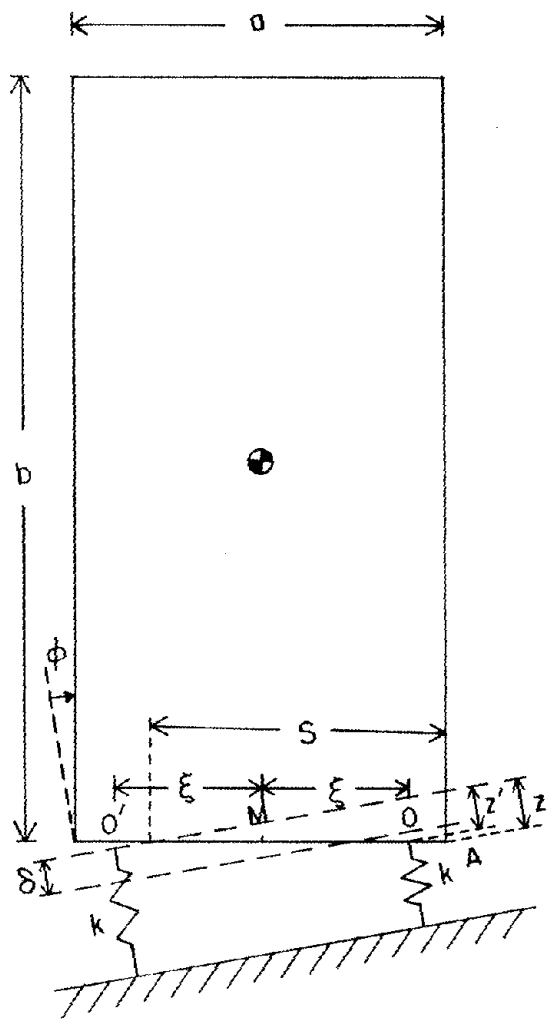

(b) Two-spring foundation

Fig. 2.5.1. Rocking block after lift-off.

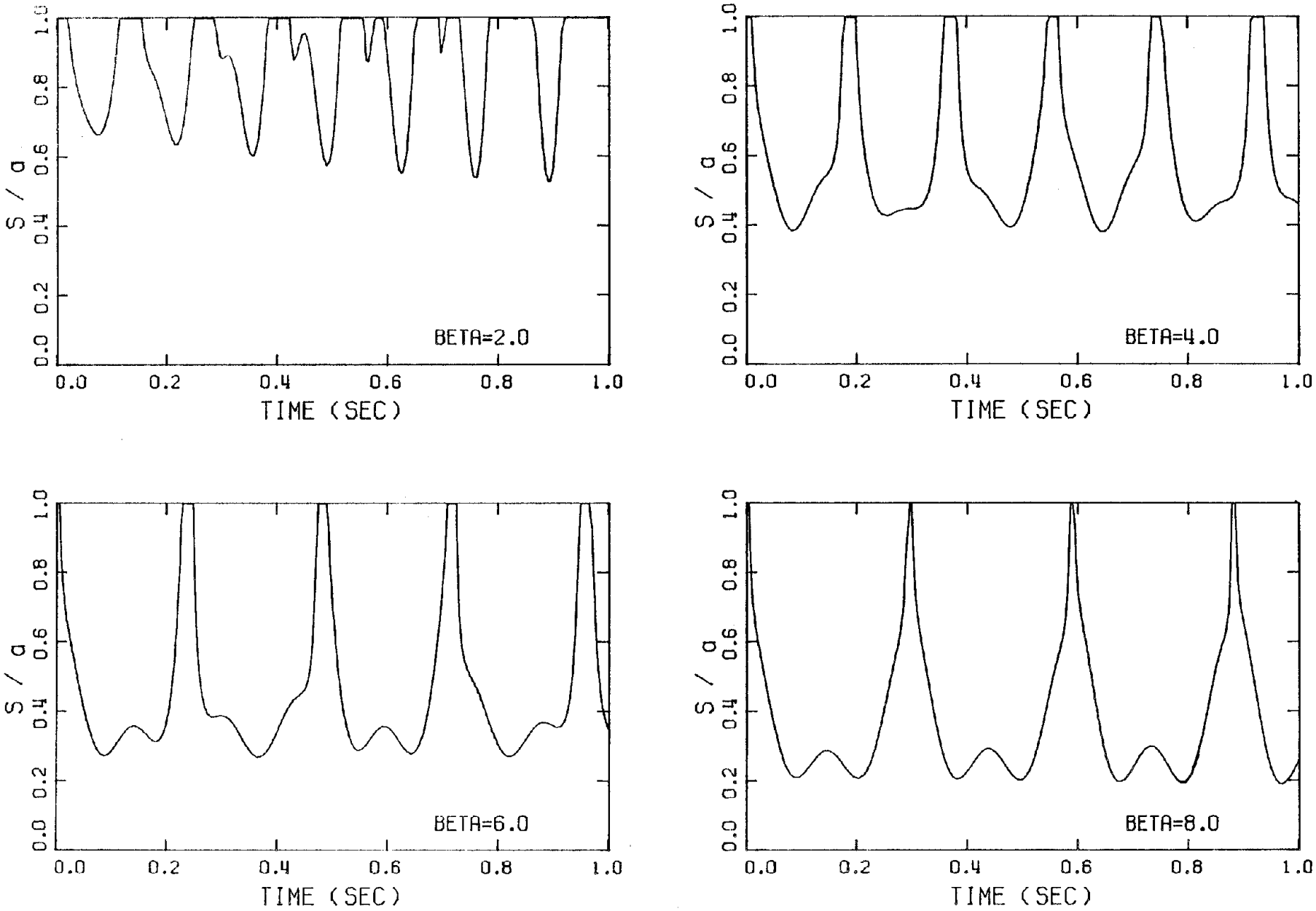

Fig. 2.5.2. Change of the normalized length of contact with time for free oscillations of a simplified model based on Millikan Library (see section 2.5.6).

oscillations of the block. Four values of the normalized impulse, $\beta = \phi^c_{max} / \phi_{cr}$, are illustrated, where ϕ^c_{max} is the maximum angle of rotation which would happen if lift-off were not allowed and ϕ_{cr} is given by (2.4.13). For these plots, equation (2.4.6) was used for the calculation of S, in which the values of ϕ and y were found by numerical integration of equations (2.4.3) and (2.4.4). More details about the procedure followed and the values of the parameters used for this example are presented in section 2.5.6.

It is seen that a complete equivalence after lift-off between the two models would require the values of k and ξ to be functions of time. Of course, this is not desirable because the simplicity of the two spring foundation would then be lost. In order to overcome this difficulty, S is replaced by a representative value, $\tilde{S}$, which is kept constant during the time of uplift. In this way, unique values of k and ξ can be determined. One representative value of $\tilde{S}$ is the average, over time, of the length of contact. In Appendix I, a parametric analysis of the exact response is made, for the case of free oscillations, in order to estimate this average; the result of this analysis is

$$\tilde{S} = \frac{a}{\sqrt{\beta}} \qquad (2.5.13)$$

i.e., $\frac{\tilde{S}}{a}$ is inversely proportional to the square root of the normalized impulse, β. Although equation (2.5.13) was derived for a horizontal impulse, it can be used to estimate $\tilde{S}$ for other horizontal ground motions. In that case, the value of ϕ^c_{max} in the expression for β should be calculated for the given excitation.

Changing S to $\tilde{S}$ in equations (2.5.9) and (2.5.11) and equating F_{2s} with F_W produces

$$k = \frac{3}{4} k_0 \tilde{S} \qquad (2.5.14)$$

Using this equation and the fact that R_A is the same for both systems, one can find the equation for ξ by equating the distances from the points of application of F_{2s} and F_W to the corner A. This gives

$$\xi = \frac{a}{2} - \frac{\tilde{S}}{3} \qquad (2.5.15)$$

Although equations (2.5.14) and (2.5.15) were derived for equivalence during lift-off only, they can be used in general for large values of β, when the time of full contact is small compared to the rocking period.

2.5.4. General Equivalence

In the previous two sections, relations between the parameters of the two-spring and the Winkler model were established so that the two models are equivalent for the two cases of full contact and uplift. However, if the rocking block vibrates in both states for significant portions of the response, neither of these sets of expressions is expected by itself to give good matching between the responses of the two models. It is needed, therefore, to combine the two cases, if possible, and find relations which can be used in general.

For a general equivalence of this type, a measurement of the expected amount of lift-off is needed. Since the ratio, β, (corresponding to the Winkler model) is the only quantity affecting the normalized average length of contact during lift-off and, in addition, can be

regarded as a measurement of the excitation, it is reasonable to employ this quantity for this purpose. Then, using equations (2.5.6), (2.5.7), (2.5.14) and (2.5.15), the parameters of an approximately equivalent two-spring model to the Winkler foundation can be given by

$$k = \frac{1}{\beta^2}\left(\frac{1}{2} k_0 a\right) + \left(1 - \frac{1}{\beta^2}\right)\left(\frac{3}{4} k_0 \tilde{S}\right) \qquad (2.5.16)$$

$$\xi = \frac{1}{\beta^2}\left(\frac{\sqrt{3}}{6} a\right) + \left(1 - \frac{1}{\beta^2}\right)\left(\frac{a}{2} - \frac{\tilde{S}}{3}\right) \qquad (2.5.17)$$

When lift-off happens for only a short time compared to the rocking period, β is close to one and the values of k and ξ resulting from equations (2.5.16) and (2.5.17) are close to the ones calculated by expressions (2.5.6) and (2.5.7). Similarly, when lift-off dominates in the response, β is much greater than one and in the limiting case, in which $\beta \to \infty$, equations (2.5.16) and (2.5.17) reduce to (2.5.14) and (2.5.15).

The fact that β is raised to the second power in equations (2.5.16) and (2.5.17) is arbitrary; the reason for choosing a quadratic dependence is to force the values of k and ξ to reach their limiting values faster when β is very large than is achieved by a linear function.

2.5.5. Estimation of the Rocking Period of Free Oscillations for the Winkler Model

As an example, let us try to estimate the rocking period of free vibrations of a block sitting on a Winkler foundation, using the equivalent two-spring model. Recall that for the two-spring system and a horizontal impulse excitation, the rocking period was found in section 2.3.6 and, according to equation (2.3.74), is given by

$$T = \frac{4}{p_1}\left[\sin^{-1}\left(\frac{1}{\beta_{2s}}\right)+\sqrt{\beta_{2s}^2-1}\right] \qquad (2.5.18)$$

in which p_1 is the natural rocking frequency during full contact and β_{2s} is the normalized impulse. For distinction, the normalized impulse corresponding to the two-spring foundation is denoted by β_{2s} and the value corresponding to the Winkler model by β. In order to calculate the rocking period of the Winkler foundation, one has to find the values of p_1 and β_{2s} which correspond to the equivalent two-spring model and then, apply equation (2.5.18) directly.

First, recall that the simplified expressions for the natural rocking frequencies during full contact (for small angles of rotation) for the two-spring and the Winkler foundation are

$$p_1 = \sqrt{\frac{2k\xi^2}{I_M}} \qquad (2.5.19)$$

and

$$p_1^* = \sqrt{\frac{k_0 a^3}{12\ I_M}} \qquad (2.5.20)$$

respectively. Using equations (2.5.16) and (2.5.17), the ratio of these frequencies can be written as

$$\frac{p_1^*}{p_1} = \frac{\beta^3}{\left[1+\left(\beta^2-1\right)\left(3-\frac{2}{\sqrt{3\beta}}\right)\right]\sqrt{1+\left(\beta^2-1\right)\frac{3}{2\sqrt{\beta}}}} \qquad (2.5.21)$$

in which, β is the normalized impulse for the Winkler foundation and expression (2.5.13) was used for the estimation of $\tilde{S}$. On the other hand, substituting the expressions of equivalence into (2.3.65) and using (2.4.13), the ratio of the critical angles at which lift-off first

happens for a horizontal excitation can be expressed as

$$\frac{\phi_{cr}^{(2s)}}{\phi_{cr}^{(W)}} = \frac{3\beta^4}{\left[1 + \left(\beta^2-1\right)\frac{3}{2\sqrt{\beta}}\right]\left[\sqrt{3} + \left(\beta^2-1\right)\left(3 - \frac{2}{\sqrt{\beta}}\right)\right]} \tag{2.5.22}$$

Also, if lift-off were not allowed, the ratio of the amplitudes of the free oscillations for the two models would be

$$\frac{\phi_{max(2s)}^{c}}{\phi_{max(W)}^{c}} = \frac{p_1^*}{p_1} \tag{2.5.23}$$

From equations (2.5.21), (2.5.22) and (2.5.23), the normalized impulse, β_{2s}, for the equivalent two-spring foundation can then be written in terms of β as

$$\beta_{2s} = \sqrt{\frac{1}{3} + \frac{(\beta^2-1)}{2\sqrt{\beta}}} \tag{2.5.24}$$

This equation implies that $\beta_{2s} < 1$ for $1 < \beta < 1.65$. For these values of β, the two-spring model does not lift-off although the Winkler system does. Note that the general equivalence, as defined by equations (2.5.16) and (2.5.17), is based on a combination of the equivalences during the two individual cases, in which both models are in full contact or lift-off. For $1 < \beta < 1.65$, therefore, equations (2.5.16) and (2.5.17) cannot be used, since the expressions for the equivalence during lift-off do not hold. Equations (2.5.6) and (2.5.7) are more appropriate to be used in this situation. In the following calculations we will assume that $\beta > 1.65$. Equation (2.5.24) is plotted in Fig. 2.5.3.

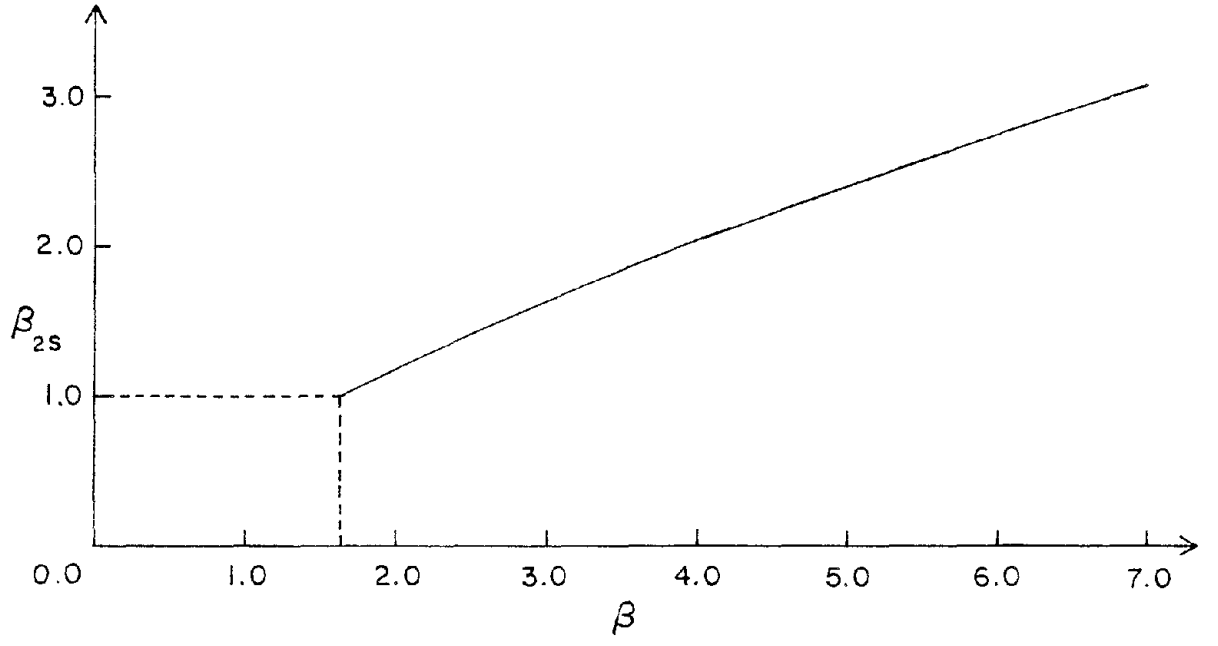

Fig. 2.5.3. Relation between the normalized impulse ratios, β and β_{2s}, of the Winkler and the equivalent two-spring model.

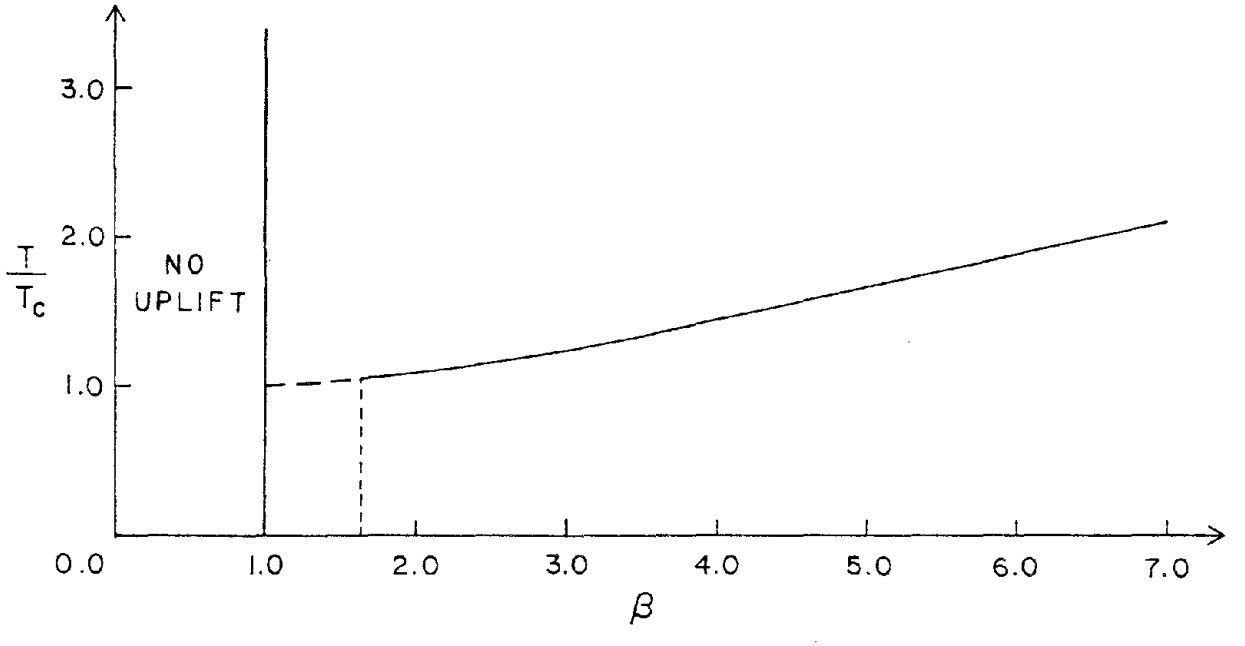

Fig. 2.5.4. Increase of the free rocking period of the Winkler model, as a result of uplift.

Substituting p_1 from equation (2.5.21) into (2.5.18), the rocking period of the Winkler model can be estimated by

$$\frac{T}{T_c} = \frac{2\beta^3\left[\sin^{-1}\left(\frac{1}{\beta_{2s}}\right)+\sqrt{\beta_{2s}^2-1}\right]}{\pi\left[1+(\beta^2-1)\left(\sqrt{3}-\frac{2}{\sqrt{3\beta}}\right)\right]\sqrt{1+(\beta^2-1)\frac{3}{2\sqrt{\beta}}}} \quad , \quad \beta > 1.65 \tag{2.5.25}$$

where β_{2s} is given by (2.5.24) and T_c is the natural rocking period for full contact given by

$$T_c = \frac{2\pi}{p_1^*}$$

The ratio $\frac{T}{T_c}$, which measures the fractional increase of the rocking period because of lift-off, is plotted versus β in Fig. 2.5.4. It is seen that for large values of β, $\frac{T}{T_c}$ is essentially proportional to β. Recall that a similar result was found for the two-spring foundation (see Fig. 2.3.6). For $\beta < 1.65$, the formula for $\frac{T}{T_c}$ can be extended linearly down to unity as

$$\frac{T}{T_c} = 1 + \frac{(\beta-1)}{0.65}\left[\left(\frac{T}{T_c}\right)_{1.65} - 1\right] \quad , \quad 1 \le \beta \le 1.65$$

or, putting $\left(\frac{T}{T_c}\right)_{1.65} = 1.063$ one gets

$$\frac{T}{T_c} = 0.903 + 0.097\beta \quad , \quad 1 \le \beta \le 1.65 \tag{2.5.26}$$

2.5.6 Numerical Example

As an example, let us consider Robert A. Millikan Memorial Library, which is located on the campus of the California Institute of Technology in Pasadena, California. For purposes of illustration we assume no deformations in the superstructure, i.e., that the building behaves like a rigid block. Millikan Library is a nine-story building, 69 × 75 feet (21.03 × 22.86 m) in plan and 144 feet (43.89 m) in height above grade and 158 feet (48.16 m) above the basement level. A plan view and a N-S section of the building are shown in Fig. 2.5.5. Assuming all the masses concentrated on the floors, the following weights of the floors may be used: roof, 2.6×10^6 lbs. (1.18×10^3t); floors 9-3, 1.95×10^6 lbs. (0.88×10^3t); floor 2, 2.43×10^6 lbs. (1.10×10^3 t); floor 1, 2.28×10^6 lbs. (1.03×10^3 t); base, 7.0×10^6 lbs. (3.18×10^3 t). With this distribution of the masses, the center of mass is located at height, h, equal to 59 ft (18 m) from the base, and the moment of inertia about the center point of the base, M, for rocking in the N-S direction is 5.5×10^9 lbs. sec.^{2} ft (7.6×10^5 t · sec^2 · m). More details about the building can be found in reference 23.

Using Veletsos' analysis,[21] Foutch[23] calculated that the rocking stiffness of the foundation in N-S direction can be modeled by a rotational spring of stiffness, K_ϕ, given by

$$r_e^2 K_\phi = 3.5 \times 10^{12} \text{ ft-lb/rad} \qquad (2.5.27)$$

where r_e is the radius of the equivalent circular base, equal to 41 feet for Millikan Library. A 28% increase of the theoretical value is included in (2.5.27) to account for embedment[47]. Assuming that the

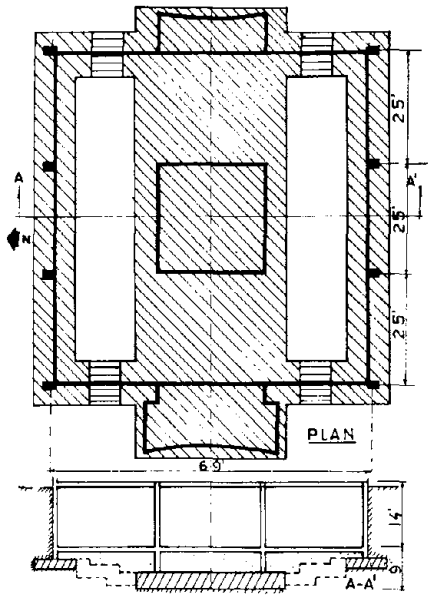

A

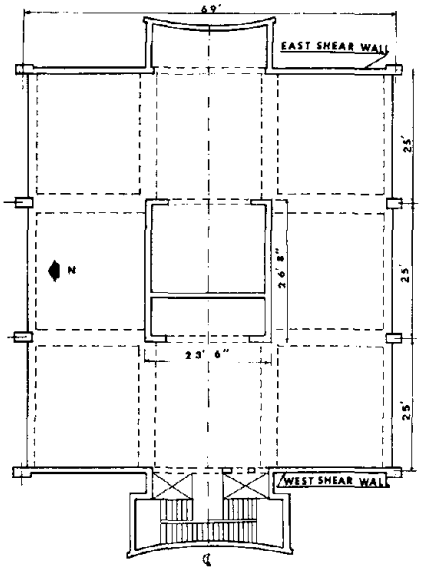

B

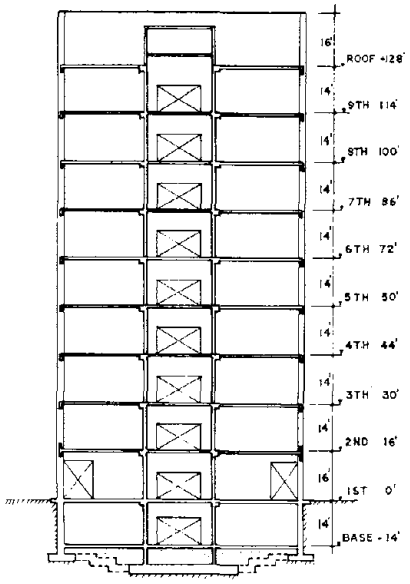

C

D

Fig. 2.5.5. Millikan Library Building: (a) foundation plan and N-S section; (b) typical floor plan; (c) a N-S section view; (d) view of building looking Northwest. (From reference 23).

building does not lift-off and equating the base moments about point M for the Winkler foundation with the moment resulting from the rotational spring, for the same angle of tilting, the following relation can be found for the Winkler model

$$k_0 = \frac{12\, r_e^2 K_\phi}{a^3} \qquad (2.5.28)$$

which results to $k_0 = 1.3 \times 10^8$ lbs/ft^2 (6.2×10^5 t/m^2). The corresponding static deflection is 0.04 in (1 mm).*

Figures 2.5.6, 2.5.7, 2.5.8 and 2.5.9 show the free vibrations of the model for β = 2, 4, 6 and 8, respectively. According to equations (2.3.62) and (2.4.8) and the definition of β, these values of β correspond to pulses: 0.15, 0.30, 0.46 and 0.61 m/sec per unit mass, respectively. For comparison, the maximum pulse in the S00E component of the El Centro earthquake of May 18, 1940 is 0.525 m/sec (see reference 53). For the Winkler response, equations (2.4.7) and (2.4.8) were used during full contact; after lift-off the nonlinear equations (2.4.3) and (2.4.4) were integrated numerically, using a Runge-Kutta method for the solution of a system of nonlinear, first order, ordinary differential equations. The time-step for the numerical integration was 0.001 sec. For the equivalent two-spring models, the response was obtained using equations (2.3.22) and (2.3.23) during full contact and equations (2.3.41) and (2.3.42) after lift-off. Note that the overturning angle, θ, in this example is 0.41 rads, i.e., more than two orders of magnitude greater than ϕ_{max} for β = 8; dramatically stronger excitation would be required for overturning.

(*) Although the rotational stiffness of this model agrees with experimental data, the resulting static deflection is very small and seems unrealistic.

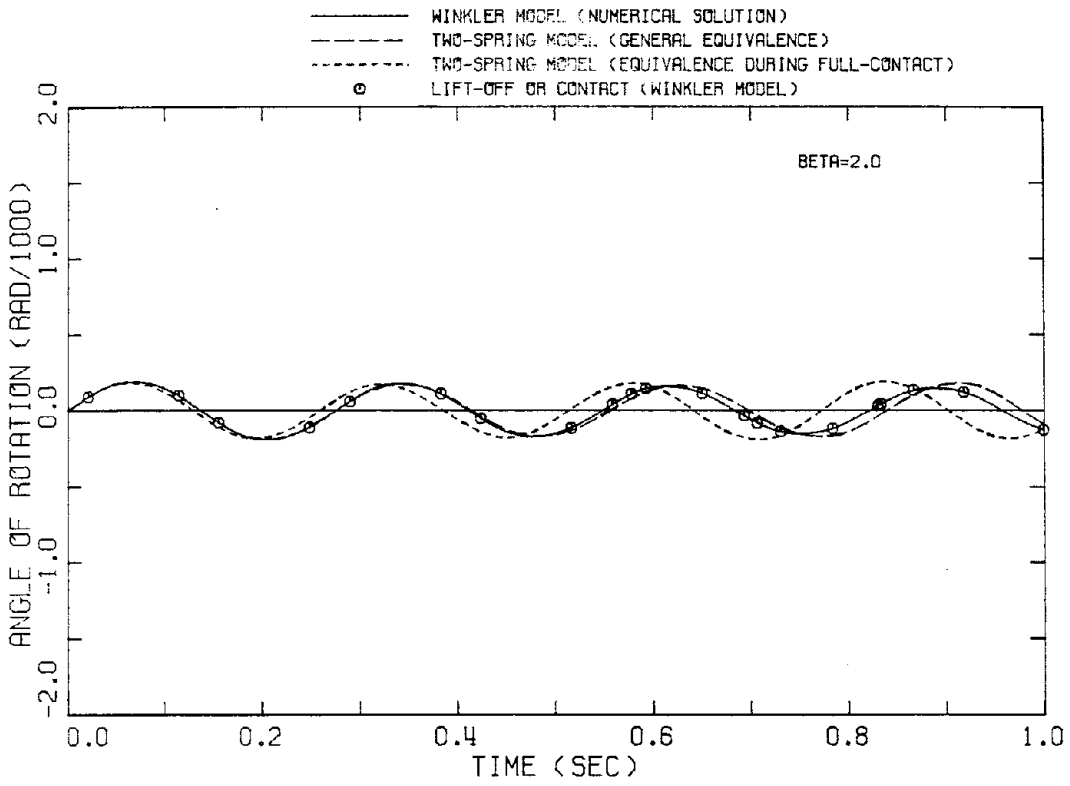

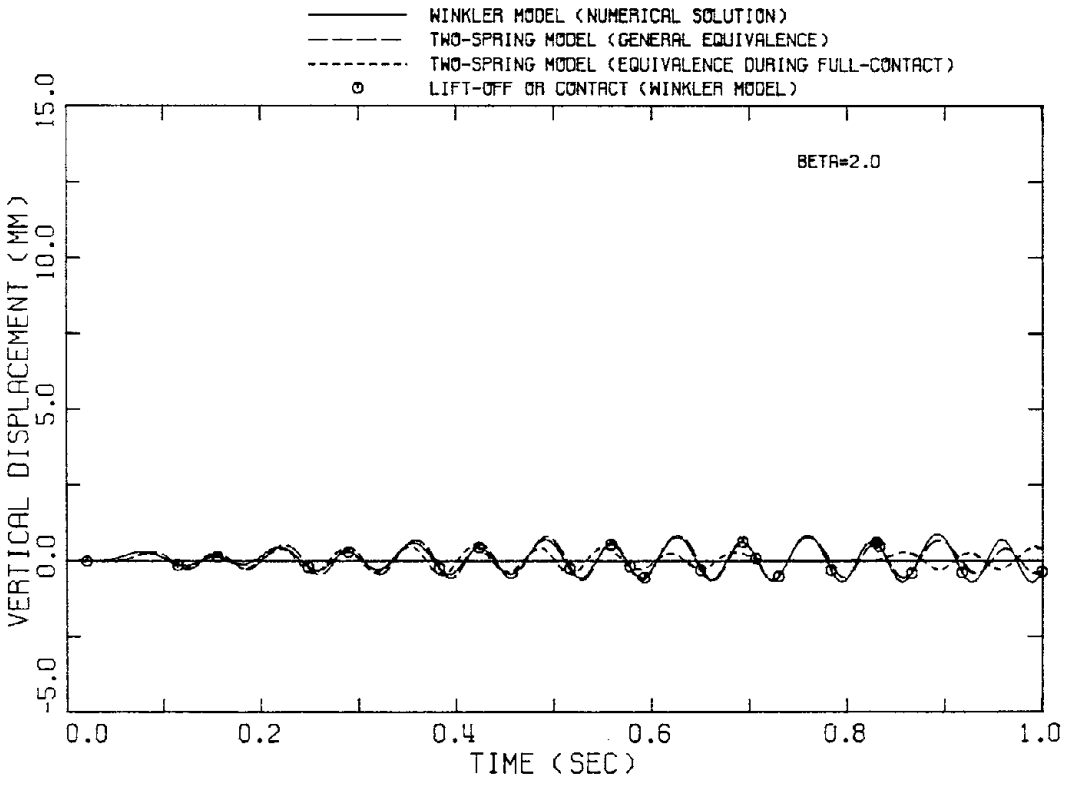

Fig. 2.5.6. Angle of rotation and vertical displacement of the center of mass for free, undamped oscillations of a simplified model of Millikan Library (β = 2).

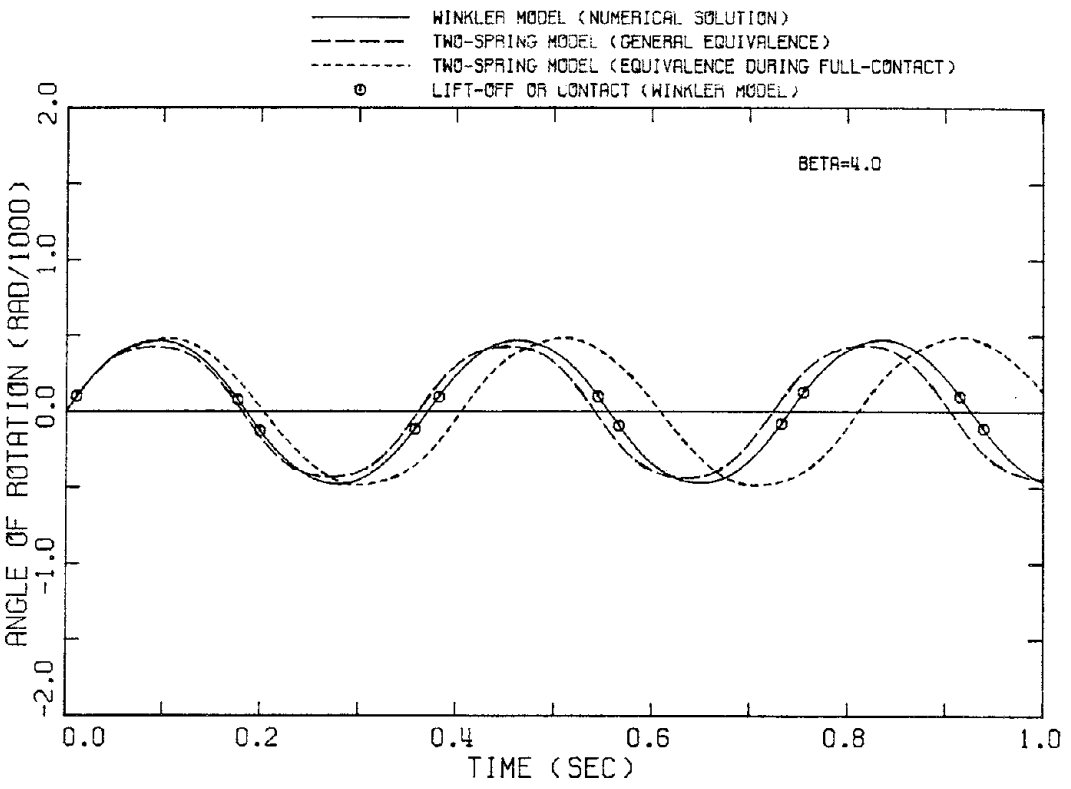

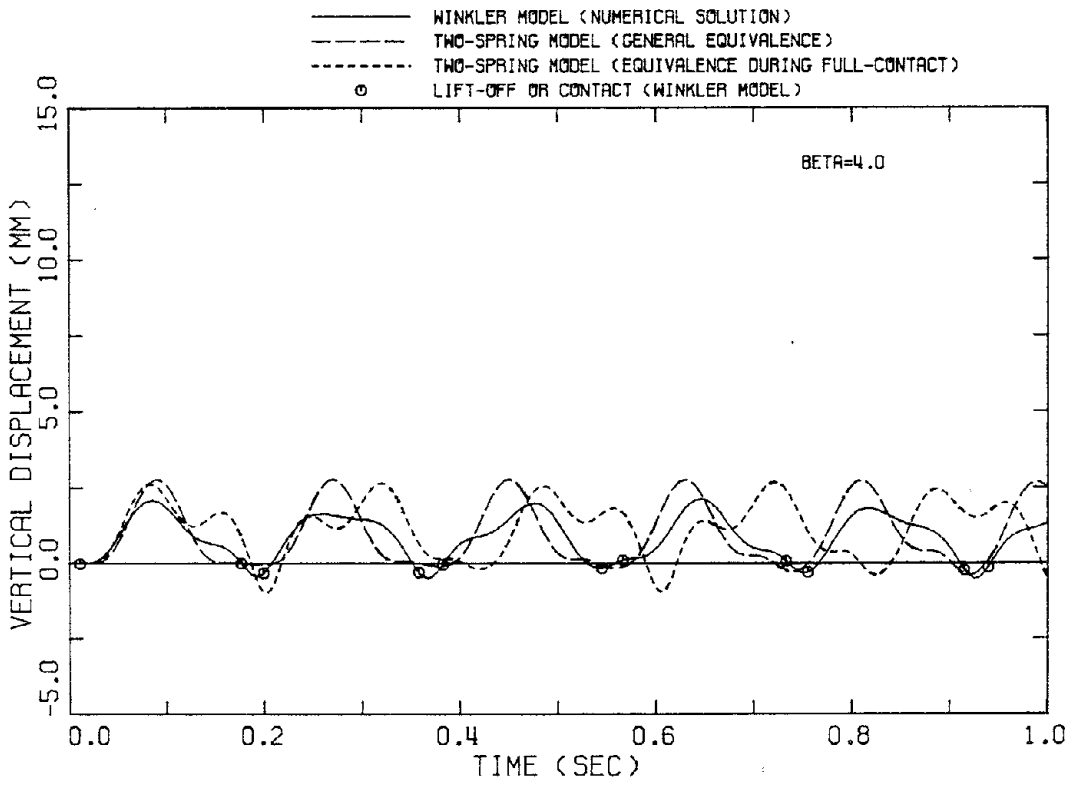

Fig. 2.5.7. Angle of rotation and vertical displacement of the center of mass for free, undamped oscillations of a simplified model of Millikan Library (β = 4).

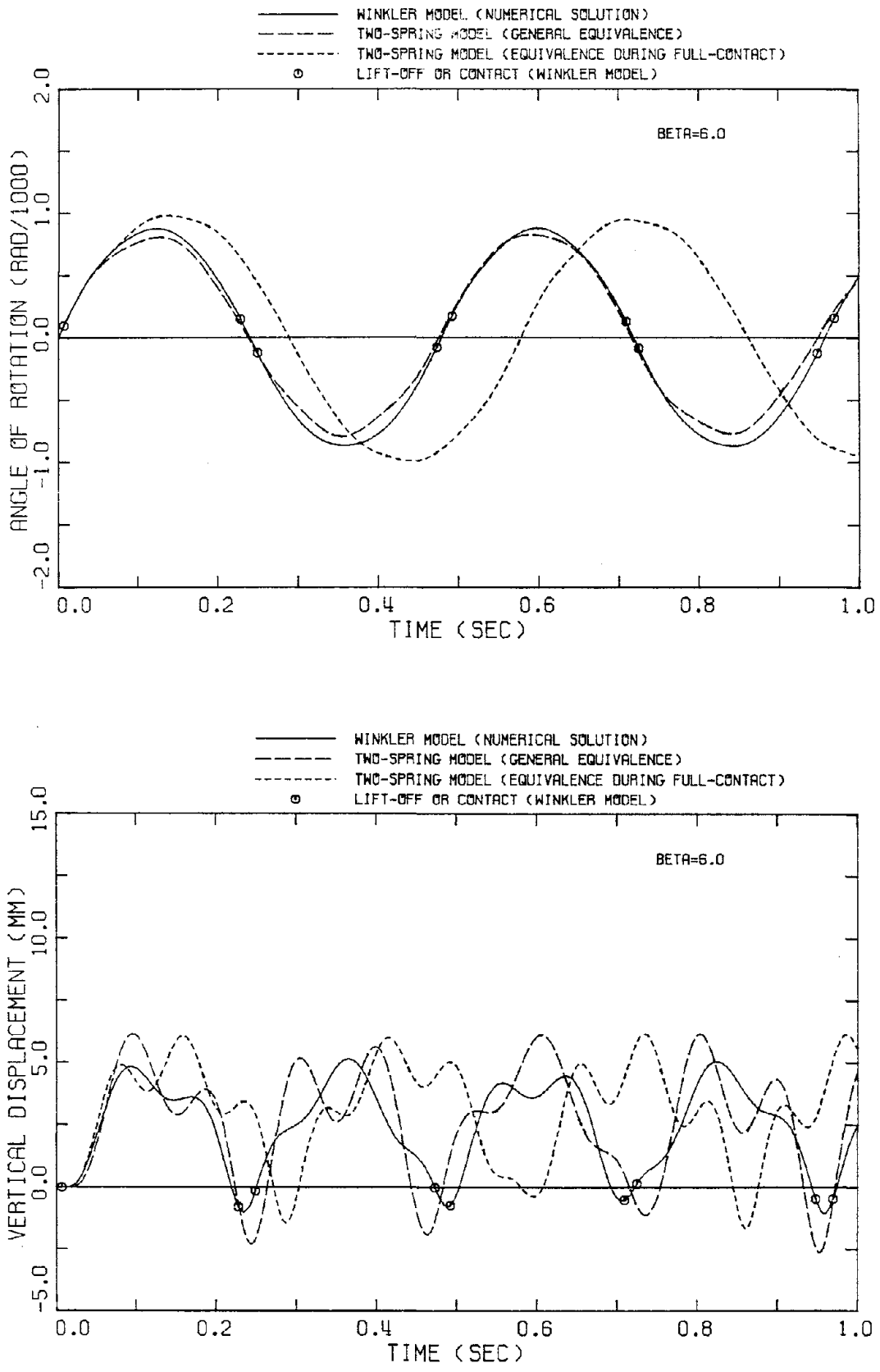

Fig. 2.5.8. Angle of rotation and vertical displacement of the center of mass for free, undamped oscillations of a simplified model of Millikan Library (β = 6).

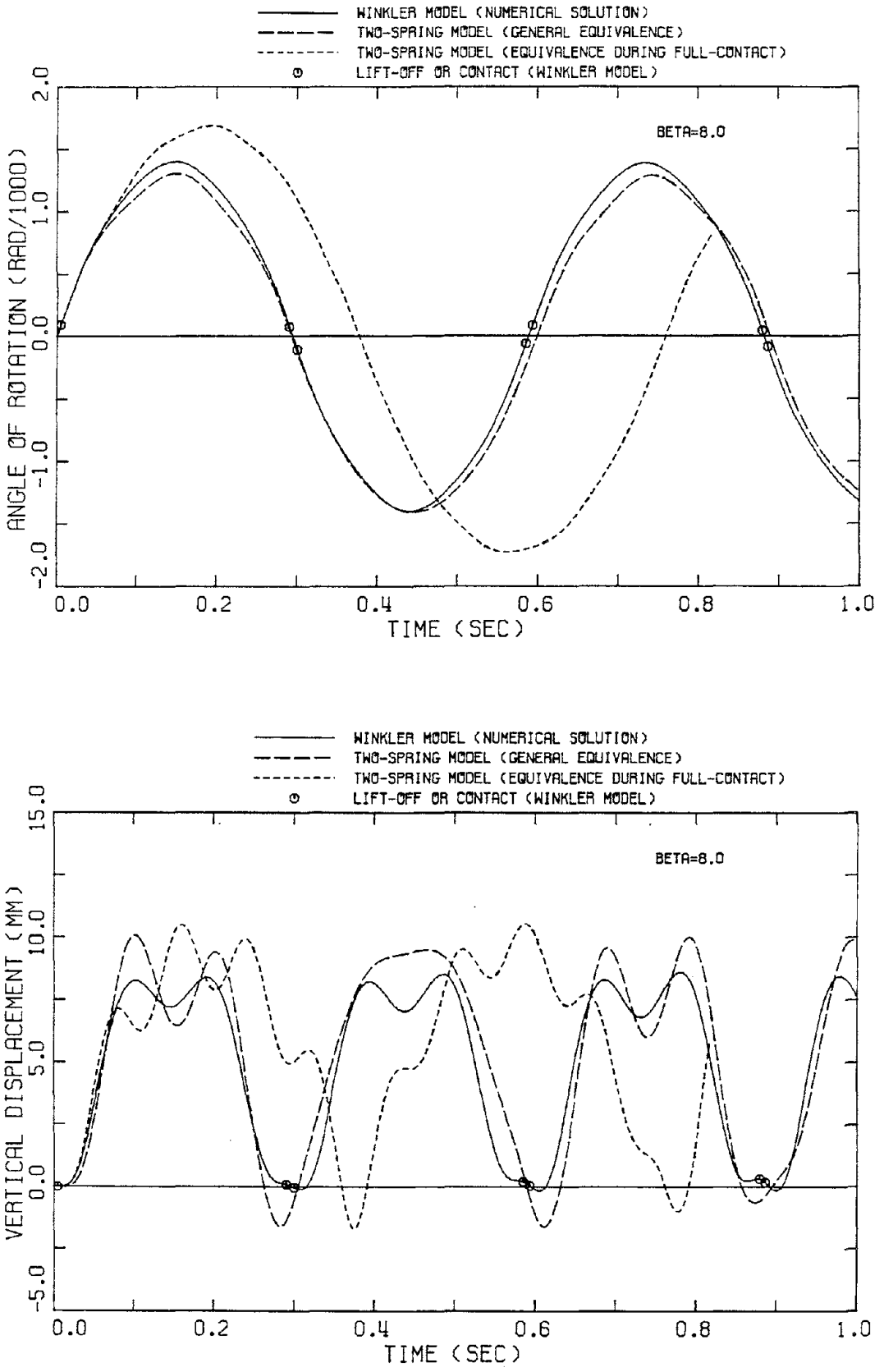

Fig. 2.5.9. Angle of rotation and vertical displacement of the center of mass for free, undamped oscillations of a simplified model of Millikan Library (β = 8).

These plots illustrate that the two-spring model, defined by equations (2.5.14) and (2.5.15) (general equivalence) can estimate very well the response of the Winkler system for practically all values of β. Equations (2.5.6) and (2.5.7) (equivalence during full-contact only), on the other hand, do not give very satisfactory results, especially for large values of β.

It is interesting to notice that the matching between the responses of the two systems is much better in the rocking direction than the vertical one. From the engineering point of view, however, one is normally more interested in the rocking response of the system, rather than the vertical motion. Under this assumption, the results of the general equivalence are very satisfactory.

The response of the two systems, initially at rest, to a horizontal harmonic excitation is shown in Fig. 2.5.10. The ground acceleration in this example was

$$\ddot{x}_G = -0.5g \times \sin\left(\frac{2\pi}{0.2}\, t\right) \tag{2.5.29}$$

where t is in seconds. In order to calculate the appropriate value of β, the following expression for ϕ^c_{max} was used

$$\phi^c_{max} = \frac{mha_0}{I_M p_1^* \left(\omega_0 - p_1^*\right)} \sin\left(\frac{2\pi\omega_0}{\omega_0 + p_1^*}\right) \tag{2.5.30}$$

in which ω_0 is the frequency of the exciting acceleration and a_0 is its amplitude. Equation (2.5.30) actually gives the first maximum value of $\phi(t)$, which would happen if lift-off were not allowed

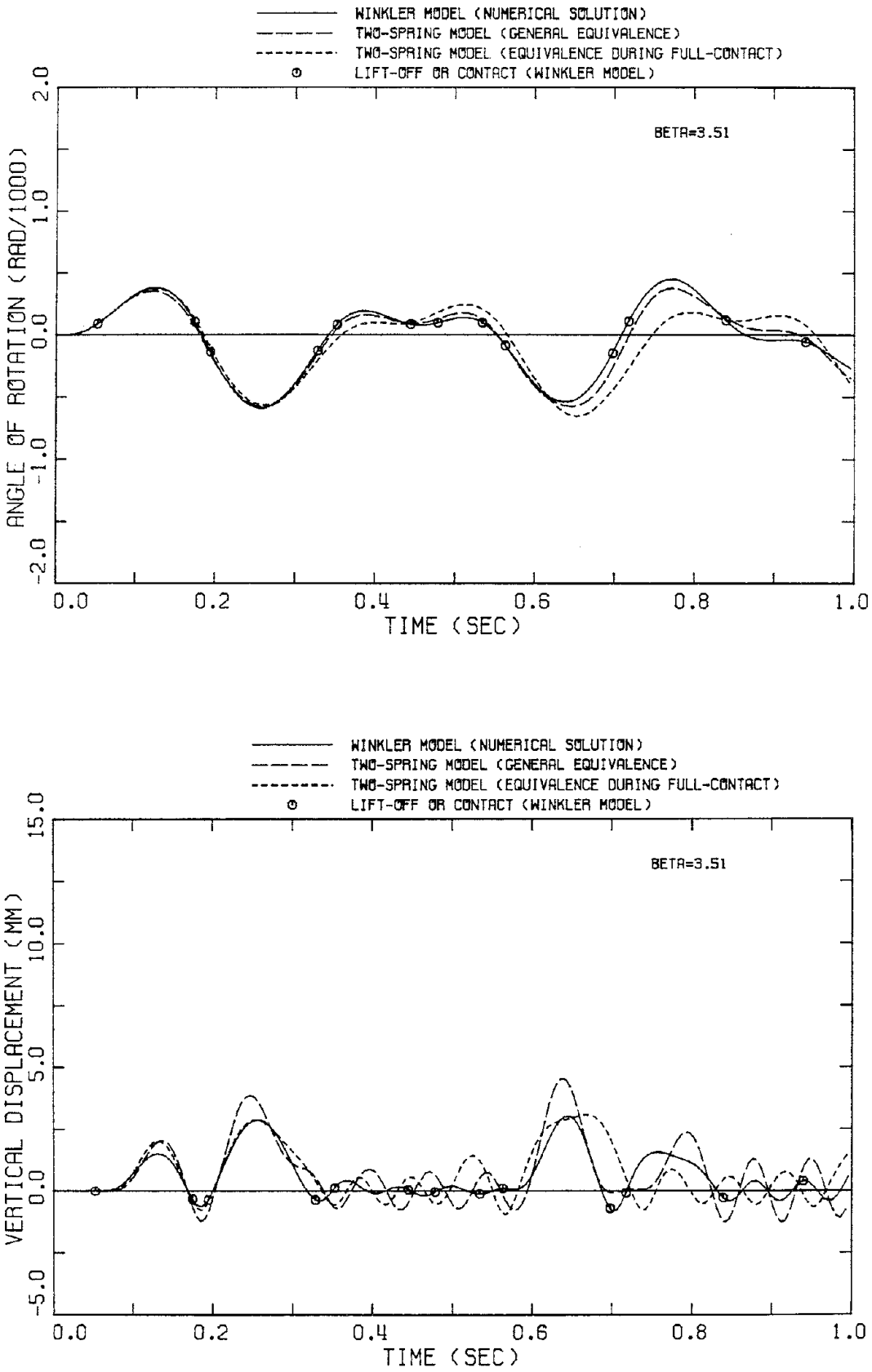

Fig. 2.5.10. Angle of rotation and vertical displacement of the center of mass for forced, undamped vibrations of a simplified model of Millikan Library (horizontal harmonic excitation).

(Winkler foundation). General equivalence again gives good results, especially for the rocking response.

Finally, the significance of lift-off on the behavior of the system is illustrated in Figs. 2.5.11, 2.5.12 and 2.5.13 where the effect of lift-off on the angle of rotation and the horizontal, relative roof acceleration ($=b\ddot{\phi}$) is shown. The Winkler model was used for these examples. The dotted lines were found using equation (2.4.8) for all times. The harmonic excitation used in the results shown in Fig. 2.5.13 is defined by equation (2.5.29). It seems that uplift tends to decrease the rocking acceleration, but the rotation can be larger or smaller, depending on the excitation.

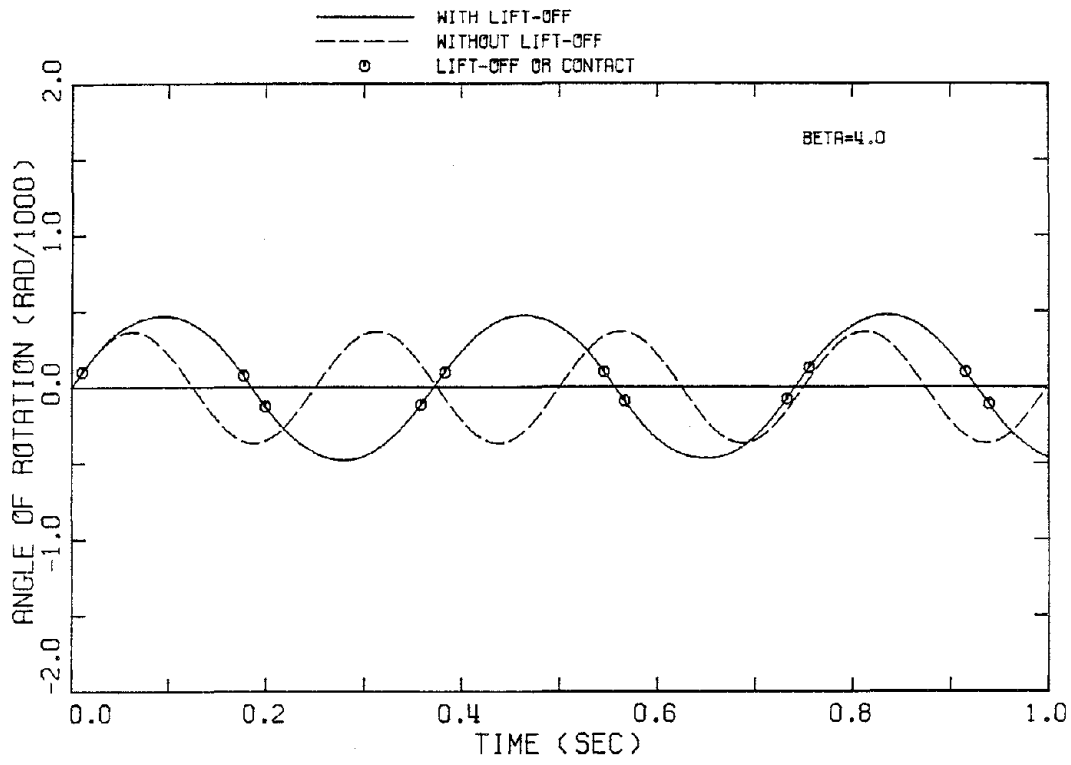

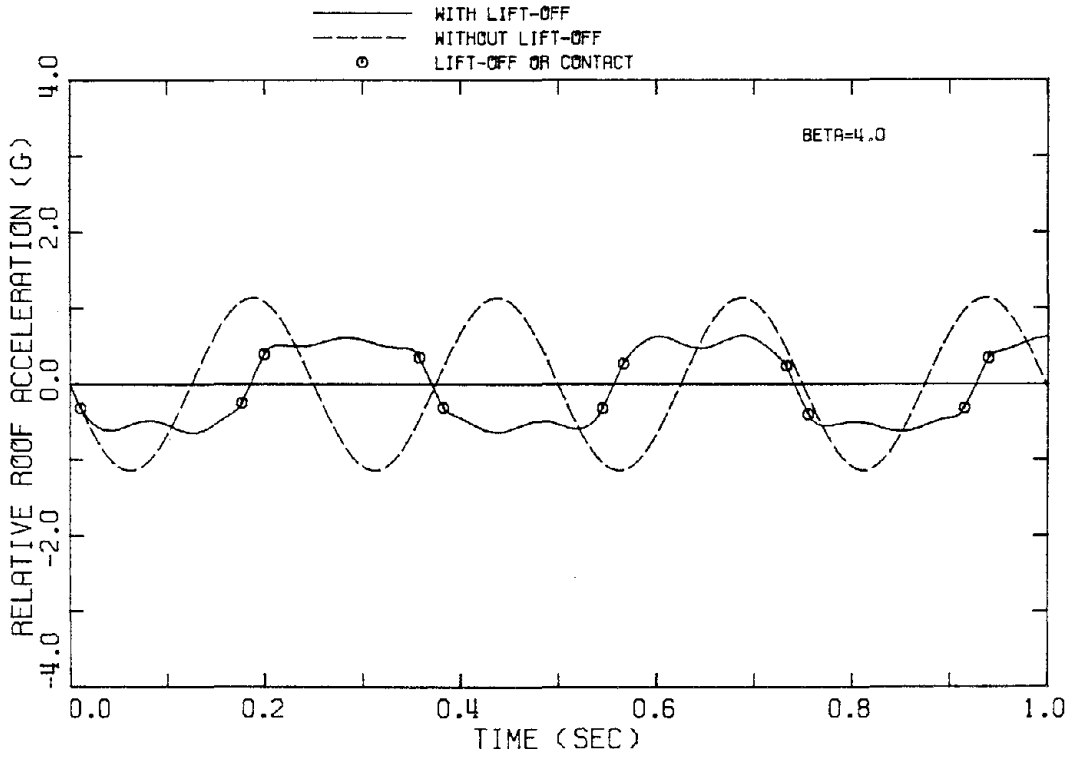

Fig. 2.5.11. Effect of lift-off on the angle of rotation and the horizontal, relative roof acceleration in the case of free vibrations ($\beta = 4$).

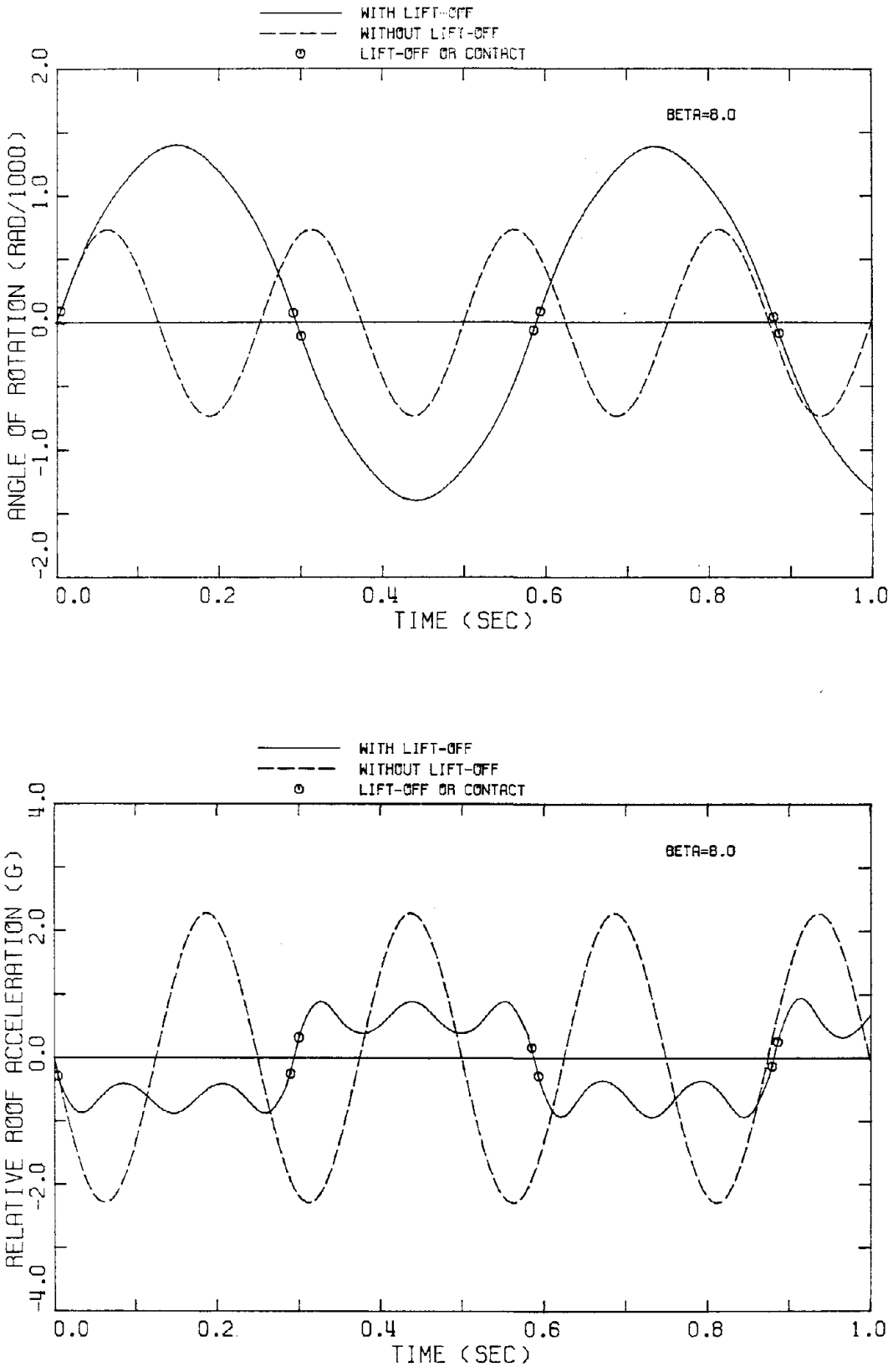

Fig. 2.5.12. Effect of lift-off on the angle of rotation and the horizontal, relative roof acceleration in the case of free vibrations (β = 8).

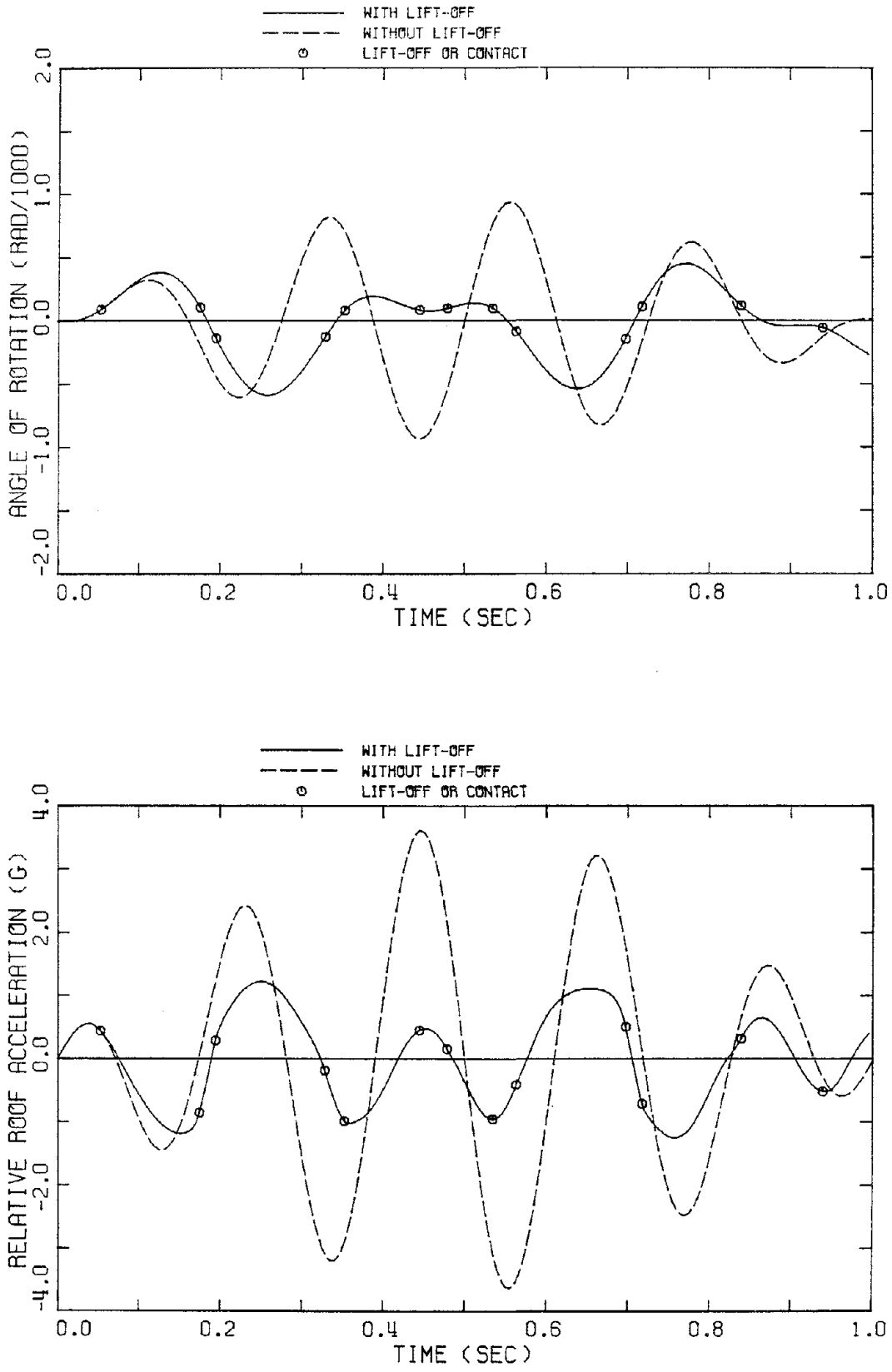

Fig. 2.5.13. Effect of lift-off on the angle of rotation and the horizontal, relative roof acceleration for harmonic excitation.

CHAPTER III

ENERGY DISSIPATING FOUNDATION MODELS

3.1 INTRODUCTION

During the earthquake response of buildings and other structures there is always some energy dissipated in the foundation because of inelastic behavior of the soil and radiation of energy through wave propagation. In very strong shaking, the energy dissipated in the foundation may in some cases be one of the more important factors in the overall response. For example, it seems that the effect of nonlinear soil behavior was one of the main reasons for the successful performance of building 41 during the San Fernando earthquake of 1971 (see Ref. 3). Furthermore, the phenomenon of radiation damping can occur for a linear or nonlinear material and is a well-established concept. The relative importance of radiation damping, in comparison to other mechanisms of energy dissipation in earthquake response, is not yet clearly understood, but there appear to be conditions under which the effect can be very large.[54]

In the simple case of a rigid block rocking on a rigid foundation, energy is dissipated every time that the pole of rotation changes from one corner of the base to the other, because of the assumed inelastic impact (see section 2.2). In contrast, the idealized models supported by elastic springs, which were used in the previous chapter to model the effects of flexible foundations, do not allow dissipation of energy and are different in this regard. In this chapter, some energy dissipating mechanisms are added to these models and their effect on the

response of the block is examined.

The first way to dissipate energy, which is studied in section 3.2, is by introducing dashpots into the models. Although viscous damping often does not have a direct physical meaning in structural dynamics, it is an attractive approach because of its simplicity and it is extensively used for modeling the hysteretic behavior of materials (e.g., equivalent viscous damping). In this first analysis, dashpots are connected in parallel with the springs for both the Winkler and the two-spring model. It should be mentioned here that the problem of assigning realistic numerical values to the spring and dashpot constants is by no means trivial and requires a careful analysis. Even for the simplest case, in which the soil is modeled by an elastic half-space, modeling by springs and dashpots implies frequency dependent coefficients (for example, see Ref. 39). In many applications, however, it seems acceptable to use representative, constant coefficients rather than coefficients depending on frequency; the resulting advantage is constant coefficients in the differential equations of motion. In the analysis that follows, the parameters of both the springs and dashpots are assumed constant and known.

Another way to introduce dissipation of energy in the foundation is by incorporating inelastic behavior into the springs. Conceptually, such an approach is probably the best way to consider the hysteretic behavior of the soil. However, its implementation involves many difficulties and it does not seem to be an attractive approach for use in design. Even the simplest case of an elastic, perfectly plastic, two-spring foundation, which is examined in section 3.3, appears unattractive

because of the many cases which should be taken under consideration.

Finally, in section 3.4 an impact mechanism is introduced into the spring foundation models which dissipates energy each time that full contact is reestablished after lift-off. As was mentioned earlier, energy is dissipated in this way during the limiting case of the rocking of a block on a rigid foundation. In addition, if the foundation were an elastic half-space, each impact would generate a pulse radiating away from the foundation toward infinity. The impact mechanism discussed in this section is introduced into the spring models of the foundation in an effort to simulate this radiation damping. Although a simple impact mechanism can be introduced without much difficulty, it seems that the effect can be modeled well by the simpler dashpot mechanism of the proceeding section.

3.2 VISCOUS DAMPING

3.2.1 Two-Spring Foundation

In Fig. 3.2.1a a rocking block on a viscously damped two-spring foundation is shown. All the assumptions used in the previous chapter (undamped case) also apply here. For the case of full-contact, the linearized equations of motion can be written as

$$m\ddot{y} + 2c\dot{y} + 2ky = -m\ddot{y}_G \tag{3.2.1}$$

$$I_M\ddot{\phi} + 2c\xi^2\dot{\phi} + (2k\xi^2 - mgh)\phi = -mh\ddot{x}_G \tag{3.2.2}$$

The solution of these equations is

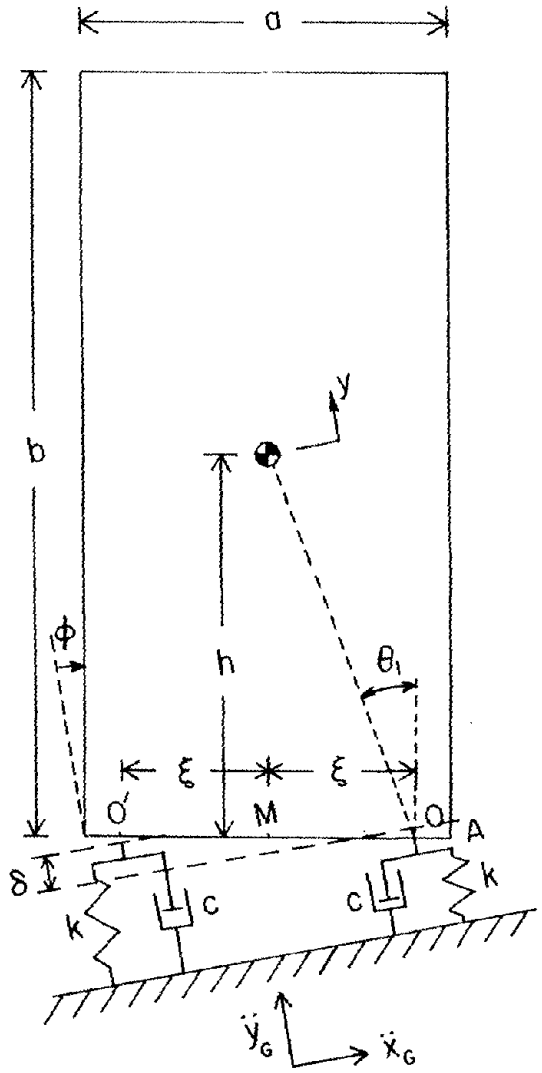

(a) Two-spring foundation

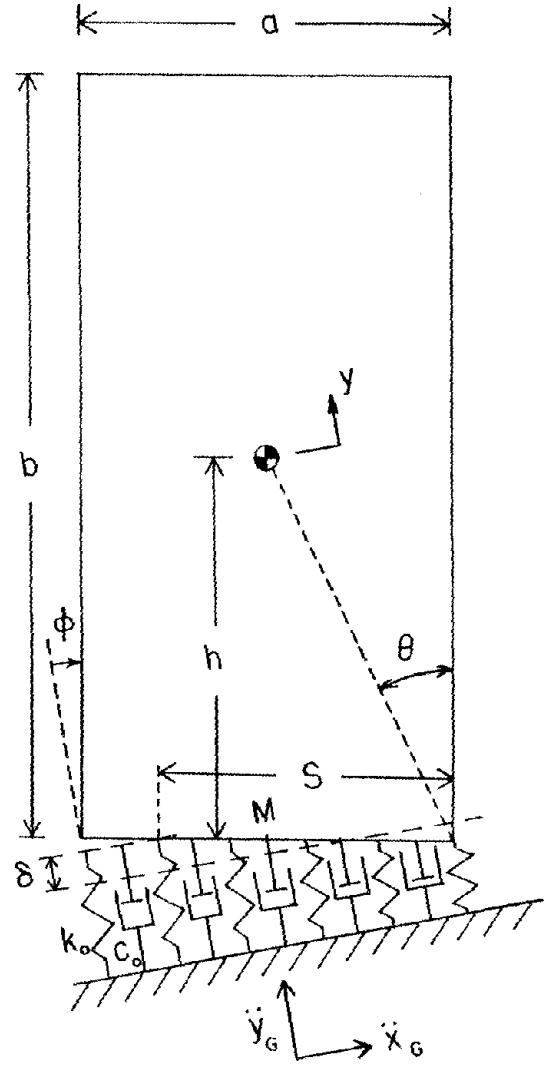

(b) Winkler foundation

Fig. 3.2.1. Rocking block on viscously damped spring foundations.

$$y(t) = e^{-\zeta_2 p_2 t}\left[y(0)\cos p_{2d}t + \left(\frac{\dot{y}(0)}{p_{2d}} + \frac{\zeta_2}{\sqrt{1-\zeta_2^2}}\,y(0)\right)\sin p_{2d}t\right]$$

$$- \frac{1}{p_{2d}}\int_0^t e^{-\zeta_2 p_2(t-\tau)}\,\ddot{y}_G(\tau)\sin p_{2d}(t-\tau)\,d\tau \qquad (3.2.3)$$

$$\phi(t) = e^{-\zeta_1 p_1 t}\left[\phi(0)\cos p_{1d}t + \left(\frac{\dot{\phi}(0)}{p_{1d}} + \frac{\zeta_1}{\sqrt{1-\zeta_1^2}}\,\phi(0)\right)\sin p_{1d}t\right]$$

$$- \frac{mh}{I_M\, p_{1d}}\int_0^t e^{-\zeta_1 p_1(t-\tau)}\,\ddot{x}_G(\tau)\sin p_{1d}(t-\tau)\,d\tau \qquad (3.2.4)$$

in which p_1 and p_2 are the undamped natural frequencies given by expressions (2.3.24) and (2.3.25), respectively, and

$$\zeta_1 = \frac{c\xi^2}{\sqrt{I_M(2k\xi^2 - mgh)}} \qquad (3.2.5)$$

$$\zeta_2 = \frac{c}{\sqrt{2km}} \qquad (3.2.6)$$

$$p_{1d} = p_1\sqrt{1-\zeta_1^2} \qquad (3.2.7)$$

$$p_{2d} = p_2\sqrt{1-\zeta_2^2} \qquad (3.2.8)$$

Comparing the damping coefficients for rocking, ζ_1, and vertical motion, ζ_2, one can write

$$\frac{\zeta_1}{\zeta_2} = \sqrt{\frac{\lambda}{1 - \alpha}} \tag{3.2.9}$$

where $\lambda = m\xi^2/I_M$ and $\alpha = \phi_{cr}/\theta_1$, ϕ_{cr} being the critical angle at which lift-off happens in the absence of vertical oscillations and θ_1 being the critical angle at which overturning occurs. As was discussed in section 2.3.6, λ diminishes as the aspect ratio b/a increases and becomes much less than one for slender blocks (see Fig. 2.3.6). Also, $\alpha << 1$, except for unrealistically soft springs. Therefore, equation (3.2.9) implies that the fraction of critical damping in rocking is significantly smaller than that for vertical vibrations, i.e., the damping in the foundation affects the rocking response of the block much less than the vertical vibrations.

After lift-off, the linearized equations of motion can be written in matrix form as (for positive angles of rotation)

$$[M]\ddot{\underset{\sim}{r}} + [C]\dot{\underset{\sim}{r}} + [K]\underset{\sim}{r} = \underset{\sim}{F} \tag{3.2.10}$$

in which

$$[M] = \begin{bmatrix} m & 0 \\ 0 & I_M/\xi^2 \end{bmatrix} \tag{3.2.11}$$

$$[C] = c\begin{bmatrix} 1 & -1 \\ -1 & 1 \end{bmatrix} \tag{3.2.12}$$

$$[K] = k\begin{bmatrix} 1 & -1 \\ -1 & 1-\alpha \end{bmatrix} \tag{3.2.13}$$

$$\underset{\sim}{F} = \begin{Bmatrix} -m\ddot{y}_G - \frac{1}{2}mg \\ -m\frac{h}{\xi}\ddot{x}_G - \frac{1}{2}mg \end{Bmatrix} \tag{3.2.14}$$

$$\underset{\sim}{r} = \begin{Bmatrix} y \\ \xi\phi \end{Bmatrix} \tag{3.2.15}$$

In the general case, in which α cannot be neglected in comparison with unity, uncoupling of the equations using principal coordinates is not possible (for a general criterion see [56]). In this case, the Laplace transform could be used for the solution of equation (3.2.10). However, for a wide range of the values of the parameters expected to be encountered in practice, a simpler approximate solution can be found as follows.

Let μ_1 and μ_2 be the eigenvalues of the matrix $[M]^{-1}[K]$ given by

$$\mu_{1,2} = \frac{k}{2m}\left\{1 + \lambda(1-\alpha) \pm \sqrt{[1+\lambda(1-\alpha)]^2 + 4\alpha^2\lambda^2}\right\} \tag{3.2.16}$$

and let $\underset{\sim}{\eta}^{(1)}$ and $\underset{\sim}{\eta}^{(2)}$ be the corresponding eigenvectors which can be written as

$$\underset{\sim}{\eta}^{(i)} = \begin{Bmatrix} \sqrt{\dfrac{\lambda}{m[\lambda + (1-\tilde{\mu}_i)^2]}} \\ (1-\tilde{\mu}_i)\sqrt{\dfrac{\lambda}{m[\lambda + (1-\tilde{\mu}_i)^2]}} \end{Bmatrix}, \quad i = 1,2 \tag{3.2.17}$$

in which

$$\tilde{\mu}_i = \mu_i/(k/m) \qquad , \quad i = 1,2 \tag{3.2.18}$$

and the normalization

$$\underset{\sim}{\eta}^{(i)T}[M]\underset{\sim}{\eta}^{(j)} = \delta_{ij} \tag{3.2.19}$$

has been used, δ_{ij} being the Kronecker delta. Equation (3.2.10) can then be written as

$$[I]\ddot{\underset{\sim}{q}} + [N]^T[C][N]\dot{\underset{\sim}{q}} + [\tilde{\mu}_i]\underset{\sim}{q} = [N]^T\underset{\sim}{F} \tag{3.2.20}$$

where [I] is the unit matrix, [N] is the modal matrix defined by

$$[N] = [\underset{\sim}{\eta}^{(1)} \quad \underset{\sim}{\eta}^{(2)}] \tag{3.2.21}$$

and $\underset{\sim}{r} = [N]\underset{\sim}{q}$. The damping matrix in this equation can be expressed as

$$[N]^T[C][N] = \frac{\lambda c}{m}\begin{bmatrix} c_{11} & -c_{12} \\ -c_{12} & c_{22} \end{bmatrix}$$

$$= \frac{\lambda c}{m}\begin{bmatrix} \dfrac{\tilde{\mu}_1^2}{\lambda + (1-\tilde{\mu}_1)^2} & \dfrac{\tilde{\mu}_1\tilde{\mu}_2}{\sqrt{[\lambda + (1-\tilde{\mu}_1)^2][\lambda + (1-\tilde{\mu}_2)^2]}} \\ \dfrac{\tilde{\mu}_1\tilde{\mu}_2}{\sqrt{[\lambda + (1-\tilde{\mu}_1)^2][\lambda + (1-\tilde{\mu}_2)^2]}} & \dfrac{\tilde{\mu}_2^2}{\lambda + (1-\tilde{\mu}_2)^2} \end{bmatrix} \tag{3.2.22}$$

In Figs. 3.2.2 and 3.2.3, the ratios c_{11}/c_{12} and c_{12}/c_{22} are plotted versus α for several values of λ. The maximum value of α was taken equal to one, since overturning happens before lift-off for $\alpha > 1$. It is clear from these plots that $c_{11} >> c_{12}$ and $c_{12} >> c_{22}$ for most combinations of λ and α, therefore, one can write,

$$[N]^T[C][N] \simeq \frac{\lambda c}{m}\begin{bmatrix} \dfrac{\tilde{\mu}_1^2}{\lambda + (1-\tilde{\mu}_1)^2} & 0 \\ \dfrac{\tilde{\mu}_1\tilde{\mu}_2}{\sqrt{[\lambda + (1-\tilde{\mu}_1)^2][\lambda + (1-\tilde{\mu}_2)^2]}} & 0 \end{bmatrix} \tag{3.2.23}$$

In this case, the solution of the matrix equation (3.2.20) can be written as

$$q_1(t) = e^{-\zeta_r P_2 t}\left[q_1(0)\cos P_{2d}t + \left(\frac{\dot{q}_1(0)}{P_{2d}} + \frac{\zeta_r}{\sqrt{1-\zeta_r^2}}\, q_1(0)\right)\sin P_{2d}t\right]$$

$$- \frac{1}{P_{2d}}\sqrt{\frac{\lambda m}{\lambda + (1-\tilde{\mu}_1)^2}}\int_0^t\left[\ddot{y}_G(\tau) + (1-\tilde{\mu}_1)\,\frac{h}{\xi}\,\ddot{x}_G(\tau) + \left(1 - \frac{\tilde{\mu}_1}{2}\right)g\right]$$

$$\times\ e^{-\zeta_r P_2(t-\tau)}\sin P_{2d}(t-\tau)\,d\tau \tag{3.2.24}$$

and

$$q_2(t) = q_2(0)\cosh P_1 t + \frac{\dot{q}_2(0)}{P_1}\sinh P_1 t\ -$$

$$- \frac{1}{P_1}\int_0^t\left[\frac{\lambda c\tilde{\mu}_1\tilde{\mu}_2\dot{r}_1(\tau)}{m\sqrt{[\lambda + (1-\tilde{\mu}_1)^2][\lambda + (1-\tilde{\mu}_2)^2]}}\ -\right.$$

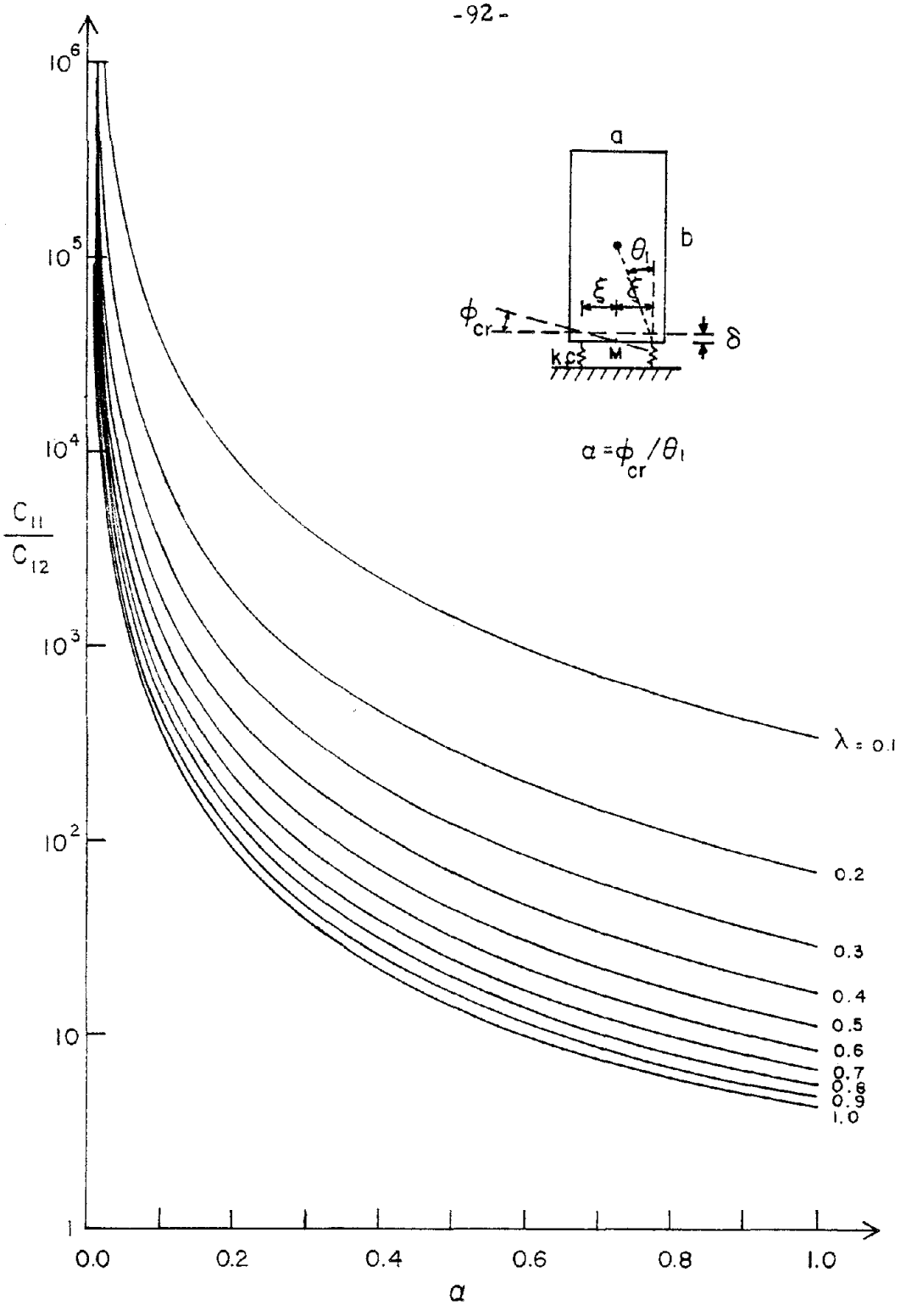

Fig. 3.2.2. Variation of c_{11}/c_{12} with α and λ.

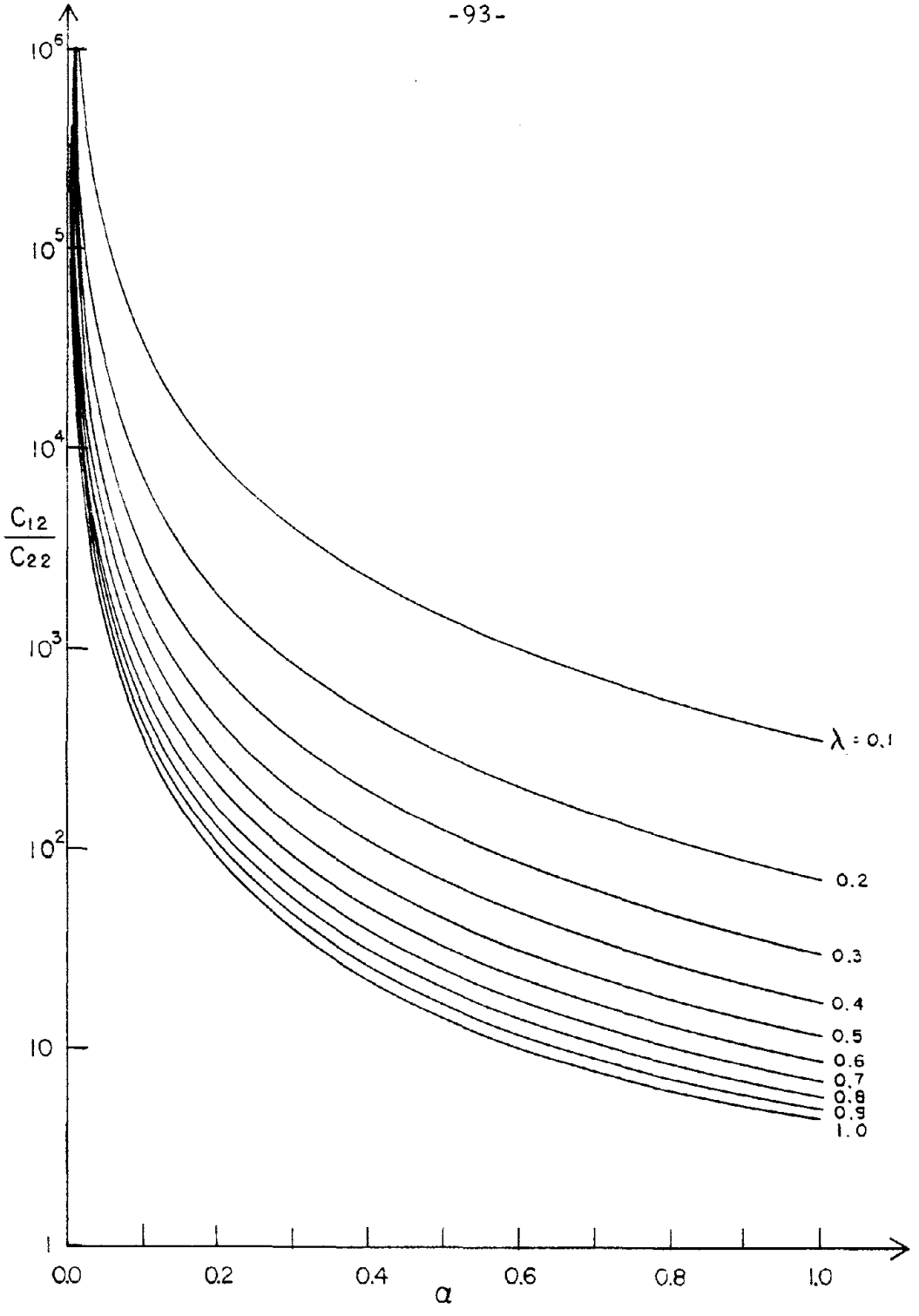

Fig. 3.2.3. Variation of c_{12}/c_{22} with α and λ.

$$- \sqrt{\frac{\lambda m}{\lambda + (1-\tilde{\mu}_2)^2}} \left[\ddot{y}_G(\tau) + (1-\tilde{\mu}_2) \frac{h}{\xi} \ddot{x}_G(\tau) + \left(1 - \frac{\tilde{\mu}_2}{2}\right) g \right] \sinh P_1(t-\tau)\, d\tau \tag{3.2.25}$$

where

$$P_1^2 = -\mu_2 \tag{3.2.26}$$

$$P_2^2 = \mu_1 \tag{3.2.27}$$

$$\zeta_r = \frac{c\lambda \sqrt{\tilde{\mu}_1^3}}{2\sqrt{km}\,[\lambda + (1-\tilde{\mu}_1)^2]} \tag{3.2.28}$$

$$P_{2d} = P_2 \sqrt{1 - \zeta_r^2} \tag{3.2.29}$$

and the origin of the time corresponds to the onset of lift-off. After the vector $\underset{\sim}{q}$ has been found, the response of the system can be determined by

$$\underset{\sim}{r}(t) = [N]\ \underset{\sim}{q}(t) \tag{3.2.30}$$

A much simpler solution can be given in the special case in which α can be neglected in comparison with one. In that case, it is convenient to use the downward displacement, Y, of point O (see Fig. 3.2.1a), measured from the equilibrium position and given by

$$Y = \xi\phi - y \tag{3.2.31}$$

instead of y. The equations of motion after lift-off can then be written in terms of ϕ and Y as

$$\ddot{Y} + \frac{c}{m}\frac{I_o}{I_M}\dot{Y} + \frac{k}{m}\frac{I_o}{I_M} Y = - \frac{mh\xi}{I_M} \ddot{x}_G + \ddot{y}_G + g\left(1 - \frac{I_o}{2I_M}\right) \tag{3.2.32}$$

$$I_o\ddot{\phi} = m\xi\ddot{Y} - mh\ddot{x}_G - m\xi\ddot{y}_G - mg\xi \tag{3.2.33}$$

The solution of equation (3.2.32) may be written as

$$Y(t) = e^{-\frac{1}{2}\zeta_2 p_2(1+\lambda)t}\left[\left(Y(0) - \delta\,\frac{(1-\lambda)}{(1+\lambda)}\right)\cos p_2\,\frac{(1+\lambda)}{2}\sqrt{\frac{2}{1+\lambda} - \zeta_2^2}\;t\right.$$

$$\left. + \frac{1}{\sqrt{\frac{2}{1+\lambda} - \zeta_2^2}}\left(\frac{2\dot{Y}(0)}{p_2(1+\lambda)} + \zeta_2 Y(0)\right)\sin p_2\,\frac{(1+\lambda)}{2}\,\sqrt{\frac{2}{1+\lambda} - \zeta_2^2}\;t\right]$$

$$- \frac{2}{p_2(1+\lambda)\sqrt{\frac{2}{1+\lambda} - \zeta_2^2}}\int_0^t e^{-\frac{1}{2}\zeta_2 p_2(1+\lambda)t}\left(\frac{mh\xi}{I_M}\,\ddot{x}_G(\tau) - \ddot{y}_G(\tau)\right)$$

$$\times\quad \sin p_2\,\frac{(1+\lambda)}{2}\quad\sqrt{\frac{2}{1+\lambda} - \zeta_2^2}(t-\tau)\,d\tau + \delta\left(\frac{1-\lambda}{1+\lambda}\right) \tag{3.2.34}$$

while double integration of equation (3.2.33) gives

$$\phi(t) = \frac{m\xi}{I_o}\left[Y(t) - \frac{h}{\xi}\,x_G(t) - y_G(t) - \frac{g}{2}\,t^2 + C_1 t + C_2\right] \tag{3.2.35}$$

in which

$$\left.\begin{aligned} C_1 &= \frac{I_o}{m\xi}\,\dot{\phi}(0) - \dot{Y}(0) + \frac{h}{\xi}\,\dot{x}_G(0) + \dot{y}_G(0) \\ C_2 &= \frac{I_o}{m\xi}\,\phi(0) - Y(0) + \frac{h}{\xi}\,x_G(0) + y_G(0) \end{aligned}\right\} \tag{3.2.36}$$

As was discussed in section 2.3.6, wherein the free oscillations of the corresponding undamped case were studied, the bracketed term in the right hand side of equation (3.2.34) can be neglected for many applications when Y(t) is substituted in equation (3.2.35). Then, for the free oscillations of the block, equation (3.2.35) implies that the

rocking response can be again approximated by an inverted parabola. Since the vertical oscillation has been neglected in the rocking motion, the motion after lift-off does not generate significant forces in the one dashpot that is still engaged. As a result, the effect of damping on this solution arises only in the initial rocking velocity (at the time of lift-off), $\dot{\phi}(0)$, which affects the value of the coefficient C_1. A more detailed analysis may be performed in this case, similar to the one done in section 2.3.6, and the apparent ratio of critical damping in rocking may be determined. This is done in the following analysis, to first order accuracy.

Let us assume that ζ_1 is small, so that terms including powers of ζ_1 greater than one can be neglected. Then one can write

$$p_{1d} \simeq p_1$$

and for a horizontal impulse excitation, equation (3.2.4) reduces to

$$\phi(t) = \phi^c_{max}\, e^{-\zeta_1 p_1 t} \sin p_1 t \qquad (3.2.37)$$

in which $\phi^c_{max} = \dot{\phi}(0)/p_1$. The time, t_o, at which lift-off first happens can then be given by the solution of equation

$$e^{-\zeta_1 p_1 t_o} \sin p_1 t_o = \frac{1}{\beta} \qquad (3.2.38)$$

in which $\beta = \phi^c_{max}/\phi_{cr}$ and $\phi_{cr} = \delta/\xi$. The angular velocity at that time is

$$\dot{\phi}(t_o) = \phi_{cr}\, p_1 \left(-\zeta_1 + \sqrt{\beta^2\, e^{-2\zeta_1 p_1 t_o} - 1} \right) \qquad (3.2.39)$$

Substituting into equations (3.2.36), the angle of rotation after lift-

off can be expressed as

$$\phi(t) = \frac{\lambda}{\xi(1+\lambda)}\left[-\frac{g}{2}t^2 + \frac{\delta}{\lambda}\left(-\zeta_1 + \sqrt{\beta^2 e^{-2\zeta_1 p_1 t_o} - 1}\right)p_1 t + \delta\left(\frac{1}{\lambda} + \frac{1-\lambda}{1+\lambda}\right)\right] \tag{3.2.40}$$

which comes from equation (3.2.35) after the harmonic part of Y(t) was neglected. This function obtains its maximum value at time, t_1, given by

$$t_1 = \frac{1}{p_1}\left(-\zeta_1 + \sqrt{\beta^2 e^{-2\zeta_1 p_1 t_o} - 1}\right) \tag{3.2.41}$$

Substituting into (3.2.40), the maximum value of the angle of rotation can be determined by

$$\phi_{max} = \phi_{cr}\left[\frac{\beta^2 e^{-2\zeta_1 p_1 t_o} - 2\zeta_1\sqrt{\beta^2 e^{-2\zeta_1 p_1 t_o} - 1} + 1}{2(1+\lambda)} + \frac{\lambda(1-\lambda)}{(1+\lambda)^2}\right] \tag{3.2.42}$$

Recall that for the undamped case it was found that the apparent rocking response can be expressed as

$$\phi^u(t) = \phi^u_{max} \sin pt \tag{3.2.43}$$

where

$$\phi^u_{max} = \phi_{cr}\left[\frac{\beta^2+1}{2(1+\lambda)} + \frac{\lambda(1-\lambda)}{(1+\lambda)^2}\right] \tag{3.2.44}$$

and $p = 2\pi/T$ is the apparent rocking frequency. An expression for T is given by equation (2.3.76).

Now, for the damped case, let ζ be the apparent fraction of critical damping. Assuming that ζ is small, one can write

$$\phi(t) = \phi^{u}_{max}\, e^{-\zeta pt} \sin pt \tag{3.2.45}$$

This function attains its maximum value when

$$pt = \tan^{-1}\left(\frac{1}{\zeta}\right) \tag{3.2.46}$$

Substituting into (3.2.45) and comparing with (3.2.42), the following equation in ζ can be obtained

$$\exp\left[-\zeta \tan^{-1}\left(\frac{1}{\zeta}\right)\right] \sin\left[\tan^{-1}\left(\frac{1}{\zeta}\right)\right] = \frac{\left(\beta^2 e^{-2\zeta_1 p_1 t_o} - 2\zeta_1 \sqrt{\beta^2 e^{-2\zeta_1 p_1 t_o} - 1} + 1\right)(1+\lambda) + 2\lambda(1-\lambda)}{(\beta^2+1)(1+\lambda) + 2\lambda(1-\lambda)} \tag{3.2.47}$$

The solution of this equation, which can be obtained by trial and error, will determine the value of the apparent ratio of critical damping. The effect of lift-off on this coefficient is shown in Fig. 3.2.4, where the ratio ζ/ζ_1 is plotted versus the normalized impulse, β, for $\lambda = 0.05$ and $\zeta_1 = 0.05$. After a small increase, which may be an error in the approximation, it is seen that the apparent damping decreases rapidly with amplitude.

This analysis can be applied to establish an equivalent linear system, similar to the one discussed in section 2.3.6. For this system lift-off is not allowed and the foundation stiffness and damping are such that the undamped rocking period is equal to T, which is given by equation (2.3.76), and the ratio of critical damping is ζ. Then the overall rocking response of the system to a horizontal excitation can be approximated by the rocking response of the equivalent linear system

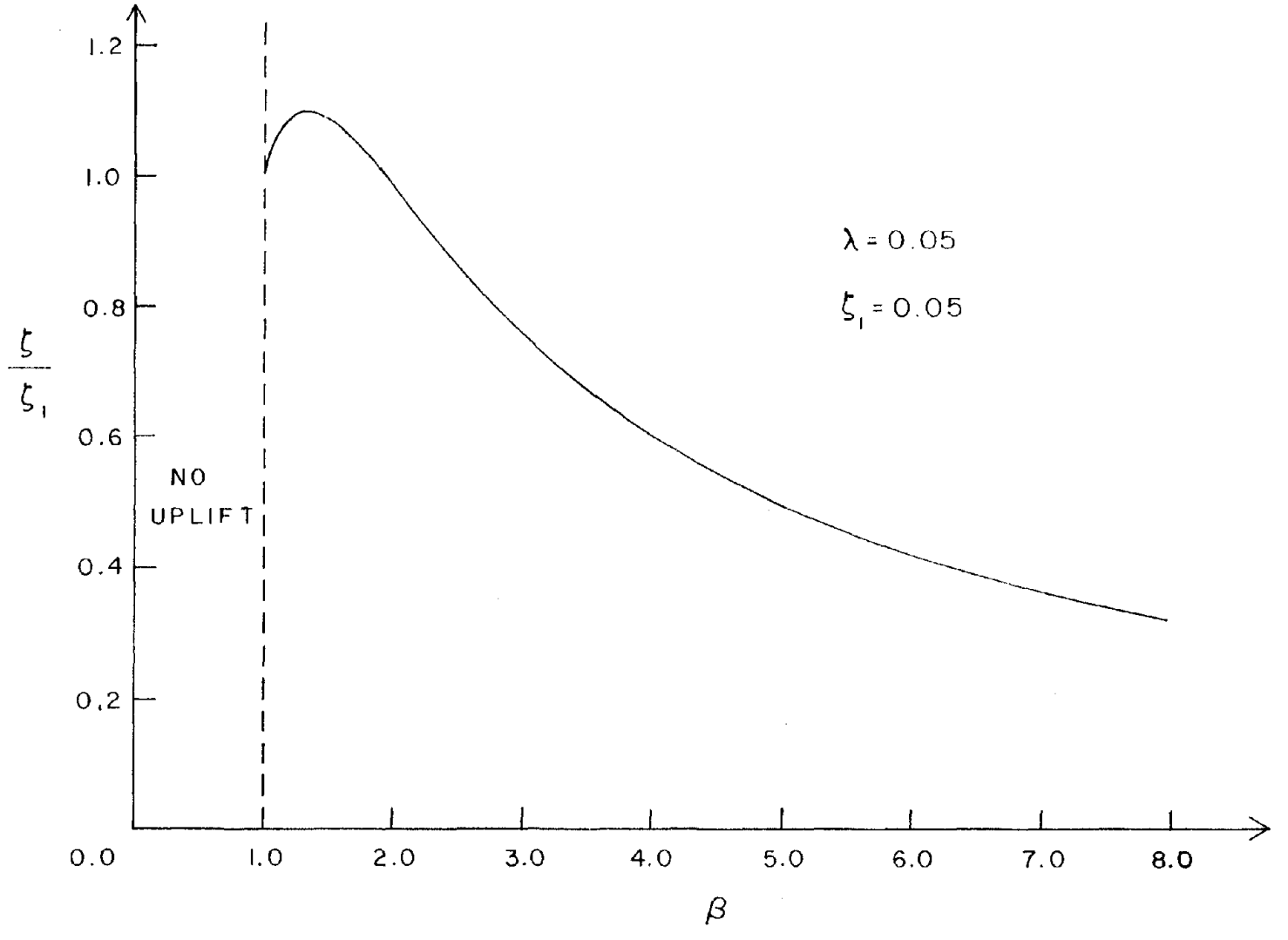

Fig. 3.2.4. Change of the apparent fraction of critical damping in rocking, ζ, with the normalized impulse, β (first order approximation).

multiplied by the correction factor, CF, given by (2.3.82).

3.2.2 Winkler Foundation

For the Winkler model, the dashpots are introduced in the foundation in parallel with the springs as shown in Fig. 3.2.1b. As in the undamped case, the equations of motion after lift-off are highly nonlinear and coupled and, apparently, they can only be solved numerically. Because of this complexity, the Winkler model is not an attractive model for simplified analyses. The linearized equations of motion during full contact and the fully nonlinear equations after lift-off are:

Full contact

$$m\ddot{y} + c_o a\dot{y} + k_o a y = -m\ddot{y}_G \tag{3.2.48}$$

$$I_M \ddot{\phi} + \frac{1}{12} c_o a^3 \dot{\phi} + k_o a\left(\frac{a^2}{12} - h\delta\right)\phi = -mh\ddot{x}_G \tag{3.2.49}$$

After lift-off

$$m\ddot{y} + c_o\left[\left(\frac{a}{2} + \frac{\delta}{\phi} - \frac{y}{\phi}\right)\dot{y} - \left(\frac{a^2}{8} - \frac{\delta^2}{2\phi^2} + \frac{\delta y}{\phi^2} - \frac{y^2}{2\phi^2}\right)\dot{\phi}\right]$$
$$+ k_o\left(\frac{a}{2}y - \frac{a^2}{8}\phi - \frac{\delta^2}{2\phi} + \frac{\delta y}{\phi} - \frac{y^2}{2\phi}\right) = -\frac{1}{2}mg - m\ddot{y}_G \tag{3.2.50}$$

$$\left(I_M + \frac{1}{2}mah\phi\right)\ddot{\phi} + c_o\left[\left(\frac{a^3}{24} - \frac{a^2h}{8}\phi + \frac{h\delta^2}{2\phi} + \frac{h\delta y}{\phi} + \frac{hy^2}{2\phi^2} + \frac{\delta^3}{3\phi^3} + \frac{y^3}{3\phi^3} + \frac{\delta^2 y}{\phi^3} + \frac{\delta y^2}{\phi^3}\right)\dot{\phi}\right.$$
$$\left. - \left(\frac{a^2}{8} - h\delta - \frac{ah}{2}\phi + hy - \frac{\delta^2}{2\phi^2} - \frac{y^2}{2\phi^2} + \frac{\delta y}{\phi^2}\right)\dot{y}\right] + k_o\left[\frac{a}{2}\left(\frac{a^2}{12} - h\delta\right)\phi\right.$$
$$\left. + \frac{ah}{2}y\phi - \left(\frac{a^2}{8} - h\delta\right)y - \frac{\delta^3}{6\phi^2} - \frac{\delta y^2}{2\phi^2} + \frac{\delta^2 y}{2\phi^2} + \frac{y^3}{6\phi^2} - \frac{hy^2}{2} - \frac{a^2}{8}h\phi^2\right]$$
$$+ \frac{1}{2}ma\ddot{x}_G\phi = -\frac{1}{2}k_o\delta\left(\frac{a^2}{4} - h\delta\right) - mh\ddot{x}_G \tag{3.2.51}$$

in which k_o and c_o are the spring and dashpot constants, respectively. The equations after lift-off, as given above, are valid only for positive angles of rotation.

For the full contact case, the equations of motion are uncoupled and can be solved directly. The undamped natural frequencies in rocking and vertical directions, p_1^* and p_2^*, are given by equations (2.4.9) and (2.4.10) and the corresponding damping coefficients are

$$\zeta_1^* = \frac{c_o a^2}{24} \sqrt{\frac{a}{k_o I_M \left(\frac{a^2}{12} - h\delta\right)}} \tag{3.2.52}$$

$$\zeta_2^* = \frac{c_o}{2} \sqrt{\frac{a}{k_o m}} \tag{3.2.53}$$

The ratio of these coefficients is

$$\frac{\zeta_2^*}{\zeta_2^*} = \sqrt{\frac{ma^2}{12\ I_M(1 - 3\alpha^*)}} \tag{3.2.54}$$

in which

$$\alpha^* = \frac{\phi_{cr}}{\theta}$$

$\phi_{cr} = \frac{2\delta}{a}$ is the critical angle at which lift-off happens in the absence of vertical oscillations and $\theta = \frac{a}{2h}$ is the overturning angle. For many applications $\alpha^* << 1$ and for slender structures, $ma^2 << 12\ I_M$. Under these conditions, equation (3.2.54) implies that the vertical oscillations during full contact are much more damped than rocking motions. Recall that the same conclusion was drawn for the two-spring foundation.

3.2.3 Equivalence between the Winkler Foundation and the Two-Spring Model

As in the undamped case, although the Winkler foundation is a commonly used model for the soil, it involves many difficulties when it is applied to the rocking of structures, because of the complicated equations of motion resulting from the varying area of contact. The two-spring foundation, on the other hand, leads to much simpler equations which can be solved analytically. An equivalence established between the two models, therefore, would allow using the two-spring model instead of the complicated continuous elastic foundation. As was discussed in the previous chapter, one seeks relations between the parameters of the two foundation models, such that the resultant vertical forces from the foundation and their points of application are the same in the two cases. For the damped problem, however, the forces resulted from the springs and the dashpots have to be distinguished and treated separately. In this way, three equations can be found for the determination of the three unknown parameters of the two-spring foundation, k, c, and ξ, in terms of the geometry of contact and the Winkler constants, k_o and c_o. Two different sets of relations can be found for the two regimes, before and after lift-off. The final expressions are:

Equivalence during full contact

$$k = \frac{k_o a}{2} \tag{3.2.55}$$

$$c = \frac{c_o a}{2} \tag{3.2.56}$$

$$\xi = \frac{a\sqrt{3}}{6} \tag{3.2.57}$$

Equivalence after lift-off

$$k = \frac{3}{4} k_o \tilde{S} \tag{3.2.58}$$

$$c = \frac{3}{4} c_o \tilde{S} \tag{3.2.59}$$

$$\xi = \frac{a}{2} - \frac{\tilde{S}}{3} \tag{3.2.60}$$

where $\tilde{S}$ is the average length of contact during uplift for the Winkler foundation. In Appendix I, an empirical formula for the estimation of $\tilde{S}$ was found for the case of undamped free oscillations [see equation (I.6)]. When damping exists, however, this formula cannot be applied directly because it is not clear which value of ϕ^c_{max} should be used. Under impulse loading, with damping, the average length of contact over each half cycle increases with

time, and eventually becomes equal to a (no lift-off). The uncertainty of the appropriate value of ϕ^c_{max} is even larger for a continuous random excitation. It is clear, however, from the example of section 2.5.6, that the equivalent two-spring model of the Winkler foundation is not very sensitive to the value of $\tilde{S}$. Also, from the engineering viewpoint, one is often primarily interested in the maximum amplitude of the response. Therefore, the maximum angle of rotation which would happen if lift-off were not allowed is suggested for the calculation of $\tilde{S}$. This value can be thought of as an estimate of the average length of contact during the half cycle at which this maximum rocking amplitude occurs. In this way, $\tilde{S}$ can be estimated by equation (I.6) with ϕ^c_{max} calculated by the solution of equation (3.2.49) or, directly, by means of response spectra.

General equivalence

For a general equivalence, the expression found for the two different regimes of full contact and uplift can be combined, similarly to the undamped case, i.e.,

$$k = \frac{1}{\beta^2}\left(\frac{1}{2}\, k_o a\right) + \left(1 - \frac{1}{\beta^2}\right)\left(\frac{3}{4}\, k_o \tilde{S}\right) \tag{3.2.61}$$

$$c = \frac{1}{\beta^2}\left(\frac{1}{2}\, c_o a\right) + \left(1 - \frac{1}{\beta^2}\right)\left(\frac{3}{4}\, c_o \tilde{S}\right) \tag{3.2.62}$$

$$\xi = \frac{1}{\beta^2}\left(\frac{a\sqrt{3}}{6}\right) + \left(1 - \frac{1}{\beta^2}\right)\left(\frac{a}{2} - \frac{\tilde{S}}{3}\right) \tag{3.2.63}$$

3.2.4 Numerical Example

As an example, let us again consider the free oscillations of a rigid block the size of Millikan Library, with the motion generated by a horizontal impulse. A description of the building and the values of the parameters were presented in section 2.5.6. The only new parameter is the damping coefficient of the Winkler foundation, c_o, which can be estimated by using Veletsos' analysis[21]; the procedure is similar to the determination of the spring constant, k_o. For Millikan Library and $\beta_\theta = 0.2$ (see [21]), the damping coefficient, C_ϕ, of the rotational dashpot is found to be

$$r_e^2\, C_\phi = 1.58 \times 10^{10} \text{ ft-lb-sec/rad} \tag{3.2.64}$$

where r_e is the radius of the equivalent circular base. The value of c_o can then be found by equating the foundation moments about point M for the Winkler foundation and the rotational spring-dashpot system, which gives

$$c_o = \frac{12(r_e^2\, C_\phi)}{a^3} \tag{3.2.65}$$

Using (3.2.64), this equation gives $c_o = 5.77 \times 10^5$ lbs-sec/ft^2

(2.82×10^3 t-sec/m^2). The corresponding ratios of critical damping during full contact, as defined by expressions (3.2.52) and (3.2.53), are $\zeta_1^* = 5.7\%$ and $\zeta_2^* = 22.7\%$.

Figures 3.2.5 and 3.2.6 show the free oscillations of the example for $\beta = 4$ and $\beta = 8$, respectively. The physical significance of these values of β is given in section 2.5.6. The value of ϕ^c_{max} was approximated by using the solution of equation (3.2.49), i.e.,

$$\phi^c_{max} = \frac{\dot{\phi}_o}{p^*_{1d}} e^{-\frac{\pi\zeta_1^*}{2\sqrt{1-\zeta_1^{*2}}}} \qquad (3.2.66)$$

in which $\dot{\phi}_o$ is the initial angular velocity. The response of the Winkler system was calculated numerically (after lift-off); for the two-spring foundation, the response was obtained via equations (3.2.3) and (3.2.4) during full contact and equations (3.2.24), (3.2.25), and (3.2.30) after lift-off. It is evident from these plots that the two-spring model, defined by the relations of the general equivalence, can match the response of the Winkler system very well, especially for small time. The matching between the two responses worsens with time, but this behavior was expected, since β was calculated using as ϕ^c_{max} the value of the maximum angle of rotation, which happens during the first half-period. From the engineering viewpoint, however, one is mainly interested in the response of the larger amplitudes, therefore, the results of the general equivalence are satisfactory.

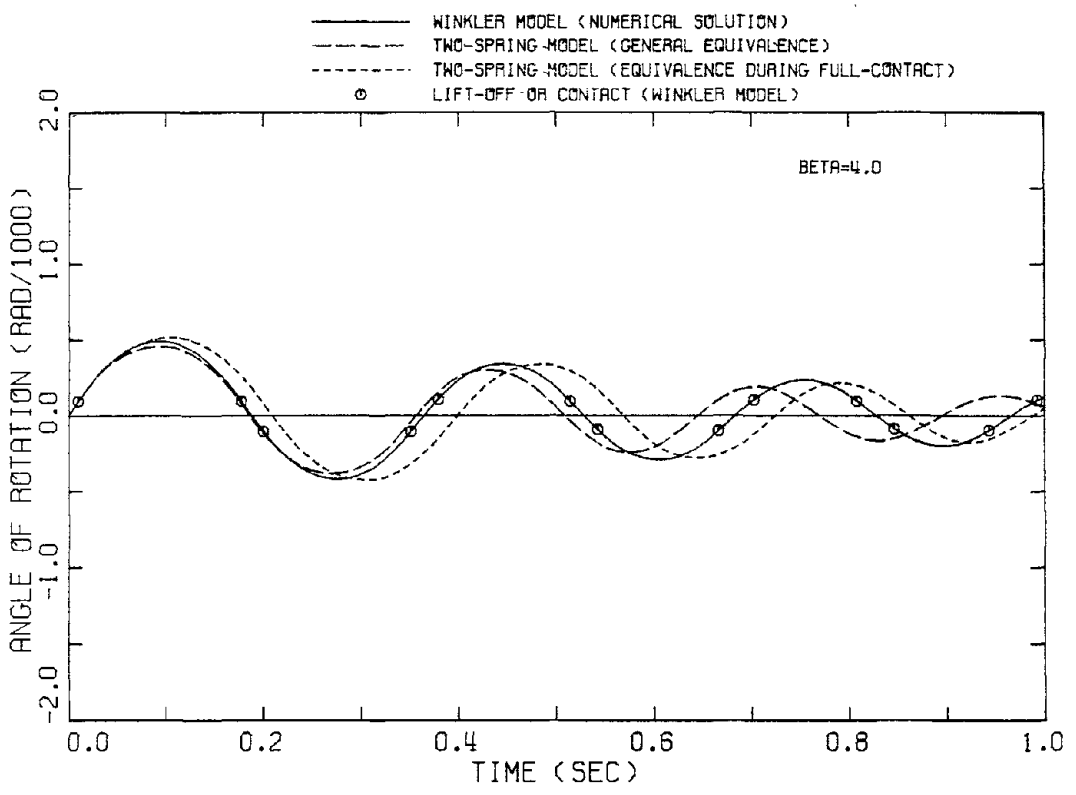

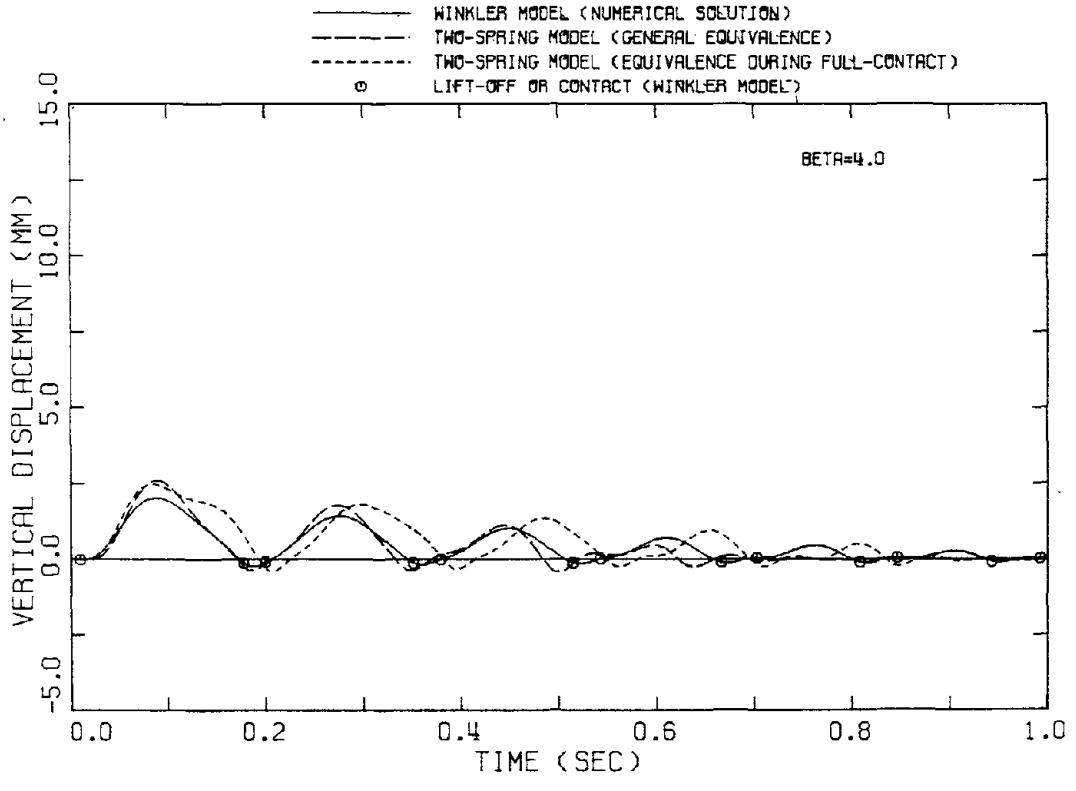

Fig. 3.2.5. Free oscillations of a simplified model of Millikan Library for $\beta = 4$.

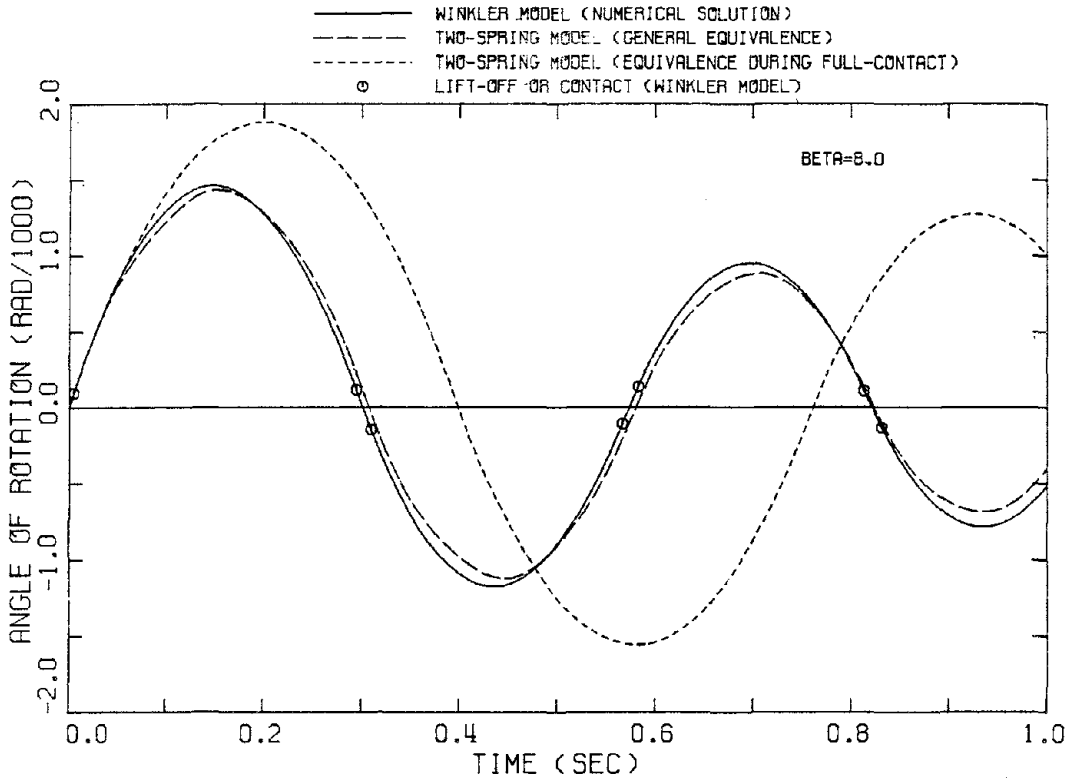

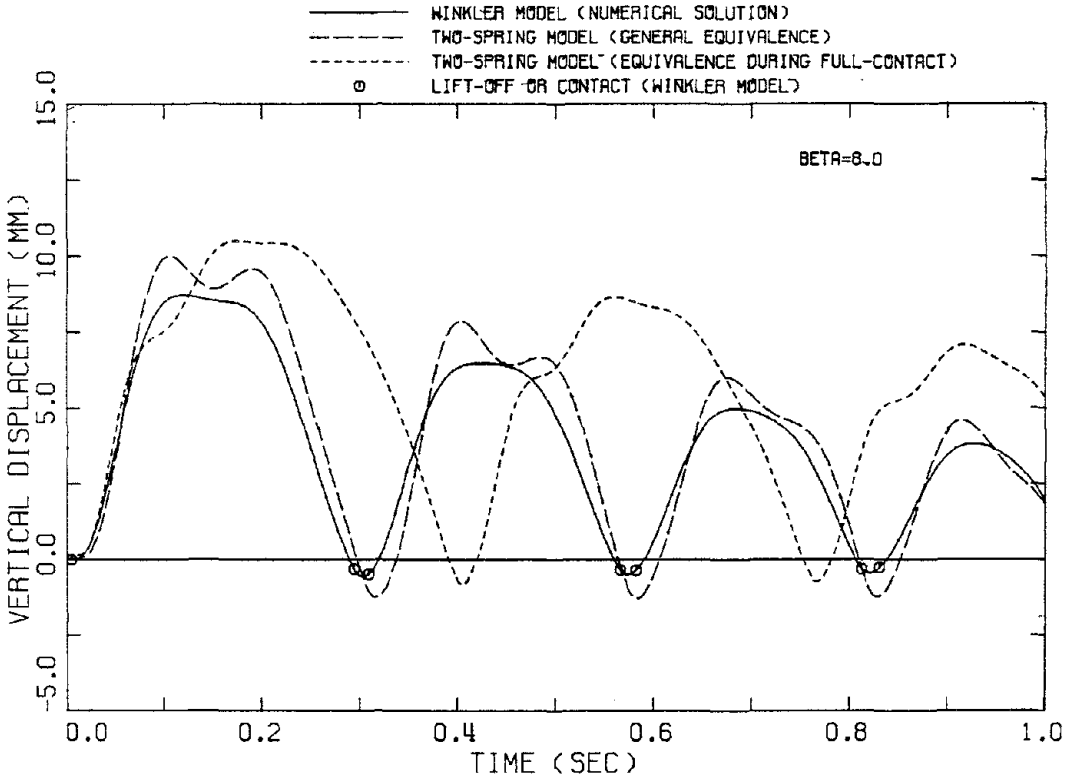

Fig. 3.2.6. Free oscillations of a simplified model of Millikan Library for $\beta = 8$.

3.3 TWO-SPRING FOUNDATION WITH ELASTIC-PERFECTLY PLASTIC SPRINGS

Inelastic action of the soil is one of the main mechanisms by which energy is dissipated in the foundation during the rocking of structures under very strong shaking. This behavior can be considered in the foundation models used earlier (Winkler or two-spring foundation) by assuming that the springs are behaving inelastically. Of course, this would introduce additional complications into the equations of motion, and the added complexity may limit the use of the model. In this section, the simplest case of a two-spring foundation with elastic-perfectly plastic springs is examined.

In Fig. 3.3.1 the force-displacement behavior of the springs is shown. We assume that the block has been rocking for some time, so that the springs at points O and O' have already experienced plastic deformations, Y_1^p and Y_2^p, respectively. Because of the different possible states of the two springs, there are five different cases which should be considered. The corresponding linearized equations of motion for these five cases are:

(a) Full contact - Elastic region

$$m\ddot{y} + 2ky = - m\ddot{y}_G - k(Y_1^p + Y_2^p) \tag{3.3.1}$$

$$I_M \ddot{\phi} + (2k\xi^2 - mgh)\phi = -mh\ddot{x}_G + k\xi(Y_1^p - Y_2^p) \tag{3.3.2}$$

(b) Full contact - Right spring in plastic region

$$m\ddot{y} + ky + k\xi\phi = -m\ddot{y}_G + F_o - \frac{1}{2} mg - kY_2^p \tag{3.3.3}$$

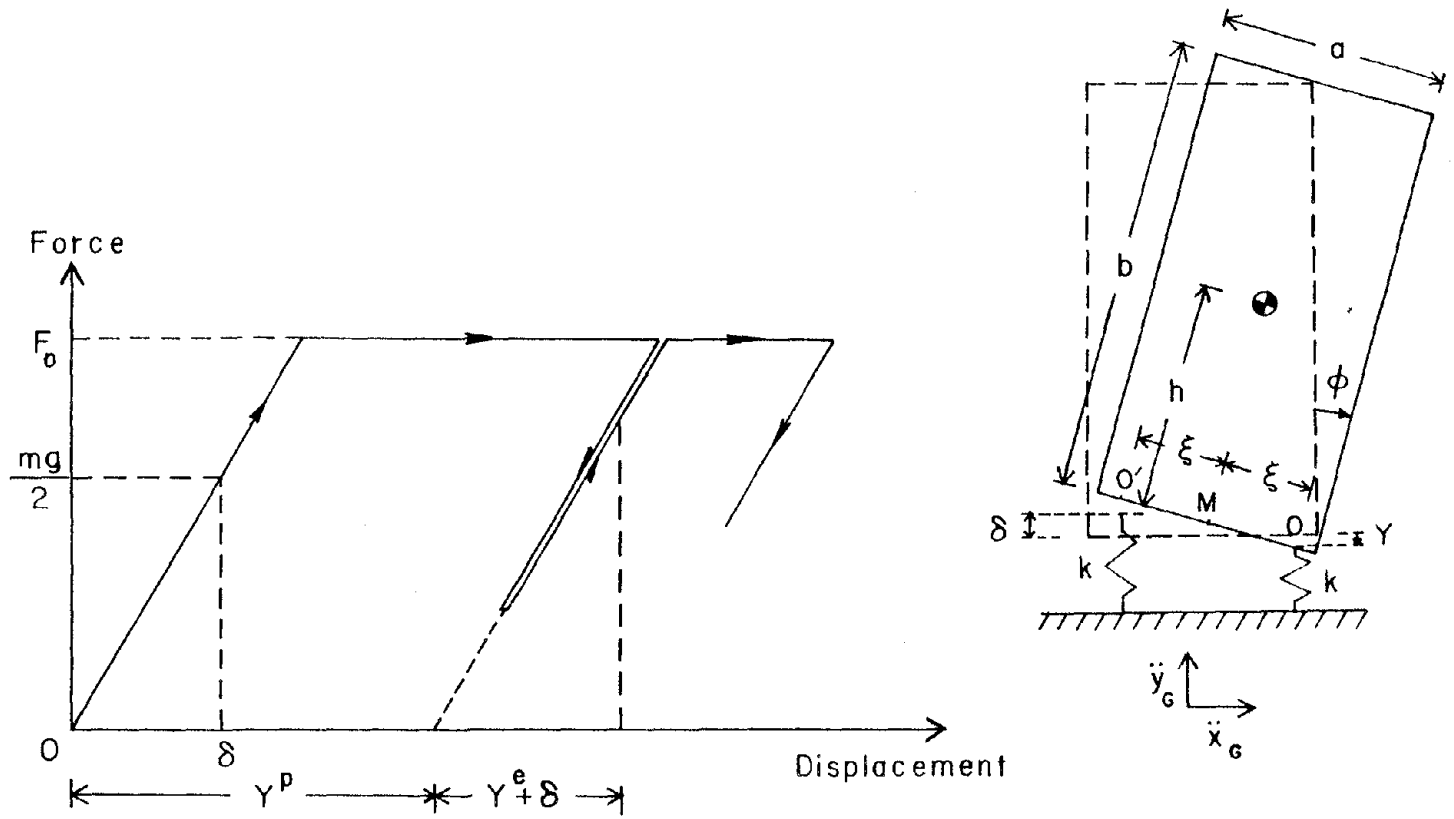

Fig. 3.3.1. Force-displacement behavior of the springs.

$$I_M\ddot{\phi} + (k\xi^2 - \frac{1}{2}mgh - F_o h)\phi + k\xi y = -mh\ddot{x}_G + \frac{1}{2}mg\xi - k\xi Y_2^p - F_o\xi \qquad (3.3.4)$$

(c) Full contact - Both springs in plastic region

$$m\ddot{y} = -m\ddot{y}_G + 2F_o - mg \qquad (3.3.5)$$

$$I_M\ddot{\phi} - 2F_o h\phi = -mh\ddot{x}_G \qquad (3.3.6)$$

(d) After lift-off - Spring in elastic region

$$m\ddot{y} + ky - k\xi\phi = -m\ddot{y}_G - \frac{1}{2}mg - kY_1^p \qquad (3.3.7)$$

$$I_M\ddot{\phi} + \left(k\xi^2 - \frac{1}{2}mgh\right)\phi - k\xi y = -mh\ddot{x}_G - \frac{1}{2}mg\xi + k\xi Y_1^p \qquad (3.3.8)$$

(e) After lift-off - Spring in plastic region

$$m\ddot{y} = -m\ddot{y}_G + F_o - mg \qquad (3.3.9)$$

$$I_M\ddot{\phi} - F_o h\phi = -mh\ddot{x}_G - F_o\xi \qquad (3.3.10)$$

in which F_o is the yield force of the springs and the angle of tilting was assumed positive. For negative ϕ, similar equations hold.

Although each of the above equations can be solved analytically, the calculation of the response of the block is complicated because the system repeatedly changes from one regime to another. Hence, one not only has to monitor the transition from full contact to lift-off and vice versa but also the states of yielding and unloading for both springs. Therefore, even the simplest case of elastic, perfectly-plastic springs does not appear to be attractive for practical applications. The difficulties are expected to increase if more complex force-displacement relations are introduced. Yielding foundation models are not examined

further in this thesis, although further research in this direction is certainly possible.

3.4 DISSIPATION OF ENERGY DURING IMPACT

Energy dissipation from impact is expected to occur in actual situations where lift-off happens. For rocking of a rigid block on a rigid foundation, Housner[1] found that energy is dissipated every time that the block hits the base and changes its pole of rotation from one corner of the base to the other. In this case, the assumed kinematics of the problem require dissipation of energy, which is described by the coefficient Q (see section 2.2). All the other foundation models introduced so far do not permit dissipation of energy upon impact.

In this section, an analysis is first made assuming that an impact is generated when the block regains full contact with the base. Then, in section 3.4.2, a mechanism is introduced which generates this kind of impact. Such a mechanism can be used together with dashpots or elastoplastic springs with both the Winkler and two-spring foundations.

3.4.1 Analysis

Consider a block rocking on a two-spring foundation and look particularly at the time when the block reestablishes contact with the left spring, after having uplifted. The simplest way to introduce dissipation of energy from impact is by assuming that the vertical velocity of point O' is suddenly reduced by some impact mechanism (see Fig. 3.4.1). This implies that $\dot{\phi}$ and $\dot{y}$ are also changed. Let $\dot{\phi}_1$ and

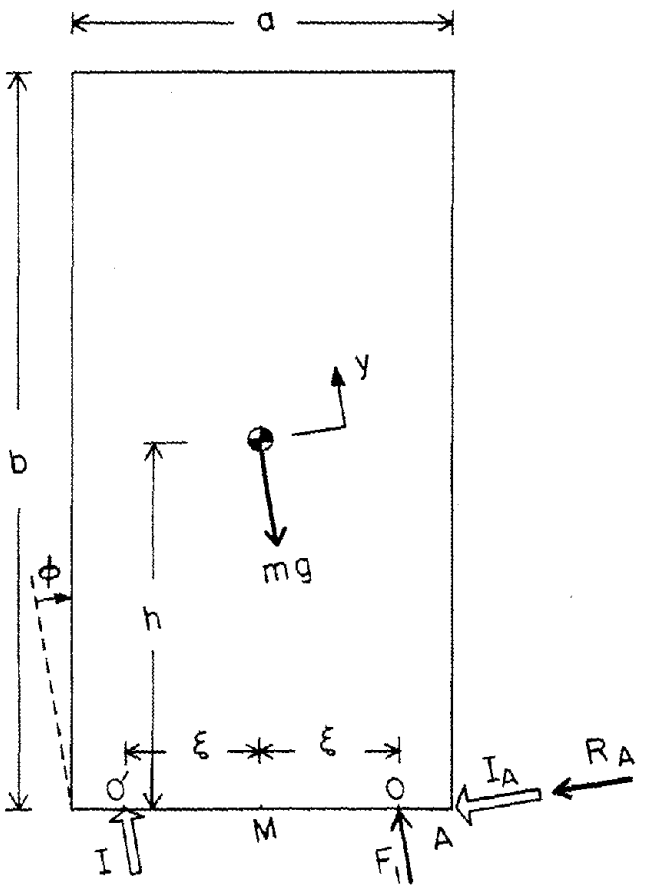

Fig. 3.4.1. Free body diagram at the time of the impact at point O'.

$\dot{y}_1$ be the corresponding values before impact, and $\dot{\phi}_2$, $\dot{y}_2$ after it. Since the velocity of point 0' is, to first order, $(\dot{y} + \xi\dot{\phi})$, one can write

$$(\dot{y}_2 + \xi\dot{\phi}_2) = \varepsilon(\dot{y}_1 + \xi\dot{\phi}_1) \tag{3.4.1}$$

where ε is a coefficient of restitution which satisfies the inequality

$$0 \leq \varepsilon \leq 1 \tag{3.4.2}$$

For the limiting case of $\varepsilon = 1$ no energy is dissipated, while for $\varepsilon = 0$ the maximum possible amount of energy is lost because of the impact against a (momentarily) rigid support.

Let I be the vertical impulse generated at point 0' and I_A be the resulting horizontal impulse at point A. Application of the impulse-momentum principle to vertical, horizontal and rocking (about the center of mass) motions and elimination of I_A finally reduces to

$$\dot{y}_2 = \dot{y}_1 + \frac{I}{m} \tag{3.4.3}$$

and

$$\dot{\phi}_2 = \dot{\phi}_1 + \frac{I(\xi + h\phi)}{I_M} \tag{3.4.4}$$

Substituting in equation (3.4.1), the impulse I can be expressed in terms of ε and the initial velocities as

$$I = -m\left(\frac{I_M}{I_o + mh\xi\phi}\right)(1 - \varepsilon)(\dot{y}_1 + \xi\dot{\phi}) \tag{3.4.5}$$

in which I_o is the moment of inertia about the point 0 or 0'.

Since the angle of rotation, ϕ, is assumed to be small, the term $mh\xi\phi$ can be neglected in comparison with I_o in the above equation.

Substituting back into equations (3.4.3) and (3.4.4) one gets the following expressions for the velocities after impact

$$\dot{y}_2 = \left(\frac{m\xi^2 + \varepsilon\ I_M}{I_o}\right)\dot{y}_1 - \frac{I_M}{I_o}(1 - \varepsilon)\ \xi\dot{\phi}_1 \tag{3.4.6}$$

$$\dot{\phi}_2 = \left(\frac{I_M + \varepsilon m\xi^2}{I_o}\right)\dot{\phi}_1 - \frac{m\xi}{I_o}(1-\varepsilon)\ \dot{y}_1 \tag{3.4.7}$$

The energy dissipated is equal to the difference of the kinetic energies before and after the impact, which gives

$$\Delta E = \frac{1}{2}\, m\, \frac{I_M}{I_o}\left(1-\varepsilon^2\right)\left(\dot{y}_1 + \xi\dot{\phi}_1\right)^2 \tag{3.4.8}$$

The maximum dissipation of energy occurs for $\varepsilon = 0$ and is

$$(\Delta E)_{max} = \frac{1}{2}\, m\, \frac{I_M}{I_o}\left(\dot{y}_1 + \xi\dot{\phi}_1\right)^2 \tag{3.4.9}$$

In order to interpret these results for the calculation of the response of the system it is necessary to use the reduced values of the velocities, as given by equations (3.4.6) and (3.4.7) as initial velocities for the full contact case. For a Winkler foundation, the value of ξ should be taken equal to a/2.

Comparison with Housner's results

As an example, let us consider the limiting case of a rigid foundation, in which $\xi = \frac{a}{2}$, $y = \frac{a}{2}\phi$ and $\varepsilon = 0$. Then, the energy loss during the impact, according to equation (3.4.8), is

$$\Delta E = \frac{1}{2}\, ma^2\, \frac{I_M}{I_o}\, \dot{\phi}_1^2 \tag{3.4.10}$$

According to Housner's results (see equation (2.2.5))

$$\dot{\phi}_2 = \dot{\phi}_1\left(1 - \frac{ma^2}{2I_o}\right)$$

therefore, the energy dissipated is

$$\Delta E = \frac{1}{2} ma^2\left(1 - \frac{ma^2}{4I_o}\right)\dot{\phi}_1^2 \qquad (3.4.11)$$

Since in this case,

$$I_M = I_o - m\frac{a^2}{4}$$

equation (3.4.11) is identical to equation (3.4.10)

3.4.2 An Impact Mechanism

In this section, an impact mechanism which reduces the velocity of point O' according to equation (3.4.1) is presented. A dashpot of constant c* is connected in series, on the top of the spring, k, and the dashpot, c, as shown in Fig. 3.4.2a. We assume that c* is large, and in the limit $c^* \to \infty$. Because of its large coefficient, the dashpot forms an essentially rigid link and, as shown in Fig. 3.4.2a, does not affect the response of the system except during impact.

At the time of impact, however, we assume that the dashpot, c*, is locked as shown in Fig. 3.4.2b, for a small time, Δt, which in the limit goes to zero. The time Δt can be viewed as the time for the dashpot plunger to move a distance Δz, unlocking the dashpot at the end of its travel. During that time, the spring, k, and the dashpot, c, are not activated, and the response is affected by the impact dashpot only. As a result, the velocity of point O' is reduced. After time Δt, the impact dashpot is unlocked, and its effect on the response ceases.

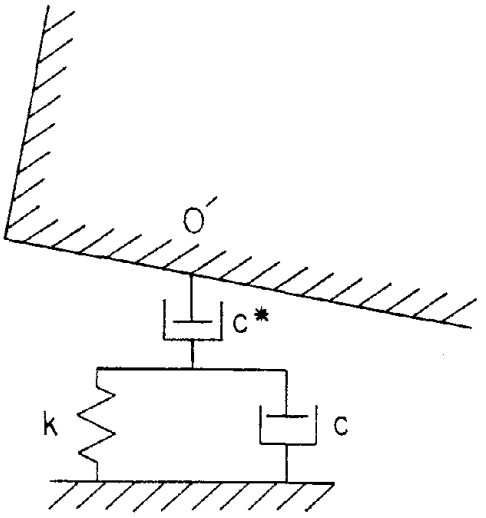

(a) Unlocked

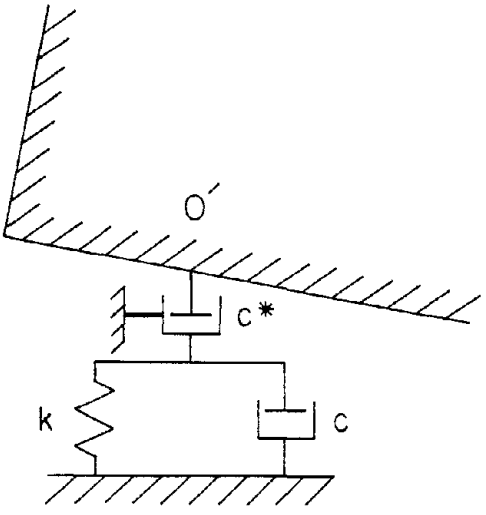

(b) Locked

Fig. 3.4.2. Impact mechanism.

Let us now look analytically at the behavior of the block during the time Δt. The vertical forces from the foundation are

$$F_1 = k(\delta - y + \xi\phi) + c(-\dot{y} + \xi\dot{\phi}) \qquad \text{at point 0}$$

$$F_2 = -c^*(\dot{y} + \xi\dot{\phi}) \qquad \text{at point 0'}$$

The governing equations of motion then, are

$$m\ddot{y} + (c^* + c)\dot{y} + (c^* - c)\xi\dot{\phi} + ky - k\xi\phi = -\frac{mg}{2} - m\ddot{y}_G \tag{3.4.12}$$

$$I_M\ddot{\phi} + (c^* - c)\xi\dot{y} + (c^* + c)\xi^2\dot{\phi} + (k\xi^2 - \frac{mgh}{2})\phi - k\xi y = -\frac{mg\xi}{2} - mh\ddot{x}_G \tag{3.4.13}$$

Let y_1, ϕ_1, $\dot{y}_1$, $\dot{\phi}_1$ be the displacements and velocities at the onset of contact. One can then write,

$$\left.\begin{aligned} y &= y_1 + \Delta y \\ \phi &= \phi_1 + \Delta\phi \end{aligned}\right\} \tag{3.4.14}$$

Substituting in equations (3.4.12) and (3.4.13) and taking under consideration that y_1, ϕ_1 satisfy equation (3.2.10), yields

$$m\Delta\ddot{y} + c^*\dot{y}_1 + (c^* + c)\Delta\dot{y} + c^*\xi\dot{\phi}_1 + (c^* - c)\xi\Delta\dot{\phi} + k\Delta y - k\xi\Delta\phi = 0 \tag{3.4.15}$$

$$I_M\Delta\ddot{\phi} + c^*\xi\dot{y}_1 + (c^* - c)\xi\Delta\dot{y} + c^*\xi^2\dot{\phi}_1 + (c^* + c)\xi^2\Delta\dot{\phi} + \left(k\xi^2 - \frac{mgh}{2}\right)\Delta\phi - k\xi\Delta y = 0 \tag{3.4.16}$$

Since $c^* \to \infty$ and $\Delta t \to 0$, the impact mechanism is expected to affect the velocities significantly, but not the displacements. It is reasonable, therefore, to assume

$$\Delta y = \Delta\phi = 0 \tag{3.4.17}$$

Also, c can be neglected in comparison with c*. Equations (3.4.15) and (3.4.16) then reduce to

$$m\Delta\ddot{y} + c^*(\Delta\dot{y} + \xi\Delta\dot{\phi}) = -c^*(\dot{y}_1 + \xi\dot{\phi}_1) \tag{3.4.18}$$

$$I_M\,\Delta\ddot{\phi} + c^*\xi(\Delta\dot{y} + \xi\Delta\dot{\phi}) = -c^*\xi(\dot{y}_1 + \xi\dot{\phi}_1) \tag{3.4.19}$$

which give

$$\frac{d}{dt}(\Delta\dot{y} + \xi\Delta\dot{\phi}) + \frac{c^*I_o}{m\,I_M}(\Delta\dot{y} + \xi\Delta\dot{\phi}) = -\frac{c^*I_o}{m\,I_M}(\dot{y}_1 + \xi\dot{\phi}_1) \tag{3.4.20}$$

At $t = 0$, $\Delta\dot{y} + \xi\Delta\dot{\phi} = 0$, therefore, the solution of (3.4.20) can be written as

$$(\Delta\dot{y} + \xi\Delta\dot{\phi}) = -(\dot{y}_1 + \xi\dot{\phi}_1)\left[1 - e^{-\left(\frac{I_o}{I_M}\frac{c^*t}{m}\right)}\right] \tag{3.4.21}$$

The final velocity of point O' at time $t = \Delta t$ is

$$(\dot{y}_2 + \xi\dot{\phi}_2) = (\dot{y}_1 + \xi\dot{\phi}_1)\, e^{-\left(\frac{I_o}{I_M}\frac{c^*\Delta t}{m}\right)} \tag{3.4.22}$$

Making the final assumption that $c^* \to \infty$ and $\Delta t \to 0$ in such a way that $c^*\Delta t$ is constant, we can put

$$\varepsilon = e^{-\left(\frac{I_o}{I_M}\frac{c^*\Delta t}{m}\right)} \tag{3.4.23}$$

Equation (3.4.22) can be written as

$$(\dot{y}_2 + \xi\dot{\phi}_2) = \varepsilon(\dot{y}_1 + \xi\dot{\phi}_1) \tag{3.4.24}$$

which is the same as equation (3.4.1). The unlocking impact dashpot, therefore, is equivalent to a coefficient of restitution, ε, which

depends on the ratio I_o/I_M, the mass, m, of the block, and the constant $c^*\Delta t$, which is a property of the dashpot. For $(c^*\Delta t) \to 0$, $\varepsilon \to 1$, and there is no energy dissipated during the impact. For $c^*\Delta t \to \infty$, $\varepsilon \to 0$ and the maximum possible amount of energy is lost. The equivalence can be checked by calculating the energy lost during the impact. This energy is equal to the work done by the impact dashpot, i.e.,

$$\Delta E = \int_0^{\Delta t} c^*\left(\dot{y} + \xi\dot{\phi}\right)^2 dt = \frac{1}{2}\, m\, \frac{I_M}{I_o}\left(1 - \varepsilon^2\right)\left(\dot{y}_1 + \xi\dot{\phi}_1\right)^2 \qquad (3.4.25)$$

which agrees with equation (3.4.8).

3.4.3 Numerical Example

The effect of the dissipation of energy during impact on the response of the block is illustrated in Fig. 3.4.3 for the same example based on Millikan Library that was used in section 3.2.4. The two-spring model (general equivalence) was used instead of the Winkler foundation. The two extreme cases of $\varepsilon = 0$ (maximum possible dissipation of energy) and $\varepsilon = 1$ (no loss of energy) are plotted with solid and fine dashed lines, respectively. It is evident that the dissipation of energy during impact may be significant for values of ε close to zero.

However, the response of the block for $\varepsilon = 0$ has the same appearance that is produced by simply adding more damping to the foundation. As it is shown in Fig. 3.4.3, the response for $\varepsilon = 0$ can be closely matched by a 130% increase of the dashpot constant, c, and neglecting the impact. This suggests that in many cases viscous damping in the foundation may adequately model the effect of dissipation of energy upon impact. Considering the nature of the other assumptions

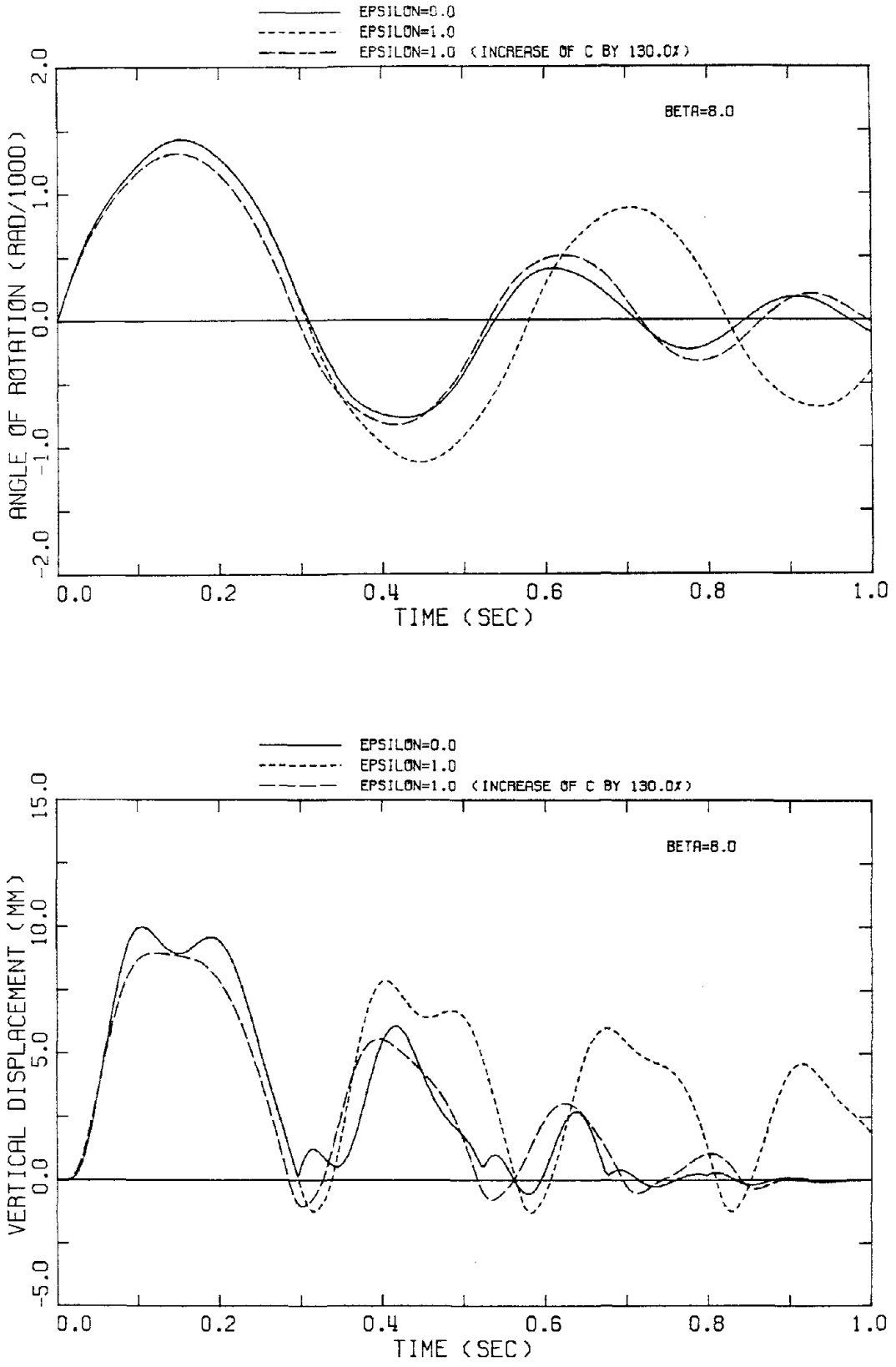

Fig. 3.4.3. Effect of impact upon free oscillations of a simplified model of Millikan Library.

made in the analysis of tipping bodies, the simple modeling of energy dissipation from impact by means of additional foundation damping would appear to be justified in most applications.

The amount of the necessary increase in the value of the damping coefficient would have to be established, however. One way to do this would be by equating the energy dissipated per cycle. The equivalent linear system established in section 3.2.1 could be used for an approximate solution.

CHAPTER IV

DYNAMICS OF FLEXIBLE SUPERSTRUCTURES

4.1 INTRODUCTION

In this chapter, the dynamics of a flexible structure rocking on a flexible foundation are examined. For simplicity, the two-spring foundation is considered. It is assumed that the equivalence between the Winkler foundation and the two-spring model, established for the case of a rocking rigid block, can again be used. The system is excited by horizontal and vertical ground accelerations, $\ddot{x}_G$ and $\ddot{y}_G$, respectively. These are strong enough to cause separation of the structure from one of the foundation springs, but not from both. No slipping between the base and the foundation is allowed, therefore, the dynamic coupling between the superstructure and the ground results in two extra degrees of freedom for the system, in addition to the degrees of freedom of the superstructure itself.

First, the simple case of a single-degree-of-freedom structure with concentrated mass is examined in section 4.2. The rocking of this simple oscillator on a rigid foundation was first examined by Meek[15]; a comparison between that solution and the response for a flexible ground is presented in section 4.2.5. The more general case of a multidegree of freedom structure rocking on a two-spring foundation is studied in section 4.3.

4.2 DYNAMICS OF A SINGLE DEGREE OF FREEDOM SUPERSTRUCTURE

4.2.1 System Considered

The system considered herein is shown in Fig. 4.2.1. The superstructure consists of a concentrated mass, m, placed at height, h, and connected with the base through a massless rod of stiffness, K, and damping constant, C. The foundation is modeled by two springs of stiffness, k, and damping, c, placed symmetrically at the corners of the base, which has length, 2ξ, and is assumed rigid and massless. The horizontal and vertical ground acceleration are denoted by $\ddot{x}_G$ and $\ddot{y}_G$, respectively, and the assumption of no slipping between the structure and the foundation is applied. Formulated this way, the system possesses three degrees of freedom, namely, rotation in the plane of motion, denoted by ϕ, vertical displacement of the mass, denoted by y, and horizontal displacement of the mass relative to the base, excluding rotations, measured by the shear deformation, u.

The system may be viewed as a highly simplified model of a single story building or other structure, or as the equivalent simple oscillator modelling a mode of vibration of a more complex vibrating system. In the latter case, the values of m, h, K, and C should be calculated by the standard earthquake engineering methods, applied for fixed-base response (e.g., see Ref. 55). The foundation parameters, k, c, and the length, ξ, can be obtained from the equations of equivalence between the Winkler and the two-spring foundation, as defined in section 3.2.3. Note that the value of β, which enters these equations,

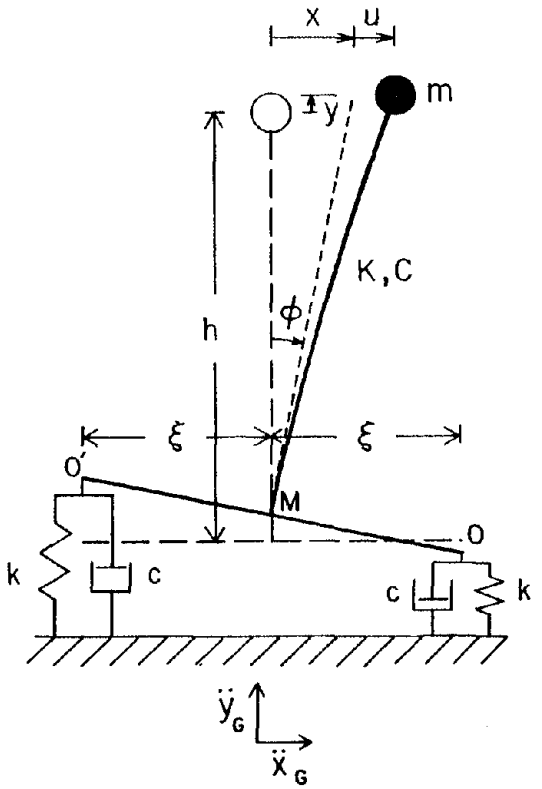

Fig. 4.2.1. Simple oscillator on a two-spring model of a rocking foundation.

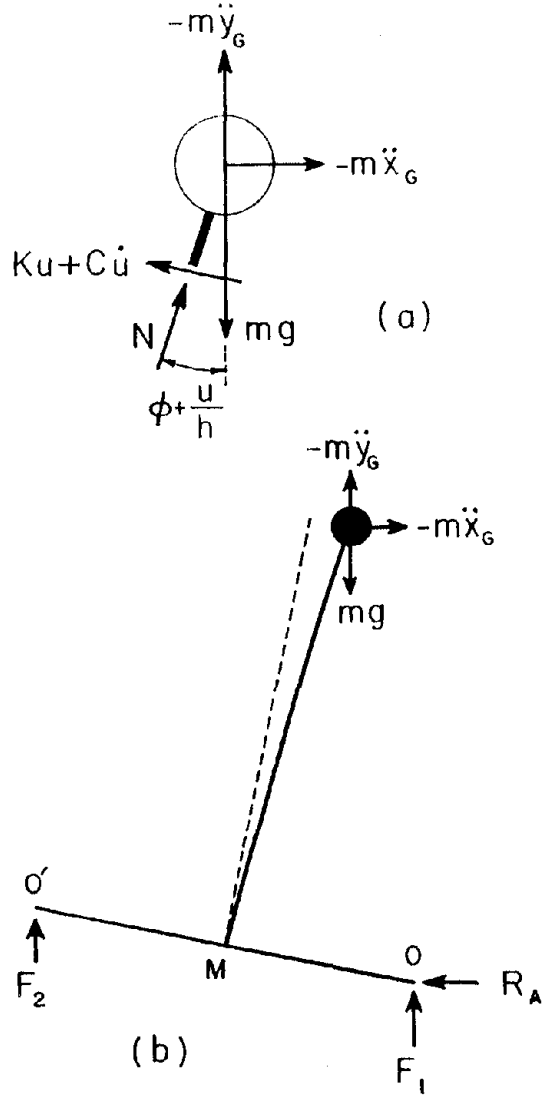

Fig. 4.2.2. Free body diagrams of the mass and the system.

should be calculated for the flexible superstructure. It should be mentioned, moreover, that the response of a multi-degree-of-freedom interacting system calculated by this method will be approximate, primarily because the effect of lift-off on the response is nonlinear and therefore the total response cannot be obtained by the superposition of the responses of the individual modes.

4.2.2 Equations of Motion

Free body diagrams for the mass and the system are shown in Figs. 4.2.2a and b. Applying Newton's second law, and assuming displacements small enough that $\sin(\phi + \frac{u}{h})$ can be replaced by $(\phi + \frac{u}{h})$ and $\cos(\phi + \frac{u}{h})$ by unity, the following equations for the mass can be derived

$$N = mg + m\ddot{y}_G + m\ddot{y} \tag{4.2.1}$$

$$mh\ddot{\phi} + m\ddot{u} + Ku + C\dot{u} - N\left(\phi + \frac{u}{h}\right) = - m\ddot{x}_G \tag{4.2.2}$$

which finally reduce to the equation

$$\ddot{x} + \ddot{u} + 2\zeta^s\omega\dot{u} + \omega^2 u - \frac{1}{h}(g + \ddot{y}_G + \ddot{y})x - \frac{1}{h}(g + \ddot{y}_G + \ddot{y})u = -\ddot{x}_G \tag{4.2.3}$$

in which

$$x = h\phi \tag{4.2.4}$$

$$\omega^2 = \frac{K}{m} \tag{4.2.5}$$

$$\zeta^s = \frac{C}{2\sqrt{Km}} \tag{4.2.6}$$

The external forces acting on the system, which are shown in Fig. 4.2.2b for positive angles of rotation, are

$$F_1 = c(-\dot{y} + \xi\dot{\phi}) + k(\delta - y + \xi\phi)$$

$$F_2 = \begin{cases} -c(\dot{y} + \xi\dot{\phi}) + k(\delta - y - \xi\phi) & , \quad \text{before lift-off} \\ 0 & , \quad \text{after lift-off} \end{cases}$$

$$R_A = -m\ddot{x}_G - m\ddot{u} - mh\ddot{\phi}$$

Then, in addition to equation (4.2.3), the other two equations of motion (in the vertical and rocking directions) are

Full contact

$$\ddot{y} + 2\zeta_2 p_2 \dot{y} + p_2^2 y = -\ddot{y}_G \tag{4.2.7}$$

$$\ddot{x} + \ddot{u} \pm \frac{\xi}{h^2}(\ddot{x}_G + \ddot{u} + \ddot{x})x + 2\zeta_2 p_2 \left(\frac{x+u}{h}\right)\dot{y} + \left(\frac{\xi}{h}\right)^2 2\zeta_2 p_2 \dot{x}$$

$$+ \left(\frac{\xi}{h}\right)^2 p_2^2 x - \frac{g}{h}(x+u) + p_2^2\left(\frac{x+u}{h}\right)y = -\ddot{x}_G \tag{4.2.8}$$

After lift-off

$$\ddot{y} + \zeta_2 p_2 \dot{y} \mp \left(\frac{\xi}{h}\right)\zeta_2 p_2 \dot{x} + \frac{p_2^2}{2} y \mp \left(\frac{\xi}{h}\right)\frac{p_2^2}{2} x = -\ddot{y}_G - \frac{g}{2} \tag{4.2.9}$$

$$\ddot{x} + \ddot{u} \pm \frac{\xi}{h^2}(\ddot{x}_G + \ddot{u} + \ddot{x})x + \zeta_2 p_2 \left[\left(\frac{\xi}{h}\right)^2 \dot{x} \mp \frac{\xi}{h}\dot{y} + \left(\frac{x+u}{h}\right)\dot{y} \mp \frac{\xi}{h}\left(\frac{x+u}{h}\right)\dot{x}\right]$$

$$+ \frac{p_2^2}{2}\left(\frac{\xi}{h}\right)^2 x - \frac{g}{2}\left(\frac{x+u}{h}\right) \mp \frac{p_2^2}{2}\left(\frac{\xi}{h}\right)y + \frac{p_2^2}{2}\left(\frac{x+u}{h}\right)y \mp \frac{p_2^2}{2}\left(\frac{\xi}{h}\right)\left(\frac{x+u}{h}\right)x$$

$$= -\ddot{x}_G \mp \frac{g\xi}{2h} \tag{4.2.10}$$

in which

$$p_2^2 = \frac{2k}{m} \tag{4.2.11}$$

$$\zeta_2 = \frac{c}{\sqrt{2km}} \tag{4.2.12}$$

Whenever a double sign appears in these equations, the upper one corresponds to positive angles of rotation and the lower one to negative ones. In this first presentation, all the nonlinear terms were kept.

4.2.3 Undamped Case

For simplicity, let us first consider the case in which there is no damping in the foundation or the superstructure. The equations of motion can then be greatly simplified.

Full contact

Subtracting equation (4.2.3) from equation (4.2.8), using (4.2.7), and dropping the nonlinear terms from the resulting expression, one gets

$$u = \left(\frac{\xi}{h}\right)^2 \frac{p_2^2}{\omega^2} x \tag{4.2.13}$$

which means that the variables u and x are not independent but linearly related to each other. Using equation (4.2.13) as a constraint, the problem reduces to the solution of two uncoupled differential equations.

Let us define

$$v(t) = u(t) + x(t) \tag{4.2.14}$$

Recall that x(t) measures the horizontal displacement of the mass, which results from the rotation, and u(t) the shear distortion.

Therefore, v(t) measures the total horizontal displacement of the mass. Equations (4.2.13) and (4.2.14) reduce to the following relations

$$x(t) = \left(\frac{\omega^2}{\omega^2 + \tilde{\alpha}^2 p_2^2}\right) v(t) \tag{4.2.15}$$

$$u(t) = \left(\frac{\tilde{\alpha}^2 p_2^2}{\omega^2 + \tilde{\alpha}^2 p_2^2}\right) v(t) \tag{4.2.16}$$

$$\tilde{\alpha} = \frac{\xi r}{h} \tag{4.2.17}$$

Note that the value of $\tan^{-1}\tilde{\alpha}$ determines the overturning angle. Substituting into (4.2.3) and dropping the nonlinear terms, one finally gets

$$\ddot{v} + \left(\frac{\tilde{\alpha}^2 \omega^2 p_2^2}{\omega^2 + \tilde{\alpha}^2 p_2^2} - \frac{g}{h}\right) v = -\ddot{x}_G \tag{4.2.18}$$

The square root of the quantity in parenthesis in the above equation will determine the natural frequency, $\tilde{\omega}$, of the soil-structure interacting system, i.e.,

$$\tilde{\omega}^2 = \frac{\tilde{\alpha}^2 \omega^2 p_2^2}{\omega^2 + \tilde{\alpha}^2 p_2^2} - \frac{g}{h} \tag{4.2.19}$$

The solution of the equations of motion can then be written as

$$y(t) = y(0) \cos p_2 t + \frac{\dot{y}(0)}{p_2} \sin p_2 t - \frac{1}{p_2} \int_0^t \ddot{y}_G(\tau) \sin p_2 (t-\tau) d\tau \tag{4.2.20}$$

$$u(t) = \frac{\tilde{\alpha}^2 p_2^2}{\omega^2 + \tilde{\alpha}^2 p_2^2} \left[v(0) \cos \tilde{\omega} t + \frac{\dot{v}(0)}{\tilde{\omega}} \sin \tilde{\omega} t - \frac{1}{\tilde{\omega}} \int_0^t \ddot{x}_G(\tau) \sin \tilde{\omega}(t-\tau) d\tau \right] \tag{4.2.21}$$

$$x(t) = h\phi(t) = \frac{\omega^2}{\omega^2 + \tilde{\alpha}^2 p_2^2} \left[v(0) \cos \tilde{\omega} t + \frac{\dot{v}(0)}{\tilde{\omega}} \sin \tilde{\omega} t - \frac{1}{\tilde{\omega}} \int_0^t \ddot{x}_G(\tau) \sin \tilde{\omega}(t-\tau) d\tau \right] \tag{4.2.22}$$

For many practical applications, the term g/h can be neglected in equation (4.2.19). Then

$$\tilde{\omega}^2 \simeq \frac{\tilde{\alpha}^2 \omega^2 p_2^2}{\omega^2 + \tilde{\alpha}^2 p_2^2} \tag{4.2.23}$$

In this case, equation (4.2.21) implies that the earthquake response of the simple oscillator-foundation system, during full contact, is equivalent to the response of a one-degree-of-freedom oscillator of natural frequency $\tilde{\omega}$, resting on a rigid foundation and subjected to effective ground acceleration equal to $(\tilde{\omega}/\omega)^2 \ddot{x}_G(t)$. This behavior was also reported by Jennings and Bielak.[19]

On the other hand, one can write

$$p_1^2 = \tilde{\alpha}^2 p_2^2 = \frac{2k\xi^2}{mh^2} \tag{4.2.24}$$

where p_1 is the approximate rocking frequency during full contact of the corresponding rigid superstructure. Then, equation (4.2.22) implies that the rocking response of the system can also be given by the response of the equivalent oscillator, if the latter is subjected to ground acceleration equal to $\frac{1}{h} (\tilde{\omega}/p_1)^2 \ddot{x}_G(t)$.

It is evident from equation (4.2.23) that $\tilde{\omega}$ is smaller than both ω and p_1. Therefore, the dynamic coupling between the structure and the foundation results in a system which is softer than either the system of the structure on a rigid foundation or the system of the rigid structure on a flexible foundation.

After lift-off

For simplicity let us consider the case of positive angles of rotation. Substituting equation (4.2.9) into (4.2.3), subtracting the resulting equation from (4.2.10), and dropping the nonlinear terms reduces to

$$\tilde{\alpha}^2 p_2^2 x - \tilde{\alpha} p_2^2 y - 2\omega^2 u + g\tilde{\alpha} = 0 \qquad (4.2.25)$$

which again is a constraint between the variables x, y, and u. In contrast to the case of full contact, however, the vertical displacement of the system is now coupled with the rotation and the shear deformation.

Making again the transformation $v(t) = u(t) + x(t)$, one gets

$$x(t) = \frac{\tilde{\alpha} p_2^2 \, y(t) + 2\omega^2 v(t) - g\tilde{\alpha}}{2\omega^2 + \tilde{\alpha}^2 p_2^2} \qquad (4.2.26)$$

$$u(t) = \frac{-\tilde{\alpha} p_2^2 \, y(t) + \tilde{\alpha}^2 p_2^2 \, v(t) + g\tilde{\alpha}}{2\omega^2 + \tilde{\alpha}^2 p_2^2} \qquad (4.2.27)$$

and the governing equations of motion reduce to

$$\ddot{y} + \frac{\omega^2 p_2^2}{2\omega^2 + \tilde{\alpha}^2 p_2^2} y - \frac{\tilde{\alpha}\omega^2 p_2^2}{2\omega^2 + \tilde{\alpha}^2 p_2^2} v = -\ddot{y}_G - g\left(\frac{\omega^2 + \tilde{\alpha}^2 p_2^2}{2\omega^2 + \tilde{\alpha}^2 p_2^2}\right) \qquad (4.2.28)$$

$$\ddot{v} + \frac{\omega^2}{2\omega^2 + \tilde{\alpha}^2 p_2^2}\left(\tilde{\alpha}^2 p_2^2 - \frac{g}{h}\right)v - \frac{\tilde{\alpha}\omega^2 p_2^2}{2\omega^2 + \tilde{\alpha}^2 p_2^2} y = -\ddot{x}_G - g\frac{\tilde{\alpha}\omega^2}{2\omega^2 + \tilde{\alpha}^2 p_2^2} \qquad (4.2.29)$$

The characteristic equation of this system of equations is

$$\tilde{\Omega}^4 + \frac{\omega^2}{2\omega^2 + \tilde{\alpha}^2 p_2^2}\left[\left(1+\tilde{\alpha}^2\right)p_2^2 - \frac{g}{h}\right]\tilde{\Omega}^2 - \frac{g}{h}\frac{\omega^4 p_2^2}{\left(2\omega^2 + \tilde{\alpha}^2 p_2^2\right)^2} = 0 \qquad (4.2.30)$$

This equation has two real and two imaginary roots, which can be written as $\pm\tilde{\Omega}_1$ and $\pm i\tilde{\Omega}_2$, where $\tilde{\Omega}_1$ and $\tilde{\Omega}_2$ are real and positive. The real roots lead to the expected hyperbolic functions in the solution.

For slender structures, $\tilde{\alpha}$ is a small quantity, therefore $\tilde{\alpha}^2$ can be neglected in comparison to unity. In this case, approximate values for $\tilde{\Omega}_1$ and $\tilde{\Omega}_2$ can be found from equation (4.2.30), which are

$$\tilde{\Omega}_1 \simeq \sqrt{\frac{g\omega^2}{h(2\omega^2 + \tilde{\alpha}^2 p_2^2)}} \qquad (4.2.31)$$

$$\tilde{\Omega}_2 \simeq \frac{\omega p_2}{\sqrt{2\omega^2 + \tilde{\alpha}^2 p_2^2}} \qquad (4.2.32)$$

The system of equations (4.2.28) and (4.2.29) can be solved by standard methods. The final expressions for the response are

$$
\begin{aligned}
y(t) = &- \frac{1}{(\tilde{\Omega}_1^2 + \tilde{\Omega}_2^2)} \left[y(0) \left(\frac{\omega^2}{2\omega^2 + \tilde{\alpha}^2 p_2^2} \left(\tilde{\alpha}^2 p_2^2 - \frac{g}{h} \right) - \tilde{\Omega}_2^2 \right) + v(0) \frac{\tilde{\alpha}\omega^2 p_2^2}{2\omega^2 + \tilde{\alpha}^2 p_2^2} \right. \\
&\left. + \frac{g}{\tilde{\Omega}_2^2 (2\omega^2 + \tilde{\alpha}^2 p_2^2)} \left(\tilde{\alpha}^2 \omega^2 p_2^2 - \left(\omega^2 + \tilde{\alpha}^2 p_2^2 \right) \tilde{\Omega}_2^2 - \frac{g\left(\omega^2 + \tilde{\alpha}^2 p_2^2 \right) \omega^2}{h\left(2\omega^2 + \tilde{\alpha}^2 p_2^2 \right)} \right) \right] \cos \tilde{\Omega}_2 t \\
&- \frac{1}{\left(\tilde{\Omega}_1^2 + \tilde{\Omega}_2^2 \right)} \left[\dot{y}(0) \left(\frac{\omega^2}{2\omega^2 + \tilde{\alpha}^2 p_2^2} \left(\tilde{\alpha}^2 p_2^2 - \frac{g}{h} \right) - \tilde{\Omega}_2^2 \right) + \dot{v}(0) \frac{\tilde{\alpha}\omega^2 p_2^2}{2\omega^2 + \tilde{\alpha}^2 p_2^2} \right] \frac{\sin \tilde{\Omega}_2 t}{\tilde{\Omega}_2} \\
&+ \frac{1}{\left(\tilde{\Omega}_1^2 + \tilde{\Omega}_2^2 \right)} \left[y(0) \left(\frac{\omega^2}{2\omega^2 + \tilde{\alpha}^2 p_2^2} \left(\tilde{\alpha}^2 p_2^2 - \frac{g}{h} \right) + \tilde{\Omega}_1^2 \right) + v(0) \frac{\tilde{\alpha}\omega^2 p_2^2}{2\omega^2 + \tilde{\alpha}^2 p_2^2} \right. \\
&\left. - \frac{g}{\tilde{\Omega}_1^2 \left(2\omega^2 + \tilde{\alpha}^2 p_2^2 \right)} \left(\tilde{\alpha}^2 \omega^2 p_2^2 + \left(\omega^2 + \tilde{\alpha}^2 p_2^2 \right) \tilde{\Omega}_1^2 - \frac{g\left(\omega^2 + \tilde{\alpha}^2 p_2^2 \right) \omega^2}{h\left(2\omega^2 + \tilde{\alpha}^2 p_2^2 \right)} \right) \right] \cosh \tilde{\Omega}_1 t \\
&+ \frac{1}{\left(\tilde{\Omega}_1^2 + \tilde{\Omega}_2^2 \right)} \left[\dot{y}(0) \left(\frac{\omega^2}{2\omega^2 + \tilde{\alpha}^2 p_2^2} \left(\tilde{\alpha}^2 p_2^2 - \frac{g}{h} \right) + \tilde{\Omega}_1^2 \right) + \dot{v}(0) \frac{\tilde{\alpha}\omega^2 p_2^2}{2\omega^2 + \tilde{\alpha}^2 p_2^2} \right] \frac{\sinh \tilde{\Omega}_1 t}{\tilde{\Omega}_1} \\
&+ \frac{\xi^2}{h} \cdot \frac{2\omega^2 + \tilde{\alpha}^2 p_2^2}{\omega^2} - g \frac{\omega^2 + \tilde{\alpha}^2 p_2^2}{\omega^2 p_2^2} \\
&+ \frac{1}{(\tilde{\Omega}_1^2 + \tilde{\Omega}_2^2)} \left[\left(\frac{\omega^2}{2\omega^2 + \tilde{\alpha}^2 p_2^2} \left(\tilde{\alpha}^2 p_2^2 - \frac{g}{h} \right) - \tilde{\Omega}_2^2 \right) \frac{1}{\tilde{\Omega}_2} \int_0^t \ddot{y}_G(\tau) \sin \tilde{\Omega}_2 (t-\tau) d\tau \right. \\
&+ \frac{\tilde{\alpha}\omega^2 p_2^2}{(2\omega^2 + \tilde{\alpha}^2 p_2^2)} \frac{1}{\tilde{\Omega}_2} \int_0^t \ddot{x}_G(\tau) \sin \tilde{\Omega}_2 (t-\tau) \, d\tau \\
&- \left(\frac{\omega^2}{2\omega^2 + \tilde{\alpha}^2 p_2^2} \left(\tilde{\alpha}^2 p_2^2 - \frac{g}{h} \right) + \tilde{\Omega}_1^2 \right) \frac{1}{\tilde{\Omega}_1} \int_0^t \ddot{y}_G(\tau) \sinh (t-\tau) \, d\tau \\
&\left. - \frac{\tilde{\alpha}\omega^2 p_2^2}{(2\omega^2 + \tilde{\alpha}^2 p_2^2)} \frac{1}{\tilde{\Omega}_1} \int_0^t \ddot{x}_G(\tau) \sinh \tilde{\Omega}_1 (t-\tau) \, d\tau \right] \qquad (4.2.33)
\end{aligned}
$$

$$
\begin{aligned}
v(t) = &- \frac{1}{\left(\tilde{\Omega}_1^2 + \tilde{\Omega}_2^2\right)} \left[y(0) \, \frac{\tilde{\alpha}\omega^2 p_2^2}{2\omega^2 + \tilde{\alpha}^2 p_2^2} + v(0) \left(\frac{\omega^2 p_2^2}{2\omega^2 + \tilde{\alpha}^2 p_2^2} - \tilde{\Omega}_2^2 \right) + \frac{\tilde{\alpha}\omega^2 \left(p_2^2 - \tilde{\Omega}_2^2\right) g}{\tilde{\Omega}_2^2 \left(2\omega^2 + \tilde{\alpha}^2 p_2^2\right)} \right] \cos \tilde{\Omega}_2 t \\
&- \frac{1}{\left(\tilde{\Omega}_1^2 + \tilde{\Omega}_2^2\right)} \left[\dot{y}(0) \, \frac{\tilde{\alpha}\omega^2 p_2^2}{2\omega^2 + \tilde{\alpha}^2 p_2^2} + \dot{v}(0) \left(\frac{\omega^2 p_2^2}{2\omega^2 + \tilde{\alpha}^2 p_2^2} - \tilde{\Omega}_2^2 \right) \right] \frac{\sin \tilde{\Omega}_2 t}{\tilde{\Omega}_2} \\
&+ \frac{1}{\left(\tilde{\Omega}_1^2 + \tilde{\Omega}_2^2\right)} \left[y(0) \, \frac{\tilde{\alpha}\omega^2 p_2^2}{2\omega^2 + \tilde{\alpha}^2 p_2^2} + v(0) \left(\frac{\omega^2 p_2^2}{2\omega^2 + \tilde{\alpha}^2 p_2^2} + \tilde{\Omega}_1^2 \right) - \frac{\tilde{\alpha}\omega^2 \left(p_2^2 + \Omega_1^2\right) g}{\tilde{\Omega}_1^2 \left(2\omega^2 + \tilde{\alpha}^2 p_2^2\right)} \right] \cosh \tilde{\Omega}_1 t \\
&+ \frac{1}{\left(\tilde{\Omega}_1^2 + \tilde{\Omega}_2^2\right)} \left[\dot{y}(0) \, \frac{\tilde{\alpha}\omega^2 p_2^2}{2\omega^2 + \tilde{\alpha}^2 p_2^2} + \dot{v}(0) \left(\frac{\omega^2 p_2^2}{2\omega^2 + \tilde{\alpha}^2 p_2^2} + \tilde{\Omega}_1^2 \right) \right] \frac{\sinh \tilde{\Omega}_1 t}{\tilde{\Omega}_1} \\
&\qquad + \xi \, \frac{2\omega^2 + \tilde{\alpha}^2 p_2^2}{\omega^2} \\
&+ \frac{1}{\left(\tilde{\Omega}_1^2 + \tilde{\Omega}_2^2\right)} \left[\frac{\tilde{\alpha}\omega^2 p_2^2}{\left(2\omega^2 + \tilde{\alpha}^2 p_2^2\right)} \frac{1}{\tilde{\Omega}_2} \int_0^t \ddot{y}_G(\tau) \sin \tilde{\Omega}_2 (t-\tau) d\tau \right. \\
&\qquad + \left(\frac{\omega^2 p_2^2}{2\omega^2 + \tilde{\alpha}^2 p_2^2} - \tilde{\Omega}_2^2 \right) \frac{1}{\tilde{\Omega}_2} \int_0^t \ddot{x}_G(\tau) \sin \tilde{\Omega}_2 (t-\tau) \, d\tau \\
&- \frac{\tilde{\alpha}\omega^2 p_2^2}{\left(2\omega^2 + \tilde{\alpha}^2 p_2^2\right)} \frac{1}{\tilde{\Omega}_1} \int_0^t \ddot{y}_G(\tau) \sinh \tilde{\Omega}_1 (t-\tau) d\tau \\
&\qquad \left. - \left(\frac{\omega^2 p_2^2}{2\omega^2 + \tilde{\alpha}^2 p_2^2} + \tilde{\Omega}_1^2 \right) \frac{1}{\tilde{\Omega}_1} \int_0^t \ddot{x}_G(\tau) \sinh \tilde{\Omega}_1 (t-\tau) d\tau \right]
\end{aligned}
\tag{4.2.34}
$$

The origin of time in these equations is at the onset of lift-off. After $y(t)$ and $v(t)$ have been found, $\phi(t)$ and $u(t)$ can be determined by equations (4.2.26) and (4.2.27).

General response

In order to calculate the total response, one has to determine at

each time step whether the system is in the state of full contact or uplift, and then apply the appropriate set of equations. When the system changes from one state to the other, the final conditions of the first case should be used as initial conditions for the next one.

A much simpler solution can be derived by neglecting the gravity terms in the left-hand side of the equations of motion, which is a good approximation for small angles of rotation. Then, the response after lift-off is given by the superposition of a parabolic and a harmonic term. Since this solution is derived as an approximate, first-mode solution for the response of a multistory structure (see section 4.3.3), it is not presented here.

4.2.4 Damped Case

If damping exists in the superstructure and the foundation, equations (4.2.13) and (4.2.25) are not valid. With damping, x and u are not linearly dependent but are related through a first-order differential equation. After lift-off, y is coupled with x and u also. Therefore, one has to solve a system of two differential equations in x and u during full contact, and a system of three differential equations in x, u, and y after uplift. This problem can be treated as a special case of the n-story superstructure, which is examined in section 4.3.

4.2.5 Example

As an example, let us consider the simple oscillator which models the first mode of Millikan Library. If $\underset{\sim}{\eta}$ is the first eigenvector, one

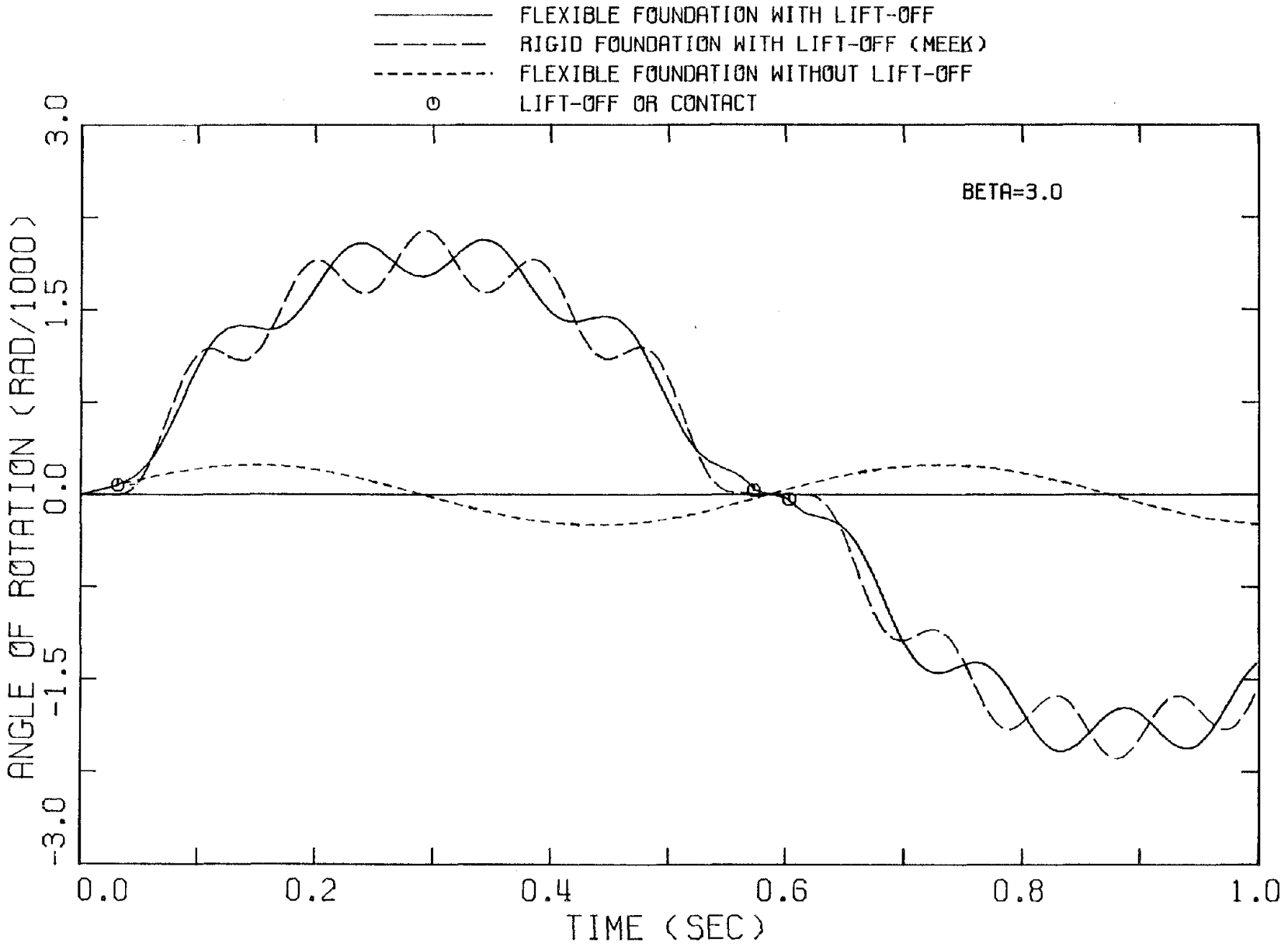

Fig. 4.2.3. Rocking response of a simple shear oscillator (horizontal impulse excitation).

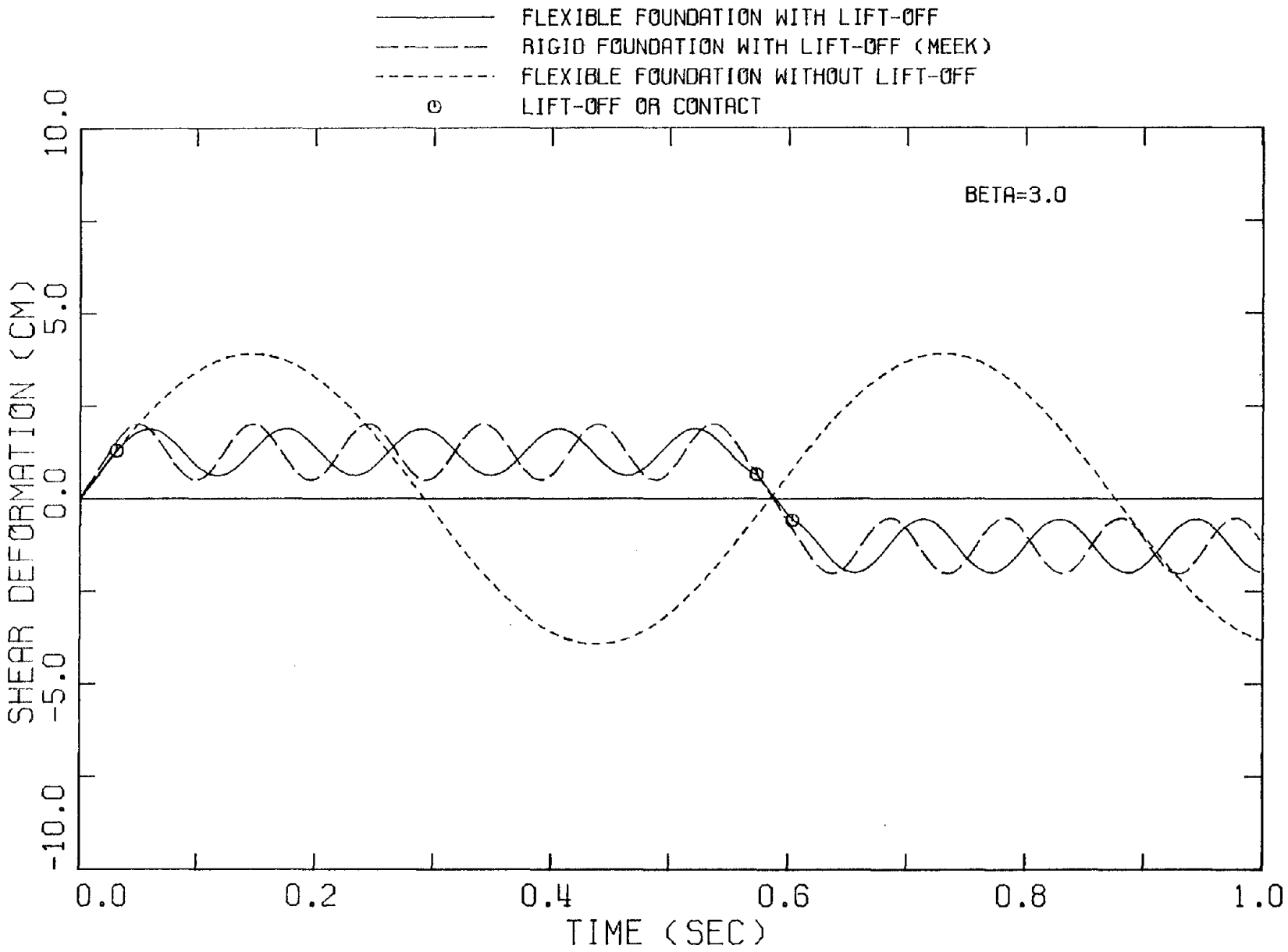

Fig. 4.2.4. Shear deformation of a simple shear oscillator (horizontal impulse excitation).

can write (according to Ref. 55)

$$m = \frac{\left[\sum_{i=1}^{10} m_i \eta_i\right]^2}{\sum_{i=1}^{10} m_i \eta_i^2} \qquad \text{and} \qquad h = \frac{\sum_{i=1}^{10} m_i h_i \eta_i}{\sum_{i=1}^{10} m_i \eta_i}$$

For Millikan Library, these expressions reduce to $m = 0.66 \times 10^3$ t-sec^2/m and $h = 32.6$ m. Also, $\omega = 1.88$ Hz. For the foundation take: $k = 6.56 \times 10^6$ t/m and $\xi = 6.07$ m. (These values were found from the Winkler stiffness used in section 2.5.6, considering the equivalent two-spring model during full contact.) Then, $\tilde{\alpha} = 0.186$, $p_2 = 22.4$ Hz, and $p_1 = \tilde{\alpha} p_2 = 4.17$ Hz.

In Figs. 4.2.3 and 4.2.4 the rocking response and shear distortion are shown for a horizontal impulse excitation. The value of β was 3, which corresponds to an initial horizontal velocity equal to 507 mm/s. It is evident from these plots that lift-off greatly affects the response of the system, since both the fixed base response (not shown) and the response for the flexible foundation in which lift-off is not allowed are much different from the solution obtained from this analysis. On the other hand, the solution obtained by Meek[15] for the rocking of the structure on a rigid foundation gives good results. It should be mentioned, however, that the foundation was quite stiff in this example; softer foundations may not yield such good agreement.

4.3 DYNAMICS OF A MULTIDEGREE OF FREEDOM STRUCTURE

4.3.1 System Considered and Equations of Motion

The system under investigation is shown in Fig. 4.3.1. The

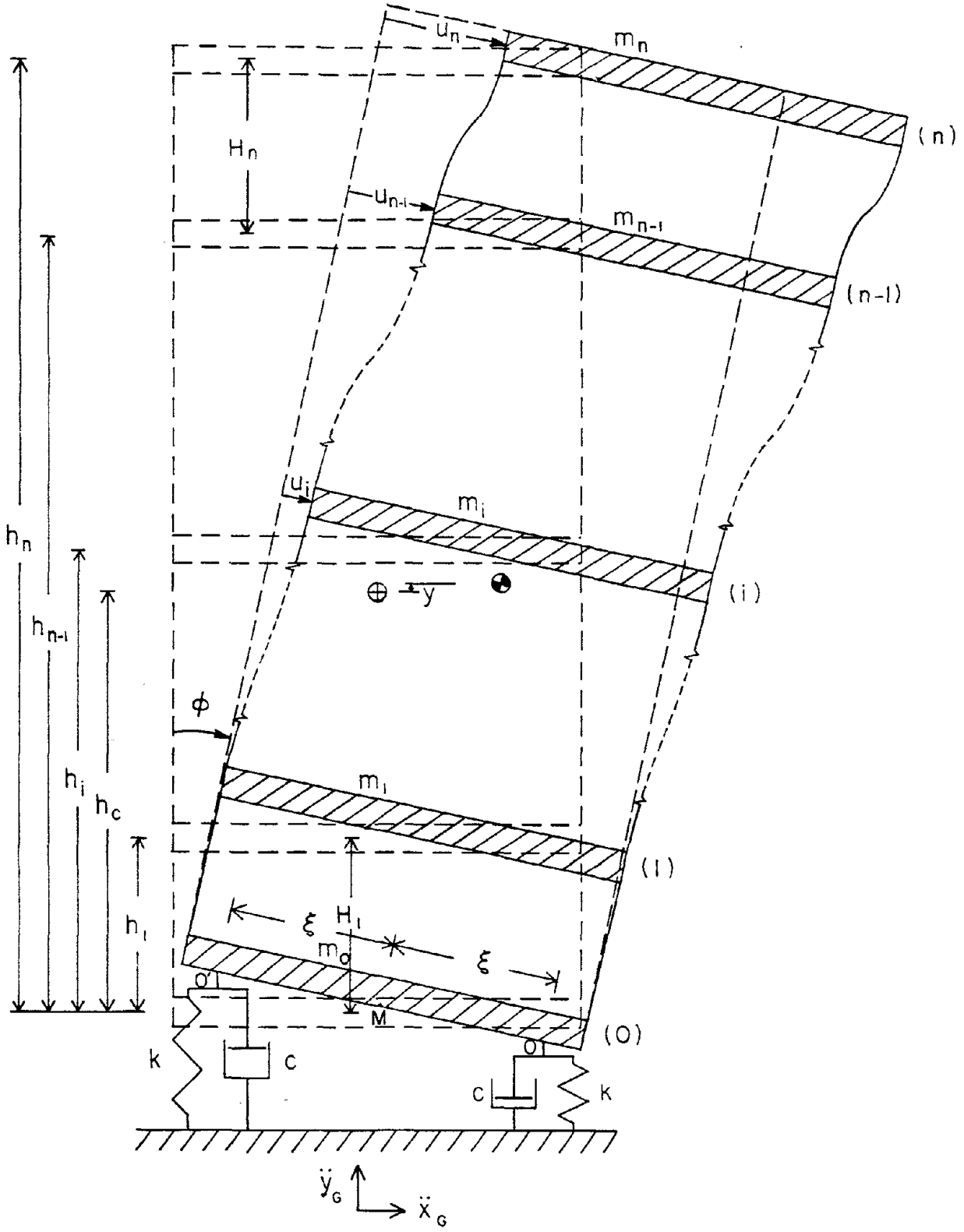

Fig. 4.3.1. Rocking n-story structure on two-spring foundation.

superstructure consists of n+1 rigid masses, concentrated at the floor levels and connected with massless, viscously damped members, so that there is one degree of freedom per floor. The building is supported by a two-spring foundation with springs of stiffness k and dashpots of constant c, placed symmetrically, a distance ξ from the center of the base, M. The system, initially at rest, is subjected to horizontal and vertical ground accelerations, $\ddot{x}_G$ and $\ddot{y}_G$ respectively, and no slippage is allowed between the base and the foundation. Formulated this way, the building-foundation system possesses n+2 degrees of freedom, namely, rotation of the structure in the plane of motion, measured by the angle ϕ, vertical translation measured by the vertical displacement of the center of mass, y, and displacement of the superstructure at the i^{th} floor relative to the base, excluding rotations, denoted by u_i, $i = 1,2,\cdots,n$.

For the special case of a superstructure deforming only in shear, the equations of motion for the building-foundation interactive system are derived in Appendix II. In general, for small displacements, the equations of motion can be written as

$$[M]\ddot{\underset{\sim}{u}} + [C]\dot{\underset{\sim}{u}} + [K]\underset{\sim}{u} = -[M](\underset{\sim}{h}\ddot{\phi} - \underset{\sim}{1}\, g\phi + \underset{\sim}{1}\, \ddot{x}_G) \tag{4.3.1}$$

and

Full contact

$$\ddot{y} + 2\zeta_2 p_2 \dot{y} + p_2^2 y = -\ddot{y}_G \tag{4.3.2}$$

$$\ddot{\phi} + \frac{1}{I_M}\sum_{i=1}^{n} m_i h_i \ddot{u}_i + 2\zeta_1 p_1 \dot{\phi} + p_1^2 \phi - \frac{g}{I_M}\sum_{i=1}^{n} m_i u_i = -\frac{mh_c}{I_M}\ddot{x}_G \tag{4.3.3}$$

After lift-off

$$\ddot{y} + \zeta_2 p_2 \dot{y} - \zeta_2 p_2 \xi\dot{\phi} + \frac{p_2^2}{2} y - \frac{p_2^2}{2} \xi\phi = -\frac{g}{2} - \ddot{y}_G \tag{4.3.4}$$

$$\ddot{\phi} + \frac{1}{I_M} \sum_{i=1}^{n} m_i h_i \ddot{u}_i + \zeta_1 p_1 \dot{\phi} - \frac{\zeta_1 p_1}{\xi} \dot{y} + \frac{p_1^2}{2} \phi - \frac{k\xi}{I_M} y - \frac{g}{2I_M} \sum_{i=1}^{n} m_i u_i =$$

$$= - \frac{mg\xi}{2I_M} - \frac{mh_c}{I_M} \ddot{x}_G \tag{4.3.5}$$

In these equations, $\underset{\sim}{u} = \{u_i\}$ and $\underset{\sim}{h} = \{h_i\}$ are column vectors; $\underset{\sim}{1}$ is the column vector with unit elements; h_i is the height of the i^{th} floor measured from the base level, and h_c is the height at which the center of mass is located; m_i is the mass of the i^{th} story, and m is the total mass, i.e., $m = \sum_{i=0}^{n} m_i$, m_o being the base mass; I_M is the total moment of inertia about the middle point of the base, M, and can be written as

$$I_M = \sum_{i=0}^{n} I_i + \sum_{i=1}^{n} m_i h_i^2 \tag{4.3.6}$$

in which I_i is the centroidal moment of inertia of the i^{th} mass; p_1, p_2, ζ_1, and ζ_2 are defined by equations (2.3.24), (2.3.25), (3.2.5), and (3.2.6), respectively, and are the characteristic frequencies and ratios of critical damping during full contact for rocking and vertical motions of the corresponding rigid superstructure; [M], [C], and [K] are the mass, damping, and stiffness matrices of the superstructure, calculated for fixed base response.

The matrix [M] is diagonal and the matrices [K] and [C] are symmetric and positive definite. For a shear structure, [K] and [C] are

tri-diagonal but this property does not hold, in general, if bending deformation is also taken under consideration. Let ω_r be the r^{th} eigenvalue of the matrix $[M]^{-1}[K]$, $\underset{\sim}{\eta}^{(r)}$ the corresponding eigenvector, and [N] the modal matrix defined by

$$[N] = [\underset{\sim}{\eta}^{(1)} \; \underset{\sim}{\eta}^{(2)} \; \cdots \; \underset{\sim}{\eta}^{(n)}] \tag{4.3.7}$$

The eigenvectors can be normalized so that

$$[N]^T [M][N] = [I] \tag{4.3.8}$$

and

$$[N]^T [K][N] = [\sim\omega^2\_] \tag{4.3.9}$$

where [I] is the identity matrix. Then, making the transformation,

$$\underset{\sim}{u}(t) = [N] \underset{\sim}{q}(t) \tag{4.3.10}$$

and substituting into equation (4.3.1) with premultiplication by $[N]^T$, one finds

$$[I]\ddot{\underset{\sim}{q}} + [N]^T [C][N]\dot{\underset{\sim}{q}} + [\sim\omega^2\_]\underset{\sim}{q} = -[N]^T[M](\ddot{h\underset{\sim}{\phi}} - \underset{\sim}{1}\, g\phi + 1\ddot{x}_G) \tag{4.3.11}$$

If the superstructure admits decomposition into classical normal modes, the matrix $[N]^T [C][N]$ will be diagonal (see Caughey and O'Kelly[56] for conditions for this to occur). It is assumed here that classical normal modes exist, since buildings seem to possess such modes over a significant range of amplitudes.

Equation (4.3.11) reduces then to a system of n uncoupled differential equations which can be written in the form

$$\ddot{q}_r + 2\zeta_r^s \omega_r \dot{q}_r + \omega_r^2 q_r = f_r(\phi,\ddot{\phi},\ddot{x}_G) , \quad r = 1,2,\cdots,n \qquad (4.3.12)$$

in which $2\zeta_r^s\omega_r$ is the r^{th} diagonal term of the matrix $[N]^T[C][N]$ and ζ_r^s is the ratio of critical damping associated with the r^{th} mode of the superstructure. The function f_r is the r^{th} component of the forcing function in the right-hand side of equation (4.3.11) and can be written as

$$f_r = - A_r\ddot{\phi} + B_r g\phi - B_r\ddot{x}_G \qquad (4.3.13)$$

where

$$A_r = \sum_{i=1}^{n} m_i h_i \eta_i^{(r)} \qquad (4.3.14)$$

$$B_r = \sum_{i=1}^{n} m_i \eta_i^{(r)} \qquad (4.3.15)$$

In the above expressions, $\eta_i^{(r)}$ is the i^{th} component of the r^{th} eigenvector.

Equation (4.3.12) can be solved for $q_r(t)$ in terms of $\phi(t)$, $\ddot{\phi}(t)$, and $\ddot{x}_G(t)$. Substitution in equations (4.3.3), (4.3.4), and (4.3.5) using (4.3.10), however, would reduce the problem to the solution of an integrodifferential equation for the case of full contact, or a system of two integrodifferential equations after lift-off. To avoid this, a solution by use of Laplace transform is proposed.

Taking the Laplace transform of equations (4.3.12) and (4.3.13),

$$\Delta_r(s)\,\bar{q}_r(s) = - (A_r s^2 - B_r g)\bar{\phi}(s) - B_r\bar{\ddot{x}}_G(s) + s[A_r\phi(0) + q_r(0)]$$

$$+ A_r\dot{\phi}(0) + \dot{q}_r(0) + 2\zeta_r^s\omega_r q_r(0) \qquad (4.3.16)$$

in which

$$\Delta_r(s) = s^2 + 2\zeta_r^s \omega_r s + \omega_r^2 \tag{4.3.17}$$

In this equation, and subsequently, s is the complex Laplace variable and a bar over a function denotes the Laplace transform.

From equation (4.3.10)

$$\bar{u}_i(s) = \sum_{r=1}^{n} n_i^{(r)} \bar{q}_r(s) \tag{4.3.18}$$

Taking the Laplace transform of equation (4.3.3), (4.3.4), and (4.3.5) and using (4.3.16) and (4.3.18), the following equations can be derived.

Full contact

$$\left[s^2 + 2\zeta_1 p_1 s + p_1^2 - \frac{1}{I_M} \sum_{r=1}^{n} \frac{\left(A_r s^2 - B_r g\right)^2}{\Delta_r(s)}\right] \bar{\phi}(s)$$

$$= \frac{1}{I_M}\left[\sum_{r=1}^{n} \frac{B_r\left(A_r s^2 - B_r g\right)}{\Delta_r(s)} - mh_c\right] \bar{\ddot{x}}_G(s)$$

$$- \frac{1}{I_M} \sum_{r=1}^{n} \frac{s\left(A_r s^2 - B_r g\right)}{\Delta_r(s)} \left[A_r \phi(0) + q_r(0)\right] -$$

$$- \frac{1}{I_M} \sum_{r=1}^{n} \frac{\left(A_r s^2 - B_r g\right)}{\Delta_r(s)} \left[A_r \dot{\phi}(0) + \dot{q}_r(0) + 2\zeta_r^s \omega_r q_r(0)\right]$$

$$+ \left[\phi(0) + \frac{1}{I_M} \sum_{i=1}^{n} m_i h_i u_i(0)\right] s + \left[\dot{\phi}(0) + 2\zeta_1 p_1 \phi(0) + \frac{1}{I_M} \sum_{i=1}^{n} m_i h_i \dot{u}_i(0)\right] \tag{4.3.19}$$

After lift-off

$$\left(s^2+\zeta_2 p_2 s+\frac{p_2^2}{2}\right)\bar{y}(s) = \left(\zeta_2 p_2 s+\frac{p_2^2}{2}\right)\xi\,\bar{\phi}(s) - \bar{\ddot{y}}_G(s) - \frac{g}{2s}$$

$$+ sy(0) + \dot{y}(0) + \zeta_2 p_2 y(0) - \zeta_2 p_2 \xi\,\phi(0) \qquad (4.3.20)$$

$$\left[s^2+\zeta_1 p_1 s+\frac{p_1^2}{2} - \frac{\left(\zeta_1 p_1 s+\frac{k\xi^2}{I_M}\right)\left(\zeta_2 p_2 s+\frac{p_2^2}{2}\right)}{s^2+\zeta_2 p_2 s+\frac{p_2^2}{2}} - \frac{1}{I_M}\sum_{r=1}^{n}\frac{A_r^2 s^4 - \frac{3}{2}A_r B_r g s^2 + \frac{1}{2}B_r^2 g^2}{\Delta_r(s)}\right]\bar{\phi}(s) =$$

$$= \frac{1}{I_M}\left[\sum_{r=1}^{n}\frac{B_r\left(A_r s^2 - \frac{1}{2}B_r g\right)}{\Delta_r(s)} - mh_c\right]\bar{\ddot{x}}_G(s) - \frac{\left(\zeta_1 p_1 s+\frac{k\xi^2}{I_M}\right)}{\xi\left(s^2+\zeta_2 p_2 s+\frac{p_2^2}{2}\right)}\bar{\ddot{y}}_G(s)$$

$$- \frac{1}{I_M}\sum_{r=1}^{n}\frac{s\left(A_r s^2 - \frac{1}{2}B_r g\right)}{\Delta_r(s)}\left[A_r\,\phi(0) + q_r(0)\right]$$

$$- \frac{1}{I_M}\sum_{r=1}^{n}\frac{\left(A_r s^2 - \frac{1}{2}B_r g\right)}{\Delta_r(s)}\left[A_r\dot{\phi}(0) + \dot{q}_r(0) + 2\zeta_r^s\omega_r q_r(0)\right]$$

$$+ s\left[\phi(0) + \frac{\left(\zeta_1 p_1 s+\frac{k\xi^2}{I_M}\right)}{\xi\left(s^2+\zeta_2 p_2 s+\frac{p_2^2}{2}\right)}\,y(0) + \frac{1}{I_M}\sum_{i=1}^{n} m_i h_i u_i(0)\right]$$

$$+ \dot{\phi}(0) + \zeta_1 p_1\phi(0) - \frac{\zeta_1 p_1}{\xi}\,y(0) + \frac{\left(\zeta_1 p_1 s+\frac{k\xi^2}{I_M}\right)}{\xi\left(s^2+\zeta_2 p_2 s+\frac{p_2^2}{2}\right)} \times$$

$$\times \left[\dot{y}(0) + \zeta_2 p_2\, y(0) - \zeta_2 p_2\, \xi\, \phi(0)\right]$$

$$+ \frac{1}{I_M} \sum_{i=1}^{n} m_i h_i \dot{u}_i(0) - \frac{mg\xi}{2I_M s} - \frac{\left(\zeta_1 p_1 s + \frac{k\xi^2}{I_M}\right)}{\xi\left(s^2 + \zeta_2 p_2 s + \frac{p_2^2}{2}\right)} \frac{g}{2s} \qquad (4.3.21)$$

The Laplace transform of equation (4.3.2) was not taken, since this equation can be solved directly by means of Duhamel's integral.

It should be mentioned here that although the system is initially at rest, all the terms in these equations involving initial conditions should be kept. This is because the system continuously changes from the state of full contact to lift-off, or vice-versa, and the final conditions of one state are used as initial conditions for the other.

For the inversion of the Laplace transform by residue theory, the zeroes of the terms in brackets in the left-hand side of equations (4.3.19) and (4.3.21) must be determined. This procedure requires the determination of the roots of an $(n+1)^{th}$ order algebraic equation in s^2 in the case of equation (4.3.19) and an $(n+2)^{th}$ order equation in the case of equation (4.3.21), which, in general, can only be done numerically. However, approximate values of the poles of these transfer functions can easily be found, as is discussed in the next section.

4.3.2 Qualitative Investigation of the Behavior of the System

For simplicity, let us first consider the undamped case. For the case of full contact, it is convenient to define the functions

$$G_1(s^2) = -\left(s^2 + p_1^2\right) \tag{4.3.22}$$

and

$$G_2(s^2) = -\frac{1}{I_M}\sum_{r=1}^{n}\frac{\left(A_r s^2 - B_r g\right)^2}{s^2 + \omega_r^2} \tag{4.3.23}$$

Note that G_2 depends on the parameters of the superstructure only, while the foundation parameters appear in the expression of G_1. If one plots the functions G_1 and G_2 versus s^2, the values of s^2 at the intersections of these two curves locate the zeroes of the bracketed expression in the left-hand side of equation (4.3.19). Let $s = \pm i\tilde{\omega}_k$, $k = 1,2,\cdots,n+1$ be those zeroes. The values of $\tilde{\omega}_k$ define the n+1 resonant frequencies of the building-foundation system. The functions G_1 and G_2 are plotted versus s^2 in Fig. 4.3.2a for the example based on Millikan Library (presented in section 4.3.3) with the two-spring foundation defined by the equations of equivalence during full contact (see section 2.5.2). An expanded view of the plot near the origin is shown in Fig. 4.3.2b.

First, note that the function G_2 is smooth with apparently constant slope, except for narrow regions around the values $s^2 = -\omega_k^2$, $k = 1,2,\cdots,n$, where its slope suddenly approaches infinity. As a result, the values of $\tilde{\omega}_k$, $k = 1,2,\cdots,n$ are expected to be close to ω_k and, at least for the higher frequencies, the relative difference between $\tilde{\omega}_k$ and ω_k is negligible. For $\tilde{\omega}_1$, however, this difference may be important, as can be seen from Fig. 4.3.2b. It is evident that $\tilde{\omega}_1$ is always smaller than ω_1 and it decreases as the foundation stiffness decreases. It can be concluded, therefore, that the higher frequencies of the building are

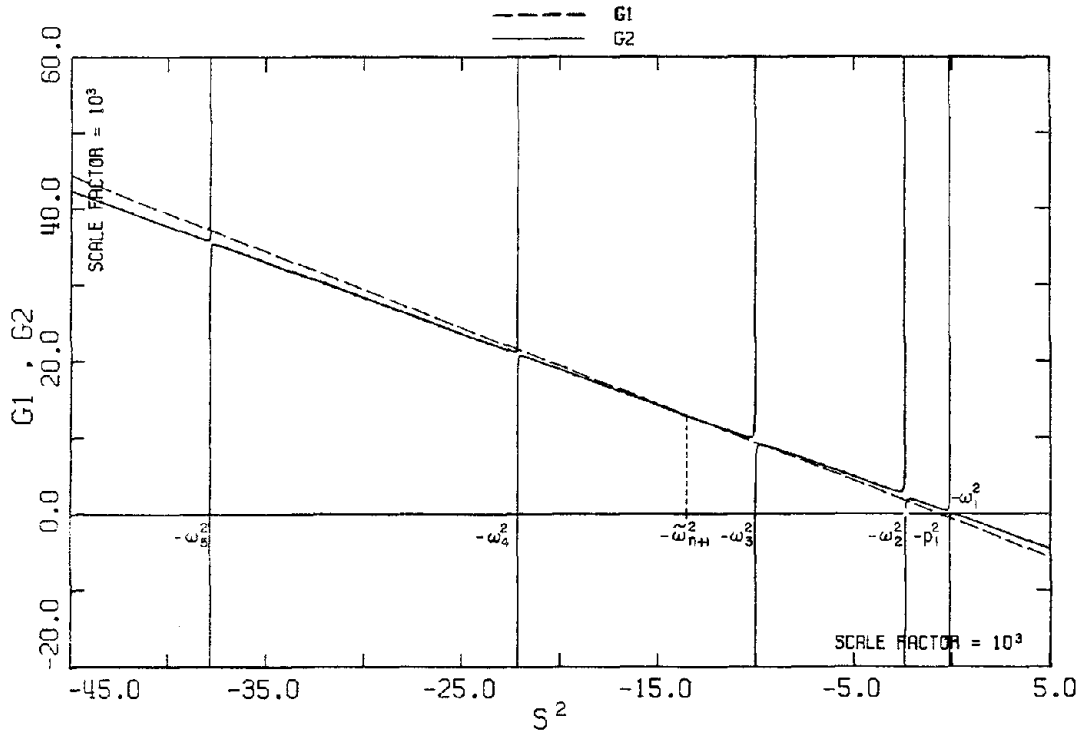

(a)

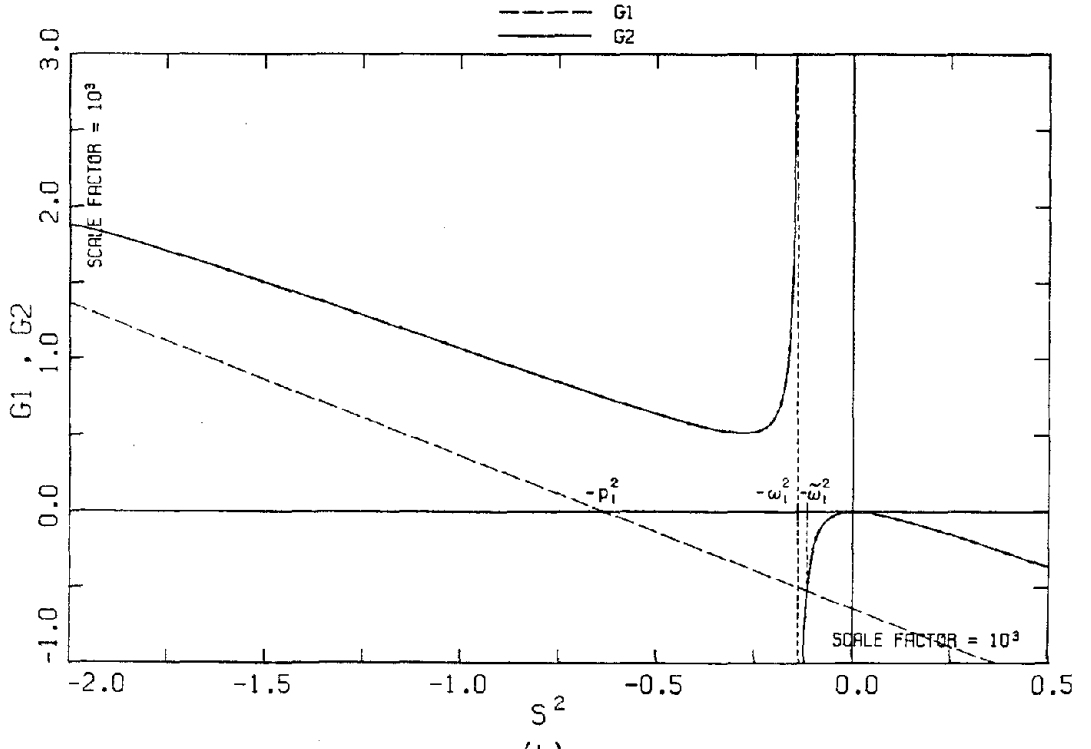

(b)

Fig. 4.3.2. Determination of the resonant frequencies of the building-foundation system during full contact.

not affected significantly by the interaction of the structure with the ground and the effect is primarily shown on the fundamental frequency, which is always reduced. These results have also been reported by other investigators of soil-structure interaction (e.g., see Jennings and Bielak[19]).

In Fig. 4.3.3, the first three terms of the series in the expression for G_2 are plotted individually. It is evident that apart from narrow regions around $s^2 = -\omega_k^2$, $k = 2,3,\cdots,n$, the first term of the series is the dominant one. Because of this behavior, equating the functions G_1 and G_2 reduces to

$$\left(I_M - A_1^2\right)s^4 + \left[I_M\left(\omega_1^2 + p_1^2\right) + 2A_1B_1g\right]s^2 + I_M\, p_1^2\, \omega_1^2 - B_1^2 g = 0 \quad (4.3.24)$$

which is a second order equation in s^2. Let s_1^2 and s_2^2 be the roots of this equation, which are both negative, and let $|s_1^2| < |s_2^2|$. One can then write: $\tilde{\omega}_1 \simeq is_1$ and $\tilde{\omega}_{n+1} \simeq is_2$. The remaining n-1 resonant frequencies of the system can be approximated by the corresponding frequencies of the building, i.e., $\tilde{\omega}_k \simeq \omega_k$, $k = 2,3,\cdots,n$.

For base excitation, the contribution of the higher modes to the response of the system decreases as the value of the corresponding eigenfrequencies increase, so the importance of the $(n+1)^{th}$ mode depends on the relative value of $\tilde{\omega}_{n+1}$ in comparison to the other resonant frequencies of the system. It can easily be concluded from Fig. 4.3.2a that $\tilde{\omega}_{n+1}$ increases with the foundation stiffness and in the limit, $\tilde{\omega}_{n+1} \to \infty$ for rigid foundations. Also, since the slope of G_1 is -1 and the slope of G_2 for large $|s^2|$ is $-A_1^2/I_M$, the value of $\tilde{\omega}_{n+1}$ increases as A_1^2 approaches I_M. Note that both A_1 and I_M depend on the

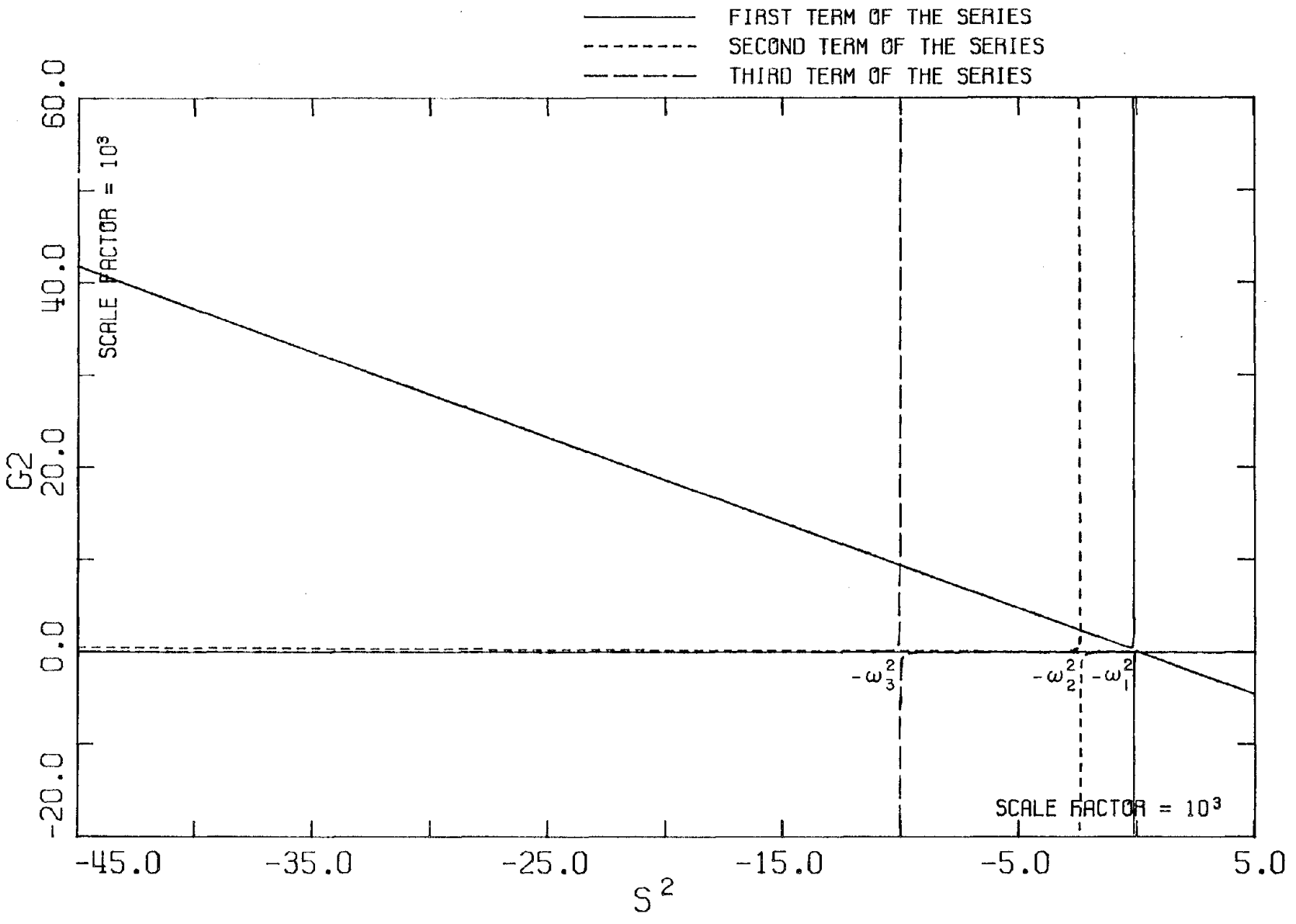

Fig. 4.3.3. Importance of each term of function $G_2(s^2)$.

properties of the building, and A_1^2 is always less than I_M.

Let us now examine the behavior of the system after lift-off. In this case we are seeking the zeroes of the transfer function which appears in the left-hand side of equation (4.3.21). Let us define the functions

$$G_3(s^2) = -\left[s^2 + \frac{p_1^2}{2} - \frac{k\xi^2 p_2^2}{2I_M\left(s^2 + \frac{p_2^2}{2}\right)} \right] \tag{4.3.25}$$

$$G_4(s^2) = -\frac{1}{I_M} \sum_{r=1}^{n} \frac{A_r^2 s^4 - \frac{3}{2} A_r B_r g s^2 + \frac{1}{2} B_r^2 g^2}{s^2 + \omega_r^2} \tag{4.3.26}$$

With this notation, the zeroes of the transfer function can be found from the points of intersection of functions G_3 and G_4, when the latter are plotted versus s^2. This plot is shown in Fig. 4.3.4a for the same example of Figs. 4.3.2 and 4.3.3; an enlarged view around the origin is shown in Fig. 4.3.4b.

It is interesting to notice that one of these points of intersection corresponds to a positive value of s^2. As a result, the response of the system consists of n+1 harmonic terms combined with a hyperbolic term. A hyperbolic term was expected in view of the results for a rigid superstructure. The existence of the real pole can be demonstrated if one keeps only the first term of the series in the expression for G_4, which again is the dominant one, except for narrow regions around $s^2 = -\omega_k^2$, $k = 2,3,\cdots,n$. Then, three of the zeroes of the transfer function can be approximated by the roots of the equation

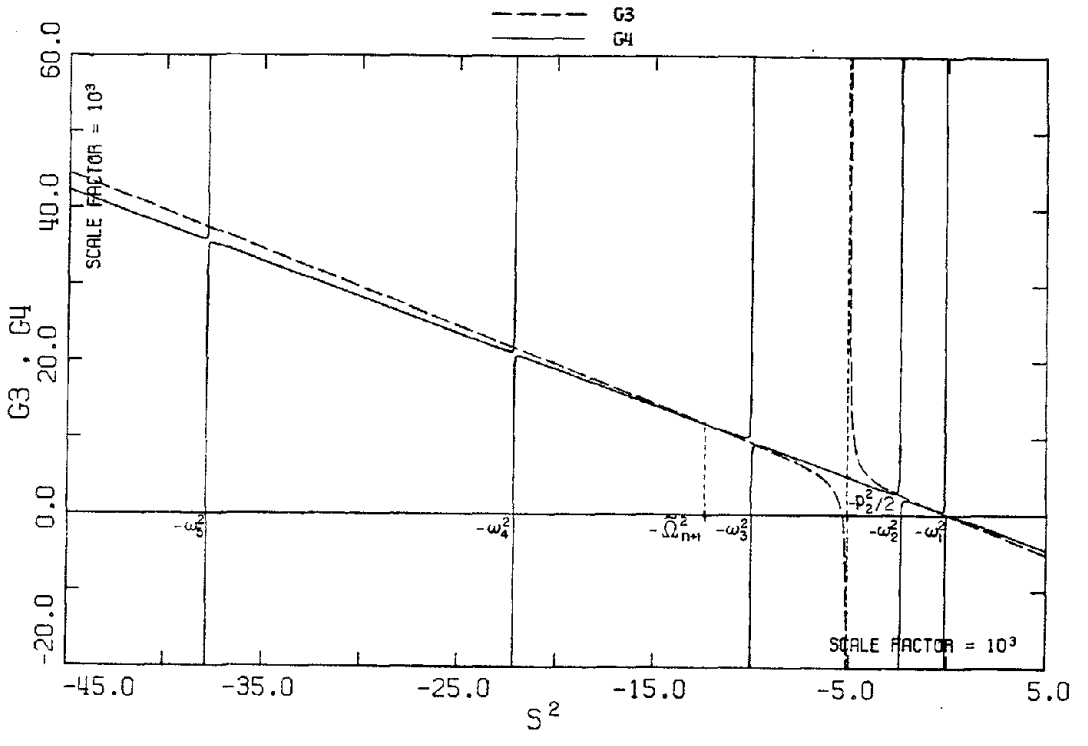

Fig. 4.3.4. Determination of resonant frequencies of the building-foundation system after lift-off.

$$I_M\left(s^2+\frac{p_1^2}{2}\right)\left(s^2+\frac{p_2^2}{2}\right)\left(s^2+\omega_1^2\right) - \frac{k\xi^2 p_2^2}{2}\left(s^2+\omega_1^2\right) -$$

$$- \left(A_1 s^4 - \frac{3}{2} A_1 B_1 g s^2 + \frac{1}{2} B_1^2 g^2\right)\left(s^2+\frac{p_2^2}{2}\right) = 0 \qquad (4.3.27)$$

which is a third order equation in s^2. The product of the three roots of this equation is equal to the negative of the ratio of the constant term to the coefficient of s^6, and can be written as

$$\frac{p_2^2}{4\left(I_M - A_1^2\right)}\left(B_1^2 g + mgh_c\omega_1^2\right)$$

Since $I_M - A_1^2 > 0$, this is a positive number and thus one of the roots of equation (4.3.27) must be positive.

Let $s = \pm i\tilde{\Omega}_k$, $k = 1,2,\cdots,n+1$ and $s = \pm\tilde{\Omega}_o$ be the zeroes of the bracketed expression in the left-hand side of equation (4.3.21). One can write $\tilde{\Omega}_k \simeq \omega_k$ for $k = 2,3,\cdots,n$, while $\tilde{\Omega}_1$, $\tilde{\Omega}_{n+1}$, and $\tilde{\Omega}_o$ can be calculated by the roots of (4.3.27). As a result of the real poles $s = \pm\tilde{\Omega}_o$, the system does not possess resonant frequencies in the classical sense. Looking at the free oscillations, however, one can identify an apparent fundamental frequency, which depends on the amplitude of the response. This apparent fundamental frequency is determined by the hyperbolic term of the response, upon which the harmonic terms are superimposed. Since the system becomes softer after lift-off, the apparent fundamental frequency is expected to be smaller than $\tilde{\omega}_1$. An approximate method of estimating this frequency by considering only the first mode of the superstructure is presented in section 4.3.3.c.

Let us now consider the damped case. During full contact, let $\tilde{\zeta}_k$, $k = 1,2,\cdots,n+1$ be the ratios of critical damping of the soil-structure interacting system. As it was shown, the eigenfrequencies of the second to n^{th} modes of the superstructure are not significantly affected by the interaction with the soil, therefore, one can write $\tilde{\zeta}_k = \zeta_k^s$ for $k = 2,3,\cdots,n$. The values of $\tilde{\zeta}_1$ and $\tilde{\zeta}_{n+1}$ can be found approximately by keeping only the first term of the series which appears in the left-hand side of equation (4.3.19). We want to determine $\tilde{\zeta}_\ell$, $\ell = 1,n+1$, so that the values

$$s = \tilde{\omega}_\ell\left(-\tilde{\zeta}_\ell \pm i\sqrt{1-\tilde{\zeta}_\ell^2}\right), \qquad \ell = 1,n+1 \tag{4.3.28}$$

satisfy approximately the equation

$$s^2 + 2\zeta_1 p_1 s + p_1^2 - \frac{\left(A_1 s^2 - B_1 g\right)^2}{I_M\left(s^2 + 2\zeta_1^s\,\omega_1 s + \omega_1^2\right)} = 0 \tag{4.3.29}$$

Substituting and keeping only the first-order terms in $\tilde{\zeta}_\ell$, one finds

$$\left(I_M - A_1^2\right)\tilde{\omega}_\ell^4 - \left[I_M\left(\omega_1^2 + p_1^2\right) + 2A_1B_1g\right]\tilde{\omega}_\ell^2 + I_M\,p_1^2\,\omega_1^2 - B_1^2 g^2 = 0 \tag{4.3.30}$$

and

$$\tilde{\zeta}_\ell = \frac{\zeta_1\left(\tilde{\omega}_\ell/\omega_1 - \omega_1/\tilde{\omega}_\ell\right) + \zeta_1^s\left(\tilde{\omega}_\ell/p_1 - p_1/\tilde{\omega}_\ell\right)}{2\left(1 - \frac{A_1^2}{I_M}\right)\frac{\tilde{\omega}_\ell^2}{\omega_1 p_1} - \left(\frac{\omega_1}{p_1} + \frac{p_1}{\omega_1} + \frac{2A_1B_1g}{I_M\,\omega_1 p_1}\right)}, \qquad \ell = 1,n+1 \tag{4.3.31}$$

Equation (4.3.30) is a second-order equation in $\tilde{\omega}_\ell^2$ and the two roots will determine the values of $\tilde{\omega}_1$ and $\tilde{\omega}_{n+1}$. After the $\tilde{\omega}_\ell$'s are found, the corresponding ratios of critical damping can be estimated

(to first order) by equation (4.3.31).

After lift-off, one can again assume that the damping coefficients, $\tilde{Z}_k$, associated with the higher modes of the system, are close to the corresponding ratios of critical damping of the superstructure, i.e., $\tilde{Z}_k \simeq \zeta_k^s$ for $k = 2,3,\cdots,n$. For the remaining modes, one considers again only the first term of the series in the left-hand side of equation (4.3.21) and assumes that the zeroes of the transfer function can be approximated by the values

$$s = \tilde{\Omega}_\ell\left(-\tilde{Z}_\ell \pm \sqrt{1 - \tilde{Z}_\ell^2}\right), \ \ell = 1,n+1, \text{ and } s = \pm\tilde{\Omega}_0 \qquad (4.3.32)$$

Working similarly, the values of $\tilde{Z}_\ell$'s can be derived.

Note that equation (4.3.30) gives the same values for $\tilde{\omega}_1$ and $\tilde{\omega}_{n+1}$ as equation (4.3.24).

In general, it can be concluded that soil-structure interaction results in a reduction of the fundamental resonant frequency of the structure, while the higher resonant frequencies are not affected significantly. If the excitation is strong enough to cause lift-off, the system becomes softer and the apparent fundamental frequency decreases even more. Since the system is now nonlinear, this frequency depends on the excitation and decreases as the amplitude of the excitation increases. Because of this behavior, the earthquake response of the uplifting system may be significantly different from the response without lift-off. The difference between the two responses, however, depends on the parameters of the structure and the foundation, and on the nature of the excitation. These features also determine whether lift-off is favorable or not to the structure.

4.3.3 Approximate Solution for Response of the First Mode

4.3.3.a Undamped case

As was done for the rocking rigid block (see section 2.3.5), the gravity terms in the left-hand side of the equations of motion can be neglected for small angles of rotation. Noting that

$$\left.\begin{aligned} \sum_{i=1}^{n} m_i h_i u_i &= \sum_{i=1}^{n} A_i q_i \\ \sum_{i=1}^{n} m_i u_i &= \sum_{i=1}^{n} B_i q_i \end{aligned}\right\} \qquad (4.3.33)$$

and keeping only the first term of the series in the right-hand side of these relations (first mode approximation), the undamped equations of motion reduce to

$$\ddot{q}_1 + A_1\ddot{\phi} + \omega_1^2 q_1 = - B_1 \ddot{x}_G \qquad (4.3.34)$$

Full contact

$$\ddot{y} + p_2^2 y = - \ddot{y}_G \qquad (4.3.35)$$

$$\ddot{\phi} + \frac{A_1}{I_M}\ddot{q}_1 + p_1^2 \phi = - \frac{mh_c}{I_M}\ddot{x}_G \qquad (4.3.36)$$

After lift-off

$$\ddot{y} + \frac{p_2^2}{2} y - \frac{p_2^2}{2}\xi\phi = - \frac{g}{2} - \ddot{y}_G \qquad (4.3.37)$$

$$\ddot{\phi} + \frac{A_1}{I_M}\ddot{q}_1 + \frac{p_1^2}{2}\phi - \frac{k\xi}{I_M} y = - \frac{mg\xi}{2I_M} - \frac{mh_c}{I_M}\ddot{x}_G \qquad (4.3.38)$$

In general for buildings, $I_M \simeq A_1^2$ and $mh_c \simeq A_1 B_1$; these relations are

exact if the centroidal moments of inertia of the floor masses are neglected and the first mode shape is a straight line. Then, for the case of full contact one can write

$$p_1^2\phi = \frac{A_1\omega_1^2}{I_M} q_1 \tag{4.3.39}$$

and the solution of the equations of motion is

$$y(t) = y(0)\cos p_2 t + \frac{\dot{y}(0)}{p_2}\sin p_2 t - \frac{1}{p_2}\int_0^t \ddot{y}_G(\tau)\sin p_2(t-\tau)d\tau \tag{4.3.40}$$

$$\phi(t) = \phi(0)\cos\tilde{\omega}_1 t + \frac{\dot{\phi}(0)}{\tilde{\omega}_1}\sin\tilde{\omega}_1 t - \frac{mh_c\omega_1^2}{I_M\tilde{\omega}_1(\omega_1^2 + p_1^2)}\int_0^t \ddot{x}_G(\tau)\sin\tilde{\omega}_1(t-\tau)d\tau \tag{4.3.41}$$

in which

$$\tilde{\omega}_1^2 = \frac{\omega_1^2 p_1^2}{\omega_1^2 + p_1^2} \tag{4.3.42}$$

and equations (2.3.52), (2.3.53) can be used for the calculation of p_1 and p_2. The normalized displacement, $q_1(t)$, can be calculated by equation (4.3.39).

After lift-off, equations (4.3.34) and (4.3.38) give

$$p_1^2\phi - \frac{2A_1\omega_1^2}{I_M} q_1 - \frac{p_1^2}{\xi} y + \frac{mg\xi}{I_M} = 0 \tag{4.3.43}$$

It is convenient again to use the downward displacement of point 0, Y, defined by (see Fig. 4.3.1)

$$Y = \xi\phi - y \tag{4.3.44}$$

With this substitution, the equations of motion reduce to

$$\left(1 + \frac{\lambda p_2^2}{2\omega_1^2}\right)\ddot{Y} + \frac{p_2^2}{2}(1+\lambda)Y = \frac{g}{2}(1-\lambda) - \lambda\frac{h_c}{\xi}\ddot{x}_G + \ddot{y}_G \tag{4.3.45}$$

$$\xi\ddot{\phi} = \frac{\lambda}{1+\lambda}\left[\left(1 - \frac{p_2^2}{2\omega_1^2}\right)\ddot{Y} - g - \frac{h_c}{\xi}\ddot{x}_G - \ddot{y}_G\right] \tag{4.3.46}$$

in which $\lambda = \frac{m\xi^2}{I_M}$ and $p_1^2 = \lambda p_2^2$. The solution of these equations can be written as

$$Y(t) = \left[Y(0) - \delta\left(\frac{1-\lambda}{1+\lambda}\right)\right]\cos P_2 t + \frac{\dot{Y}(0)}{P_2}\sin P_2 t + \delta\frac{(1-\lambda)}{(1+\lambda)} - \frac{2\omega_1^2}{P_2(2\omega_1^2+\lambda p_2^2)}\int_0^t\left[\lambda\frac{h_c}{\xi}\ddot{x}_G(\tau) - \ddot{y}_G(\tau)\right]\sin P_2(t-\tau)\,d\tau \tag{4.3.47}$$

$$\phi(t) = \frac{\lambda}{\xi(1+\lambda)}\left[\left(1 - \frac{p_2^2}{2\omega_1^2}\right)Y(t) - \frac{h_c}{\xi}x_G(t) - y_G(t) - \frac{g}{2}t^2 + C_1 t + C_2\right] \tag{4.3.48}$$

where,

$$P_2^2 = \frac{\omega_1^2 p_2^2(1+\lambda)}{2\omega_1^2 + \lambda p_2^2} \tag{4.3.49}$$

and

$$C_1 = \frac{(1+\lambda)}{\lambda}\xi\dot{\phi}(0) - \left(1 - \frac{p_2^2}{2\omega_1^2}\right)\dot{Y}(0) + \frac{h_c}{\xi}\dot{x}_G(0) + \dot{y}_G(0) \tag{4.3.50}$$

$$C_2 = \frac{(1+\lambda)}{\lambda}\xi\phi(0) - \left(1 - \frac{p_2^2}{2\omega_1^2}\right)Y(0) + \frac{h_c}{\xi}x_G(0) + y_G(0) \tag{4.3.51}$$

After $Y(t)$ and $\phi(t)$ have been calculated, $y(t)$ and $q_1(t)$ can be found by equations (4.3.44) and (4.3.43). Recall that this solution is valid for

positive angles of rotation only and that the origin of the time is at the onset of lift-off.

When the system changes from full contact to uplift or vice-versa, the final conditions of the one regime should be used as initial conditions for the other one. At that time, the constraints given by equations (4.3.39) and (4.3.43) both hold. Differentiation of these equations, however, gives constraints upon the velocities which cannot hold simultaneously. This inconsistency, which is due to the approximations considered, has only a local effect and does not affect the overall response. The appropriate values of the initial velocities which should be used can be calculated using the principle of conservation of momentum as follows.

Assume that the system changes from full contact to uplift and that the final velocities for the full-contact regime are $\dot{\phi}_0$, $\dot{q}_{1\,0}$ and $\dot{y}_0$. Assuming that the horizontal momentum does not change, one can write

$$mh_c\dot{\phi}_0 + B_1\dot{q}_{1\,0} = mh_c\dot{\phi}(0) + B_1\dot{q}_1(0) \qquad (4.3.52)$$

Matching of the vertical momenta before and after lift-off requires that $\dot{y}(0) = \dot{y}_0$. Then, using (4.3.39) and (4.3.43), (4.3.52) reduces to

$$\dot{\phi}(0) = \frac{2(\omega_1^2+p_1^2)}{(2\omega_1^2+p_1^2)}\dot{\phi}_0 + \frac{p_1^2}{(2\omega_1^2+p_1^2)\,\xi}\dot{y}_0 \qquad (4.3.53)$$

For Y(t), one should take

$$\dot{Y}(0) = \frac{2(\omega_1^2+p_1^2)}{(2\omega_1^2+p_1^2)}\xi\,\dot{\phi}_0 - \frac{2\omega_1^2}{(2\omega_1^2+p_1^2)}\dot{y}_0 \qquad (4.3.54)$$

Now, assume that the building goes from uplift to full contact and that $\dot{\phi}_0$ and $\dot{Y}_0$ are the final velocities for the uplift regime. Working similarly, the initial velocities, $\dot{\phi}(0)$ and $\dot{y}(0)$, for the case of full contact are

$$\dot{\phi}(0) = \frac{\omega_1^2}{(\omega_1^2+p_1^2)}\dot{\phi}_0 + \frac{p_1^2}{2(\omega_1^2+p_1^2)\xi}\dot{Y}_0 \qquad (4.3.55)$$

and

$$\dot{y}(0) = \xi\dot{\phi}_0 - \dot{Y}_0 \qquad (4.3.56)$$

It should be noted that under the assumptions considered here (i.e., zero centroidal moments of inertia of the floor masses and linear first mode) conservation of the horizontal and vertical momenta during lift-off or contact implies conservation of the kinetic energy, too.

4.3.3.b Damped Case

For the case of full contact, again considering the approximate solution, we can assume for small damping that q_1 and ϕ are related according to equation (4.3.39). The fundamental ratio of critical damping, $\tilde{\zeta}_1$, can be found by equation (4.3.31), which for the approximations considered here reduces to

$$\tilde{\zeta}_1 = -\frac{\zeta_1\left(\frac{\tilde{\omega}_1}{\omega_1} - \frac{\omega_1}{\tilde{\omega}_1}\right) + \zeta_1^s\left(\frac{\tilde{\omega}_1}{p_1} - \frac{p_1}{\tilde{\omega}_1}\right)}{\frac{\omega_1}{p_1} + \frac{p_1}{\omega_1} + \frac{2mh_c g}{I_M \omega_1 p_1}} \qquad (4.3.57)$$

Then, the solution can be written as

$$y(t) = e^{-\zeta_2 p_2 t}\left[y(0)\cos p_2 t + \left(\frac{\dot{y}(0)}{p_2} + \zeta_2 y(0)\right)\sin p_2 t\right]$$

$$- \frac{1}{p_2}\int_0^t e^{-\zeta_2 p_2 (t-\tau)}\ddot{y}_G(\tau)\sin p_2(t-\tau)d\tau \qquad (4.3.58)$$

$$\phi(t) = e^{-\tilde{\zeta}_1 \tilde{\omega}_1 t}\left[\phi(0)\cos \tilde{\omega}_1 t + \left(\frac{\dot{\phi}(0)}{\tilde{\omega}_1} + \tilde{\zeta}_1\phi(0)\right)\sin \tilde{\omega}_1 t\right]$$

$$- \frac{mh_c\omega_1{}^2}{I_M\tilde{\omega}_1(\omega_1{}^2+p_1{}^2)}\int_0^t e^{-\tilde{\zeta}_1\tilde{\omega}_1(t-\tau)}\ddot{x}_G(\tau)\sin\tilde{\omega}_1(t-\tau)d\tau \qquad (4.3.59)$$

After lift-off, we can again assume that equation (4.3.43) holds for small damping. The differential equation for Y(t) in this case is expected to be

$$\left(1 + \frac{\lambda p_2{}^2}{2\omega_1{}^2}\right)\ddot{Y} + \zeta_2 p_2(1+\lambda)\dot{Y} + \frac{p_2{}^2}{2}(1+\lambda)Y = \frac{g}{2}(1-\lambda) - \lambda\frac{h_c}{\xi}\ddot{x}_G + \ddot{y}_G \qquad (4.3.60)$$

Note that a similar behavior was found for the rigid superstructure in section 3.2.1. Then,

$$Y(t) = e^{-Z_2 P_2 t}\left[\left(Y(0) - \delta\frac{(1-\lambda)}{(1+\lambda)}\right)\cos P_2 t + \left(\frac{\dot{Y}(0)}{P_2} + Z_2 Y(0)\right)\sin P_2 t\right]$$

$$+ \delta\frac{(1-\lambda)}{(1+\lambda)} - \frac{2\omega_1{}^2}{P_2{}^2(2\omega_1{}^2+\lambda p_2{}^2)}\int_0^t e^{-Z_2P_2(t-\tau)}\left[\lambda\frac{h_c}{\xi}\ddot{x}_G(\tau) - \ddot{y}_G(\tau)\right]\times$$

$$\times \sin P_2(t-\tau)d\tau \qquad (4.3.61)$$

in which

$$Z_2 = \frac{\zeta_2 \sqrt{(1+\lambda)(2\omega_1^2 + \lambda p_2^2)}}{2\omega_1} \qquad (4.3.62)$$

The angle of rotation, $\phi(t)$, can be again calculated by equation (4.3.48).

4.3.3.c. Estimation of the Fundamental Period

Let us consider the undamped free oscillations of the system, excited by a horizontal impulse. In this case, the vertical oscillations are not excited before the building lifts off for the first time, which happens at time, t_0, given by

$$t_0 = \frac{1}{\tilde{\omega}_1} \sin^{-1}\left(\frac{1}{\beta}\right) \qquad (4.3.63)$$

In this equation, β is the normalized impulse and it is equal to the ratio of the maximum angle of rotation, ϕ^c_{max}, which would occur if uplift were not allowed, over the critical angle, ϕ_{cr}, at which lift-off happens in the absence of vertical oscillations.

At time $t = t_0$, the angular velocity, $\dot{\phi}_0$, can be written as

$$\dot{\phi}_0 = \phi_{cr}\tilde{\omega}\sqrt{\beta^2-1} \qquad (4.3.64)$$

Using equations (4.3.53) and (4.3.54) to calculate $\dot{\phi}(0)$ and $\dot{Y}(0)$ and substituting in (4.3.50) one finally gets

$$C_1 = \frac{g}{\tilde{\omega}_1}\sqrt{\beta^2-1} \qquad (4.3.65)$$

As can be seen from equation (4.3.48), the angle of rotation after lift-off consists of a harmonic function of frequency P_2 superimposed

upon a parabola. This parabolic term attains its maximum value at time $t_1 = \frac{C_1}{g}$, i.e.

$$t_1 = \frac{1}{\tilde{\omega}_1}\sqrt{\beta^2 - 1} \tag{4.3.66}$$

It is reasonable to assume that a quarter of the apparent fundamental period, T, has ellapsed at this time. Therefore, one can write

$$\frac{T}{\tilde{T}_{1c}} = \frac{2}{\pi}\left[\sin^{-1}\left(\frac{1}{\beta}\right) + \sqrt{\beta^2 - 1}\right] \tag{4.3.67}$$

in which $\tilde{T}_{1c} = \frac{2\pi}{\tilde{\omega}_1}$ is the fundamental period of the interacting system when lift-off is not allowed. It is seen that the apparent fundamental period increases rapidly with the value of the normalized impulse, and for large values of β, $\frac{T}{\tilde{T}_{1c}}$ is essentially proportional to β. Recall that the same behavior was found for the case of the free oscillations of a rocking block [see equation (2.3.76)]. A plot of equation (4.3.67) is shown in Fig. 2.3.6.

Let T_1 be the fundamental period of the building for fixed-base response. In this case, (4.3.67) becomes

$$\frac{T}{T_1} = \sqrt{1 + \frac{\omega_1^2}{p_1^2}}\left[\sin^{-1}\left(\frac{1}{\beta}\right) + \sqrt{\beta^2 - 1}\right] \tag{4.3.68}$$

Since p_1 can be thought as a measure of the foundation stiffness, it can be concluded from this equation that the apparent period, T, increases as the foundation becomes softer.

4.3.4. Example

As an example, let us consider again a simplified model of the Millikan Library building. The dimensions and masses of the floors are given in section 2.5.6. For the calculation of the stiffness matrix, [K], the procedure used by Foutch[23] was employed. According to this method, the flexibility matrix of the model was first calculated by applying unit loads separately at each floor level and computing the resulting floor displacements. These displacements were found using the plane stress solution for the displacement of the centerline of a rectangular cantilever beam with a concentrated load applied at the end (e.g., see [57]). The resulting flexibility matrix was then inverted to obtain the stiffness matrix, [K]. As proposed by Foutch, the total moment of inertia of the east and west shear walls was taken equal to 6.64×10^4 ft^4 and Young's modulus (for 4,000 psi concrete) was 3.6×10^6 psi.

The eigenfrequencies and the corresponding eigenvectors of the fixed-base model were then calculated from the matrix $[M]^{-1}[K]$. The resulting values for the five first eigenfrequencies are given in Table 4.3.1 together with the corresponding values of A_i's and B_i's [see equations (4.3.14) and (4.3.15)]. The normalized values of the five first eigenvectors are given in Table 4.3.2.

The ratios of critical damping for the superstructure were taken equal to 6.5% for the first mode and 5% for the others. The values for the first two modes were suggested by McVerry[58] and are based on the response of the building during the San Fernando earthquake of February, 1971. Since no information was available for the values of

TABLE 4.3.1

Calculated Values of the First Five Eigenfrequencies and Corresponding Values of Ai and Bi for the Fixed-Base Model of Millikan Library

No.	Eigenfrequency (Hz)	$Ai\sqrt{1000}$	$Bi\sqrt{1000}$
1	1.88	26.55	0.814
2	7.81	-2.89	-0.462
3	16.0	0.709	0.228
4	23.7	-0.174	-0.136
5	31.0	0.102	0.099

TABLE 4.3.2

First Five Normalized Eigenvectors $\left(x\sqrt{1000}\right)$ for the Fixed-Base Model of Millikan Library

Floor Level	1	2	3	4	5
1	0.067	-0.469	0.917	-1.173	1.453
2	0.192	-0.984	1.498	-1.183	0.415
3	0.336	-1.300	1.245	0.069	-1.200
4	0.507	-1.437	0.470	1.256	-1.085
5	0.697	-1.359	-0.481	1.342	0.596
6	0.901	-1.065	-1.178	0.259	1.452
7	1.112	-0.588	-1.302	-1.027	0.269
8	1.326	0.012	-0.788	-1.372	-1.260
9	1.537	0.659	0.147	-0.454	-0.944
10	1.743	1.270	1.103	0.944	0.787

the fractions of critical damping for the other modes, they were arbitrarily taken equal to 5%.

For the foundation (Winkler model), the stiffness and damping considered were: $k_0 = 6.24 \times 10^5$ t/m^2 and $c_0 = 2.82 \times 10^3$ t $\cdot$ sec/m. These values are equal to the ones calculated in sections 2.5.6 and 3.2.4.

The S16E component of the accelerogram recorded at Pacoima Dam during the San Fernando earthquake ($M_L = 6.3$) was used as the ground acceleration. The first 15 seconds of this record are shown in Fig. 4.3.5. The peak acceleration is -11.48 m/sec^2 (= 1.17g) and the peak velocity is -1.13 m/sec.

The equations of motion were integrated numerically using the Runge-Kutta method and a time step of 0.001 seconds. Only the first five modes were included in the calculation. First, the continuous, full contact case was solved by using the equivalent two-spring model for the Winkler foundation (see section 3.2.3). The value of ϕ^c_{max} was calculated and the corresponding value of β was found to be 3.96. For distinction, here, β denotes the equivalent normalized impulse corresponding to the Winkler model and β_{2s} the one corresponding to the two-spring foundation. [For a relation between β_{2s} and β see (2.5.24)]. After β was estimated, a new two-spring model, based on the equations for general equivalence, was defined. For this model, $k = 5.05 \times 10^6$ t/m, $c = 2.28 \times 10^4$ t $\cdot$ sec/m, $\xi = 6.93$ m and $\beta_{2s} = 2$. The resulting characteristic frequencies of the foundation were: $p_1 = 4.02$ Hz and $p_2 = 14.1$ Hz, and the corresponding ratios of critical damping: $\zeta_1 = 5.7\%$ (in rocking) and $\zeta_2 = 20\%$ (in vertical). The critical angle at which lift-off occurs is 0.187×10^{-3} rad, which corresponds to a rigid body movement of 0.8 cm at the roof

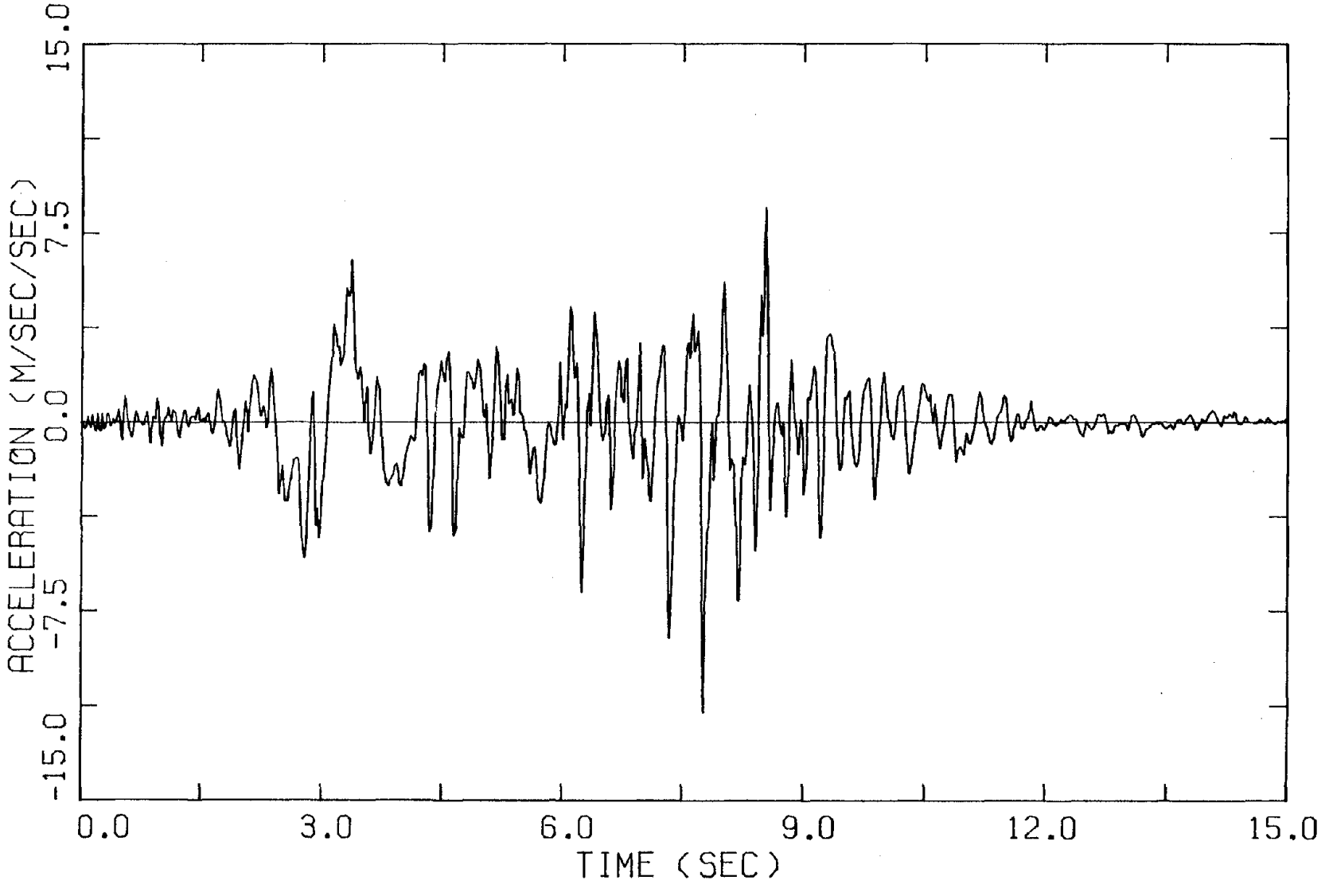

Fig. 4.3.5. S16E component of the Pacoima Dam record, San Fernando, California, Earthquake, February 9, 1971.

level. This model was then subjected to the same ground acceleration, allowing lift-off. The resulting response is presented in Figs. 4.3.6 - 4.3.12. For comparison, the response without allowing lift-off and the approximate, first-mode solution are also shown.

In Figs. 4.3.6 and 4.3.7, the deflections of the 5th and 10th (roof) floors relative to the base, excluding rotations, are shown. It is evident that lift-off significantly affects the deflection history of the building, although the amplitude is not much affected in this example. The first-mode solution is very close to the total response, which means that the response of the structure is dominated by the first mode. The higher frequency components, which are apparent in the exact and approximate solutions, but not in the response without lift-off, are due to the dynamic coupling of the deformation with the vertical oscillations.

Similar observations hold for the absolute accelerations of the 5th and 10th floor levels, which are shown in Figs. 4.3.8 and 4.3.9, respectively. It is seen that uplift results in somewhat higher accelerations, compared to the case without lift-off. The approximate solution includes all the main features of the response except the high frequency components which are due to the contribution of the higher modes.

In Fig. 4.3.10, the angle of rotation is shown. The first lift-off at 2.5 seconds can be correlated with the large pulse in the accelerogram at this time. It is seen that the angle of rotation is increased tremendously by the uplift, compared to the response without lift-off. It should be noted, however, that this response was calculated for a

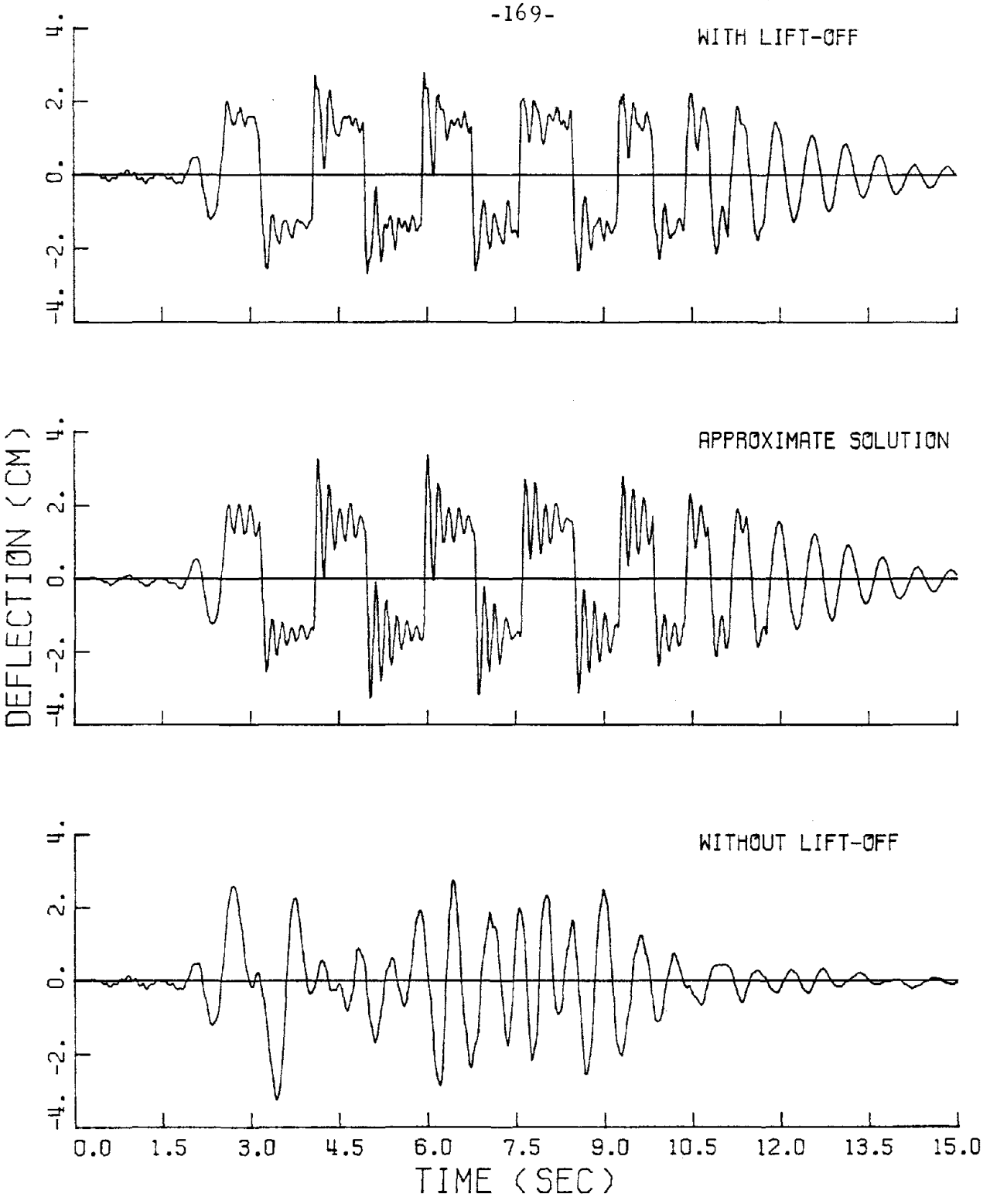

Fig. 4.3.6. Fifth floor deflection with respect to the base, excluding rotations, of a model of Millikan Library subjected to the Pacoima Dam ground acceleration.

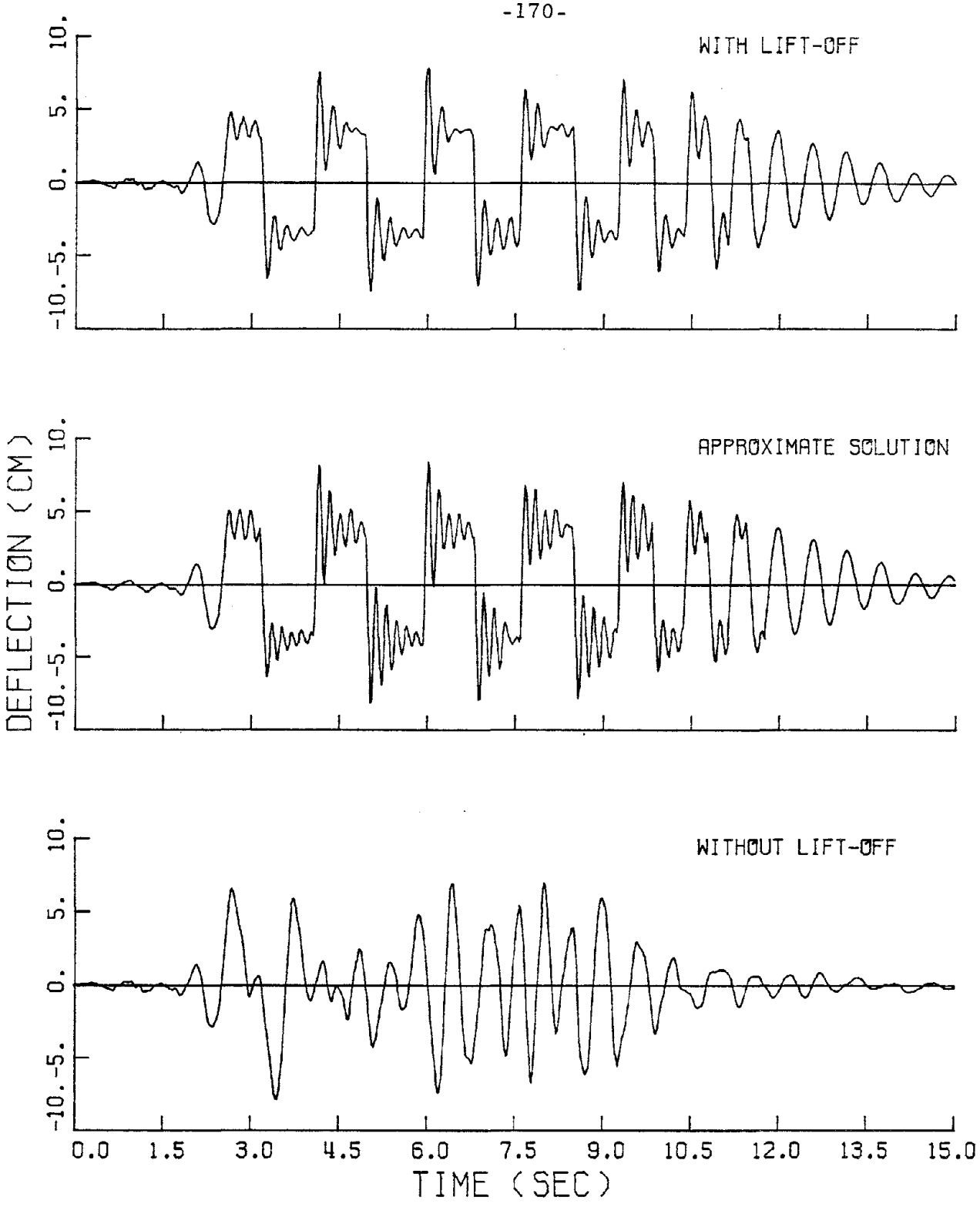

Fig. 4.3.7. Roof deflection with respect to the base, excluding rotations, of a model of Millikan Library subjected to the Pacoima Dam ground acceleration.

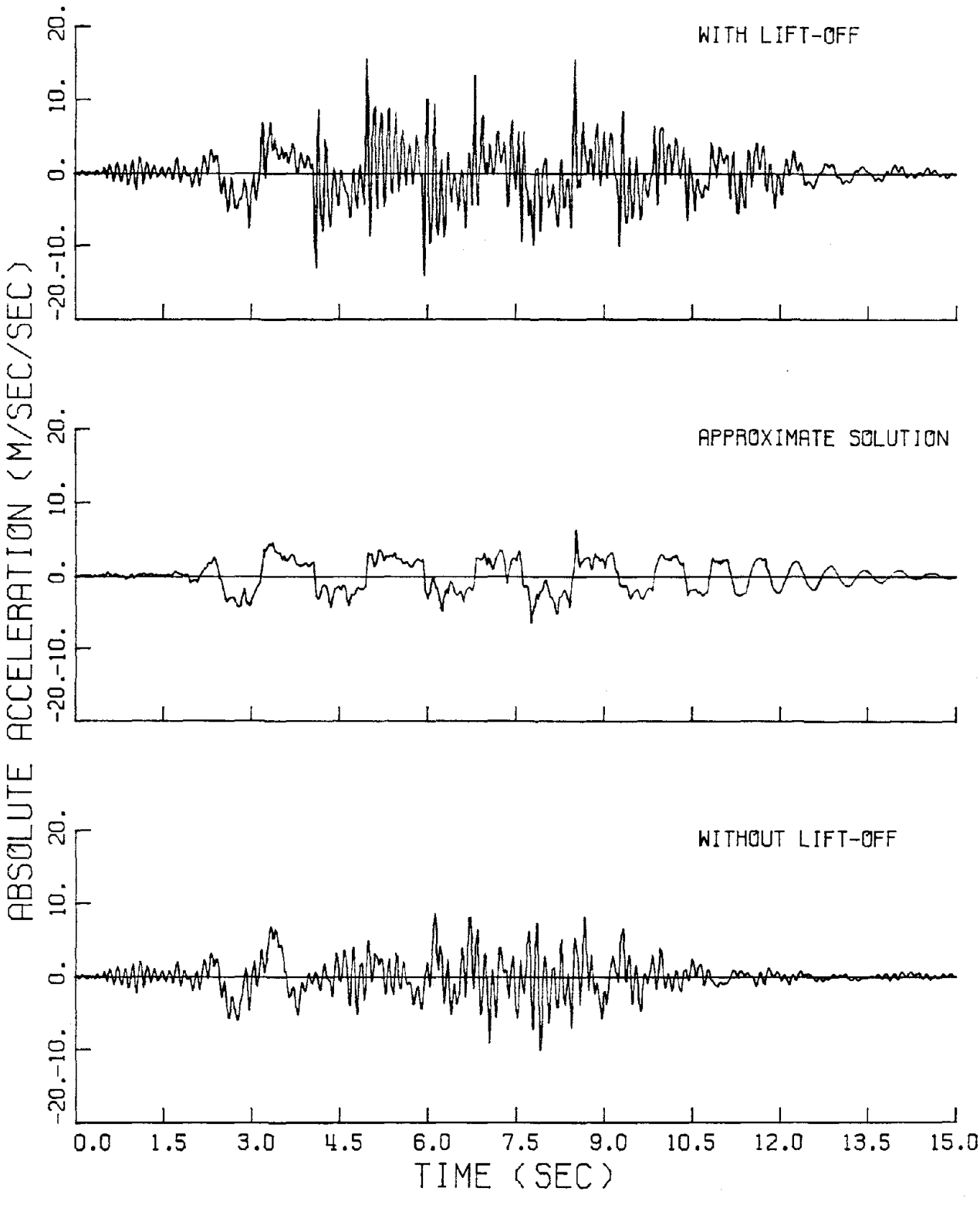

Fig. 4.3.8. Fifth floor absolute acceleration of a model of Millikan Library subjected to the Pacoima Dam ground acceleration.

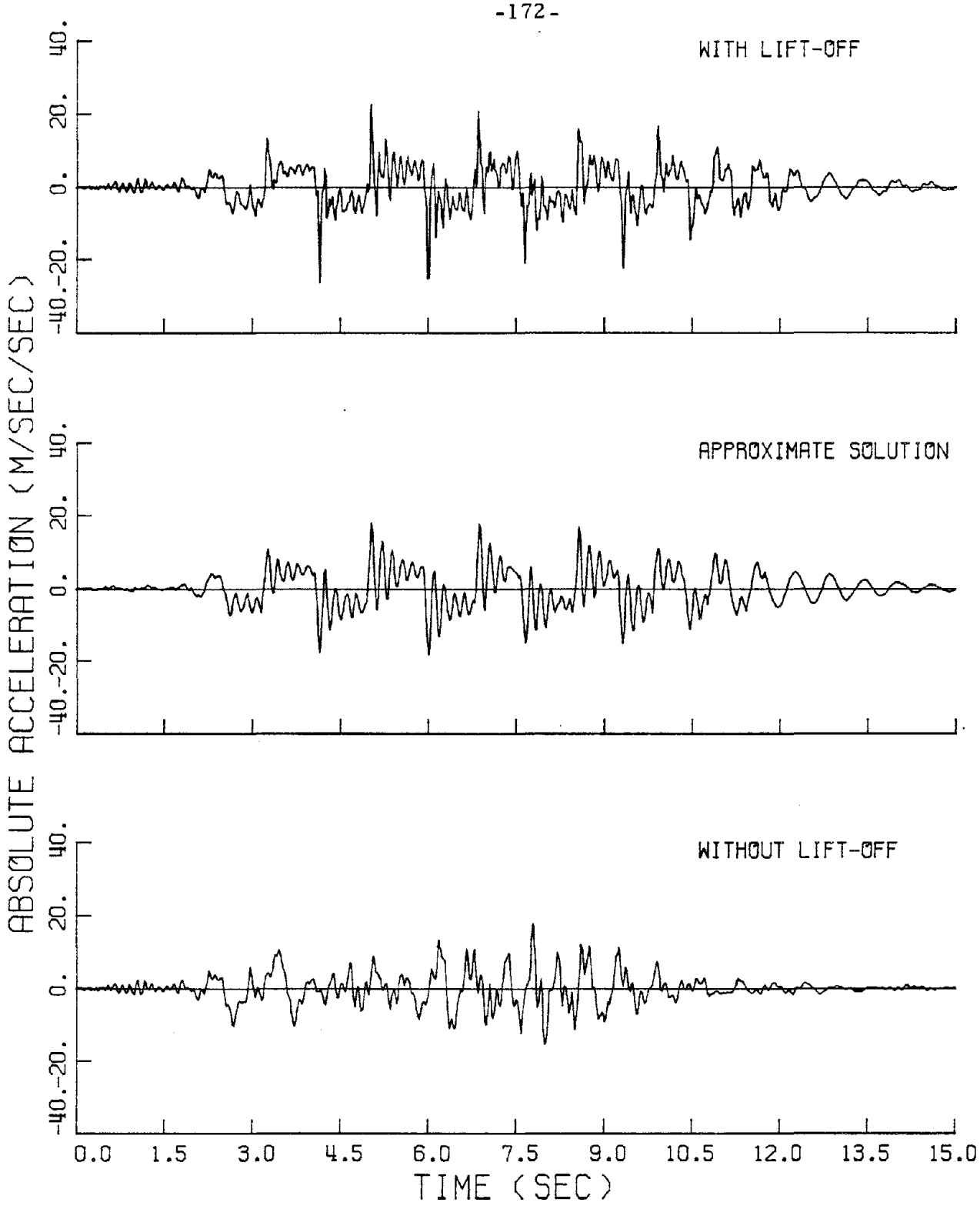

Fig. 4.3.9. Roof absolute acceleration of a model of Millikan Library subjected to the Pacoima Dam ground acceleration.

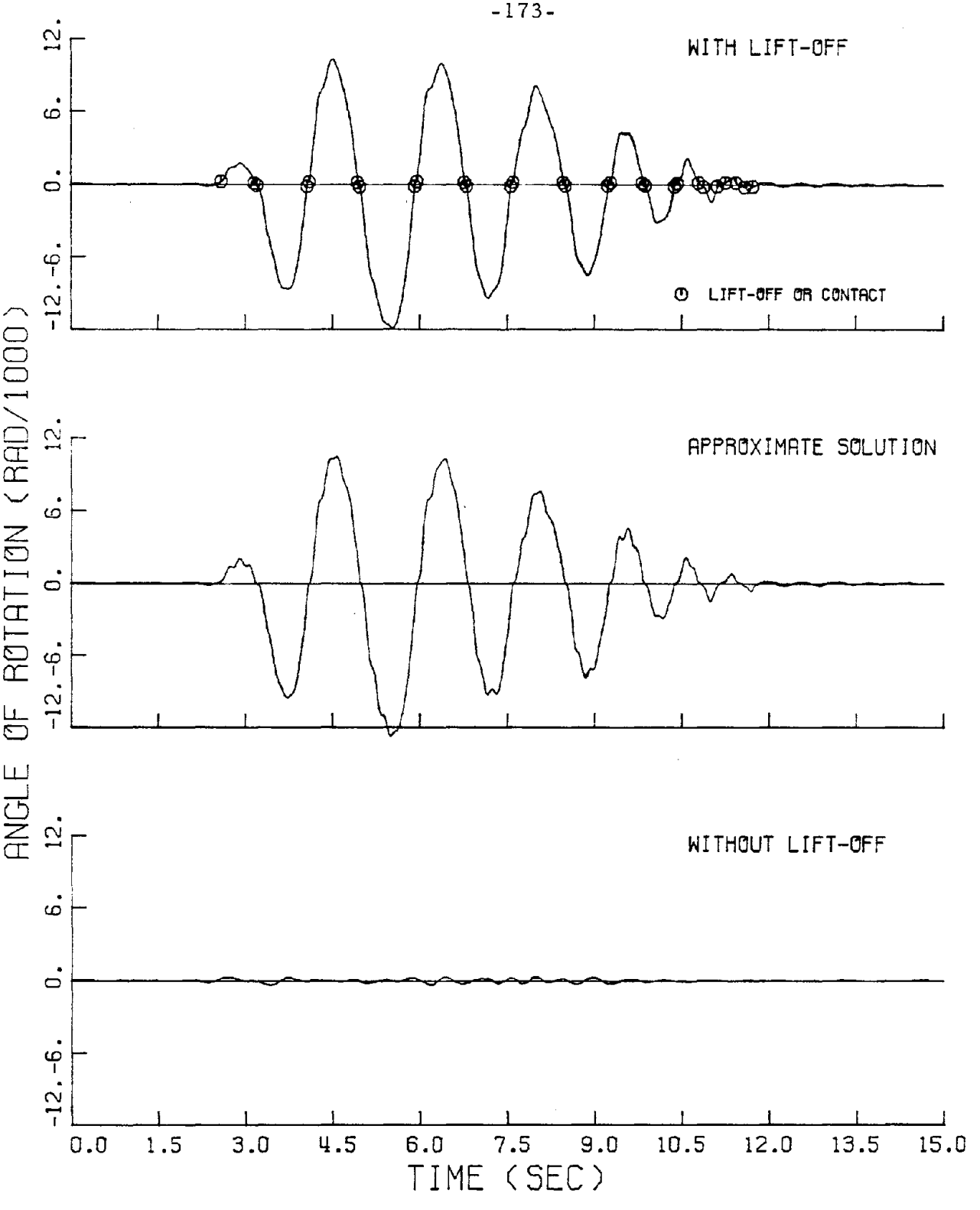

Fig. 4.3.10. Angle of rotation of a model of Millikan Library subjected to the Pacoima Dam ground acceleration.

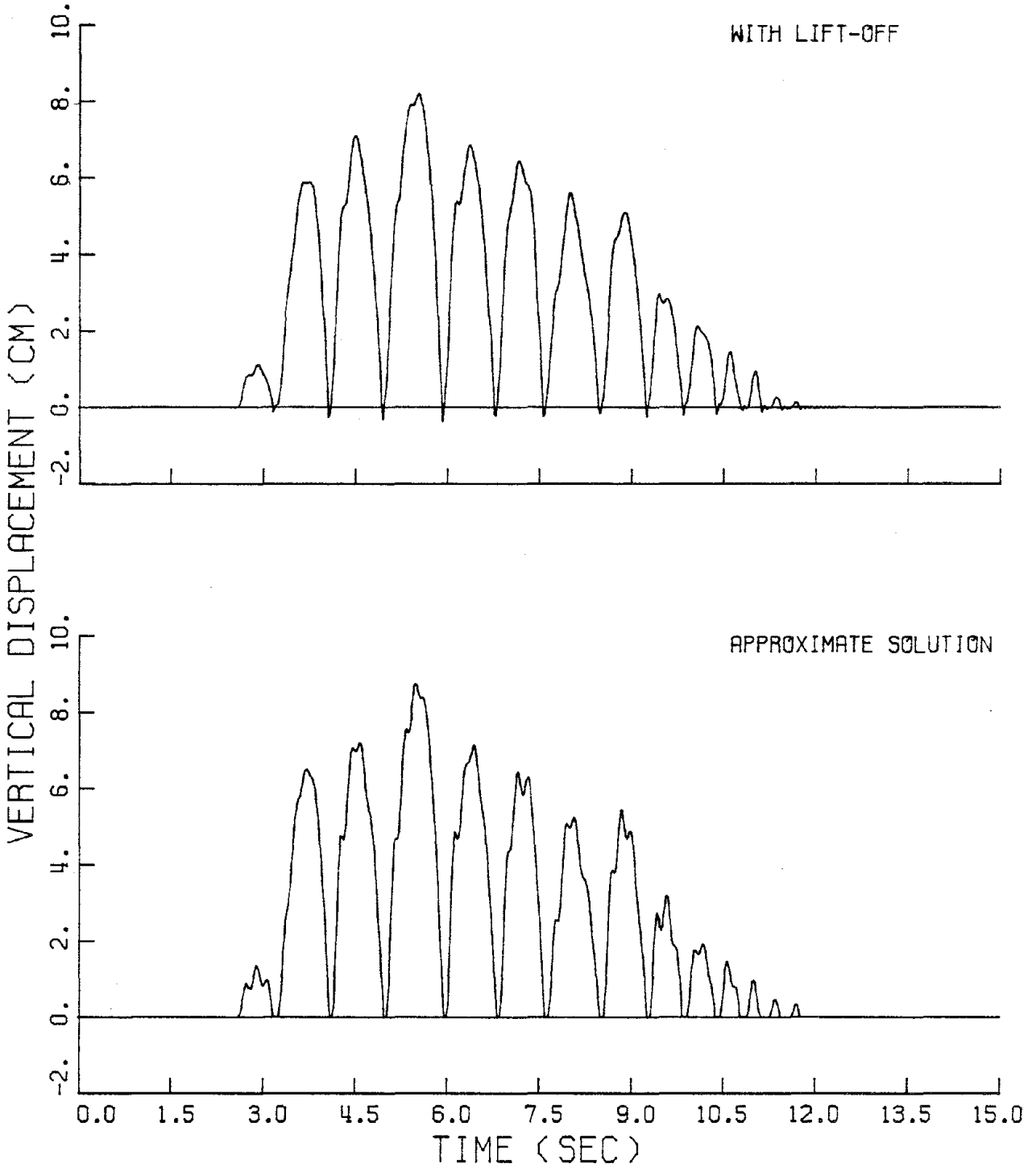

Fig. 4.3.11. Vertical displacement of the center of mass of a model of Millikan Library subjected to the Pacoima Dam ground acceleration.

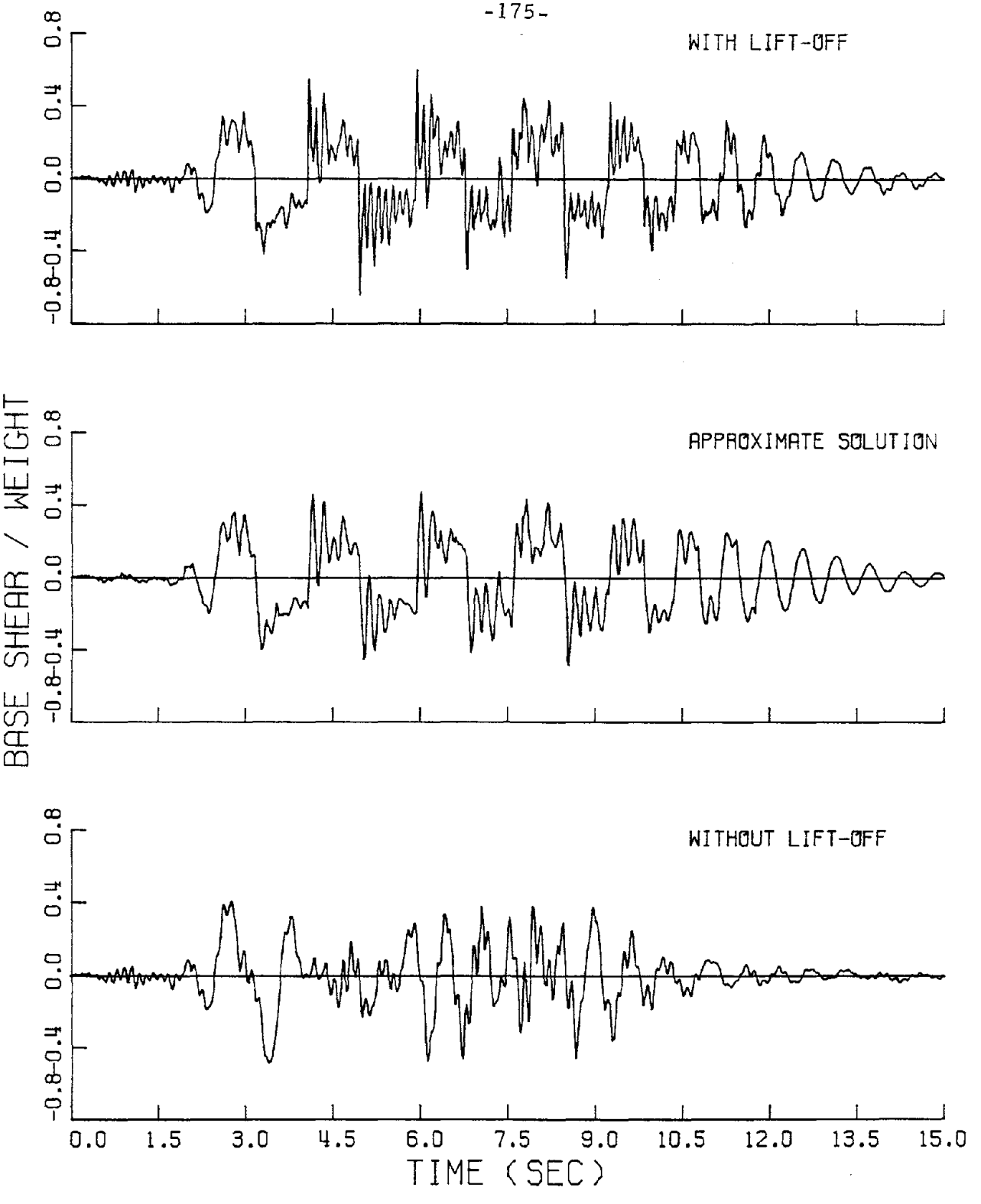

Fig. 4.3.12. Base shear force of a model of Millikan Library subjected to the Pacoima Dam ground acceleration.

very strong ground shaking and stiff foundation conditions. Also, the restraining effects of embedment and foundation details were not considered (except for the calculation of the foundation stiffness). The amplitude of the rocking response changes nonlinearly with the amplitude of the excitation and decreases significantly for smaller excitations. This behavior is illustrated in Fig. 4.3.13, in which the rocking response for 80% of the Pacoima record is shown. It can be seen that a 20% reduction in the excitation caused an 85% reduction in the amplitude of ϕ. In contrast to the behavior of the angle of rotation, the nonlinear effect of lift-off is not as evident in the deflection of the building model, as can be verified by comparison of Figs. 4.3.7 and 4.3.14.

The vertical displacement of the center of mass is shown in Fig. 4.3.11 for the exact and the approximate solutions. Since $y = \xi|\phi| - Y$ and Y is small (of the order of magnitude of the static deflection, δ), this displacement is essentially proportional to the angle of rotation.

In Fig. 4.3.12, the ratio of the base shear force to the weight of the building is shown. This force was calculated by the equation (see Appendix II)

$$Q_1 = N_1\left(\phi + \frac{u_1}{h_1}\right) + \sum_{i=1}^{10} m_i\left(\ddot{x}_G + h_i\ddot{\phi} + \ddot{u}_i\right)$$

in which N_1 is the base axial force, given by

$$N_1 = \left(\sum_{i=1}^{10} m_i\right)(g + \ddot{y})$$

Since this shear force mainly depends on the absolute accelerations of

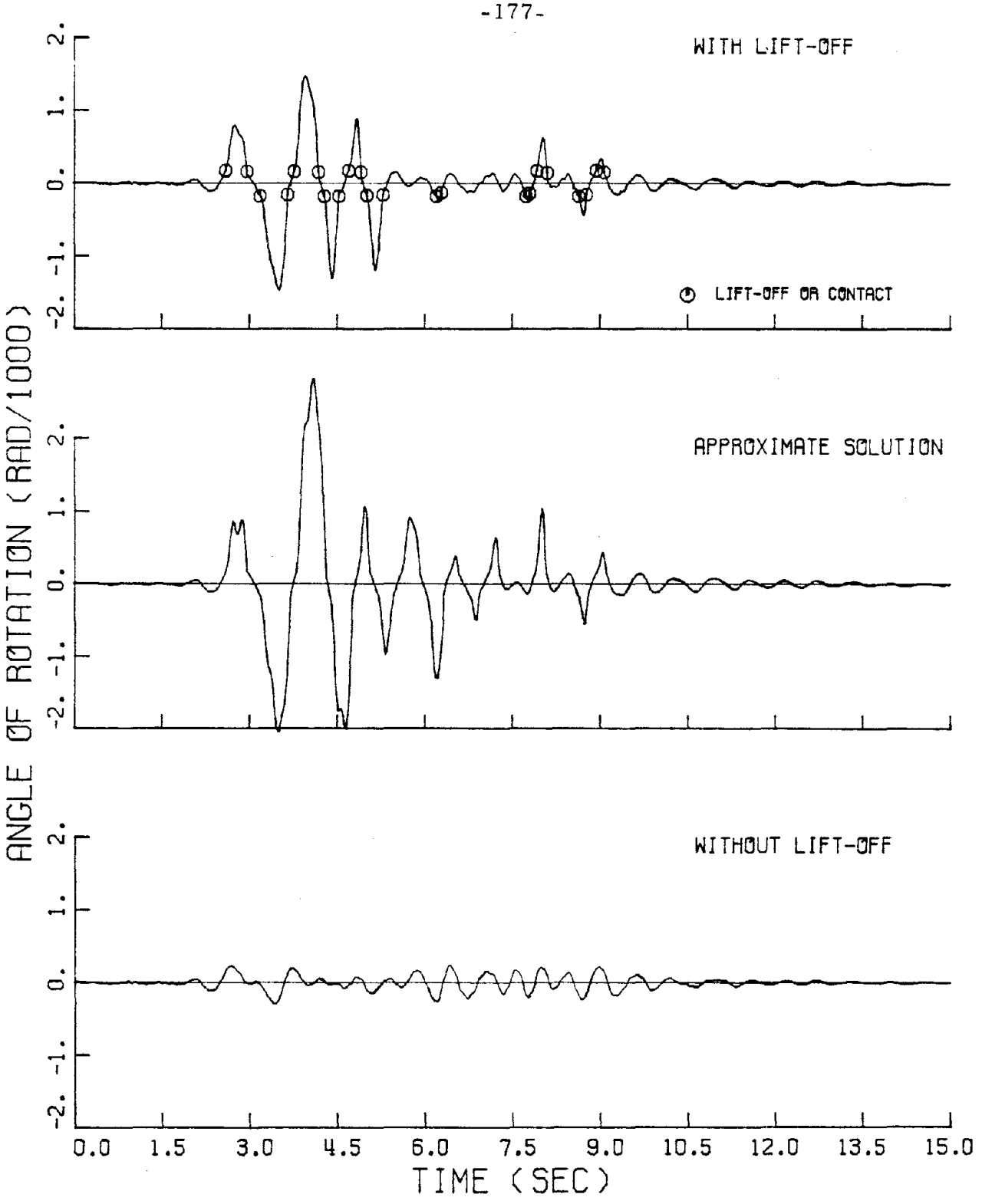

Fig. 4.3.13. Angle of rotation of a model of Millikan Library subjected to 80% of the Pacoima Dam ground acceleration.

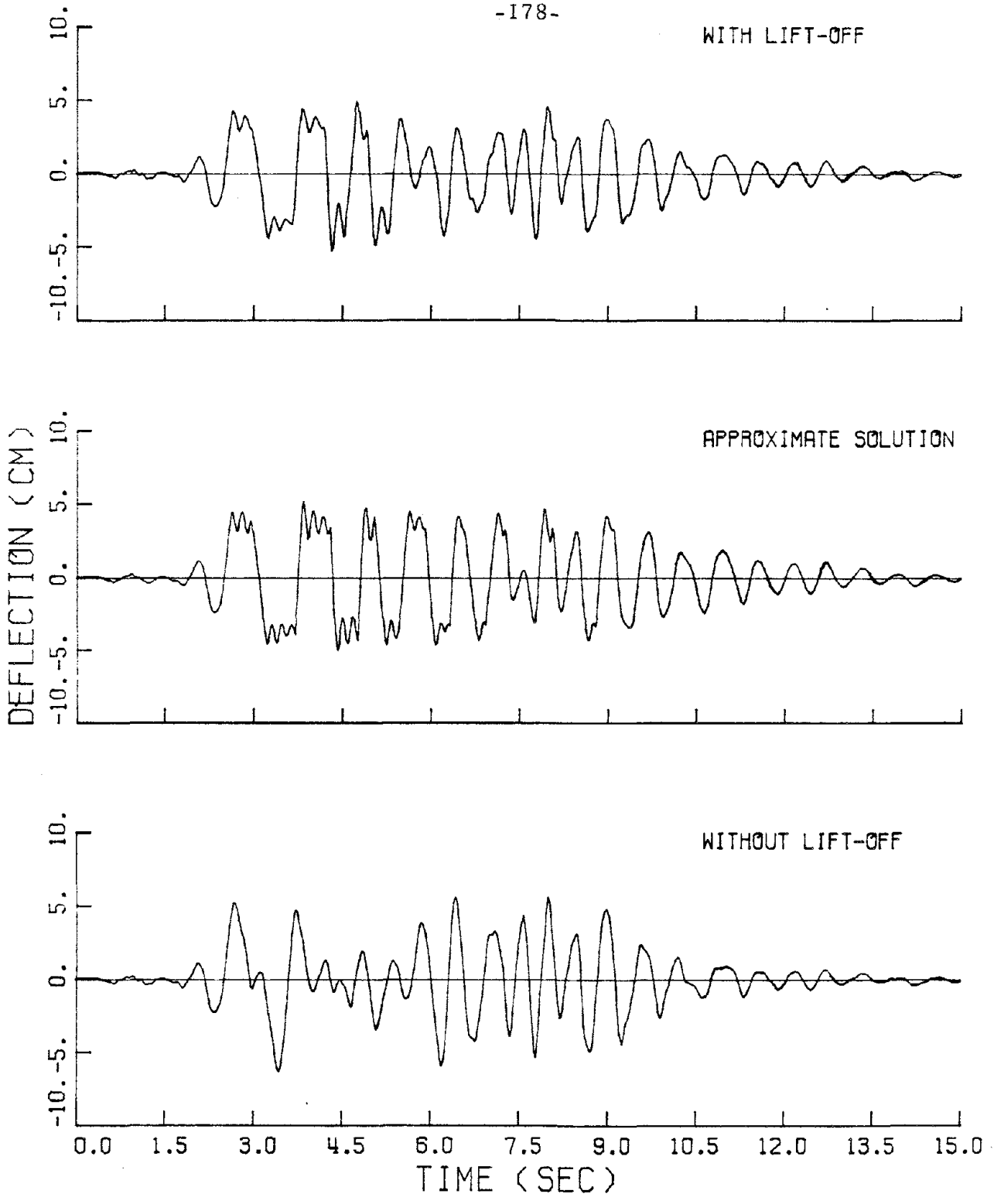

Fig. 4.3.14. Roof deflection with respect to the base, excluding rotations, of a model of Millikan Library subjected to 80% of the Pacoima Dam ground acceleration.

the floors, the same comments made for the accelerations apply here. It is seen that the amplitude of the base shear force for the uplifting system is slightly higher than for the case without lift-off. This conclusion, however, should not be generalized and, as it was mentioned in the analysis, rocking on the foundation and uplifting may or may not be favorable for the building, depending upon the characteristic parameters of the structure and upon the nature of the ground shaking.

CHAPTER V

SUMMARY AND CONCLUSIONS

Summary

The principal result of this thesis is a detailed presentation of the dynamic behavior of simplified structures supported by flexible foundations which permit uplift. Some approximate models for foundations allowing uplift, suitable for design calculations, have been presented also. The analysis was limited to two types of foundations: the continuous elastic foundation (the well-known Winkler model) and a two-spring foundation in which the structure is supported by two springs symmetrically placed under the base. The structure was not allowed to slip horizontally on the foundation; therefore, in addition to the degrees of freedom of the superstructure, the system possessed two more degrees of freedom in rocking and vertical motions.

In general, the equations of motion for the two-spring model are much simpler than the corresponding equations for the Winkler foundation. Based on this observation, relations between the parameters of the two models were derived so that the responses are similar. In this way, the equivalent two-spring model can be used instead of the Winkler foundation. The Winkler foundation is commonly used in soil mechanics, but leads to quite complicated equations when uplift is permitted. Since the behavior of the uplifting systems is nonlinear, the equations of equivalence depend on the expected amount of lift-off, which is measured by the "normalized impulse." This quantity is proportional to the maximum angle of rotation which would occur under pulse loading if lift-off were not allowed. Although the equations of equivalence

were derived for a rigid superstructure and a horizontal impulse excitation, the results can be extended to account for flexible superstructures and other types of dynamic loading.

For the case of a rigid superstructure and an undamped two-spring foundation, the equations of motion were solved analytically for any horizontal and/or vertical ground motion. Simpler approximate solutions were also developed. The response after lift-off is dominated by hyperbolic functions; these exponential terms can be approximated by a parabola for many applications. Using the approximate solution, the apparent rocking period of free oscillations was determined. Then, an equivalent linear system was defined; this system is not allowed to uplift and its parameters depend on the normalized impulse. The advantage of this approximate method is that it greatly simplifies the solution and it even permits the use of response spectra for the estimation of the maximum angle of rotation. Note that the value of the normalized impulse can also be calculated from response spectra.

In an effort to introduce dissipation of energy into the foundation to account for the inelastic behavior of the soil as well as the radiation of energy in the form of stress waves, three different mechanisms were examined. First, viscous damping was introduced by placing dashpots in parallel with the springs. For the two-spring foundation, the equations of motion were solved analytically, while the corresponding equations for the Winkler model were highly nonlinear and were solved numerically. The equations of equivalence between the two models were extended to take the damping into consideration. For the

two-spring foundation, simple, approximate solutions were also derived, similar to those for the undamped case.

As a second way to dissipate energy in the foundation, springs with inelastic behavior were considered. The simple case of elastic-perfectly plastic springs and the two-spring foundation was examined. Although the equations of motion for each regime of the response can be linearized and solved analytically, the many conditions of possible contact and yielding which must be considered make this method unattractive for design purposes.

Finally, the disssipation of energy caused by the inelastic impact, which occurs when the block regains full contact with the foundation, was also examined. Since the elastic springs, even with dashpots in parallel, do not permit this kind of energy dissipation, an impact mechanism was developed which can be used with both the two-spring and the Winkler model, along with other energy dissipating mechanisms. The impact mechanism causes a reduction in the velocities during the impact and can be easily implemented.

The equations of equivalence between the two-spring and the Winkler foundation, which were derived for the rigid block, hold for flexible superstructures, too, provided only that the base of the structure be rigid. The analysis for flexible superstructures was therefore limited to a viscously damped, two-spring foundation. First the response of a simple shear oscillator was examined and then a multi-degree-of-freedom structure was considered. For the case of the multistory structure, it was assumed that the fixed-base response admits decomposition into classical normal modes. An approximate, first-mode solution was also

derived. Like that for the rocking rigid block, the solution of the equations of motion after lift-off includes exponential terms.

Conclusions

In general, it can be said that lift-off results in a softer vibrating system which behaves nonlinearly, overall, although the response is composed of a sequence of linear responses. For the case of the rocking rigid block, the apparent rocking period of the system increases with the amount of lift-off and for large amplitudes of the response the increase is essentially proportional to the normalized impulse. For the case of a flexible superstructure, the effect of uplift is mainly shown in the apparent fundamental period of the system which also increases in the same way, compared to the period before lift-off. Note that the latter period is always larger than the fundamental period of the fixed-base response of the superstructure, because of the deformability of the foundation. In contrast to the first mode, the second and higher modes of the superstructure are not affected significantly by either the soil-structure interaction or the uplift.

Another effect of lift-off on the response is that vertical oscillations are excited even for purely horizontal excitation. Although for many potential applications, including the response of buildings, the vertical vibrations are of relatively minor interest, they may sometimes be important for very strong excitations since complete separation is possible. The possibility of complete separation increases with the value of the normalized impulse and with the width-to-height ratio of the structure. For very short and wide structures, if horizontal

slipping can, in fact, be prevented, complete separation is possible for any horizontal excitation strong enough to cause partial lift-off.

For a rigid block rocking on a Winkler foundation, the length of contact between the base and the foundation decreases as the amount of lift-off increases. A parametric analysis showed that the average length of contact, with respect to time, is inversely proportional to the square root of the normalized impulse.

When damping is included in the foundation, the apparent ratio of critical damping in rocking has a general tendancy to decrease with the amount of lift-off. It should be noted that introduction of damping into the foundation results in sigificantly more damping for vertical motion than for rocking. As a result, the possibility of complete separation reduces in this case.

Considering our present level of understanding of response with lift-off, it seems that for engineering purposes viscous damping is the simplest and most efficient method to account for energy dissipation in the foundation. Inelastic springs are conceptually better for modeling the hysteretic behavior of the soil but, as was mentioned earlier, this approach does not appear to be attractive for applications. On the other hand, several numerical examples showed that an increase in the dashpot coefficients is sufficient to account approximately for the dissipation of energy during impact.

Because of the significant reduction of the fundamental frequency of the system caused by lift-off, the dynamic behavior of a structure allowed to uplift may be very different from the response without lift-off. For the rigid superstructure, lift-off tends to decrease the

rocking acceleration while the angle of rotation may be larger or smaller. For flexible superstructures, it seems that uplift always increases the angle of rotation but the effects on the deflection and the resulting stresses are not clear. In general, it cannot be concluded whether uplift is beneficial to the structure or not, since this depends on the parameters of the system and the characteristics of the excitation.

There is an important limitation in the analysis for flexible superstructures, if the results are to be applied for the calculation of the response of buildings. In this case, the details of the foundation design, the degree of embedment and the deformability of the base may need to be considered. These factors may significantly affect the dynamic characteristics of the foundation, particularly at the large amplitudes of response associated with possible lift-off.

An analysis of the problem with other models of the foundation is certainly an attractive subject for future research. As a first step, modeling of the soil by an elastic half-space should be considered. Next, nonlinear but more realistic models of the soil could be examined. Further research could be conducted for buildings with embeded foundations and with flexible bases. Of course, these considerations would complicate the formulation of the problem significantly and would probably require numerical solutions, e.g., by finite element methods. The analyses may not be attractive for practical applications but could guide simpler approaches to the problem. In addition, such investigations would lead to a clearer understanding of the phenomenon of uplift and its effect on the response of structures.

REFERENCES

1. Housner, G.W., "The Behavior of Inverted Pendulum Structures During Earthquakes," Bulletin of the Seismological Society of America, Vol. 53, No. 2, Feb. 1963, pp. 403-417.
2. Hanson, R.D., "Behavior of Liquid-Storage Tanks," The Great Alaska Earthquake of 1964, Engineering, National Academy of Sciences, Washington, D.C., 1973, p. 334.
3. Oldham, R.D., "Report on the Great Earthquake of 12th June 1897," Memoirs of Geological Survey of India, Geological Survey of India, Vol. XXIX, Calcutta, 1899.
4. Rutenberg, A., Jennings, P.C. and Housner, G.W., "The Response of Veterans Hospital Building 41 in the San Fernando Earthquake," Report No. EERL 80-03, Earthquake Engineering Research Laboratory, California Institute of Technology, Pasadena, California, May 1980.
5. Kirkpatrick, P., "Seismic Measurements by the Overthrow of Columns," Bulletin of the Seismological Society of America, Vol. 17, No. 2, June 1927, pp. 95-109.
6. Ikegami, R. and Kishinoue, F., "A Study on the Overturning of a Rectangular Column," Bulletin of the Earthquake Research Institute of Japan, Vol. 24, 1946, pp. 11-18 (in Japanese).
7. Ikegami, R. and Kishinoue, F., "A Study on the Overturning of Rectangular Columns in the Case of the Nankai Earthquake," Bulletin of the Earthquake Research Institute of Japan, Vol. 25, 1947, pp. 49-55 (in Japanese).

8. Kobayashi, H., "Overturning of a Simple Body and the Seismic Coefficient," Transactions of the Architectural Institute of Japan, Vol. 8, Sept. 1950 (in Japanese).

9. Yasumi, M. and Akao, S., "Overturning of Prismatic Columns Due to An Earthquake," Technology Reports of the Osaka University, Vol. 1, Nos. 10-24, Oct. 1951, pp. 192-200.

10. Otsuki, Y., "Study on the Rocking Vibration of a Simple Body," Data No. 40 of the Committee of Vibration, Architectural Institute of Japan, 1956 (in Japanese).

11. Aslam, M., Godden, W.G. and Scalise, D.T., "Earthquake Rocking Response of Rigid Bodies," Journal of the Structural Division, American Society of Civil Engineers, Vol. 106, No. ST2, Feb. 1980, pp. 377-392.

12. Yim, C.S., Chopra, A.K. and Penzien, J., "Rocking Response of Rigid Blocks to Earthquakes," Report No. UCB/EERC 80-02, Earthquake Engineering Research Center, University of California, Berkeley, California, Jan. 1980.

13. Ishiyama, Y., "Review and Discussion on Overturning of Bodies by Earthquake Motions," BRI Research Paper No. 85, Building Research Institute, Ministry of Construction, June 1980.

14. Beck, J.L. and Skinner, R.I., "The Seismic Response of a Reinforced Concrete Bridge Pier Designed to Step," Earthquake Engineering and Structural Dynamics, Vol. 2, No. 4, Apr-June 1974, pp. 343-358.

15. Meek, J.W., "Effects of Foundation Tipping on Dynamic Response," Journal of the Structural Division, American Society of Civil Engineers, Vol. 101, No. ST7, July 1975, pp. 1297-1311.

16. Sexton, H.J., Discussion of reference 15, Journal of the Structural Division, American Society of Civil Engineers, Vol. 102, No. ST6, June 1975, pp. 1262-1263.

17. Parmelee, R.A., Perelman, D.S., Lee, S.L. and Keer, L.M., "Seismic Response of Structure-Foundation Systems," Journal of the Engineering Mechanics Division, American Society of Civil Engineers, Vol. 94, No. EM6, Dec. 1968, pp. 1295-1315.

18. Lee, T.H. and Wesley, D.A., "Soil-Structure Interaction of Reactor Structures Subjected to Seismic Excitation," Proceedings of the First International Conference on Structural Mechanics in Reactor Technology, Berlin, Sept. 1971, Paper K3/5.

19. Jennings, P.C. and Bielak, J., "Dynamics of Building-Soil Interaction," Bulletin of the Seismological Society of America, Vol. 63, No. 1, Feb. 1973, pp. 9-48.

20. Roesset, J.M., Whitman, R.V. and Dobry, R., "Modal Analysis for Structures with Foundation Interaction," Journal of the Structural Division, American Society of Civil Engineers, Vol. 99, No. ST3, March 1973, pp. 399-416.

21. Veletsos, A.S. and Meek, J.W., "Dynamic Behavior of Building-Foundation Systems," Earthquake Engineering and Structural Dynamics, Vol. 3, No. 2, Oct.-Dec. 1974, pp. 121-138.

22. Veletsos, A.S. and Nair, D.V.V., "Seismic Interaction of Structures on Hysteretic Foundations," Journal of the Structural Division, American Society of Civil Engineers, Vol. 101, No. ST1, Jan. 1975, pp. 109-129.

23. Foutch, D.A., "A Study of the Vibrational Characteristics of Two Multistory Buildings," Report No. EERL 76-03, Earthquake Engineering Research Laboratory, California Institute of Technology, Pasadena, California, Sept. 1976.

24. Goschy, Bela, "Soil-Foundation-Structure Interaction," Journal of the Structural Division, American Society of Civil Engineers, Vol. 104, No. ST5, May 1978, pp. 749-761.

25. Muto, K., Umemura, H. and Sonobe, Y., "Study of the Overturning Vibrations of Slender Structures," Proceedings of the Second World Conference on Earthquake Engineering, Tokyo, 1960.

26. Huckelbridge, A.A. and Clough, R.W., "Earthquake Simulation Tests of a Steel Frame Allowed to Uplift," Paper presented at the ASCE/EMD Specialty Conference on Dynamic Response of Structures, Instrumentation, Testing Methods and System Identification, held at the University of California, Los Angeles, California, March 30-31, 1976.

27. Huckelbridge, A.A., "Earthquake Simulation Tests of a Nine-Story Steel Frame with Columns Allowed to Uplift," Report No. UCB/EERC 77-23, Earthquake Engineering Research Center, University of California, Berkeley, California, Aug. 1977.

28. Clough, R.W. and Huckelbridge, A.A., "Earthquake Simulation Tests of a Three-Story Steel Frame with Columns Allowed to Uplift," Report No. UCB/EERC 77-22, Earthquake Engineering Research Center, University of California, Berkeley, California, Aug. 1977.

29. Huckelbridge, A.A. and Clough, R.W., "Seismic Response of an Uplifting Building Frame," Paper presented at the ASCE Annual Convention, San Francisco, California, Oct. 17-21, 1977.

30. Clough, R.W. and Huckelbridge, A.A., "The Effect of Column Uplift in Building Frames During Earthquakes," Paper presented at the SEAOC Convention, Coronado, California, 1977.

31. Morris, D.V., "Centrifugal Modeling of Earthquake Phenomena," To be published in the Journal of the Geotechnical Engineering Division, American Society of Civil Engineers.

32. Priestley, M.J.N., Evison, R.J. and Carr, A.J., "Seismic Response of Structures Free to Rock on Their Foundations," Bulletin of the New Zealand National Society of Earthquake Engineering, Vol. 11, No. 3, Sept. 1978, pp. 141-150.

33. Priestley, M.J.N., McManus, K.J. and Carr, A.J., "Seismic Rocking Response of Flexible Structures," To be published in the Journal of the Structural Division, American Society of Civil Engineers.

34. Wolf, J.P., "Soil-Structure Interaction with Separation of Base Mat from Soil (Lifting-off)," Nuclear Engineering and Design, Vol. 38, No. 2, Aug. 1976, pp. 357-384.

35. Wolf, J.P., "Seismic Response Due to Travelling Shear Wave Including Soil-Structure Interaction with Base Mat Uplift," Earthquake Engineering and Structural Dynamics, Vol. 5, No. 4, Oct.-Dec. 1977, pp. 337-363.

36. Wolf, J.P. and Skrikerud, P.E., "Seismic Excitation with Large Overturning Moments: Tensile Capacity, Projecting Base Mat or

Lifting-off?," Nuclear Engineering and Design, Vol. 50, No. 2, Oct. 1978, pp. 305-321.

37. Singh, P., "Seismic Behavior of Braces and Braced Steel Frames," Report No. UMEE 77R1, Department of Civil Engineering, University of Michigan, July 1977.

38. Bervig, D.R. and Chen, C., "Stability and Toe Pressure Calculation of a Reactor Building Subject to Seismic Disturbance," Transactions of the Third International Conference on Structural Mechanics in Reactor Technology, Imperial College, London, Sept. 1975, Paper K3/7.

39. Hsieh, T.K., "Foundation Vibrations," Proceedings of the Institute of Civil Engineers, Vol. 22, June 1962, pp. 211-225.

40. Whitman, R.V. and Richart, F.E., "Design Procedures for Dynamically Loaded Foundations," Journal of the Soil Mechanics and Foundations Division, American Society of Civil Engineers, Vol. 93, No. SM6, Nov. 1967, pp. 169-193.

41. Richart, F.E., Woods, R.O. and Hall, J.R., Vibration of Soils and Foundations, Prentice Hall, 1970.

42. Veletsos, A.S. and Wei, Y.T., "Lateral and Rocking Vibrations of Footings," Journal of the Soil Mechanics and Foundations Division, American Society of Civil Engineers, Vol. 97, No. SM9, Sept. 1971, pp. 1227-1249.

43. Luco, J.E. and Westmann, R.A., "Dynamic Response of Circular Footings," Journal of the Engineering Mechanics Division, American Society of Civil Engineers, Vol. 97, No. EM5, Oct. 1971, pp. 1381-1395.

44. Weissmann, G.F., "Tilting Foundations," Journal of the Soil Mechanics and Foundations Division, American Society of Civil Engineers, Vol. 98, No. SM1, Jan. 1972, pp. 59-78.

45. Sarrazin, M.A., Roesset, J.M. and Whitman, R.V., "Dynamic Soil-Structure Interaction," Journal of the Structural Division, American Society of Civil Engineers, Vol. 98, No. ST7, July 1972, pp. 1525-1544.

46. Newmark, N.M. and Rosenblueth, E., Fundamentals of Earthquake Engineering, Prentice Hall, 1972, pp. 93-101.

47. Luco, J.E. and Westmann, R.A., "Dynamic Response of a Rigid Footing Bonded to an Elastic Half Space," Journal of Applied Mechanics, American Society of Mechanical Engineers, Vol. 39, No. E2, June 1972, pp. 527-534.

48. Bolt, B.A., Earthquakes, A Primer, W. H. Freeman and Co., San Francisco, 1978, pp. 112-115.

49. Morrill, B.J., "Evidence of Record Vertical Accelerations at Kagel Canyon During the Earthquake," The San Fernando, California, Earthquake of February 9, 1971, A Preliminary Report Published jointly by the U.S. Geological Survey and the National Oceanic and Atmospheric Administration, Geological Survey Professional Paper 733, 1971, pp. 177-181.

50. "Strong Motion Earthquake Accelerograms," Vol. II, Part C, Report No. EERL 72-51, Earthquake Engineering Research Laboratory, California Institute of Technology, Pasadena, California, Febr. 1973, p. 9.

51. "Earthquake in Romania, March 4, 1977, An Engineering Report," National Research Council and Earthquake Engineering Research Institute, National Academy Press, Washington, D.C., 1980, p. 6.

52. "Strong Motion Earthquake Accelerograms," Vol. II, Part B, Report No. EERL 72-50, Earthquake Engineering Research Laboratory, California Institute of Technology, Pasadena, California, Feb. 1973, p. 51.

53. Housner, G.W., "Statistics of Pulses on Strong Motion Accelerograms," Proceedings of the N.S.F. Seminar-Workshop on Strong Ground Motion, Rancho Santa Fe, Febr. 1978, pp. 60-64.

54. Luco, J.E., "Linear Soil-Structure Interaction," Report No. UCRL-15272, Seismic Safety Margins Research Program, Lawrence Livermore Laboratory, Livermore, California, July 1980.

55. Wiegel, R.L., Editor, Earthquake Engineering, Prentice-Hall, 1970, p. 102.

56. Caughey, T.K. and O'Kelly, M.E.J., "General Theory of Vibration of Damped Linear Dynamic Systems," Dynamics Laboratory, California Institute of Technology, Pasadena, California, June 1973.

57. Housner, G.W. and Vreeland, T., Jr., "The Analysis of Stress and Deformation," Division of Engineering and Applied Science, California Institute of Technology, Pasadena, California, 1965, p. 104.

58. McVerry, G.H., "Frequency Domain Identification of Structural Models from Earthquake Records," Report No. EERL 79-02, Earthquake Engineering Research Laboratory, California Institute of Technology, Pasadena, California, Oct. 1979.

59. Duncan, W.J., Thom, A.S. and Yound, A.D., Mechanics of Fluids, Edward Arnold, 2nd Edition, 1970, pp. 191-192.

APPENDIX I

ESTIMATION OF THE AVERAGE LENGTH OF CONTACT BETWEEN THE BLOCK AND THE UNDAMPED WINKLER FOUNDATION DURING FREE OSCILLATIONS

Assuming that the mass of the block is uniformly distributed, there are only six parameters involved in the response of the block, namely: the mass, m; the height, h, at which the center of mass is located; the width of the base, a; the stiffness of the springs of the Winkler foundation, k_0; the acceleration of gravity, g; and the initial angular velocity, $\dot{\phi}_0$, caused by the horizontal impulse. Instead of the last quantity, however, the maximum angle of rotation, ϕ^c_{max}, which would happen if lift-off were not allowed, is used in the following. As equation (2.4.8) implies, these quantities are related to each other by the expression

$$\phi^c_{max} = \frac{\dot{\phi}_0}{p_1^*} \tag{I.1}$$

in which p_1^* is the rocking frequency during full contact. The advantage of using ϕ^c_{max} is that the results can then be extended to other horizontal excitations, also.

Let $\tilde{S}$ be the average length of contact during uplift. Then, according to Buckingham's Π-theorem,[59] the dimensionless quantity $\frac{\tilde{S}}{a}$ can be expressed as a function of three other dimensionless quantities, Π_1, Π_2 and Π_3, which here are chosen to be

$$\Pi_1 = \frac{h}{a} \tag{I.2}$$

$$\Pi_2 = \frac{\delta}{a} = \frac{mg}{k_0 a^2} \tag{I.3}$$

$$\Pi_3 = \phi^c_{max} \tag{I.4}$$

The function which relates $\frac{\tilde{S}}{a}$ with the Π_i's can be found by examining the dependence of $\frac{\tilde{S}}{a}$ on each of these dimensionless quantities while the other two are kept constant.

The results of such an analysis are shown in Fig. I.1 (isolated points). The response of the system was found using equations (2.4.7) and (2.4.8) during full contact and equations (2.4.3) and (2.4.4) after lift-off. The latter equations were integrated numerically, via Runge-Kutta method for the solution of a system of first order, nonlinear, ordinary differential equations. The value of the length of contact, S, at each time step during uplift, was calculated according to equation (2.4.6) and $\tilde{S}$ was taken equal to the numerical average of these values. The values of the parameters used and the numerical results are shown in Tables I.1, I.2 and I.3. In these tables, the values of the maximum angle of rotation, ϕ_{max}, and the rocking period, T, are also presented and compared with the corresponding values, which would occur if lift-off were not allowed, ϕ^c_{max} and T_c, respectively.

From the first plot of Fig. I.1, it is seen that $\frac{\tilde{S}}{a}$ is independent of $\frac{h}{a}$; Figs. I.1.b and I.1.c imply that

$$\frac{\tilde{S}}{a} = C_1 + C_2\left(\frac{\delta}{a}\right)^{\alpha_1} \left(\phi^c_{max}\right)^{\alpha_2} \tag{I.5}$$

where C_1 , C_2, α_1 and α_2 are constants, which have to be determined. For the limiting case, however, of a rigid foundation, both δ and $\tilde{S}$ reach zero, therefore, C_1 must vanish. The values of C_2, α_1 and α_2 were found

TABLE I.1

Variation of $\frac{\tilde{S}}{a}$ with Π_1

a (m)	h (m)	m $\left(\frac{t\cdot sec^2}{m}\right)$	k_0 $\left(\frac{t}{m^2}\right)$	ϕ_{cr} (rad)	$\frac{1}{\beta} = \frac{\phi_{cr}}{\phi^c_{max}}$	T_c (sec)	(Π_1) $\frac{h}{a}$	(Π_2) $\frac{mg}{k_0 a^2}$	(Π_3) ϕ^c_{max}	$\frac{\tilde{S}}{a}$	T (sec)	$\frac{T}{T_c}$	ϕ_{max} (rad)	$\frac{\phi_{max}}{\phi^c_{max}}$
10.	4.	40.	8,000.	9.81×10^{-4}	0.13333	0.265	0.4	4.905×10^{-4}	7.3575×10^{-3}	0.33057	0.677	2.551	1.268×10^{-2}	1.724
10.	6.	60.	12,000.	"	"		0.6	"	"	complete separation				
10.	8.	80.	16,000.	"	"	0.475	0.8	"	"	0.34361	1.095	2.319	1.338×10^{-2}	1.818
10.	10.	100.	20,000	"	"	0.581	1.0	"	"	0.36664	1.324	2.279	1.363×10^{-2}	1.853
10.	12.	120.	24,000.	"	"	0.691	1.2	"	"	0.35204	1.571	2.273	1.364×10^{-2}	1.854
10.	14.	140.	28,000.	"	"	0.803	1.4	"	"	0.36488	1.818	2.265	1.368×10^{-2}	1.859
10.	16.	160.	32,000.	"	"	0.914	1.6	"	"	0.35557	2.071	2.265	1.379×10^{-2}	1.874
10.	18.	180.	36,000.	"	"	1.027	1.8	"	"	0.36346	2.327	2.266	1.386×10^{-2}	1.884
10.	20.	200.	40,000.	"	"	1.139	2.0	"	"	0.35622	2.586	2.270	1.389×10^{-2}	1.888
10.	25.	250.	50,000.	"	"	1.422	2.5	"	"	0.35732	3.247	2.283	1.400×10^{-2}	1.903
10.	30.	300.	60,000.	"	"	1.707	3.0	"	"	0.35819	3.929	2.302	1.410×10^{-2}	1.916
10.	35.	350.	70,000.	"	"	1.993	3.5	"	"	0.35518	4.625	2.321	1.420×10^{-2}	1.930
10.	40.	400.	80,000.	"	"	2.279	4.0	"	"	0.35566	5.344	2.345	1.431×10^{-2}	1.945
10.	50.	500.	100,000.	"	"	2.856	5.0	"	"	0.35230	6.838	2.394	1.453×10^{-2}	1.975
10.	60.	600.	120,000.	"	"	3.436	6.0	"	"	0.34979	8.421	2.451	1.477×10^{-2}	2.007

TABLE I.2

Variation of $\frac{\tilde{s}}{a}$ with Π_2

a (m)	h (m)	m $\left(\frac{t\cdot sec^2}{m}\right)$	k_0 $\left(\frac{t}{m^2}\right)$	ϕ_{cr} (rad) $\times 10^3$	$\frac{1}{\beta} = \frac{\phi_{cr}}{\phi^c_{max}}$	T_c (sec)	(Π_1) $\frac{h}{a}$	(Π_2) $\frac{mg}{k_0 a^2}$	(Π_3) ϕ^c_{max}	$\frac{\tilde{s}}{a}$	T (sec)	$\frac{T}{T_c}$	ϕ_{max} (rad)	$\frac{\phi_{max}}{\phi^c_{max}}$
10.	5.	50.	4,000.	2.452	0.981	0.499	0.5	1.23×10^{-3}	0.0025	0.99417	0.502	1.007	0.0025	1.000
10.	5.	"	5,000.	1.962	0.785	0.446	"	0.98×10^{-3}	"	0.91996	0.453	1.017	0.00251	1.003
10.	5.	"	6,000.	1.635	0.654	0.407	"	0.82×10^{-3}	"	0.85516	0.424	1.043	0.00253	1.012
10.	5.	"	7,000.	1.401	0.560	0.376	"	0.70×10^{-3}	"	0.79596	0.406	1.079	0.00257	1.026
10.	5.	"	8,000.	1.226	0.490	0.352	"	0.61×10^{-3}	"	0.74081	0.396	1.125	0.00261	1.043
10.	5.	"	9,000.	1.090	0.436	0.332	"	0.54×10^{-3}	"	0.69113	0.392	1.182	0.00265	1.061
10.	5.	"	10,000.	0.981	0.392	0.315	"	0.49×10^{-3}	"	0.64790	0.390	1.240	0.00270	1.081
10.	5.	"	12,000.	0.817	0.327	0.287	"	0.41×10^{-3}	"	0.57856	0.391	1.362	0.00280	1.121
10.	5.	"	14,000.	0.701	0.280	0.266	"	0.35×10^{-3}	"	0.53032	0.394	1.482	0.00290	1.161
10.	5.	"	16,000.	0.613	0.245	0.249	"	0.31×10^{-3}	"	0.50208	0.396	1.593	0.00300	1.201
10.	5.	"	18,000.	0.545	0.218	0.234	"	0.27×10^{-3}	"	0.46654	0.402	1.715	0.00321	1.282
10.	5.	"	20,000.	0.490	0.196	0.222	"	0.25×10^{-3}	"	0.43447	0.410	1.844	0.00356	1.423
10.	5.	"	25,000.	0.392	0.157	0.199	"	0.20×10^{-3}	"	0.39236	0.429	2.158	0.00394	1.577

TABLE I.3

Variation of $\frac{\tilde{S}}{a}$ with Π_3

a (m)	h (m)	m $\left(\frac{t\cdot sec^2}{m}\right)$	k_0 $\left(\frac{t}{m^2}\right)$	ϕ_{cr} (rad)	$\frac{1}{\beta} = \frac{\phi_{cr}}{\phi^c_{max}}$	T_c (sec)	(Π_1) $\frac{h}{a}$	(Π_2) $\frac{mg}{k_0 a^2}$	(Π_3) $\phi^c_{max} \times 10^3$	$\frac{\tilde{S}}{a}$	T (sec)	$\frac{T}{T_c}$	ϕ_{max} (rad) $\times 10^{-3}$	$\frac{\phi_{max}}{\phi^c_{max}}$
10.	5.	50.	10,000.	9.81×10^{-4}	0.981	0.315	0.5	4.905×10^{-4}	1.00	0.99558	0.320	1.017	1.000	1.000
10.	5.	"	"	"	0.785	"	"	"	1.25	0.92077	0.322	1.023	1.254	1.003
10.	5.	"	"	"	0.654	"	"	"	1.50	0.85643	0.329	1.046	1.518	1.012
10.	5.	"	"	"	0.561	"	"	"	1.75	0.79694	0.340	1.081	1.7955	1.026
10.	5.	"	"	"	0.491	"	"	"	2.00	0.74066	0.355	1.128	2.086	1.043
10.	5.	"	"	"	0.392	"	"	"	2.50	0.64790	0.390	1.240	2.7025	1.081
10.	5.	"	"	"	0.327	"	"	"	3.00	0.57974	0.429	1.364	3.363	1.121
10.	5.	"	"	"	0.280	"	"	"	3.50	0.53341	0.465	1.478	4.067	1.162
10.	5.	"	"	"	0.245	"	"	"	4.00	0.50145	0.501	1.592	4.808	1.202
10.	5.	"	"	"	0.218	"	"	"	4.50	0.46533	0.539	1.713	5.796	1.288
10.	5.	"	"	"	0.196	"	"	"	5.00	0.43272	0.580	1.843	7.145	1.429
10.	5.	"	"	"	0.178	"	"	"	5.50	0.40999	0.622	1.977	8.4205	1.531
10.	5.	"	"	"	0.164	"	"	"	6.00	0.39549	0.661	2.101	9.468	1.578
10.	5.	"	"	"	0.140	"	"	"	7.00	0.37737	0.726	2.308	10.311	1.473
10.	5.	"	"	"	0.123	"	"	"	8.00	complete separation				

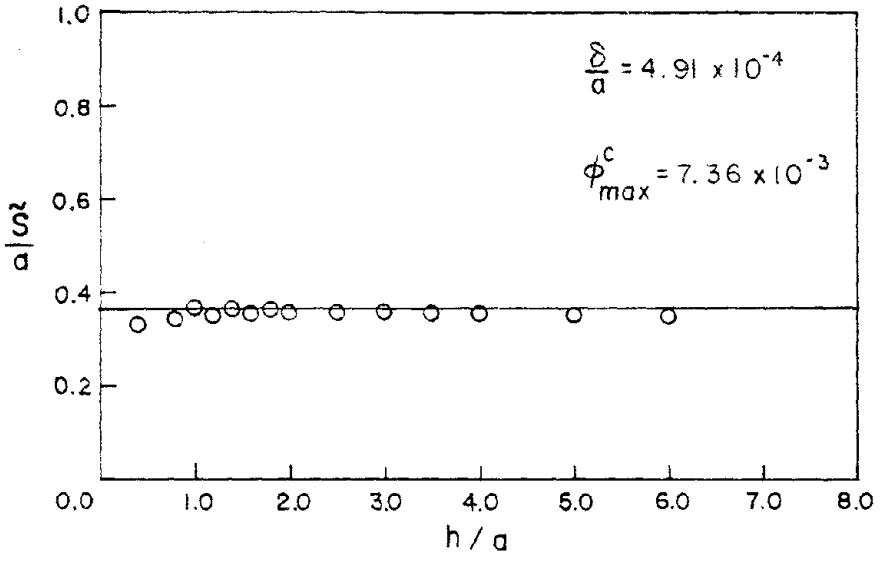

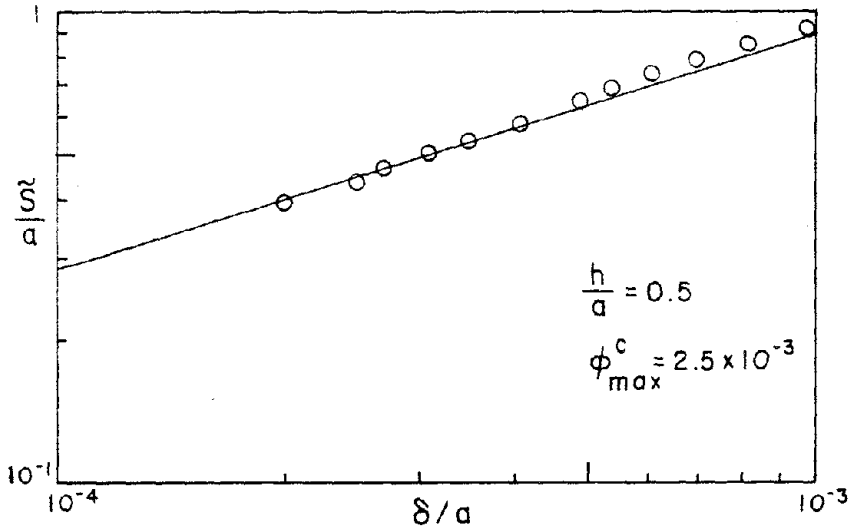

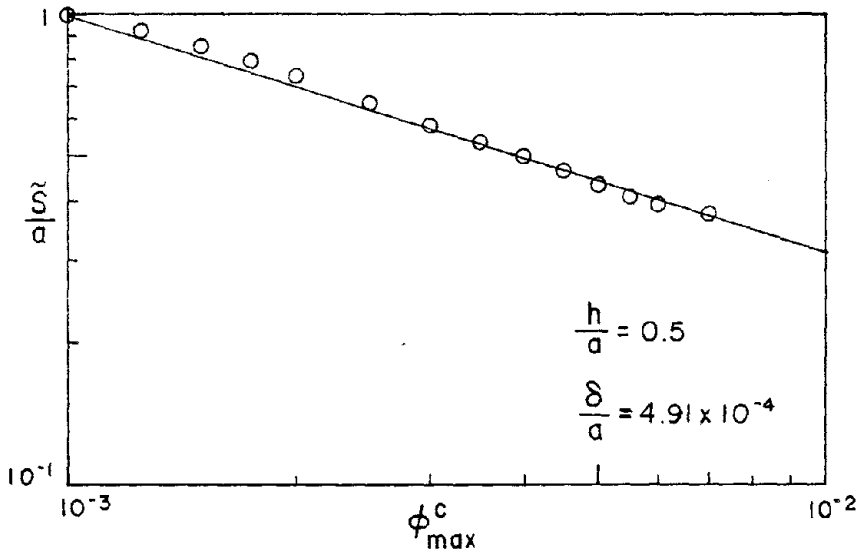

Fig. I.1. Dependence of $\left(\frac{\tilde{S}}{a}\right)$ on: (a) $\frac{h}{a}$, (b) $\frac{\delta}{a}$, (c) ϕ^c_{max}.

by a least square analysis and are

$$C_2 = 1.27$$

$$\alpha_1 = 0.51$$

$$\alpha_2 = -0.54$$

Noting that $C_2 \cong \sqrt{2}$ and that $\alpha_1 \cong -\alpha_2 \cong \frac{1}{2}$, the following simple formula can be written

$$\frac{\tilde{S}}{a} = \sqrt{\frac{1}{\beta}} \qquad (I.6)$$

where

$$\beta = \frac{\phi^c_{max}}{\phi_{cr}} \qquad (I.7)$$

In equation (I.7), ϕ_{cr} is the critical angle at which lift-off happens in the absence of vertical oscillations, given by

$$\phi_{cr} = \frac{2\delta}{a} \qquad (I.8)$$

The fitting of formula (I.6) with the calculated data is good, as it can be seen from the plots of Fig. I.1, where expression (I.6) is plotted with a solid line. In Fig. I.2, all these data, plus more points corresponding to other combinations of the dimensionless parameters, are plotted together with equation (I.6). It seems that this simple equation accurately estimates the value of $\tilde{S}$.

Although the empirical expression (I.6) cannot be proven analytically, it can be shown that the value of $\frac{\tilde{S}}{a}$ is close to the

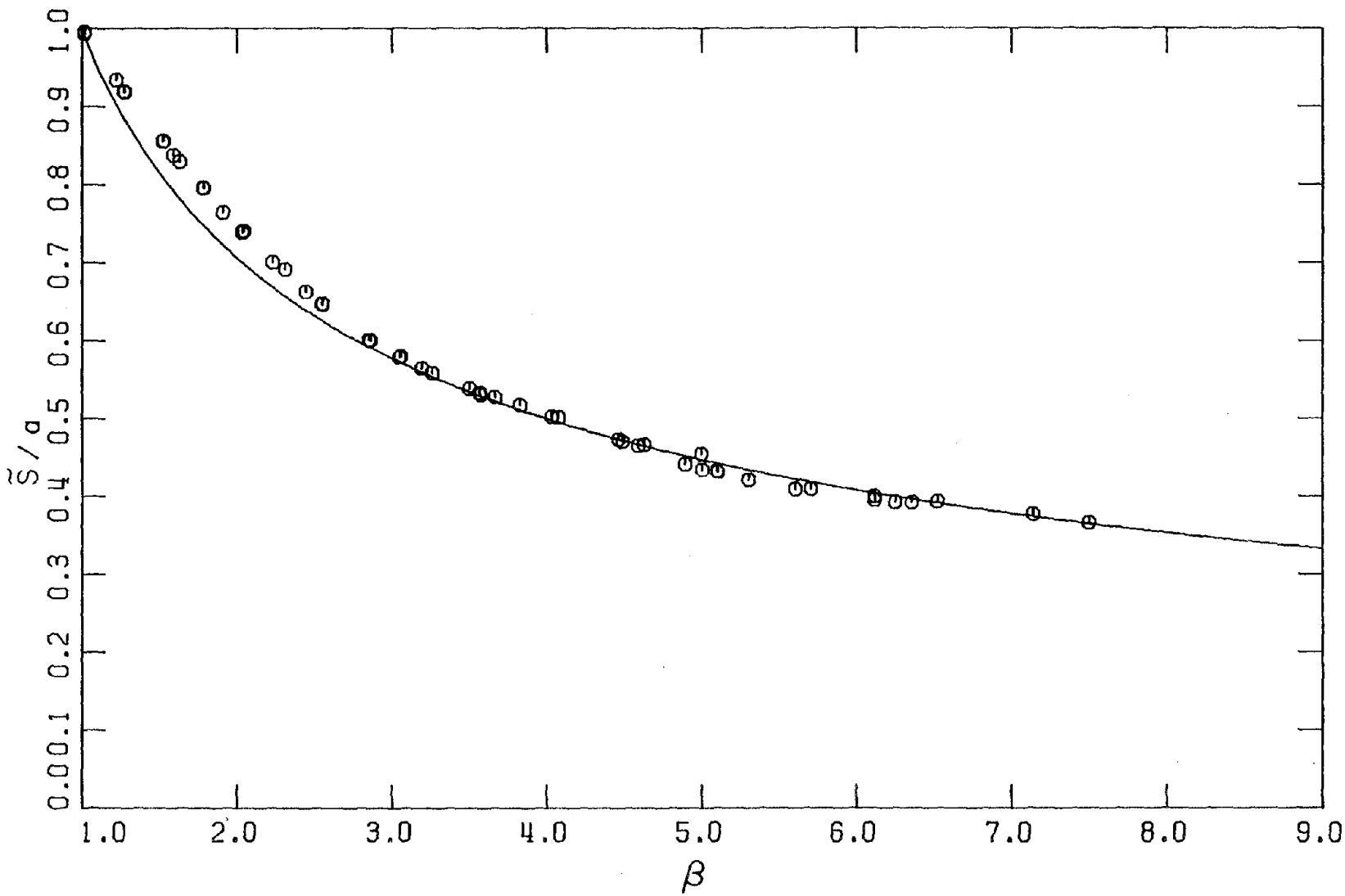

Fig. I.2. Variation of the average length of contact with the normalized impulse, β.

value predicted by (I.6). To do that, let us first recall that the pole of rotation, P, before lift-off is located at the middle-point of the base, M. After lift-off and for positive angles of rotation, P is moving to the right. In the following, it is assumed that P lies on line L-L and the distance, ℓ, depends on the amount of lift-off (see Fig. I.3). The following expression can then be written

$$\frac{S}{a} = \frac{\phi_{cr}}{\phi}\left(1 - \frac{\ell_1}{a}\right) + \frac{\ell_1}{a} \tag{I.9}$$

The maximum angle of rotation, ϕ_{max}, and the rocking frequency, p, can be estimated by the response of the equivalent two-spring model (equivalence during full contact), which is defined by equations (2.5.6) and (2.5.7). Using equations (2.3.81) and (2.3.74), one can write,

$$\phi_{max} = \phi_{cr}^{(2s)}\left[\frac{1+\lambda}{2}\left(\beta_{2s}^2 - 1\right) + 1\right] \tag{I.10}$$

$$p = p_1 \frac{\pi}{2\left[\sin^{-1}\left(\frac{1}{\beta_{2s}}\right) + \sqrt{\beta_{2s} - 1}\right]} \tag{I.11}$$

in which $\phi_{cr}^{(2s)}$ and β_{2s} are the corresponding values of the critical angle and the normalized impulse for the two-spring foundation, and

$$p_1 = \sqrt{\frac{2k\xi^2}{I_M}} \tag{I.12}$$

Equations (2.5.6) and (2.5.7) imply that

$$\phi_{cr}^{(2s)} = \sqrt{3}\,\phi_{cr} \tag{I.13}$$

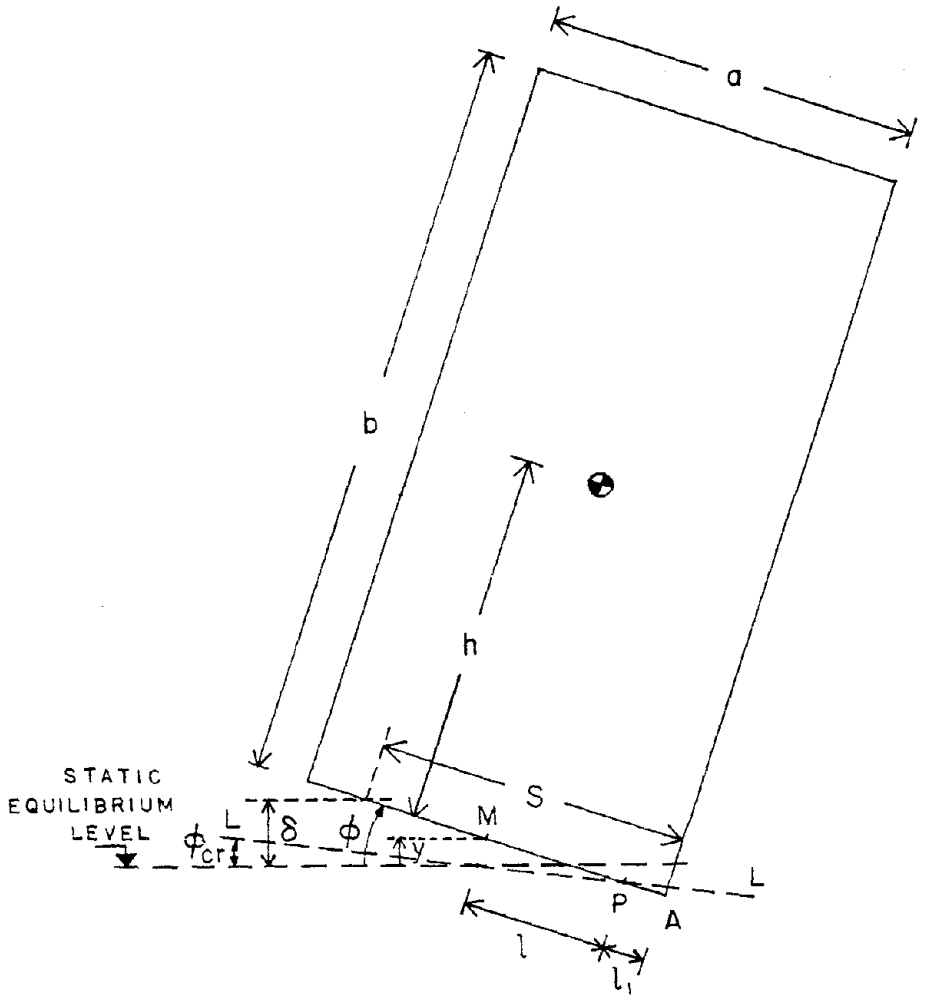

Fig. I.3. Length of contact and pole of rotation after lift-off for a rocking block on a Winkler foundation.

$$\beta_{2s} = \frac{\beta}{\sqrt{3}} \tag{I.14}$$

Since $\beta_{2s} < 1$ for $\beta < \sqrt{3}$, the two-spring model does not lift-off for $1 \leq \beta \leq \sqrt{3}$. In that case, the following expressions apply

$$\phi_{max} = \beta_{2s}\, \phi_{cr}^{2s} = \beta\, \phi_{cr} \tag{I.15}$$

$$p = p_1 \tag{I.16}$$

For simplcity, let us assume that $\lambda << 1$. Then, one can write

$$\phi(t) = \begin{cases} \beta\, \phi_{cr} \sin pt & , \quad 1 \leq \beta \leq \sqrt{3} \\ \dfrac{\sqrt{3}}{2}\, \phi_{cr}\left(\dfrac{\beta^2}{3} + 1\right) \sin pt & , \quad \beta \geq \sqrt{3} \end{cases} \tag{I.17}$$

Substituting in (I.9) and taking the average of $\frac{\tilde{S}}{a}$ from the time of lift-off, t_o, to $t = \frac{\pi}{2p}$ (i.e. $t = \frac{T}{4}$) gives

$$\frac{\tilde{S}}{a} = \frac{\left(1 - \frac{\ell_1}{a}\right) G_1 \ell n\, G_2}{\frac{\pi}{2} - \sin^{-1} G_1} + \frac{\ell_1}{a} \tag{I.18}$$

in which

$$G_1 = \begin{cases} \dfrac{1}{\beta} & , \quad 1 \leq \beta \leq \sqrt{3} \\ \dfrac{2}{\sqrt{3}\left(\dfrac{\beta^2}{3} + 1\right)} & , \quad \beta \geq \sqrt{3} \end{cases} \tag{I.19}$$

and

$$G_2 = \begin{cases} \beta + \sqrt{\beta^2 - 1} & , \quad 1 \leq \beta \leq \sqrt{3} \\ \frac{\sqrt{3}}{2}\left(\frac{\beta^2}{3} + 1\right) + \frac{1}{2}\sqrt{3\left(\frac{\beta^2}{3} + 1\right)^2 - 1} & , \quad \beta \geq \sqrt{3} \end{cases} \tag{I.20}$$

In these expressions, t_o was calculated from equation

$$\sin pt_o = G_1 \tag{I.21}$$

as equation (I.17) suggests.

The rocking equation of motion can be written as

$$I_P\ddot{\phi} + \frac{1}{2} k_0 S^2\left(\ell_1 - \frac{S}{3}\right)\phi - mgh\,\phi = mg\ell \tag{I.22}$$

where I_P is the moment of inertia about the pole, P. Neglecting the term mgh ϕ and putting $I_P \cong I_M$ (for small λ), the rocking frequency can be expressed as

$$p = \sqrt{\frac{k_0 \tilde{S}^2\left(\ell_1 - \frac{\tilde{S}}{3}\right)}{2I_M}} \tag{I.23}$$

in which S was substituted by $\tilde{S}$ and ℓ_1 was assumed constant, equal to some average value. Using equations (I.11), (I.12), (I.16) and (I.23) one can write

$$\left(\frac{\tilde{S}}{a}\right)^2\left[\frac{\ell_1}{a} - \frac{\tilde{S}}{3a}\right] = \frac{G_3}{6} \tag{I.24}$$

where

$$G_3 = \begin{cases} 1 & , \quad 1 \le \beta \le \sqrt{3} \\ \dfrac{\pi^2}{4\left[\sin^{-1}\left(\dfrac{\sqrt{3}}{\beta}\right) + \sqrt{\dfrac{\beta^2-3}{3}}\right]^2} & , \quad \beta \ge \sqrt{3} \end{cases} \tag{I.25}$$

Eliminating $\frac{\ell_1}{a}$ from (I.18) and (I.24), the following equation for $\frac{\tilde{S}}{a}$ can be obtained

$$\left(\frac{\tilde{S}}{a}\right)^3 \left[\frac{\frac{\pi}{2} - \sin^{-1}G_1}{\frac{\pi}{2} - \sin^{-1}G_1 - G_1 \ell n\, G_2} - \frac{1}{3}\right] - \left(\frac{\tilde{S}}{a}\right)^2 \left[\frac{G_1 \ell n\, G_2}{\frac{\pi}{2} - \sin^{-1}G_1 - G_1 \ell n\, G_2}\right] - \frac{G_3}{6} = 0 \tag{I.26}$$

The real root of this equation is plotted versus β in Fig. I.4. In the same plot, the corresponding values of equation (I.6) are shown. Although the agreement of the two curves is only approximate, it can be concluded that the behavior of $\frac{\tilde{S}}{a}$ is similar to $1/\sqrt{\beta}$, taking under consideration the many approximations used in the derivation of equation (I.26).

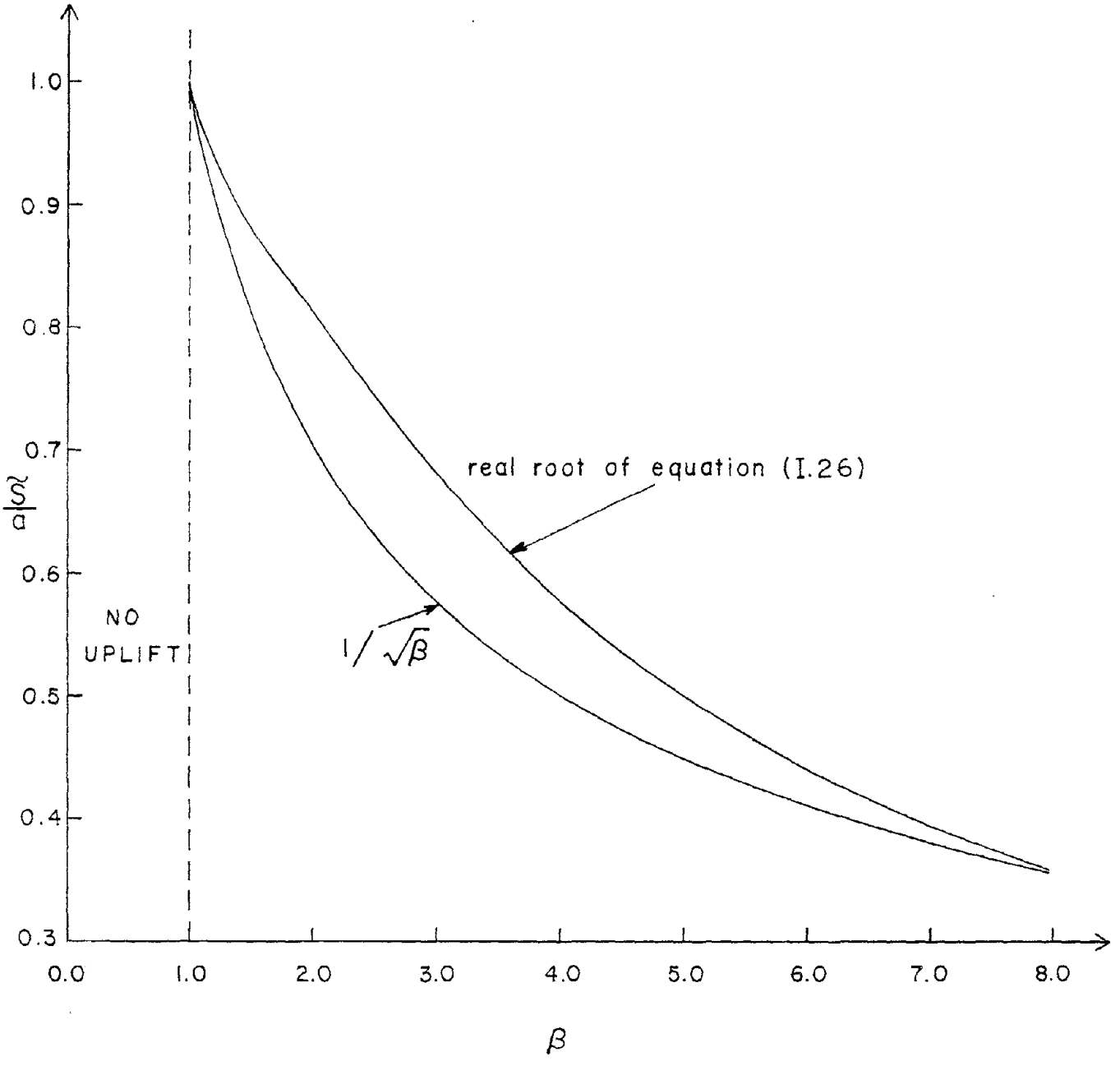

Fig. I.4. Comparison of the approximate analytical values of $\left(\frac{\tilde{S}}{a}\right)$ with the results of equation (I.26).

APPENDIX II

EQUATIONS OF MOTION FOR A ROCKING n-STORY SHEAR STRUCTURE (TWO-SPRING FOUNDATION)

Let us consider a system of coordinates (x_o,y_o,z_o) applied at the center of mass, CM, as shown in Fig. II.1, and rotating with the structure, with angular velocity $\underset{\sim}{\omega}_o$ with respect to the reference system (x,y,z). Let $\underset{\sim}{\Omega}_i$ be the relative angular velocity of the mass m_i with respect to the system (x_o,y_o,z_o). Then, the angular momentum, $\underset{\sim}{H}_i$, of this mass with respect to its center of mass can be written in matrix form as

$$\{H_i\} = [I_i]\{\omega_o\} + [I_i]\{\Omega_i\} \tag{II.1}$$

or, in vector form as

$$\underset{\sim}{H}_i = \underset{\sim}{H}'_i + \underset{\sim}{H}''_i \tag{II.2}$$

where $\underset{\sim}{H}'_i$ and $\underset{\sim}{H}''_i$ are angular momenta associated with the velocities $\underset{\sim}{\omega}_o$ and $\underset{\sim}{\Omega}_i$, respectively, and $[I_i]$ is the inertia matrix of mass m_i. Similarly, the total angular momentum of the system with respect to the center of mass, CM, is

$$H_{CM} = H'_{CM} + H''_{CM} \tag{II.3}$$

Let $(\underset{\sim}{v}_i)_r$ be the velocity of the center of mass of the i^{th} mass, relative to the system (x_o,y_o,z_o). Then

$$\underset{\sim}{H}'_{CM} = \sum_{i=0}^{n} \underset{\sim}{H}'_i + \sum_{i=0}^{n} \underset{\sim}{\rho}_i \times m_i(\underset{\sim}{\omega}_o \times \underset{\sim}{\rho}_i) \tag{II.4}$$

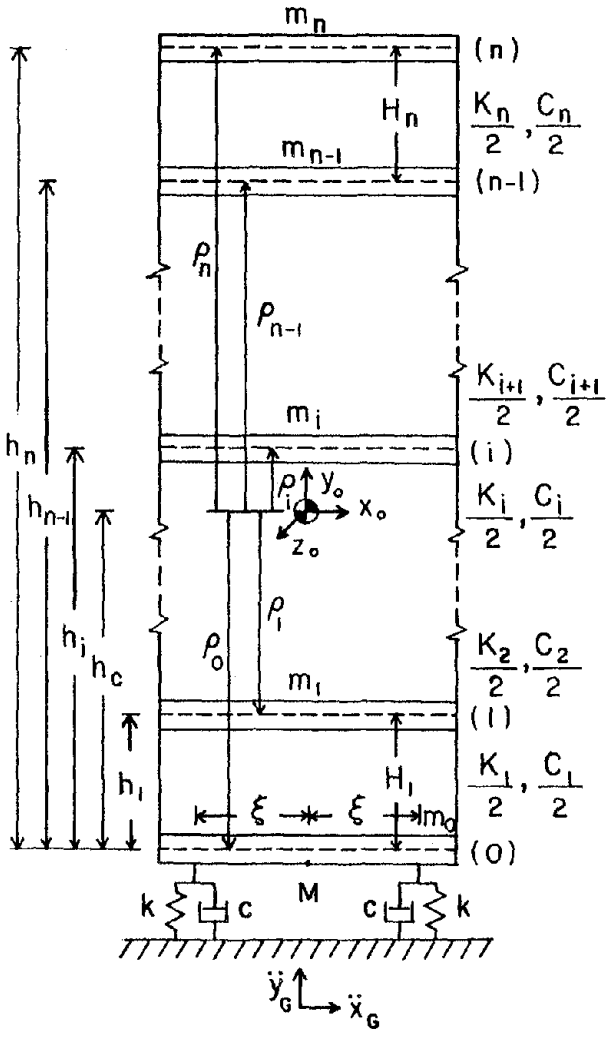

Fig. II.1. n-story structure on two-spring foundation.

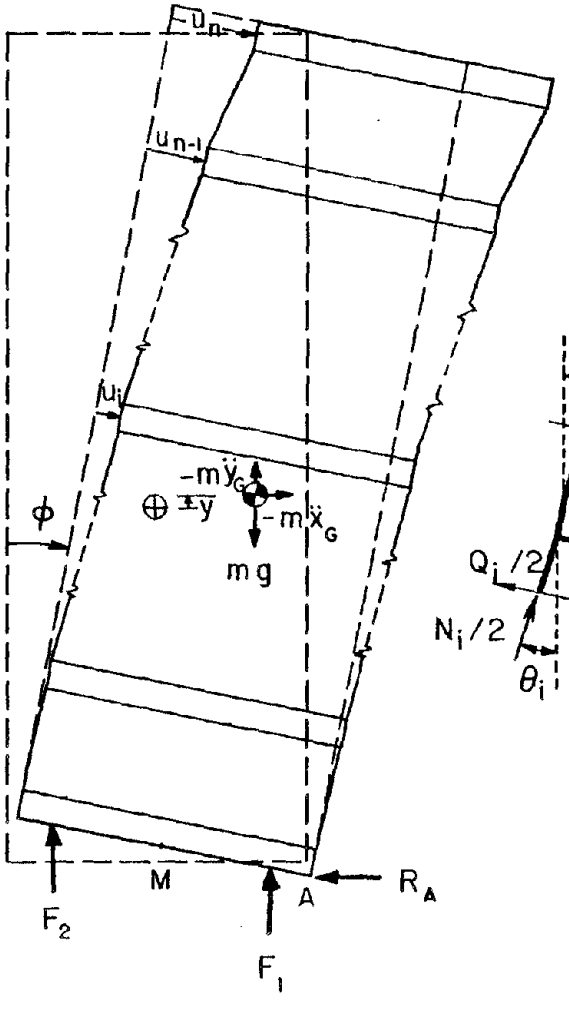

Fig. II.2. Free body diagram of the system.

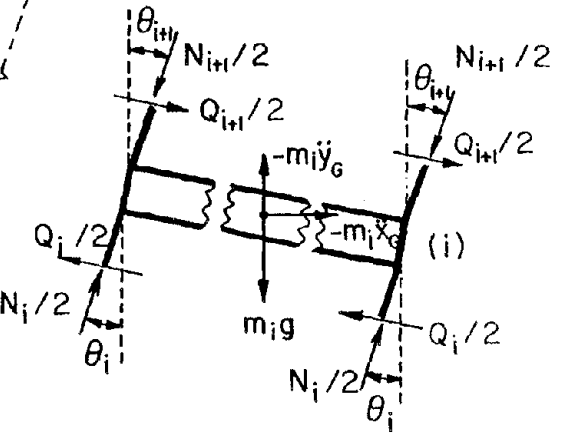

Fig. II.3. Free body diagram of the i^{th} mass.

and

$$\underset{\sim}{H}''_{CM} = \sum_{i=0}^{n} \underset{\sim}{H}''_i + \sum_{i=0}^{n} \underset{\sim}{\rho}_i \times m_i (\underset{\sim}{v}_i)_r \tag{II.5}$$

But, in our case,

$$\underset{\sim}{\omega}_0 = \begin{Bmatrix} 0 \\ 0 \\ -\dot{\phi} \end{Bmatrix} \tag{II.6}$$

and

$$\underset{\sim}{\Omega}_i = \underset{\sim}{0} \quad , \qquad i = 0,1,2,\cdots,n \tag{II.7}$$

which implies that

$$\underset{\sim}{H}''_i = \underset{\sim}{0} \quad , \qquad i = 0,1,2,\cdots,n \tag{II.8}$$

Since there is rotation about the z-axis only, we consider the equations associated with this axis only. Equations (II.4) and (II.5) give

$$H'_{CM} = - \sum_{i=0}^{n} \left(I_i + m_i \rho_i^2 \right) \dot{\phi} \tag{II.9}$$

$$H''_{CM} = - \sum_{i=0}^{n} m_i \rho_i \left(\dot{u}_i - \dot{u}_c \right) \tag{II.10}$$

where u_i and u_c are the shear deformations of the i^{th} story and the center of mass, respectively (see Fig. II.2).

Applying the equation of motion:

$$M_{CM} = \dot{H}_{CM} \tag{II.11}$$

the following equation can be obtained

$$-M_{CM} = I_{CM}\ddot{\phi} + \sum_{i=0}^{n} m_i\rho_i\ddot{u}_i \tag{II.12}$$

in which M_{CM} and I_{CM} are the moment of the external forces and the moment of inertia about the center of mass, respectively, and the identities

$$\sum_{i=0}^{n} m_i\rho_i = 0 \tag{II.13}$$

$$\sum_{i=0}^{n} I_i + m_i\rho_i^2 = I_{CM} \tag{II.14}$$

were employed.

Application of Newton's second law in the horizontal direction gives

$$R_A = -m(h_c\ddot{\phi} + \ddot{u}_c + \ddot{x}_G) \tag{II.15}$$

where $m = \sum_{i=0}^{n} m_i$ is the total mass. Then two of the equations of motion for the system can be found from equation (II.12) and application of Newton's second law in the vertical direction. For tilting to the right and neglecting the nonlinear terms, one gets

Full contact

$$m\ddot{y} + 2c\dot{y} + 2ky = -m\ddot{y}_G \tag{II.16}$$

$$I_M\ddot{\phi} + \sum_{i=0}^{n} m_i h_i\ddot{u}_i + 2c\xi^2\dot{\phi} + 2\left(k\xi^2 - \frac{1}{2}mgh_c\right)\phi - g\sum_{i=0}^{n} m_i u_i = -mh_c\ddot{x}_G \tag{II.17}$$

After lift-off

$$m\ddot{y} + c\dot{y} - c\xi\dot{\phi} + ky - k\xi\phi = -\frac{1}{2}mg - m\ddot{y}_G \tag{II.18}$$

$$I_M \ddot{\phi} + \sum_{i=0}^{n} m_i h_i \ddot{u}_i + c\xi^2\dot{\phi} - c\xi\dot{y} + \left(k\xi^2 - \frac{1}{2} mgh_c\right)\phi - k\xi y$$

$$- \frac{g}{2} \sum_{i=0}^{n} m_i u_i = -\frac{1}{2} mg\xi - mh_c\ddot{x}_G \qquad \text{(II.19)}$$

where I_M is the moment of inertia about the middle-point of the base, M, given by

$$I_M = I_{CM} + mh_c^2 \qquad \text{(II.20)}$$

The following expressions were also used for the derivation of equations (II.17) and (II.19)

$$\sum_{i=0}^{n} m_i u_i = mu_c \qquad \text{(II.21)}$$

$$\sum_{i=0}^{n} m_i \ddot{u}_i = m\ddot{u}_c \qquad \text{(II.22)}$$

$$h_i = h_c + \rho_i \qquad \text{(II.23)}$$

Note that for the mass m_o, $u_o = \dot{u}_o = \ddot{u}_o = 0$.

The remaining n equations of motion can be found by examining each mass separately. A free-body diagram of the i^{th} mass ($i = 1,2,\cdots,n-1$) is shown in Fig. II.3. The equation of motion in the vertical direction can be written as

$$N_i = N_{i+1} + m_i(g + \ddot{y}_G + \ddot{y}) \ , \qquad i = 1,2,\cdots,n-1 \qquad \text{(II.24)}$$

in which the terms $Q_i \sin\left(\frac{u_i - u_{i-1}}{h_i - h_{i-1}}\right)$ and $Q_{i+1} \sin\left(\frac{u_{i+1} - u_i}{h_{i+1} - h_i}\right)$ were neglected as of second order. For i = n, the corresponding equation is

$$N_n = m_n(g + \ddot{y}_G + \ddot{y}) \tag{II.25}$$

For $i = n-1$,

$$N_{n-1} = N_n + m_{n-1}(g + \ddot{y}_G + \ddot{y}) = (m_{n-1} + m_n)(g + \ddot{y}_G + \ddot{y})$$

As can be easily verified by induction, the following formula can be used in general:

$$N_i = \left(\sum_{\ell=i}^{n} m_\ell\right)(g + \ddot{y}_G + \ddot{y}) \ , \qquad i = 1,2,\cdots,n \tag{II.26}$$

Then, the equation of motion in the horizontal direction is

$$\begin{aligned} &m_i(h_i\ddot{\phi} + \ddot{u}_i) + (C_i + C_{i+1})\dot{u}_i - C_i\dot{u}_{i-1} - C_{i+1}\dot{u}_{i+1} \\ &+ (K_i + K_{i+1})u_i - K_iu_{i-1} - K_{i+1}u_{i+1} - m_ig\phi \\ &-m_ig\left(\frac{u_i - u_{i-1}}{H_i}\right) - \left(\sum_{\ell=i+1}^{n} m_\ell\right) g\left(\frac{u_i - u_{i-1}}{H_i} - \frac{u_{i+1} - u_i}{H_{i+1}}\right) = -m_i\ddot{x}_G \end{aligned} \tag{II.27}$$

for $i = 1,2,\cdots,n-1$, where $H_i = h_i - h_{i-1}$ and θ_i is assumed small, so that one can write

$$\cos\theta_i \simeq 1 \qquad \text{and} \qquad \sin\theta_i \simeq \phi + \frac{u_i - u_{i-1}}{H_i} \tag{II.28}$$

The corresponding equation for the n^{th} mass has to be derived independently and is

$$m_n(h_n\ddot{\phi} + \ddot{u}_n) + C_n(\dot{u}_n - \dot{u}_{n-1}) + K_n(u_n - u_{n-1}) -$$

$$- m_n g\phi - m_n g\left(\frac{u_n - u_{n-1}}{H_n}\right) = - m_n \ddot{x}_G \qquad \text{(II.29)}$$

The equations of motion derived here were verified by rederiving them using Lagrange's equations. The author expresses his sincere thanks to Mr. Dirceu Bothelo, who did this derivation.

Equations (II.27) and (II.29) can be written in matrix form as

$$[M]\underset{\sim}{\ddot{u}} + [C]\underset{\sim}{\dot{u}} + [K]\underset{\sim}{u} = -[M]\underset{\sim}{h}\ddot{\phi} + \underset{\sim}{m}g\phi - \underset{\sim}{m}\ddot{x}_G \qquad \text{(II.30)}$$

where

$$\underset{\sim}{u} = \{u_i\} \quad , \quad i = 1,\cdots,n \qquad \text{(II.31)}$$

$$\underset{\sim}{h} = \{h_i\} \quad , \quad i = 1,\cdots,n \qquad \text{(II.32)}$$

$$\underset{\sim}{m} = \{m_i\} \quad , \quad i = 1,\cdots,n \qquad \text{(II.33)}$$

$$[M] = [\sim m_i \sim] \quad , \quad i = 1,\cdots,n \qquad \text{(II.34)}$$

and $[C] = [C_{ij}]$, $[K] = [K_{ij}]$ are tridiagonal matrices, defined by

$$C_{ij} = \begin{cases} C_i + C_{i+1} & , \ i = j = 1,\cdots,n-1 \\ C_i & , \ i = j = n \\ -C_i & , \ j = i-1 \\ -C_{i+1} & , \ j = i+1 \\ 0 & , \ \text{otherwise} \end{cases} \qquad \text{(II.35)}$$

$$K_{ij} = \begin{cases} K_i + K_{i+1} - g\left(\dfrac{m_i^*}{H_i} + \dfrac{m_{i+1}^*}{H_{i+1}}\right) & , \ i = j = 1, \cdots, n-1 \\ K_i - \dfrac{m_i^* g}{H_i} & , \ i = j = n \\ -K_i + \dfrac{m_i^* g}{H_i} & , \ j = i-1 \\ -K_{i+1} + \dfrac{m_{i+1}^* g}{H_{i+1}} & , \ j = i+1 \\ 0 & , \text{ otherwise} \end{cases} \qquad \text{(II.36)}$$

in which

$$m_i^* = \sum_{\ell=i}^{n} m_\ell \qquad \text{(II.37)}$$

and

$$H_i = h_i - h_{i-1} \qquad , \ i = 1, \cdots, n \qquad \text{(II.38)}$$